Released Oct. 1976

EVANS, Robert

Ph. D. Jan. 1977

STERIC STABILIZATION

A Thesis

submitted in fulfilment of

the requirements for

the degree of Doctor of Philosophy

by

Robert Evans

Department of Physical Chemistry

University of Sydney

February, 1976

PREFACE

This thesis is the result of a general study of the phenomenon of steric stabilization, which is the stabilization of colloidal dispersions by adsorbed macromolecules. The main objectives were:

i) to develop a theory, in terms of experimentally determinable quantities, which gives a satisfactory prediction of the distance dependence of the interaction between monodisperse sterically stabilized latex particles.

ii) to consider the use of Flory's free volume theory of polymer solutions as a means of improving the theory of steric stabilization.

iii) to ensure that the experimentally observed correlation between the critical flocculation point of a sterically stabilized latex and the Θ-point for the stabilizer in free solution is reflected in the predictions of the theory.

iv) to prepare and characterize a sterically stabilized latex which flocculates on heating in a non-aqueous medium.

v) to study the effects of pressure on the critical flocculation point of sterically stabilized latices and on its correlation with the Θ-point for the stabilizer in free solution.

vi) to investigate the use of low molecular weight non-ionic polymers as flocculants for sterically stabilized latices.

vii) to determine the quantitative effect of van der Waals attraction (as calculated using Lifshitz theory) on the total interaction in sterically stabilized latices.

Much of the work presented here has been published. Copies of all available papers of which I am a joint author are supplied with this thesis. One paper (no.11 on the list of publications) was not available at the time of submission. Publication no.8 contains results obtained by P.M. Went (B.Sc. Hons., University of Sydney, 1974) which I presented at the Australian Polymer Symposium (5th National Convention of the R.A.C.I.) Canberra, 1974. Publication no.1 refers to results included in my B.Sc. Hons. thesis (University of Sydney, 1971). Unless otherwise indicated, the results in this thesis are original and have not previously been submitted for examination.

I would like to acknowledge the assistance of the many people with whom I have been associated at the University of Sydney; I especially wish to thank the following:

Dr. D.H. Napper for his supervision, encouragement and enthusiasm,

Assoc. Prof. R.J. Hunter who, as acting Head of the Department of Physical Chemistry (1971) allowed me to undertake the studies for this degree,

Prof. W.J. Moore, present Head of the Department of Physical Chemistry,

Mr. J.B. Smitham and Mr. R. Feigin for numerous enlightening discussions and for their comments on chapters II and III,

Dr. A.H. Ewald for the use of the C.S.I.R.O. pressure apparatus and advice on the construction and use of the modified apparatus used in chapter II,

Mr. L. Edney who constructed the high pressure bomb and rapid mixing apparatus and who offered valuable suggestions for their modification,

Mr. B. Alcorn for the photographs in chapters II and III.

Financial support of these studies was provided by the Australian Research Grants Committee. The award of a Commonwealth Postgraduate

Scholarship is gratefully acknowledged.

ROBERT EVANS

18th February, 1976.

PUBLICATIONS

1. The Preparation of Aqueous Entropically Stabilized Latices.
   Evans,R., Davison,J.B. and Napper,D.H., J. Polymer Sci., B10, 449 (1972).

2. Steric Stabilization I - Comparison of Theories with Experiment.
   Evans,R. and Napper,D.H., Kolloid-Z-Z. Polym., 251, 409 (1973).

3. Steric Stabilization II - A Generalization of Fischer's Solvency Theory.
   Evans,R. and Napper,D.H., Kolloid-Z-Z. Polym., 251, 329 (1973).

4. On the Calculation of Van der Waals Attraction Between Latex Particles.
   Evans,R. and Napper,D.H., J. Colloid and Interface Sci., 45, 138 (1973).

5. Flocculation of Latices by Low Molecular Weight Polymers.
   Evans,R. and Napper,D.H., Nature, 246, 34 (1973).

6. Enhanced Steric Stabilization.
   Dobbie,J.W., Evans,R., Gibson,D.V., Smitham,J.B. and Napper,D.H.,
   J. Colloid and Interface Sci., 45, 557 (1973).

7. Analytical Theories of the Steric Stabilization of Colloidal Dispersions.
   Smitham,J.B., Evans,R. and Napper,D.H., Trans. Faraday Soc., 71, 285 (1975).

8. The Chemical Reactivities of Macromolecules Attached to an Interface.
   Went,P.M., Evans,R. and Napper,D.H., J. Polymer Sci., 49, 159 (1975).

9. A Correlation Between Critical Flocculation Pressures and Theta-Pressures.
   Evans,R., Napper,D.H. and Ewald,A.H., J. Colloid and Interface Sci., 51,
   552 (1975).

10. Enthalpic Stabilization in Non-aqueous Media.
    Evans,R. and Napper,D.H., J. Colloid and Interface Sci., 52, 260 (1975).

11. Theoretical Prediction of the Elastic Contribution to Steric Stabilization. Evans,R., Smitham,J.B. and Napper,D.H., Kolloid-Z-Z. Polym., accepted for publication (1975).

ABBREVIATIONS FOR POLYMERS

PAA	poly(acrylic acid)
PAAm	polyacrylamide
PAN	polyacrylonitrile
PDMS	polydimethylsiloxane
PE	polyethylene
PEO	poly(ethylene oxide)
PHS	poly(12-hydroxystearate)
PIB	polyisobutylene
PMAA	poly(methacrylic acid)
PMMA	poly(methyl methacrylate)
PPO	poly(propylene oxide)
PVA	poly(vinyl acetate)
PVOH	poly(vinyl alcohol)
PVP	polyvinylpyrrolidone
PLMA	poly(lauryl methacrylate)

CONTENTS

CHAPTER I

STERIC STABILIZATION

GLOSSARY OF SYMBOLS FOR CHAPTER I

(excluding appendices)

A	area per particle at slip-plane of close-packed monodisperse latex
a	particle radius
d_0	surface separation of spheres along line of centres
F	force along line of centres
F_N	normal component of force
ΔG_M	free energy of mixing
ΔG_M^E	excess free energy of mixing per unit area
ΔG_{os}	osmotic free energy of interaction per unit area for two uncharged sterically stabilized flat plates
ΔG_{os}^u	ΔG_{os} for uniform segment density model
ΔG_{el}	elastic free energy of interaction per unit area for two sterically stabilized flat plates
ΔG_{el}^R	ΔG_{el} for random flight model
ΔG_{el}^u	ΔG_{el} for uniform segment density model
ΔG_{el}^G	ΔG_{el} for Gaussian model
ΔG_T	total free energy of interaction per unit area for two sterically stabilized flat plates
ΔH_M^E	excess enthalpy of mixing per unit area
k	Boltzmann constant
L	measured barrier layer thickness
L'	contour length of polymer chain
ℓ	length of polymer segment

$\langle M \rangle$	average polymer molecular weight
$\langle M_n \rangle$	number-average polymer molecular weight
$\langle M_w \rangle$	weight-average polymer molecular weight
N_A	Avagadro's number
n_s	number of segments per polymer chain
n_1	number of solvent molecules
n_2	number of polymer molecules
P_T	total disjoining pressure of sterically stabilized latex
P_{os}	excess osmotic pressure in an uncharged sterically stabilized latex
P_{el}	elastic pressure in a sterically stabilized latex
P_A	van der Waals attraction pressure in a latex
P_T^u	P_T for uniform segment density model
P_{os}^u	P_{os} for uniform segment density model
P_{el}^u	P_{el} for uniform segment density model
R	gas constant
R_{el}	elastic interaction parameter for sterically stabilized flat plates
R_{el}^u	R_{el} for uniform segment density model
R_{el}^G	R_{el} for Gaussian model
R_{el}^R	R_{el} for random flight model
R_{el}^A	quadratic approximation for R_{el}
$\langle r^2 \rangle_0^{\frac{1}{2}}$	unperturbed r.m.s. end-to-end distance of polymer chain
$\langle r^2 \rangle^{\frac{1}{2}}$	r.m.s. end-to-end distance of polymer chain ($= \alpha \langle r^2 \rangle_0^{\frac{1}{2}}$)
S_{el}	elastic interaction parameter for sterically stabilized spheres

S_{el}^{u}	S_{el} for uniform segment density model
S_{el}^{G}	S_{el} for Gaussian model
S_{el}^{R}	S_{el} for random flight model
S_{el}^{A}	S_{el} quadratic approximation for S_{el}
ΔS_{M}^{E}	excess entropy of mixing per unit area
ΔS_{el}	elastic entropy of compression of an adsorbed chain between two flat plates
ΔS_{el}^{u}	ΔS_{el} for uniform segment density model
ΔS_{el}^{G}	ΔS_{el} for Gaussian model
T	absolute temperature
V	volume after deformation
V_0	volume before deformation
V_1	volume of solvent molecule
$\bar{V}_1$	molar volume of solvent
V_2	volume of polymer molecule
$\bar{V}_2$	molar volume of polymer
V_s	volume of polymer segment
v_2	volume fraction of polymer in solution
v_{sp}	specific volume of polymer
v_x	volume fraction of polymer in adsorbed layer at a distance x from the adsorbing surface
$\bar{v}$	mean volume fraction of polymer in adsorbed layer
$\hat{v}_d$	normalised volume fraction distribution on one coated flat plate with a second plate at distance d.

$\hat{v}_{d'}$	mirror image of $\hat{v}_d$ on second plate
$\hat{v}_\infty$	$\hat{v}_d$ for $d \to \infty$
ΔV_{os}^u	osmotic free energy of interaction for two uncharged sterically stabilized particles (uniform segment density model)
ΔV_{el}^R	elastic free energy of interaction for two sterically stabilized particles (random flight model)
ΔV_{el}^u	elastic free energy of interaction for two sterically stabilized particles (uniform segment density model)
ΔV_T	total free energy of interaction for two sterically stabilized particles
α	intramolecular expansion factor
δ	reduced distance of separation of coated flat plates (= d/L)
δ_0	reduced distance of separation of coated spheres (= d_0/L)
$\delta_{x,y,z}$	ratios of the dimensions of a volume element after deformation to those before deformation
δ_{yz}	ratio of the dimensions of a volume element parallel to an adsorbing surface (= $\delta_y = \delta_z$)
Θ	theta or Flory temperature
κ_1	enthalpy of dilution parameter at infinite dilution
μ_1^E	relative excess chemical potential of solvent
ν	number of adsorbed polymer chains per unit area of one surface
ξ	extension parameter for adsorbed polymer chains (= $L/\langle r^2 \rangle^{\frac{1}{2}}$)
π^E	excess osmotic pressure
$\hat{\rho}_d$	normalized segment density distribution of adsorbed polymer on a flat plate with a second plate at distance d

$\hat{\rho}_{d'}$	mirror image of $\hat{\rho}_d$ on second plate
$\hat{\rho}_\infty$	$\hat{\rho}_d$ when $d \to \infty$
τ	tetrahedral angle ($= \cos^{-1}(-1/3)$)
ϕ_0	apparent maximum volume fraction of core particles when $d = 0$
ϕ_p	theoretical volume fraction of core particles
ϕ_{pm}	measured volume fraction of core particles
χ	reduced residual chemical potential of solvent or exchange free energy parameter
χ_1	χ in the limit of infinite dilution
χ_2	initial slope of χ versus polymer concentration plot
χ_i	coefficients of power series expansion of χ in terms of polymer concentration ($i = 1,2,3 \ldots.$)
χ'	exchange free energy parameter
χ'_i	coefficients of power series expansion of χ' in terms of polymer concentration ($i = 1,2,3 \ldots.$)
ψ_1	entropy of dilution parameter at infinite dilution
ω	weight of adsorbed polymer per unit area

1. INTRODUCTION

One of the most significant experimental observations to be made in the field of steric stabilization is that the limit of stability correlates, in general, with the Θ-point for the stabilizing macromolecules in free solution (1-5). Exceptions have been noted (6) but these are usually associated with extremes in experimental conditions (e.g., poor anchoring, multipoint anchoring), which will be discussed in more detail in the following section.

The general thermodynamic conditions relating to the point of incipient instability of a latex have been presented by Napper (7) and can be illustrated using a stability diagram (Fig.1). In a later chapter we shall use a similar diagram to indicate the influence of pressure on a latex. Note that all temperature changes can be represented by transition parallel to the entropy axis and that the enthalpy axis is an impassable barrier (T = 0 K). A latex which is entropically stabilized or combined entropically/enthalpically stabilized cannot be made enthalpically stabilized (or vice versa) unless ΔH and ΔS are changed (e.g., by changing the solvent medium (8)).

We may introduce the close correlation between the Θ-point and the critical flocculation point by placing

$$\Delta H_M^E \simeq \Delta H$$

and

$$\Delta S_M^E \simeq \Delta S$$

in Fig.1, where ΔH_M^E and ΔS_M^E are the excess enthalpy and entropy of mixing

Fig.1. Stability diagram for sterically stabilized dispersions - methods of thermal flocculation. Distance from the $\Delta G = 0$ line is exaggerated for reasons of clarity.

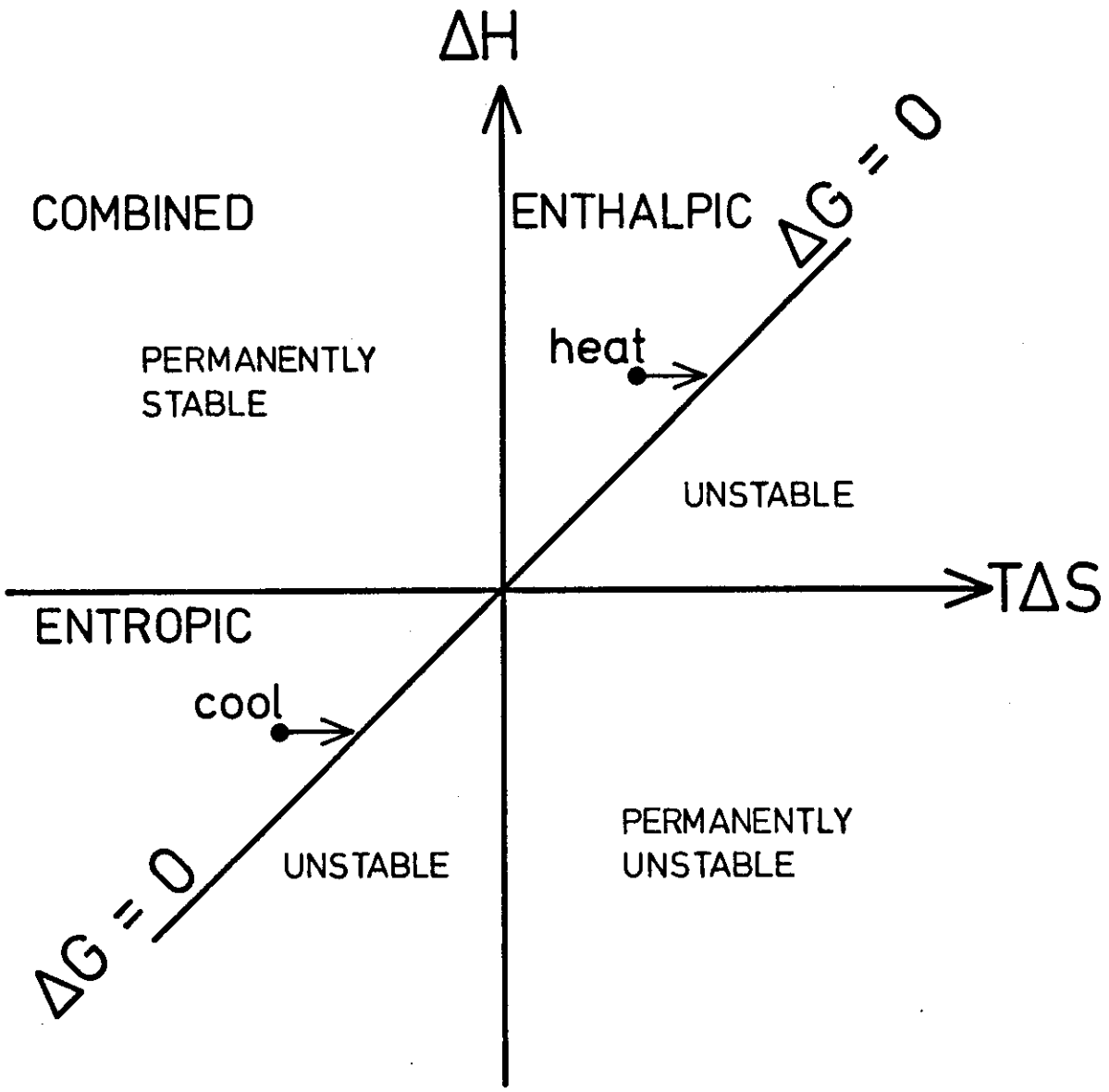
ΔH
COMBINED
ENTHALPIC
ΔG = 0
PERMANENTLY
STABLE
heat
UNSTABLE
TΔS
ENTROPIC
cool
ΔG = 0
UNSTABLE
PERMANENTLY
UNSTABLE

free stabilizer polymer with solvent medium (but only include second and perhaps third virial coefficients). Essentially, we are saying that all other contributions play a relatively small part in determining the point of incipient instability of a sterically stabilized latex. Obvious exceptions include (i) elastically stabilized latices (9,10) for which ΔH_M^E and ΔS_M^E are negligible compared with the configurational entropy change of the stabilizer and (ii) charged particles, which could remain stable in aqueous media of low ionic strength even when the interpenetration of adsorbed polymers is favourable.

In theory, we are concerned with uncharged particles stabilized by non-ionic macromolecules; consequently we may ignore electrostatic effects. In practice, electostatic contributions are likely to be small in non-aqueous media and in aqueous media of high ionic strength. Generally, studies of the flocculation behaviour of sterically stabilized dispersions in aqueous media require ionic strengths of the order of 1 (11), which is more than sufficient to negate any electrostatic effects due to charged particles or ionic stabilizers. We feel justified, therefore, in ignoring these effects for the majority of cases.

To begin this chapter, we discuss the development of previous theories and compare them with published experimental results. After enumerating some of the inadequacies of these theories, we develop a more general theory which allows, in part, for the concentration dependence of the interaction parameter. In addition, we present a simple means of estimating the elastic interaction between sterically stabilized particles for the case of uniform stabilizer density. The derivation of this elastic effect is not intended to be rigorous,

but gives similar results to those obtained by random walk statistics, which often require extensive numerical calculations (12,13).

After extending the theory to spheres, using the Derjaguin approximation (14), we present a general method for calculating the excess pressure of a stable concentrated latex in terms of the volume fraction of core particles or the particle separation. The theory will be compared with some experimental results (from the literature), which describe the distance dependence of the steric interaction. As will be shown, the experimental systems studied in the literature are far from being ideal model systems. This makes comparison with theory very difficult. All numerical calculations will be performed using the uniform segment density model described in the text so as not to intrude on a subsequent thesis by Smitham that will discuss other distribution functions (e.g., Gaussian, exponential). Finally, we shall demonstrate that our theory predicts the experimentally observed correlation between the point of incipient instability of sterically stabilized latices and the Θ-point for the stabilizer in free solution.

As steric stabilization theory is based mainly on the theory of polymer solutions, we also looked at the possibility of using a "state of the art" polymer solution theory such as Flory's free volume theory (FVT). The results of this investigation will be discussed in appendix 1.1.

2. COMPARISON OF PREVIOUS THEORIES WITH EXPERIMENT

There have been many attempts (e.g.,11,12,15-27) in the past quarter century to formulate qualitative and, more recently, quantitative theories of steric stabilization. It has been shown (6) that the "entropy theories" (e.g., 16,18,19-23) suffer from the serious neglect of solvency contributions. Recent experimental studies (1-5) on model sterically stabilized latices show that the solvency of the dispersion medium critically determines their stability. Neglect of the dispersion medium leads to the erroneous conclusion that all sterically stabilized dispersions are stable solely by virtue of the configurational entropy of the adsorbed polymer chains. Fischer (17), in 1958, was the first to acknowledge the importance of solvency. His stability theory is based upon the generation of an excess osmotic pressure caused by an increase in stabilizer concentration in the interaction zone. The resulting solvent diffusion gradient opposes this increase in concentration, thereby resisting the approach of the particles. A uniform segment density in each stabilizer sheath is assumed.

Meier (12) and Hesselink et al (13,28,29) have derived segment density distribution functions for adsorbed "tails" and "loops" at planar interfaces and have calculated the configurational entropic repulsion between opposing pairs of such interfaces. Meier's calculations are incorrect owing to the inclusion of certain forbidden conformations in his segment density distributions. Both authors have combined this entropy of repulsion with a solvency term based on Fischer's result but using their calculated segment densities. However, in spite of this seemingly great improvement in the quantitative accuracy of the theory, the Hesselink, Vrij and Overbeek (HVO) formulation (13)

is at odds with the experimental evidence (1-5,30,31). Moreover, while Fischer's model behaves at least qualitatively in accordance with experiment, the HVO model seems to fail even at this level. Before going into possible reasons for this disagreement, the predictions of the above proposed theories will be compared with available experimental results.

In essence, Fischer's theory states that the free energy of repulsion ΔG_R between sterically stabilized particles is directly proportional to the second virial coefficient (A_2) of the polymer in free solution:

$$\Delta G_R \propto A_2$$

Qualitatively, this theory predicts (i) that instability should be evident in solvents worse than Θ-solvents (since A_2 becomes negative), (ii) that the point of incipient flocculation should occur close to the Θ-point where $A_2 = 0$ and (iii) that no marked dependence of the incipient flocculation point upon the molecular weight of the stabilizer or the particle radius should be observed. All of these qualitative predictions have been confirmed by experiment (1-5,30, 31).

The corresponding predictions of the HVO theory are represented in Fig.2 (13). Incipient flocculation lines,above which the dispersions are stable, are calculated for dispersions of flat plates stabilized by tails. Similar results are expected for loops. If the Derjaguin method (14) is used to calculate the repulsion for spheres from the repulsion for flat plates, qualitatively similar findings regarding stability are evident (32). The intramolecular expansion factor α is represented on the abscissa in Fig.2. This is a measure of the quality of solvency of the dispersion medium for the stabilizing macromolecules.

Fig.2. Lines of demarcation between stable and unstable dispersions of flat plates according to the HVO theory. M is the molecular weight of the adsorbed tails, α is the intramolecular expansion factor (α = 1.00 at the Θ-point).

Lines: (1) square particles of side 200 nm ,

(2) square particles of side 100 nm .

Amount of adsorbed polymer = 2×10^{-8} g cm^{-2}

Hamaker constant = 10×10^{-21} J.

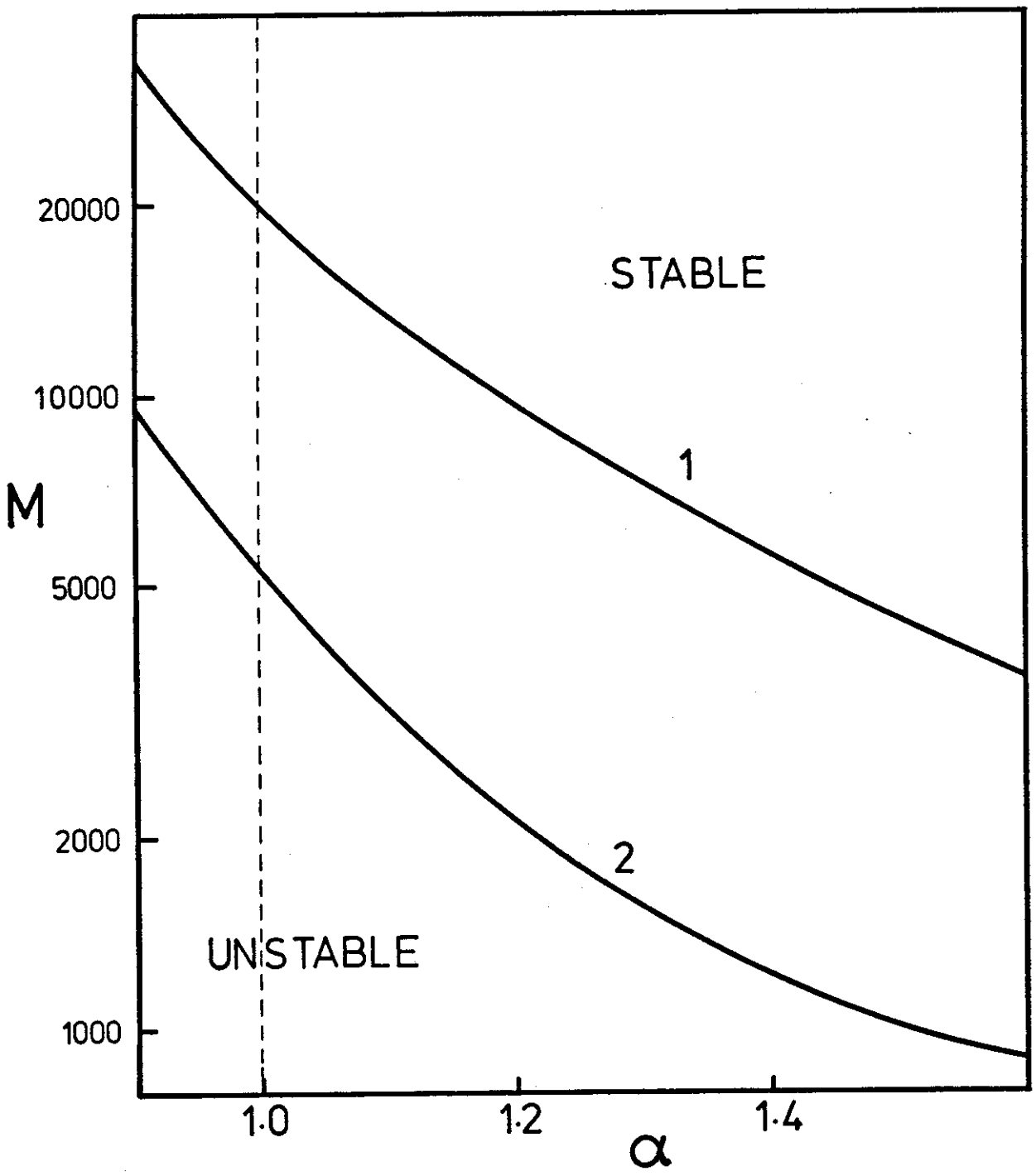
20000
10000
5000
2000
1000
M
STABLE
1
2
UNSTABLE
1·0
1·2
1·4
α

TABLE 1

Molecular Weight Dependence of the Critical Flocculation Temperature (6)

Stabilizing Moiety	<M>	Cft/K	Θ/K
PEO	1.0×10^6	317 ± 2	315 ± 3
PEO	8.0×10^5	316	316
PEO	3.2×10^5	315	314
PEO	9.6×10^4	316	315
PEO	4.9×10^4	316	314
PEO	2.3×10^4	314	315
PEO	1.0×10^4	318	319
PAA	9.8×10^3	287 ± 2	287 ± 5
PAA	1.9×10^4	289	287
PAA	5.2×10^4	283	287
PAA	9.0×10^4	281	287

Results for PEO are from ref.2 and those for PAA are from ref.5.

The following comparisons of the predictions of the HVO theory (13) with experiment may be made:

i) Stability is predicted in solvents worse than Θ-solvents ($\alpha < 1.00$). There is no special significance placed on the points corresponding to $\alpha = 1.00$ (i.e., the Θ-point). Table 1 displays some typical experimental results which show that the Θ-point corresponds closely to the limit of stability of sterically stabilized dispersions. Over forty different critical flocculation points (cfp's) have been shown to correlate with the corresponding Θ-points for the stabilizing macromolecules in free solution (1-5,30,31). The same conclusion is reached whether flocculation is induced by addition of non-solvent, by heating or cooling the latices or by applying pressure (see chapter on high pressure studies). This correlation is not apparent in Fig. 2.

ii) The HVO theory implies that the cfp is strongly dependent on the molecular weight (M) of the stabilizer (Fig. 2). We have shown (6) that, according to the HVO theory, two latices stabilized by polymer chains which differ in molecular weight by a factor of ten should differ in their cfp's by ~ 100 K. Again, we see from Table 1 that this prediction is not substantiated by experiment. The critical flocculation temperatures (cft's) of the latices stabilized by poly(ethylene oxide) (PEO) were achieved by heating; the cft's of the latices stabilized by poly(acrylic acid) (PAA) (5) were achieved by cooling. Note that the molecular weight of the PEO varies over three decades and that of the PAA varies over one decade. Cft variations are at least an order of magnitude less than those predicted by

the HVO theory. The molecular weight dependence of the cfp observed by Heller (33,34) and Molau (35-37) has been explained in terms of desorption or lateral movement of stabilizer in the interaction zone (6). Such effects are expressly forbidden by the HVO model which requires the stabilizer to be irreversibly anchored to the particle surface. Heller (34) found that electrostatically stabilized dispersions which were additionally stabilized by unanchored PEO could be flocculated by, e.g.,0.5 M KCl at 20 C. We have confirmed this observation and repeated the experiment using anchored PEO of similar molecular weight. The latices stabilized by anchored PEO are stable in 0.5 M KCl and, in fact, stable in 3.0 M KCl, which is a much worse solvent for PEO. HVO have suggested (13) that the observed insensitivity to molecular weight may be due, in part, to extra adsorption of the PEO segments. This would decrease the nominal molecular weight. Apart from the arguments against this possibility proposed in ref.6 it seems highly unlikely that polymer molecules with molecular weights ranging from 10^4 to 10^6 would automatically adsorb to give loops of such a constant molecular weight that the cft corresponds with the Θ-point for the polymer in free solution. Indeed, the extension data is against this proposal (38). This process would have to allow automatically for particle size and surface concentration of polymer.

iii) The HVO theory predicts stability to be possible in solvents considerably worse than Θ-solvents. Moreover, they assume that the stabilizer has the same solution properties whether or not it is adsorbed (i.e., their stability curves are constructed using the free solution properties). For the purposes of the model this is not unreasonable. However, the only

instances which have been recorded in which sterically stabilized latices were shown to be stable in worse solvents than Θ-solvents can be explained in terms of "enhanced" steric stabilization (39). We have observed that stabilizer molecules, even when anchored at a sufficient number of points along the chain, cease to exhibit the free solution properties. It is then no longer valid to compare the cfp with the Θ-point in free solution.

iv) The HVO theory predicts that the stability of latices should be inversely proportional to the particle radius in Derjaguin's approximation. Our results show that the cfp's of aqueous and non-aqueous latices are relatively insensitive to the particle radius (1,2,5).

So far we have seen that the entropy theories proposed by Mackor and van der Waals (15,16), Jäckel (18) and Clayfield and Lumb (19-23) fail as general theories because they ignore the effect of the solvent medium completely. We found that Fischer's solvency theory (17) is in qualitative agreement with experiment but it cannot be used for situations in which the particles are separated by distances less than the barrier layer thickness (compression region). This theory also disregards virial coefficients higher than the second and represents the stabilizer segment density distribution as a step function; thus the quantitative aspects of the theory are in doubt. Finally, we have seen that the hybrid entropy plus solvency theory of Meier (12) and Hesselink (13,28, 29) fails to predict the stability properties of model latices (1-5,30,31).

We will now examine the more recent solvency theories (24-27,40,41). Basically, they all state that the free energy of repulsion is zero at the Θ-

point because only excess mixing terms are considered. The belief that the entropic volume restriction or elastic contribution is unimportant relative to the mixing or osmotic contibution is supported by the conclusions of Doroszkowski and Lambourne (40) whose experiments on steric barriers are explained best by models which ignore volume restriction. Ottewill and Walker (24) have interpreted Fischer's model (17) in terms of dilute polymer solution theory (42). Doroszkowski and Lambourne (40) allow relaxation of segments away from the lens-shaped interaction zone, as does Bagchi (25). Napper, Evans and Smitham (27,41) use an interpenetration and compression model applied to uniform, Gaussian and Hesselink-type segment density distribution functions.

The only osmotic theory which does not predict a close correlation between the cfp and the Θ-point is that of Bagchi (25,26), although the author states expressly that these points coincide. His error lies in an improper "improvement" in the formulation of the free energy of mixing in the interaction zone. In the past, the concentration dependence of both the entropy and enthalpy of mixing has been ignored. Bagchi has included the full concentration dependent entopy term from the lattice theory (42) but has ignored the concentration dependence of the enthalpy. Inclusion of one without the other results in the destruction of the correlation between the cfp and the Θ-point.

Recently, Dolan and Edwards (43,44) have developed a novel theory of steric stabilization which incorporates both elastic and osmotic contributions in a single model. They treat the entire problem as one of configurational repulsion. The presence of the solvent is accounted for indirectly by assigning a thermodynamic excluded volume to the polymer. The number of possible

configurations of the adsorbed polymer chains is reduced by: i) the excluded volume of the polymer on the surface considered; ii) the excluded volume of the polymer on the surface of the second approaching particle; iii) the surface of the second approaching particle.

By using a self-consistent field approach, which was originated by Hartree (45) and adapted by Edwards (46), allowance can be made for the change in configuration of the adsorbed polymer due to the excluded volume effect. The self-consistent field approach involves extensive iterative computations and the problem cannot as yet be solved analytically. Basically, the method consists of replacing the required segment density distribution by a self-consistent potential field and solving the random walk problem in the presence of this field. The field itself is the solution to this random walk problem. For a general treatment of the self-consistent field approach to the excluded volume effect, see Yamakawa (47).

Unfortunately, the complete theory of steric stabilization, as proposed by Dolan and Edwards (44), is analytically intractable. Nevertheless, such a theory is necessary if only to compare it with the entropy plus solvency theories. Shortcomings of the theory include the neglect of the concentration dependence of the interaction parameter χ (42) (embodied in their excluded volume parameter $u \propto (\frac{1}{2} - \chi_1)$) and its present inability to account for negative excluded volumes (i.e., $\chi_1 < \frac{1}{2}$). Until the theory is extended to negative values of u, no reliable predictions can be made concerning the cfp of sterically stabilized particles.

Approximations for the excluded volume effect have been presented by Dolan and Edwards (44) but these offer no advantage over the Flory-Krigbaum type mixing effect. In fact, the best approximation to the complete solution is probably that given by the usual entropy plus solvency theories.

One final point to note is that when the excluded volume is zero (i.e., at the Θ-point) the results of Dolan and Edwards coincide with those of Hesselink et al for random flight chains. Dolan and Edwards have derived very useful approximations for the configurational entropy of confined adsorbed random flight chains (43) and we shall have occasion to use their results in the section on elastic repulsion.

3. BARRIER LAYER THICKNESS AND PARTICLE SIZE IN MODEL LATICES

The comparison of theory with experiment requires that the latices conform to the specifications of a single model. A general theory that describes the behaviour of all possible types of latex has not been formulated. In the meantime a series of theoretical models that, hopefully, approximate to the real latices must be postulated. The comparative dearth of experimental results available at present indicates that many of the models so far suggested in the literature have not been tested satisfactorily for validity.

The most popular models in use (13,24,25,40,41,48) all rely upon polymer solution theory and statistical thermodynamics, all assume irreversible stabilizer adsorption and all neglect the effects of bound charges. Despite their apparent similarity, they yield not only quantitatively different but also qualitatively different predictions. It appears that, in part, the disagreement is a consequence of the approximations made on the basis of a single parameter. This parameter is the ratio of the barrier layer thickness L to the particle radius a. Apart from a mention of enhanced steric stabilization, the following discussion applies only to stabilizers which do not interact specifically with the particle surface except through the anchor polymer.

i) $a \ll L$

Under these conditions, the adsorbed polymer is essentially unperturbed by the presence of the particle. We have, in effect, a very large polymer molecule in free solution with a small particle imbedded in the centre.

The particle creates a "super" polymer molecule by adsorbing several stabilizer polymer molecules, thus reducing the translational entropy of the polymer. During collisions, the particles present small cross-sections to the approaching polymer chains. Configurational changes should therefore be small and the elastic or volume restriction effect (12) negligible. In any case, before the elastic effect can begin to operate, so much stabilizer would have interpenetrated that solution thermodynamics easily determines stability. In fact, the flocculation process would be very similar to that of phase separation of "infinite" molecular weight polymer (27).

ii) $a \sim L$

The polymer is perturbed by the particle and must extend into the solvent medium in order to partially regain lost configurational entropy resulting from the loss of available space (53). Under these conditions we expect that stability is still determined by the solution properties of the polymer which, according to the lattice model (42), are reasonably independent of the configuration of the polymer as long as it remains constant (49). In highly concentrated latices (50-52), when the external pressure is made to overcome this thermodynamic contribution, the elastic effect can become important. All latices are expected to resist compression at some stage, even when flocculated, because of the elastic effect, which is relatively insensitive to solvency conditions. The high curvature of the particles also reduces the elastic effect with regard to stability in uncompressed latices (40). In a flocculated latex, the elastic and thermodynamic(or osmotic)effects tend to balance when the particles are separated by a certain equilibrium distance at which the

interaction energy is a minimum. If a flocculated latex were so concentrated that the average interparticle distance were significantly less than this equilibrium distance, then the latex would appear to be stable. For example, a latex of particle radius 100 nm and with a stabilizer layer of thickness 30 nm would probably resist compression to much less than a volume corresponding to an interparticle separation of ~30 nm, even when the segment mixing term is favourable. The elastic effect, as we shall see, becomes dominant fairly soon after the particles start to compress the adsorbate. For the above latex, apparent stability should be observed at core particle volume fractions greater than ~0.5 since there is no opportunity for the particles to form preferential contacts. The result would presumably be a gel-like latex such as that observed by Cairns and Ottewill (50). Similarly, electrostatically stabilized dispersions, which are stable, can be flocculated at high concentrations because the electrostatic potential barrier is overcome by the confining boundary of the latex. Thus the term "stability" is used in the present context to describe the resistance to spontaneous aggregation in dilute latices.

iii) $a \gg L$ (including flat plates)

Elastic repulsion may significantly contribute to stability in this extreme case. The configuration of the stabilizer polymer may be sufficiently perturbed by the particle to render free solution thermodynamics inapplicable to the adsorbed polymer, unless the stabilizer chains are long. The reason for this stipulation is that short polymer chains have been found to be much more affected by adsorption than long chains; experimental

results (e.g.,54,55) indicate that short chains can be almost fully extended when adsorbed at one end. Terminal adsorption of (uncharged) long chains could not reasonably be expected to result in such an unfavourable configuration. For example, if we consider a freely jointed chain of n segments, each of length ℓ, the one-dimensional root-mean-square end-to-end distance is $\ell(n/3)^{\frac{1}{2}}$ (42). Suppose that adsorption changes this dimension by a factor ξ normal to the interface. The absolute change is $\ell(n/3)^{\frac{1}{2}}(\xi - 1)$ and the change measured in units of the contour length ($n\ell$) is $(\xi - 1)(3n)^{-\frac{1}{2}}$. This last expression can be considered a measure of the perturbation caused by extension. Monte Carlo calculations (56) indicate that ξ is insensitive to chain length. According to these simple calculations, we would expect the perturbation to increase with decreasing chain length. By using very large particles or flat plates, therefore, we could have long adsorbed chains and still have $a >> L$. The chains would be only slightly perturbed so that free solution thermodynamics should give a reasonable guide to the behaviour of the stabilizer (and latex). More often, the particles would be of average size (~100 nm) and, in order to satisfy the condition that $a >> L$, the stabilizer would have to be in the form of short tails and/or loops. Long chains may be transformed to short loops by multipoint anchoring, which could result in enhanced steric stabilization (39). In fact, enhanced steric stabilization may be partially attributable to the intervention of the elastic effect. Large particle/short chain latices would be expected to exhibit stability in worse than Θ-solvents if the tendency for the stabilizer to overlap is overcome by the configurational entropy loss before sufficient segment-segment contacts are made to ensure

flocculation. Finally, if the stabilizer layer is very thin, van der Waals attraction may cause flocculation regardless of the properties of the adsorbed layer.

Variation of the ratio a/L in experimental model latices would be expected to yield results which supported the solvency theories (Fischer, Napper and Evans, Bagchi, Doroszkowski and Lambourne, Ottewill and Walker) when a/L is not too large, and the solvency plus entropy theories (Meier, Hesselink) when a/L is very large and L is small (short chains).

In the following sections we shall develop a theory of steric stabilization which allows for the concentration dependence of both the entropy and enthalpy of mixing.

4. A GENERAL THEORY WHICH ALLOWS FOR THE CONCENTRATION DEPENDENCE OF χ

The excess free energy of dissolution of stabilizer polymer in the solvent medium can be obtained by a straightforward application of Flory's theory for concentrated polymer solutions (42), modified to allow for the concentration dependence of the interaction parameter. Approach of the coated particles during Brownian collisions results in changes in stabilizer concentration and the concomitant free energy changes contribute to the total interaction potential between the particles.

We make the assumption that the osmotic and elastic or configurational effects are separable. At present, alternative assumptions (44) lead to non-analytical solutions, as in the self-consistent field approach of Dolan and Edwards (43,44,46).

4.1. Free Energy of Mixing Adsorbed Polymer and Solvent

According to the original lattice theory (42), the free energy of mixing n_2 polymer molecules with n_1 solvent molecules is given by

$$\Delta G_M = kT(n_1 \ln v_1 + n_2 \ln v_2 + \chi' n_1 v_2) \qquad \{1\}$$

where v_1 and v_2 are the volume fractions of solvent and polymer in the mixture and χ' is the contact exchange free energy parameter for the particular system considered. Our use of this expression will be confined to calculations involving adsorbed polymer. The second term within the brackets of eq.{1} arises from the entropy associated with the number of ways of distributing the centres of gravity of the polymer molecules over the volume of the mixture

compared with distributing them over the volume of the pure polymer. Since the average configuration of the macromolecules is overwhelmingly dominant, we can neglect all others in our entropy calculations (57). The position of the centre of gravity of a polymer molecule attached to an interface may be assumed fixed at the average position under a given set of equilibrium conditions. Only one arrangement is possible for fixed points, therefore the ideal entropy of attached polymers is $\ln 1 = 0$.

The excess free energy of mixing attached polymers with solvent is

$$\Delta G_M^E = kT\, n_1\{\ln(1 - v_2) + \chi' v_2\} \qquad \{2\}$$

$$= kT \frac{V}{V_1}(1 - v_2)\{\ln(1 - v_2) + \chi' v_2\} \qquad \{3\}$$

where $n_1 = \frac{Vv_1}{V_1}$

$v_1 = (1 - v_2)$

V_1 = volume of solvent molecule

V = volume of solution .

This equation holds only for uniform v_2. In general, v_2 depends on position in V; the free energy of mixing must be found by summing over all volume elements small enough to contain a uniform local segment density:

$$\delta(\Delta G_M^E) = \frac{kT}{V_1}(1 - v_2)\{\ln(1 - v_2) + \chi' v_2\}\delta V \quad . \qquad \{4\}$$

Differentiation of this expression with respect to n_1 and multiplication by Avogadro's number yields the excess chemical potential of the solvent:

$$\mu_1^E = RT\{\ln(1 - v_2) + v_2 + \chi v_2^2\} \quad . \qquad \{5\}$$

χ is an exchange free energy parameter not necessarily equal to χ' unless they are independent of v_2. Originally (42), χ and χ' were assumed to be independent of concentration. This assumption is still made by workers in the field of steric stabilization (e.g.,12,13,24-27,44), although it is well established that χ and χ' depend strongly on concentration for the majority of systems (49).

χ is often expressed (e.g.,58) as a power series in v:

$$\chi = \chi_1 + \chi_2 v_2 + \chi_3 v_2^2 + \ldots . \qquad 6\}$$

To allow for differentiation, Koningsveld et al (58,59) have shown that if χ' is given by

$$\chi' = \chi_1' + \chi_2' v_2 + \chi_3' v_2^2 + \ldots . \qquad \{7\}$$

the coefficients are related by

$$\chi_i = i(\chi_i' - \chi_{i+1}') \quad , \qquad \{8\}$$

where i is an integer greater than zero. Summing on both sides we have

$$\sum_{i=1}^{\infty} \frac{\chi_i}{i} = \sum_{i=1}^{\infty} \chi_i' - \sum_{i=1}^{\infty} \chi_{i+1}'$$

$$= \chi_1' \quad .$$

Similarly,

$$\chi_2' = \sum_{i=2}^{\infty} \frac{\chi_i}{i} \quad ,$$

$$\chi_3' = \sum_{i=3}^{\infty} \frac{\chi_i}{i} \qquad \text{etc.}$$

In general,

$$\chi'_j = \sum_{i=j}^{\infty} \frac{\chi_i}{i} \quad . \qquad \{9\}$$

Therefore

$$\chi' v_2 = v_2 \sum_{i=1}^{\infty} \frac{\chi_i}{i} + v_2^2 \sum_{i=2}^{\infty} \frac{\chi_i}{i} + v_2^3 \sum_{i=3}^{\infty} \frac{\chi_i}{i} + \ldots .$$

$$= \sum_{j=1}^{\infty} v_2^j \sum_{i=j}^{\infty} \frac{\chi_i}{i} \quad . \qquad \{10\}$$

As a power series in v_2,

$$\ln(1 - v_2) = - \sum_{j=1}^{\infty} \frac{v_2^j}{j} \qquad \{11\}$$

Substituting eqs.{10} and {11} into eq.{4} we find the free energy of mixing in the volume element as a power series in v_2:

$$\delta(\Delta G_M^E) = \frac{kT}{V_1} (1 - v_2) \sum_{j=1}^{\infty} v_2^j \left(\sum_{i=j}^{\infty} \frac{\chi_i}{i} - \frac{1}{j} \right) \delta V$$

$$= \frac{kT}{V_1} \sum_{i=1}^{\infty} \frac{v_2^{i+1}}{i} \left(\frac{1}{i+1} - \chi_i \right) \delta V - \frac{kT}{V_1} v_2 \left(1 - \sum_{i=1}^{\infty} \frac{\chi_i}{i} \right) \delta V \quad . \qquad \{12\}$$

Summing over all volume elements, we arrive at the total free energy of mixing in the adsorbed layer:

$$\Delta G_M^E = \frac{kT}{V_1} \sum_{i=1}^{\infty} \frac{1}{i} \left(\frac{1}{i+1} - \chi_i \right) \int_0^{\infty} v_2^{i+1} dV - \frac{kT}{V_1} \left(1 - \sum_{i=1}^{\infty} \frac{\chi_i}{i} \right) \int_0^{\infty} v_2 dV \qquad \{13\}$$

It is general practice (e.g.,13,44) to assume that the surface coverage of polymer is high enough to make the segment density uniform in any surface parallel to the adsorbing surface. v_2 depends only on the direction normal to the surface (denoted the x-direction). Therefore, the free energy of dissolution per unit area is

$$\Delta G_M^E = \frac{kT}{V_1} \sum_{i=1}^{\infty} \frac{1}{i} \left(\frac{1}{i+1} - \chi_i\right) \int_0^{\infty} v_x^{i+1} dx - \frac{kT}{V_1}\left(1 - \sum_{i=1}^{\infty} \frac{\chi_i}{i}\right) \int_0^{\infty} v_x dx \qquad \{14\}$$

where v_x is the volume fraction of polymer at a distance x from the surface.

If $\hat{v}_\infty$ is the normalized volume fraction distribution when the second barrier is at infinite distance, $\hat{v}_d$ the corresponding distribution at separation d and $\bar{v}$ the average segment density in one adsorbed layer of experimental thickness L, we have

$$\Delta G_M^E(\infty) = \frac{2kT}{V_1} \sum_{i=1}^{\infty} (\bar{v}L)^{i+1} \frac{1}{i}\left(\frac{1}{i+1} - \chi_i\right) \int_0^{\infty} \hat{v}_\infty^{i+1} dx - \frac{2kT}{V_1} \bar{v}L\left(1 - \sum_{i=1}^{\infty} \frac{\chi_i}{i}\right), \qquad \{15\}$$

where

$$\bar{v} = \frac{\nu n_s V_s}{L},$$

ν = number of adsorbed chains per unit area of one surface

n_s = number of segments per chain

V_s = volume of one segment.

This is the normalised free energy of dissolution of adsobed polymer per unit area of <u>two</u> flat plates separated by a distance $d = \infty$. The corresponding expression for any distance d is:

$$\Delta G_M^E(d) = \frac{kT}{V_1} \sum_{i=1}^{\infty} (\bar{v}L)^{i+1} \frac{1}{i}\left(\frac{1}{i+1} - \chi_i\right) \int_0^d (\hat{v}_d + \hat{v}_{d'})^{i+1} dx - \frac{2kT}{V_1} \bar{v}L\left(1 - \sum_{i=1}^{\infty} \frac{\chi_i}{i}\right), \quad \{16\}$$

where $\hat{v}_{d'}$ is the mirror image of $\hat{v}_d$ on the second surface (12).

4.2. Mixing Term for the Interaction of Two Coated Flat Plates

The change in free energy during the approach of the two coated surfaces is

$$\Delta G_{OS} = \Delta G_M^E(d) - \Delta G_M^E(\infty) \quad , \quad \{17\}$$

where the subscript OS indicates that this is an osmotic effect. Thus

$$\Delta G_{OS} = \frac{kT}{V_1} \sum_{i=1}^{\infty} \frac{(\bar{v}L)^{i+1}}{i} \left(\frac{1}{i+1} - \chi_i\right) \left\{\int_0^d (\hat{v}_d + \hat{v}_{d'})^{i+1} dx - 2\int_0^{\infty} \hat{v}_{\infty}^{i+1} dx\right\}. \quad \{18\}$$

This free energy may be expressed in terms of normalized segment density distributions ($\hat{\rho}$) by placing

$$\hat{\rho} = \hat{v} \qquad \text{(Note: } \rho V_s = v\text{)}$$

and

$$\bar{v} = \frac{\nu n_s V_s}{L} \quad :$$

$$\Delta G_{OS} = \frac{kT}{V_1} \sum_{i=1}^{\infty} \frac{(\nu n_s V_s)^{i+1}}{i} \left(\frac{1}{i+1} - \chi_i\right) \left\{\int_0^d (\hat{\rho}_d + \hat{\rho}_{d'})^{i+1} dx - 2\int_0^{\infty} \hat{\rho}_{\infty}^{i+1} dx\right\} . \quad \{19\}$$

The first term of the series in eq.{19} is:

$$\Delta G_{OS(i=1)} = \frac{2kT}{V_1} V_s^2 n_s^2 \nu^2 (\tfrac{1}{2} - \chi_1) \{\int_0^d \hat{\rho}_d^2 dx + \int_0^d \hat{\rho}_d \hat{\rho}_{d'} dx - \int_0^\infty \hat{\rho}_\infty^2 dx\} \quad \{20\}$$

which is the equation used by Meier (12), Hesselink et al (13) and Evans and Napper (27) for the change in free energy of mixing per unit area between approaching coated plates. By including a further term we can allow, to some extent, for the concentration dependence of χ. The next term in the series is:

$$\Delta G_{OS(i=2)} = \frac{kT}{V_1} V_s^3 n_s^3 \nu^3 (\frac{1}{3} - \chi_2) \{\int_0^d \hat{\rho}_d^3 dx + \frac{3}{2} \int_0^d \hat{\rho}_d^2 \hat{\rho}_{d'} dx + \frac{3}{2} \int_0^d \hat{\rho}_d \hat{\rho}_{d'}^2 dx - \int_0^\infty \hat{\rho}_\infty^3 dx\}. \{21\}$$

Although this and higher terms have previously been neglected, it can be shown that the ratio of $G_{OS(i=2)}$ to $G_{OS(i=1)}$ is often of the order of $\bar{v}$ when the stabilizer layers overlap extensively.

4.3. Extension to Spherical Particles

The Derjaguin approximation provides a convenient method of calculating the interaction between spheres from that between flat plates (14). The great advantage of such a general procedure is its independence of the nature and distance dependence of the interaction energy. The only major disadvantage is that it can only be used with precision for particles of radius appreciably greater than the range of the interactions (which can usually be arranged experimentally). We shall use this consistent procedure in preference to the more artificial geometric approaches (e.g.,25,52) which rely heavily on the geometry of the interaction zone.

The potential energy of interaction between two identical spheres of radius a, whose surfaces are separated by the distance d_0 (measured along the line of centres), is (14):

$$\Delta V_{OS} = \pi a \int_{d_0}^{\infty} \Delta G_{OS} d(d) \quad . \qquad \{22\}$$

This is the osmotic contribution from the change in free energy of mixing. ΔG_{OS} is obtained from eq.{18}. After substitution:

$$\Delta V_{OS} = \pi a L \frac{kT}{V_1} \sum_{i=1}^{\infty} \frac{(\bar{v}L)^{i+1}}{i} \left(\frac{1}{i+1} - \chi_i\right) \int_{\delta_0}^{\infty} \{\int_0^d (\hat{v}_d + \hat{v}_{d'})^{i+1} dx - 2\int_0^{\infty} \hat{v}_{\infty}^{i+1} dx\} d(\delta) \quad , \qquad \{23\}$$

where separations of the particles are measured in units of the barrier layer thickness L ($\delta_0 = d_0/L$ and $\delta = d/L$).

As $\delta_0 \to \infty$ $\quad \hat{v}_d \to \hat{v}_{\infty}$

and $\quad \hat{v}_{d'} \to \hat{v}_{\infty}$.

To use these expressions, we must formulate the segment density or volume fraction distribution functions and find χ_i.

In these derivations, we have expanded the logarithmic entropy term and, in so doing, eliminated the significance of the point $v_2 = 1$, which is the maximum possible value of the polymer volume fraction. Under most circumstances this point will not be approached and if it is, no existing theory of steric stabilization will apply. However, for the sake of completeness, we include in appendix 1.2 a treatment of the above work which retains the logarithmic form of the entropy of mixing.

5. THE CONCENTRATION DEPENDENCE OF χ.

5.1. Theory

The solvency conditions under which the osmotic free energy of interpenetration and compression (eq.{18}) becomes zero are given by:

$$\sum_{i=1}^{\infty} \chi_i = \sum_{i=1}^{\infty} \frac{1}{i+1} \qquad \{24\}$$

The simplest set of solutions which satisfies this equation is

$$\chi_i = \frac{1}{i+1} \ . \qquad \{25\}$$

When $i = 1$ we have the familiar relationship (42)

$$\chi_1 = \tfrac{1}{2},$$

which is used to represent χ in dilute solutions at the Θ-point and is legitimate whether χ is concentration dependent or not. However, it is also common practice to use $\chi_1 = \frac{1}{2} = \chi_1'$ (eq.{1}) for dilute solutions at the Θ-point (e.g.,13,25,27). This is valid <u>only</u> when χ' and χ are independent of concentration. To be precise, in the limit of infinite dilution, at the Θ-point (eq.{9}):

$$\chi_1' = \sum_{i=1}^{\infty} \frac{\chi_i}{i} = 1 \qquad \{26\}$$

and $\chi_1' = \frac{1}{2}$ only when $\sum_{i=2}^{\infty} \frac{\chi_i}{i} = \frac{1}{2}$. The significance of this last stipulation

is that all higher powers of concentration (than the second) in the combinatorial entropy term are made to cancel with those in the enthalpy term; i.e., the third and higher virial coefficients are placed equal to zero under all conditions. It has been shown theoretically that the third virial coefficient is likely to be negligible at the Θ-point (42,60). However, its neglect in good solvents may make a significant difference to the distance dependence of the interaction between coated particles. This difference may be particularly noticable when the theory is applied to the results of experiments performed on highly concentrated latices (50-52) in which segment densities can be very high indeed.

Although we cannot avoid the difficulty of requiring that $\sum_{i=1}^{\infty} \frac{\chi_i}{i} = 1$ at the Θ-point, we can start by assuming that $\chi_1 = \frac{1}{2}$ and $\chi_2 = \frac{1}{3}$ are reasonable at the Θ-point; which leaves us with

$$\sum_{i=3}^{\infty} \frac{\chi_i}{i} = \frac{1}{3} \quad . \qquad \{27\}$$

There are indications that even $\chi_3 = \frac{1}{4}$ is not unreasonable (see below). The only ad hoc assumption needed in that case would be

$$\sum_{i=4}^{\infty} \frac{\chi_i}{i} = \frac{1}{4} \qquad \{28\}$$

Equation {28} is partially justifiable in that our theory requires that a Θ-solvent behaves as such for all concentrations of polymer. Such a solvent would be a perfect Θ-solvent. We do not expect the theory to apply, in practice, when the polymer concentration exceeds 20-30%. Additionally, according

to statistical theory (60,61), all of the virial coefficients are positive (in good solvents) if the superposition approximation is valid (60). Accordingly, in good solvents, $\chi_i < \frac{1}{i+1}$ and the only way we can have $\sum_{i=1}^{\infty} \frac{\chi_i}{i} = 1$ at the Θ-point is for <u>each</u> χ_i to approach $\frac{1}{i+1}$ from below (although not necessarily at the same rate). Thus statistical theory supports eq.{25} as a thermodynamically valid set of solutions to eq.{24}.

Having accepted that $\chi_1 = \frac{1}{2}$ and $\chi_2 = \frac{1}{3}$ at the Θ-point, we go further and suggest that

$$\chi_2 = \frac{2\chi_1}{3} \qquad \{29\}$$

is a reasonable first approximation near the Θ-point. The theoretical justification for the dependence of χ_2 on χ_1 is as follows (62):

i) $(\frac{1}{2} - \chi_1)$ and $(\frac{1}{3} - \chi_2)$ are related directly to the second and third osmotic virial coefficients Γ_2 and Γ_3 because they are coefficients of the square and cube of the concentration respectively. Expanding eq.{5} for example:

$$\mu_1^E = -RT\{(\tfrac{1}{2} - \chi_1)v_2^2 + (\tfrac{1}{3} - \chi_2)v_2^3 + \ldots . \} .$$

The excess osmotic pressure of the solution is

$$\pi^E = -\frac{\mu_1^E}{\bar{V}_1} = +\frac{RT}{\bar{V}_1}\{(\tfrac{1}{2} - \chi_1)v_2^2 + (\tfrac{1}{3} - \chi_2)v_2^3 + \ldots . \} .$$

However, using c as the polymer concentration (42,46),

$$\pi^E = \pi^E_{c=0}(\Gamma_2 c^2 + \Gamma_3 c^3 + \ldots .) .$$

This is a virial expansion with Γ_2 and Γ_3 as the second and third coefficients (the ideal term is zero). Quantitatively, the lattice approach is unsatisfactory for predicting the behaviour of Γ_3 (62), therefore we will not equate Γ_2 with $(\frac{1}{2} - \chi_1)$ or Γ_3 with $(\frac{1}{3} - \chi_2)$. It is expected, however, that when Γ_2 and Γ_3 are zero, $\chi_1 = \frac{1}{2}$ and $\chi_2 = \frac{1}{3}$.

ii) Stockmayer and Casassa (60) have shown that when Γ_2 is zero, Γ_3 is zero. Even for an array of hard spheres this is true (60). We may infer that as $\chi_1 \to \frac{1}{2}$, $\chi_2 \to \frac{1}{3}$, in keeping with the abovementioned requirements of statistical theory. Equation {29} was chosen as the simplest possible form of the dependence of χ_2 on χ_1 which allows the third virial coefficient to vanish with the first. At most, eq.{29} may be considered a semi-empirical relationship, useful for many systems when χ_1 is not too different from $\frac{1}{2}$. We will now test eq.{29} on several systems reported in the literature.

5.2. Experimental Evidence

The data and results of free volume theory calculations represented in Figs.3 to 8 were transcribed from the following references:

Fig.	ref(s).
3a	63
3b	59,64
4a	65
4b	66
5	67,68

Fig.	ref(s).
6a	69,70
6b	71
7a	69,72
7b	71
8a	73
8b	74

Only two systems could be found that were investigated under Θ-conditions: polyisobutylene (PIB) in benzene at 297.5 K (63,68) and polystyrene (PS) in cyclohexane at 307 K (59,75). Both systems, as pointed out by Krigbaum and Geymer (62), exhibit $\chi_2 \simeq \frac{1}{3}$ (lines 1). Even the additional assignment of $\chi_3 = \frac{1}{4}$ (lines 2) gives a reasonable fit to the data at high concentrations. The general placement of $\chi_i = \frac{1}{i+1}$ at the Θ-point is not justified by this experimental evidence; instead we must limit our use of the interaction formulae to moderate concentrations. Note that in Figs.4b and 7b the two sets of data for polydimethylsiloxane (PDMS) in benzene yield χ_1 values which may be accurate to only ±0.03. This is a totally unacceptable situation. The temperature dependence of χ_1 is such that $|\partial\chi_1/\partial T| \sim 10^{-3}$ K^{-1} may be considered typically of the right order of magnitude (59,67,68,75) near the Θ-point. Therefore, an error of ±0.03 in χ_1 could result in a very large uncertainty in Θ (~30 K). Since no theory can as yet accurately predict the Θ-point of a polymer solution from first principles, we are forced to fit the theory to the experimental data - particularly in the region of the Θ-point, which must be found accurately.

Fig. 3. Concentration dependence of the interaction parameter χ.

(a) PIB in benzene at 298 K,

(b) PS in cyclohexane at 307 K.

Lines: (1) $\chi = \frac{1}{2}(1 + 2v_2/3)$,

(2) $\chi = \frac{1}{2}(1 + 2v_2/3 + v_2^2/2)$,

(3) Predictions of free volume theory (FVT).

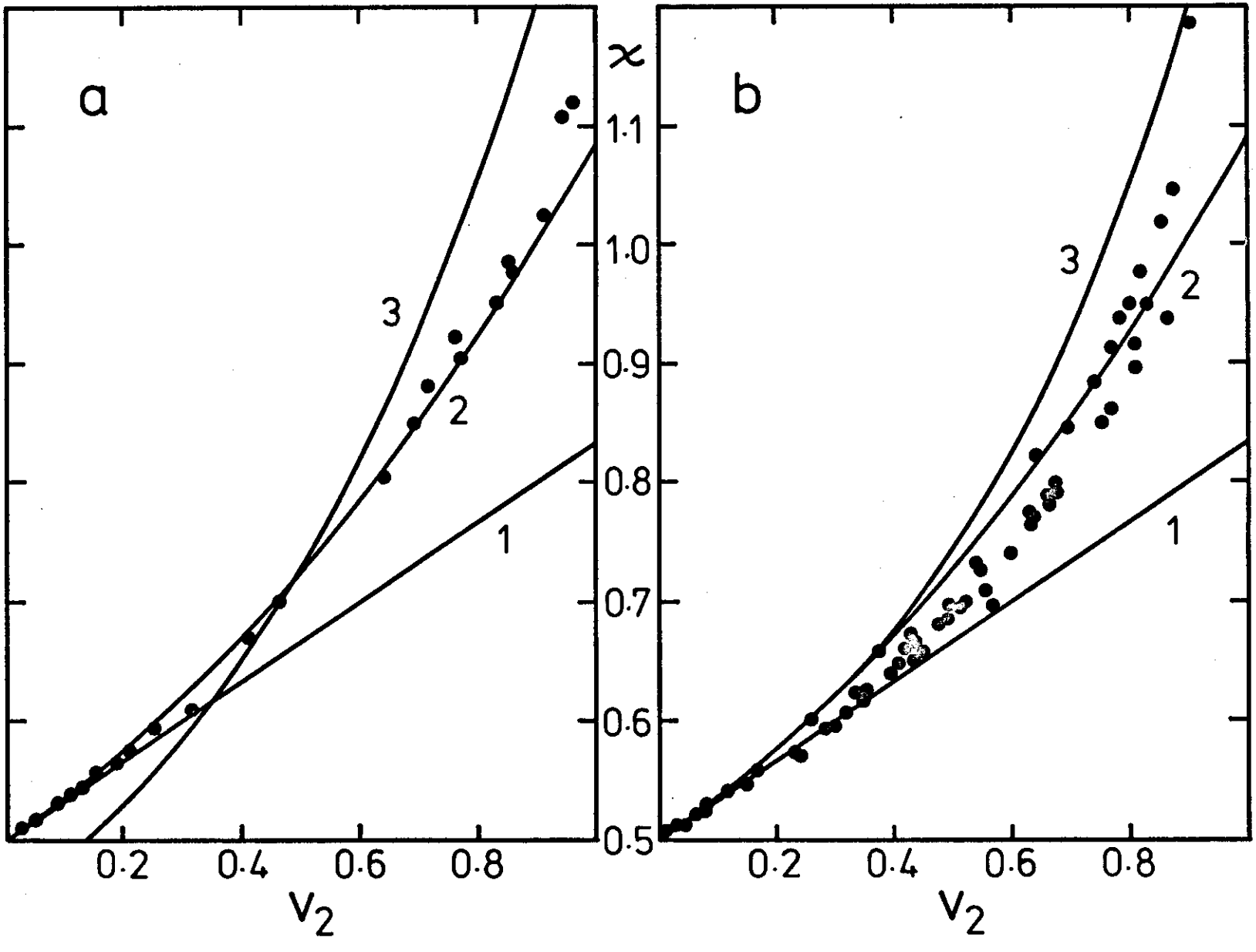
a
b
3
2
1
x
1.1
1.0
0.9
0.8
0.7
0.6
0.5
0.2
0.4
0.6
0.8
v_2

Fig.4. Concentration dependence of the interaction parameter χ.

(a) PIB in n-pentane at 298 K,

(b) PDMS in benzene at 298 K.

Lines: (1) $\chi = \chi_1(1 + 2v_2/3)$,

(2) FVT .

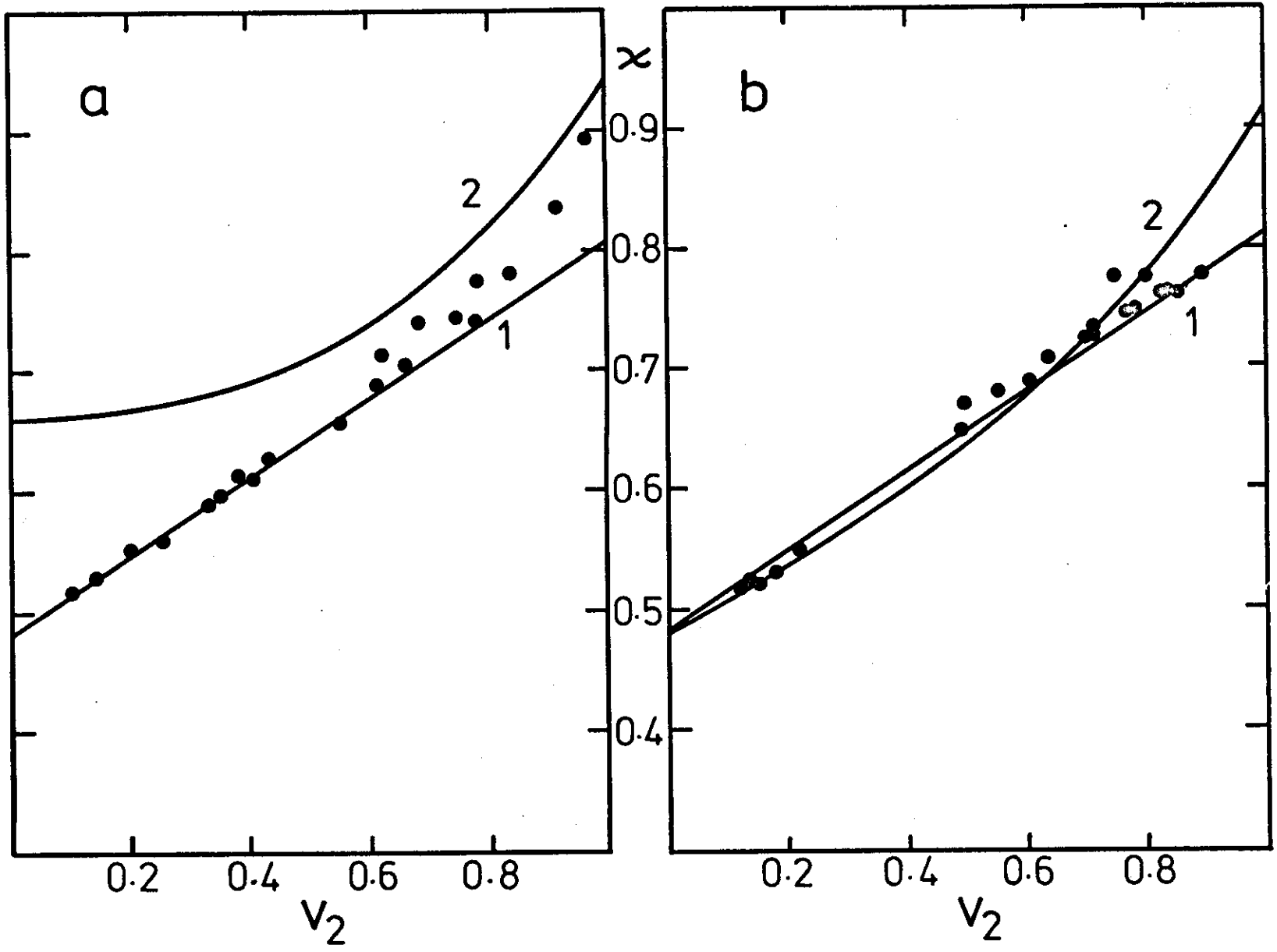
a
b
2
1
2
1
x
0·9
0·8
0·7
0·6
0·5
0·4
0·2
0·4
0·6
0·8
0·2
0·4
0·6
0·8
V_2
V_2

Fig.5. Concentration dependence of the interaction parameter χ.

Lines: (1) PDMS in chlorobenzene at 298 K,

(2) PDMS in chlorobenzene at 333 K,

(3) PDMS in toluene at 293 K,

(4) PIB in benzene at 297.5 K,

all lines fitted to $\chi = \chi_1(1 + 2v_2/3)$.

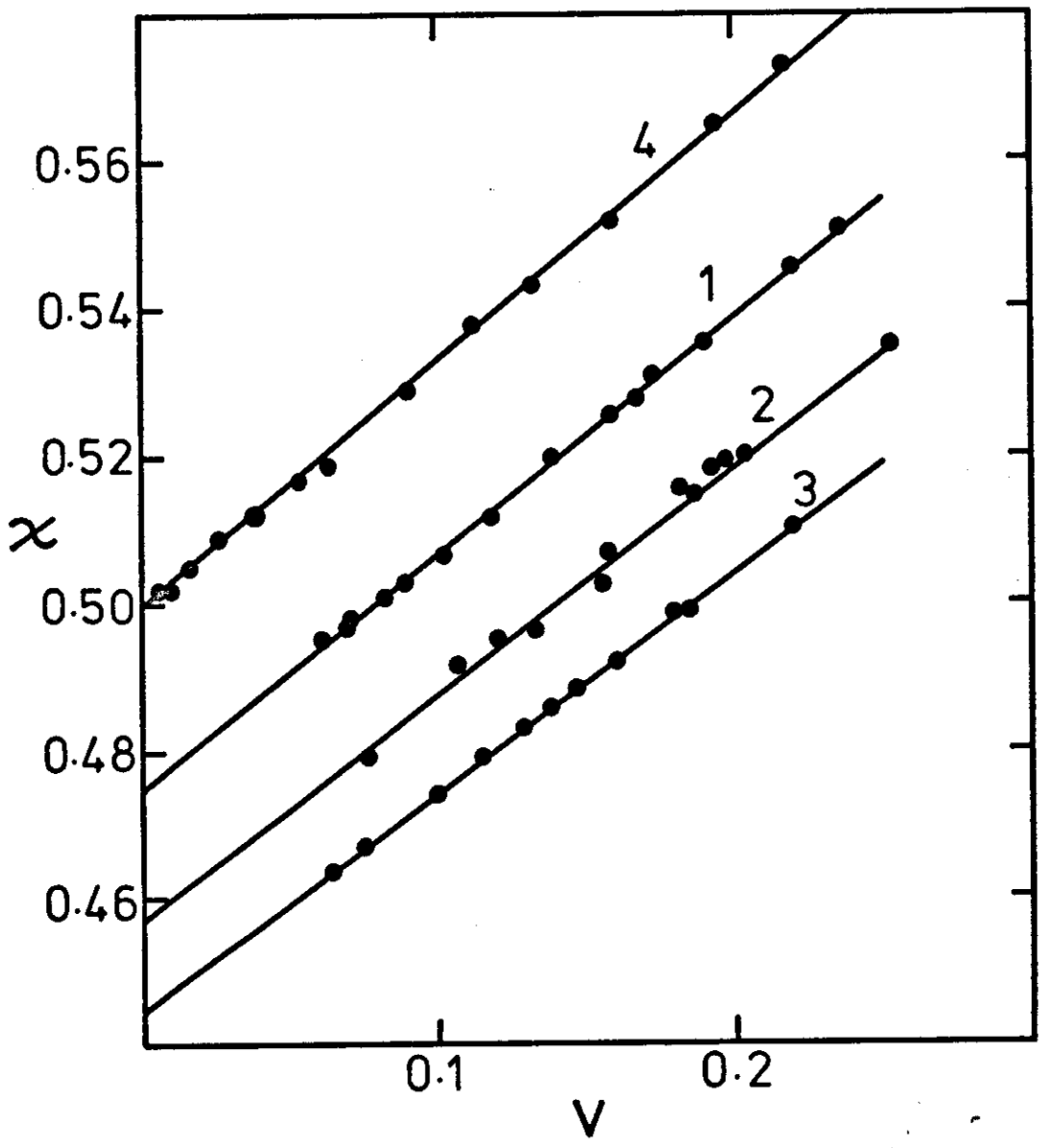
0·56
0·54
0·52
0·50
0·48
0·46
χ
0·1
0·2
V
4
1
2
3

Fig.6. Concentration dependence of the interaction parameter χ.

(a) PS in methyl ethyl ketone at 298 K,

(b) PDMS in toluene at 298 K.

Lines: (1) $\chi = \chi_1(1 + 2v_2/3)$,

(2) FVT .

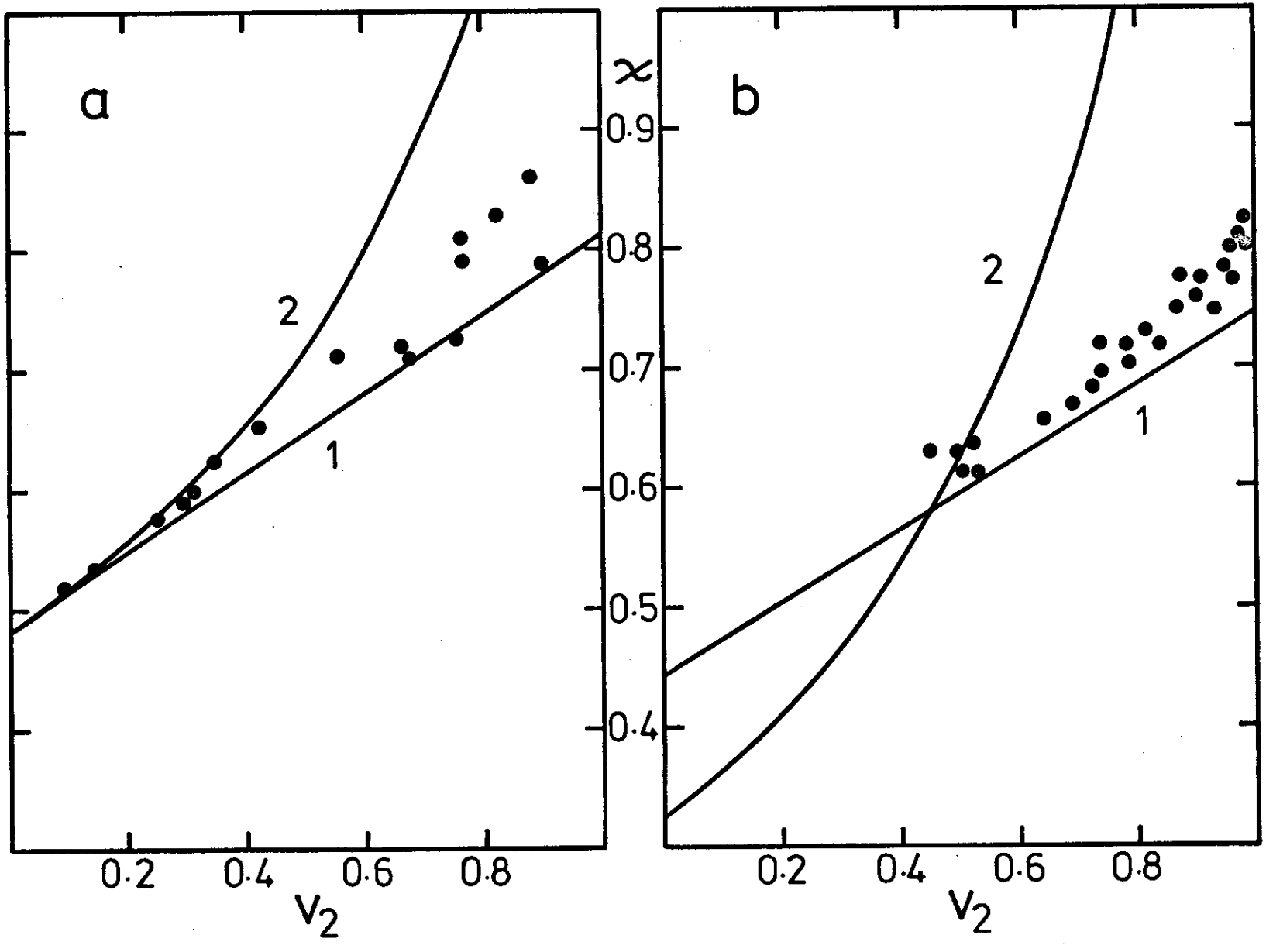
a
b
x
0.9
0.8
0.7
0.6
0.5
0.4
0.2
0.4
0.6
0.8
v_2
1
2

Fig.7. Concentration dependence of the interaction parameter χ.

(a) PS in ethylbenzene at 298 K,

(b) PDMS in benzene at 298 K.

Lines: (1) $\chi = \chi_1(1 + 2v_2/3)$,

(2) FVT .

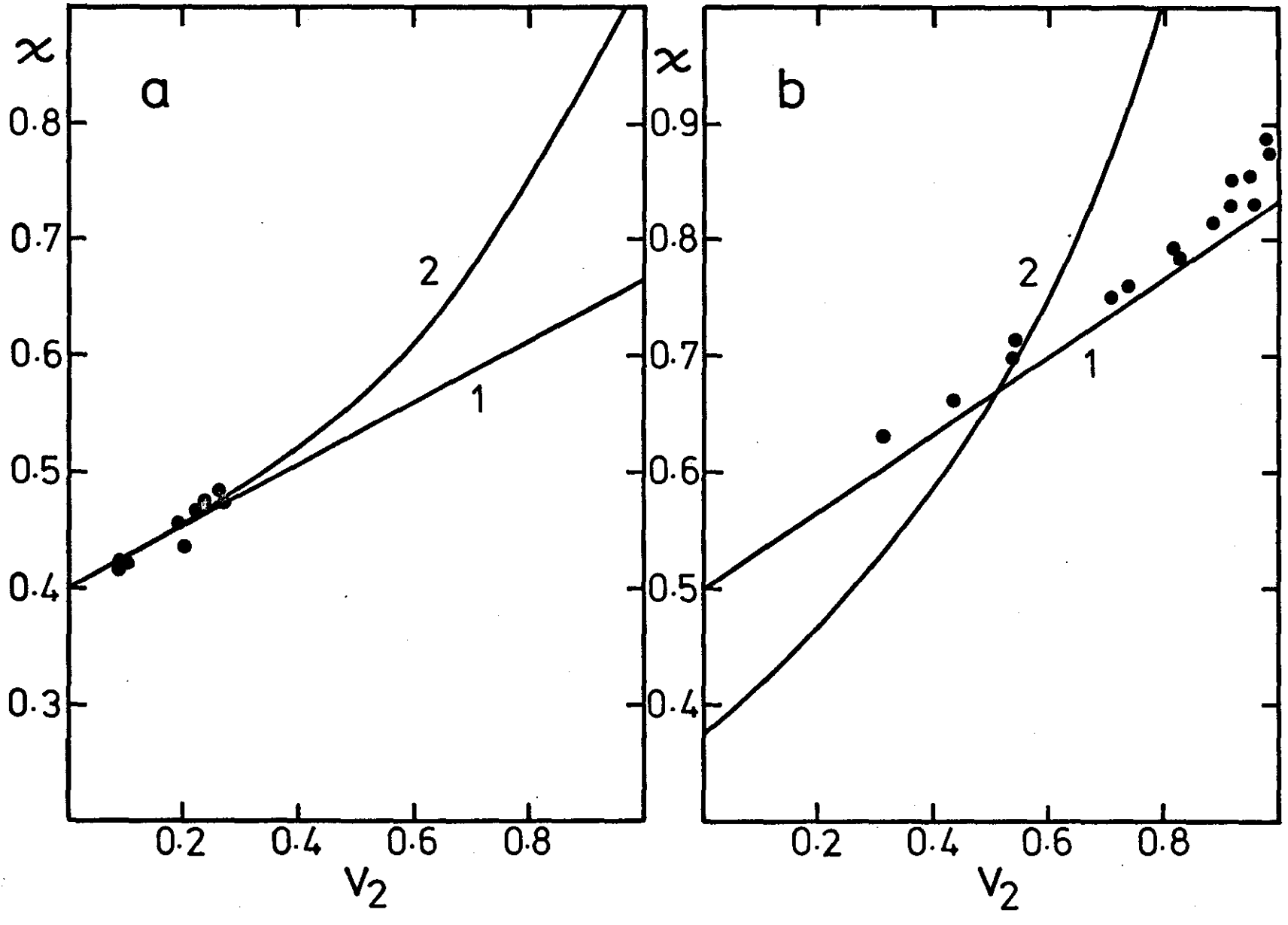
a
b
x
V_2
0.8
0.7
0.6
0.5
0.4
0.3
0.9
0.2
0.4
0.6
0.8
1
2

Fig.8. Concentration dependence of the interaction parameter χ.

(a) PIB in n-octane at 298 K.

Lines: (1) $\chi = \chi_1(1 + 2v_2/3)$,fitted,

(2) FVT.fitted

(b) PEO in benzene.

Lines: (3) $\chi = \chi_1(1 + 2v_2/3)$; T = 330.9 K,

(4) $\chi = \chi_1(1 + 2v_2/3)$; T = 333.2 K,

(5) FVT; T = 330.9 K.

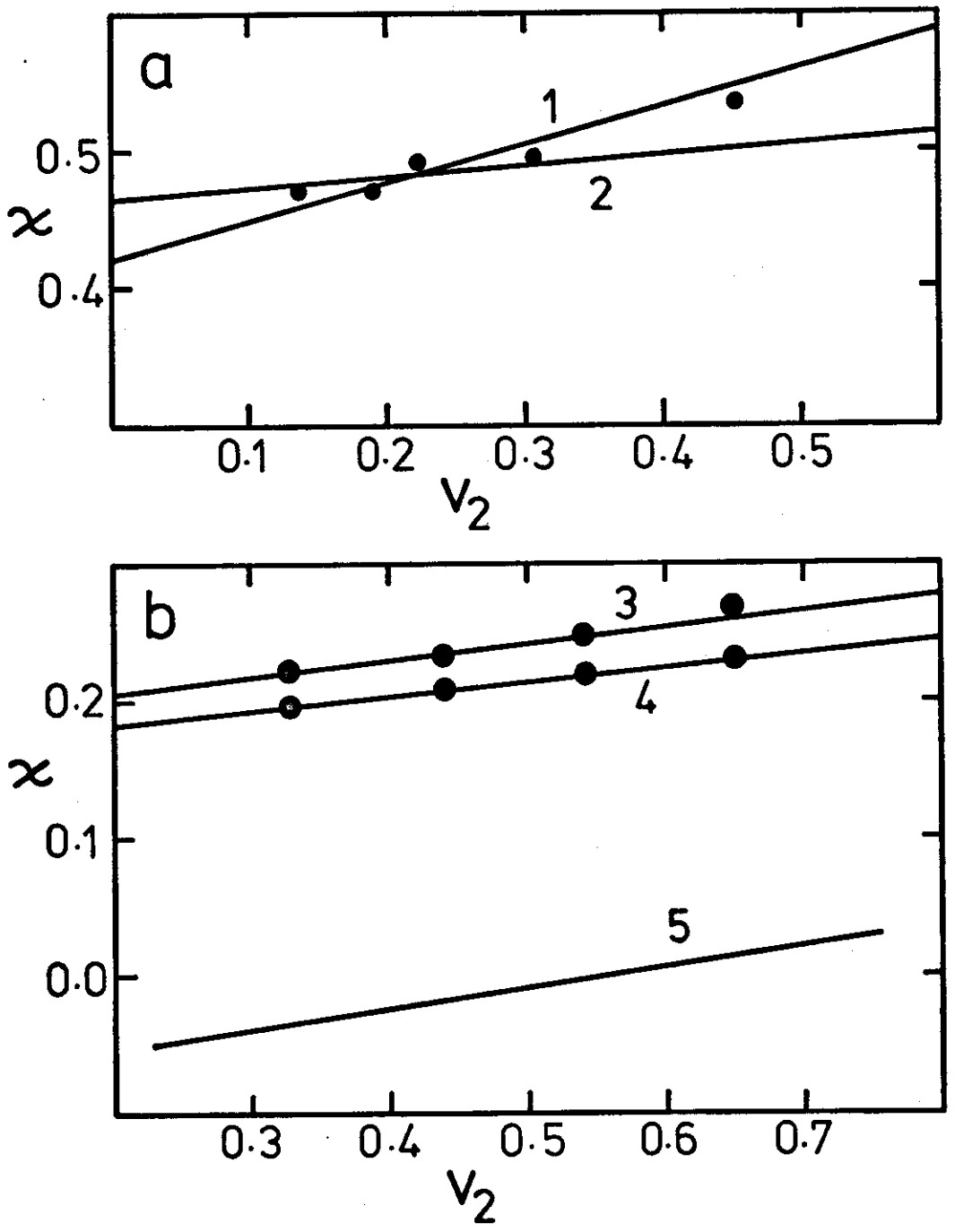
a
1
2
0.5
0.4
χ
0.1
0.2
0.3
0.4
0.5
V_2
b
3
4
5
0.2
0.1
0.0
χ
0.3
0.4
0.5
0.6
0.7
V_2

In most cases, free volume theory can be made to fit the data quite well. It should be pointed out that the free volume theory predictions in, for example, Figs.6b and 7b have been fitted to the heat of dilution data at intermediate polymer concentrations (71). Therefore, a poor fit at very low concentrations is expected. Note also, our steric stabilization theory is based upon polymer volume fractions while segment fractions are most often employed in modern polymer solution theories (49). Although this does not significantly effect our present results, future theories of steric stabilization may use segment fractions. We take a brief look at the possibility of using Flory's free volume theory in appendix 1.1.

Although the semi-empirical approximation $\chi_2 = \frac{2\chi_1}{3}$ is not expected to be useful far from the Θ-point, we include some results (74) for PEO in benzene which behave unusually "well" considering the large magnitude of $(\frac{1}{2} - \chi_1)$ (see Fig.8b).

Instances were found in the literature that definitely do not follow the simple theory. The most notable example is PS in toluene (69) for which χ actually decreases with increasing concentration. Apparently, even free volume theory cannot account for this phenomenon (69). Other examples include PDMS in dimethylsiloxane oligomers (71) which tend to have a reasonably constant χ; again, free volume theory is of little help.

Such systems are, however, far from the Θ-point. For example, the Θ-temperature for the system PS/toluene is ~160 K (42) and the measurements

which yield a negative concentration dependence of χ were taken at 298 K.

Our studies are concerned mainly with the point of incipient instability of sterically stabilized latices. As we remarked earlier, this point is usually associated with the Θ-point of the stabilizer in free solution. Therefore, the behaviour of χ very close to Θ is of the greatest interest and our attention is accordingly concentrated on Fig.3. Summarizing the experimental comparisons, we have:

1. $\chi_1 = \frac{1}{2}$ at Θ,
2. $\chi_2 \simeq \frac{1}{3}$ at Θ,
3. $\chi_3 \simeq \frac{1}{4}$ is not unreasonable at Θ,
4. $\sum_{i=4}^{\infty} \frac{\chi_i}{i}$ is unknown but less than $\frac{1}{4}$ at Θ,
5. $\chi_2 = \frac{2\chi_1}{3}$ is an acceptable semi-empirical approximation for many systems.

We now apply this theory to steric stabilization. The above results may be applied in general, but henceforth we shall use the uniform segment density model.

6. UNIFORM SEGMENT DENSITY MODEL

It has been found (41) that, given the barrier layer thickness L as measured experimentally and the amount of adsorbed polymer ω or ν, the distance dependence of the osmotic interaction is not very sensitive to the exact form of the segment density distribution. The results so far presented apply to any distribution. We will henceforth resort to a uniform segment density model primarily because of its extreme ease of manipulation. The model will be shown, in section 9, to give a reasonable indication of the behaviour of real systems.

A further simplifying assumption which we make and which has been made by other authors (40,25,76) is to maintain a uniform total segment density distribution at all separations less than d = 2L. Previous authors (40,25) have used this condition to allow continuous relaxation of stabilizer away from the interaction zone. If this were the case, a very large elastic repulsion would occur owing to a loss in configurational freedom of the polymer. Neglect of this elastic effect may be partially justified in that experimental determinations of the parameters describing the free solution properties of polymers must automatically include any configurational relaxation effects due to interpenetration. It seems very unlikely that configurational relaxation of adsorbed chains can be accounted for entirely by these experimental parameters.

An alternative explanation involves no configurational relaxation until d = L at which point elastic effects commence (see next section). We merely

assume that the segment density distribution is such that overlap results in the same free energy change as would be obtained from the osmotic component of the uniform segment density "denting" process (see Bagchi (25,26)). The result is a distribution less abrupt than a step function. We have "softened" the interaction free energy and obtained a model more physically realistic than the continuous relaxation model which ignores the configurational consequences of relaxation.

There is, as yet, no experimental confirmation of the accuracy of any proposed segment density distribution apart from apparent barrier layer thickness measurements (e.g.,55). We suspect that there will be no unique form for the distribution in real systems and that the form will depend on the method of preparation of the latex (e.g., whether the stabilizer is adsorbed onto the preformed particles or the particles are grown in the presence of the stabilizer). It has been suggested by Edwards and Freed (77) that high molecular weight polymers are probably not in configurational equilibrium because of the time required to anneal. If kinetic factors are dominant or if the time taken to produce a latex is too short to allow configurational equilibrium of the stabilizer, the adsorbed chains will be permanently in a thermodynamically unfavourable configuration.

A further point concerns whether the real chains can be considered "production" chains (47). Configurational statistics of adsorbed polymers are generally studied using random flight methods. Consider, for example, an adsorbed "loop". The number of ways in which the polymer can be "grown" starting from and ending at the surface has generally been accepted (e.g.,12,

28,29,43) as indicating the configurational entropy of a loop. In other words, each loop has been formed by "producing" a chain. Suppose now that the chain already exists as an adsorbed loop. A great many of the configurations possible for the production chain are no longer possible because covalent bonds would have to be broken in order to make these configurations accesible. This problem does not exist in principle for free linear chains or adsorbed "tails"; however, in practice, the unravelling of knots may take far too long to allow continuous equilibration.

The difference between having a knot and having a simple loop could be a matter of a very small deviation during the growth of a production chain, but a matter of virtual permanence for an already existing chain.

In effect, the validity of random flight methods (including Monte Carlo experiments) in steric stabilization relies upon the assumption that the formation of knots is directly proportional to the number of possible configurations at <u>each</u> distance of separation of the particles in a given system. A "knot", in this context, is any configuration which cannot change in a time much shorter than the collision time of two particles. This assumption may be reasonable at low polymer concentrations but as the concentration increases the approach to equilibrium should become slower (cf. denting mechanism (25)). The study of polymer dynamics by inelastic neutron scattering techniques (78) may be very useful in this area.

Other complications for real systems include possible surface interactions

which alter the segment density distribution (39), the coexistence of loops and tails and the polydispersity of the adsorbed polymer. The complete description of the segment density distribution of real adsorbed polymers may prove to be impossible from a theoretical viewpoint, which is why the relative insensitivity of the interaction to the distribution is encouraging.

We begin our simplification of eq.{18} for the flat plate case by placing

$$\hat{v}_d = \hat{v}_{d'} = \frac{1}{d} \qquad \{30\}$$

and

$$\hat{v}_\infty = \hat{v}_L = \frac{1}{L} \quad . \qquad \{31\}$$

Thus

$$\Delta G^u_{OS} = \frac{2RTL}{\bar{V}_1} \sum_{i=1}^{\infty} \frac{\bar{v}^{i+1}}{i} \left(\frac{1}{i+1} - \chi_i\right)\{(2/\delta)^i - 1\} \ , \qquad \{32\}$$

where $\bar{V}_1$ is the molar volume of solvent, R is the gas constant and the superscript u indicates the uniform segment density model.

Interaction starts at a particle surface separation of 2L or $\delta = 2$. Evaluation of eq.{18} requires the substitution:

$$\int_0^\infty \hat{v}_\infty^{i+1} dx = \int_0^{2L} \hat{v}_L^{i+1} dx \quad . \qquad \{33\}$$

We have shown that up to moderate polymer concentrations, $\chi = \chi_1(1 + 2v_2/3)$. Neglecting terms of the order $\bar{v}^4$ in eq.{32}, we find for the osmotic interaction between sterically stabilized flat plates:

$$\Delta G^{u}_{OS} = \frac{2RTL}{\bar{V}_1}(\tfrac{1}{2} - \chi_1)\bar{v}^2(\frac{2}{\delta} - 1)\{1 + \frac{\bar{v}}{3}(\frac{2}{\delta} + 1)\} \quad . \qquad \{34\}$$

Proceeding in the same manner from eq.{23}, we have the osmotic interaction between equal spheres:

$$\Delta V^{u}_{OS} = 4\pi a \frac{RTL^2}{\bar{V}_1}\Big[\bar{v}^2(\tfrac{1}{2} - \chi_1)(\ln\frac{2}{\delta_0} + \frac{\delta_0}{2} - 1) + \sum_{i=2}^{\infty}\frac{\bar{v}^{i+1}}{i(i-1)}(\frac{1}{i+1} - \chi_i)\{(\frac{2}{\delta_0})^{i-1} + (i-1)\frac{\delta_0}{2} - i\}\Big], \qquad \{35\}$$

which simplifies to:

$$\Delta V^{u}_{OS} \simeq 4\pi a \frac{RTL^2}{\bar{V}_1}(\tfrac{1}{2} - \chi_1)\bar{v}^2\{\ln\frac{2}{\delta_0} + \frac{\delta_0}{2} - 1 + \frac{2\bar{v}}{3}(\frac{2}{\delta_0} + \frac{\delta_0}{2} - 2)\} + O(\bar{v}^4) \quad . \qquad \{36\}$$

The above equations are, in effect, first order perturbation approximations and as such cannot be used when terms of order $\bar{v}^3$ become comparable with terms of order $\bar{v}^2$. If these terms are comparable, then we are not justified in ignoring $O(\bar{v}^4)$. Estimation of χ_3 is much more difficult than the estimation of χ_2 from experimental data since we require the curvature of the χ versus v_2 plots. Although $\chi_3 \simeq \frac{1}{4}$ may be reasonable at Θ, the uncertainty in experimental data precludes any reliable estimate away from Θ. Since we cannot extend the equation to higher terms readily, we must resort to the conditions that

$$\bar{v} \leq 0.15$$

and

$$\delta_0 \geq 0.5$$

although these conditions are sensitive to the behaviour of χ.

7. ELASTIC REPULSION

When the distance of separation of two sterically stabilized particles is less than the maximum possible extension of a stabilizer molecule, elastic repulsion may begin to contribute to stabilization. This repulsion was first proposed from a phenomenological viewpoint by Jäckel (18). The elastic term arises from the loss in configurational entropy of the stabilizer chains during approach of the particles and, as such, is equivalent to the volume restriction effect proposed by Meier (12), Hesselink (13) and, more recently, by Dolan and Edwards (43,44). By using the term "elastic" in this context we are following the nomenclature of Flory (42).

In this section we shall extend a slightly modified version of the results of Dolan and Edwards (43) to cover the elastic interaction between spheres. For the purposes of utilizing the uniform segment density model, we derive a further expression for elastic repulsion based upon the condition that the stabilizer layer is in thermodynamic equilibrium when uncompressed. We use the initial premise that each adsorbed polymer molecule can be replaced by an equivalent confined ideal gas molecule. Both of the above models will be compared with that of the one-dimensional deformation of Gaussian chains (42, 48).

7.1. Extension of Formulae of Dolan and Edwards to Spheres

Dolan and Edwards, in their first paper on configurational repulsion (43), derived approximate closed expressions for the elastic free energy of mono-

terminally adsorbed chains confined between parallel flat plates. Their approximation applied to large separations of coated flat plates yields:

$$\Delta G_{el}^{R} = -2kT\nu \ln\{1 - 2\exp(\frac{-3d^2}{2\ell L'})\} \qquad \{37\}$$

where ν = number of monodisperse chains per unit area on one plate,

ℓ = length of one segment,

L' = contour length of a chain,

d = separation of the plates,

superscript R indicates random flight model and subscript el refers to the elastic effect.

Placing $L' = n_s\ell$, where n_s is the number of segments per chain, we see that

$$\ell L' = n_s\ell^2 ,$$

which is the mean-square end-to-end distance of the unperturbed hypothetical freely jointed chain in free space. The Markoff nature of the chain (named after A.A. Markoff who formulated the general form of the random flight problem in 1912 (79)) is indicated by the fact that the mean-square end-to-end distance is directly proportional to the number of segments n_s (47).

The r.m.s. end-to-end distance of a real polymer chain differs from $(n_s\ell^2)^{\frac{1}{2}}$ in two ways. First, the inclusion of bond angle and rotational restrictions and any other "short range" effects usually results in an increase in the r.m.s. end-to-end distance (80). Second, excluded volume ("long range") effects cause not only a change in this characteristic distance, but also a change in the form of the segment density distribution function (46,47).

It has been shown that the short range effects do not destroy the Markoff nature of an unperturbed chain (47,80) as long as the number of segments is large enough. We may therefore write, for the unperturbed r.m.s. end-to-end distance $\langle r^2 \rangle_0^{\frac{1}{2}}$ of a <u>real</u> chain:

$$\langle r^2 \rangle^{\frac{1}{2}} \propto (n_s \ell^2)^{\frac{1}{2}} \quad .$$

Excluded volume or long range effects depend upon the entire segment density distribution. According to Yamakawa (47), for example, the peripheral regions of a free chain are expanded more than the internal regions by the effect of a positive segmental excluded volume. Uniform expansion does not occur and therefore we cannot strictly write:

$$\langle r^2 \rangle^{\frac{1}{2}} = \alpha \langle r^2 \rangle_0^{\frac{1}{2}} \qquad \{38\}$$

for the perturbed r.m.s. end-to-end distance of a real chain. The Markoff nature has been destroyed because α depends upon the number of segments in the chain (46,47,80). Several authors (e.g.,46,47,80) have found that

$$\langle r^2 \rangle \propto n_s^{\gamma} \quad ,$$

where $\gamma \simeq 1.2$.

Despite the non-Markoff nature of perturbed chains, the results of Dolan and Edwards (44) suggest that a fourfold increase in chain length results in negligible change in free energy of an adsorbed chain when the separation of the surfaces remains at a constant <u>reduced</u> distance $d/(\ell L')^{\frac{1}{2}}$. This appears to be true for both the random flight chains and for chains with excluded volume.

For our purposes, therefore, it seems reasonable to use eq.{38} and treat

all real chains as Markoff chains. Naturally, this argument must break down when the chains are short (47) but, for the present, we shall simply replace $\ell L'$ by $\langle r^2 \rangle$ in eq.{37} and consider the result as applying to equivalent freely jointed chains:

$$\Delta G_{el}^{R} = -2kT\nu \ln\{1 - 2\exp(\frac{-3d^2}{2\langle r^2 \rangle})\} \quad . \qquad \{39\}$$

We emphasise that our use of $\langle r^2 \rangle^{\frac{1}{2}}$ as a unit of length does not mean that we have accounted for interpenetrational excluded volume effects; it is merely a scaling factor which gives a better indication of the range of the interaction than does $(\ell L')^{\frac{1}{2}}$ or $\langle r^2 \rangle_0^{\frac{1}{2}}$.

We have assumed above that the dimensions of an adsorbed chain are affected by the same amount as those of a free chain. Expanding eq.{39}, we have:

$$\Delta G_{el}^{R} = 2kT\nu\{2\exp(\frac{-3d^2}{2\langle r^2 \rangle}) + 2\exp(\frac{-3d^2}{\langle r^2 \rangle}) + \frac{8}{3}\exp(\frac{-9d^2}{2\langle r^2 \rangle}) + ...\} \quad . \qquad \{40\}$$

Neglect of all but the leading term leads to an underestimate of the repulsion of 23% at $d = \langle r^2 \rangle^{\frac{1}{2}}$. Retention of the second term reduces this error to 6%. If the coefficient of the second term is arbitrarily increased from 2 to 2.5, the error in ΔG_{el} is reduced to less than 2% for all $d \geq \langle r^2 \rangle^{\frac{1}{2}}$. Therefore, to a good approximation (better, in fact, than the parent expression {39}, which is itself and approximation):

$$\Delta G_{el}^{R} = 2kT\nu\{2\exp(\frac{-3d^2}{2\langle r^2 \rangle}) + 2.5\exp(\frac{-3d^2}{\langle r^2 \rangle})\} \quad . \qquad \{41\}$$

One problem associated with the application of this equation, and the

similar equations of Hesselink (13) and Meier (12), to our model lies in the difference between the reduced distances used. We have found it more convenient to use the parameter $\delta = d/L$ where L is the measured barrier layer thickness. If we place

$$\xi = L/\langle r^2 \rangle^{\frac{1}{2}} \quad , \qquad \{42\}$$

which is an experimental ratio identical to the extension factor f in ref.41, we find:

$$\Delta G^R_{el} = 2kT\nu\{2\exp(-\tfrac{3}{2}\,\xi^2\delta^2) + 2.5\exp(-3\xi^2\delta^2)\} \quad . \qquad \{43\}$$

Once again, we may apply the Derjaguin method (14) to find the elastic repulsion between two coated spheres:

$$\Delta V^R_{el} = \pi aL \int_{\delta_0}^{\infty} \Delta G^R_{el}\, d(\delta) \qquad \{44\}$$

where $\delta = d_0/L$ and d_0 = surface separation of spheres. Therefore,

$$\Delta V^R_{el} = 2\pi akT\nu L\xi^{-1}(\pi/3)^{\frac{1}{2}}\{2^{\frac{1}{2}}\,\mathrm{erfc}(3/2)^{\frac{1}{2}}\,\xi\delta_0 + (5/4)\mathrm{erfc}\,3^{\frac{1}{2}}\xi\delta_0\} \quad , \qquad \{45\}$$

where erfc is the complementary error function (81).

The complementary error function is readily calculated from a slightly modified version of a polynomial approximation in the "Handbook of Mathematical Functions" (81):

$$\mathrm{erfc}(x) = (1 + x(a_1 + x(a_2 + x(a_3 + x(a_4 + x(a_5 + a_6x))))))^{-16} \qquad \{46\}$$

with an error of less than 3×10^{-7} ,

where $a_1 = .07052\ 30784$

$a_2 = .04228\ 20123$

$a_3 = .00927\ 05272$

$a_4 = .00015\ 20143$

$a_5 = .00027\ 65672$

$a_6 = .00004\ 30638$.

By placing

$$\Delta V_{el}^{R} = 2\pi akT\nu L\ S_{el}^{R} \qquad \{47\}$$

we have

$$S_{el}^{R} = \xi^{-1}(\pi/3)^{\frac{1}{2}}\{2^{\frac{1}{2}}\ \mathrm{erfc}(3/2)^{\frac{1}{2}}\ \xi\delta_0 + (5/4)\mathrm{erfc}\ 3^{\frac{1}{2}}\xi\delta_0\} \quad . \qquad \{48\}$$

This expression holds for

$$\delta_0 \gtrsim \xi^{-1} \quad . \qquad \{49\}$$

From eq.{48} we can construct a family of curves relating S_{el}^{R} to δ_0 for differing values of ξ (Fig.9). These results will be compared with those of two other segment density distributions in the following sections.

7.2. Construction of a Model Consistent with Uniform Segment Density Requirement

We mentioned previously that the choice of segment density distribution does not seriously affect the distance dependence of the osmotic contribution (41) as long as the experimental barrier layer thickness and the amount of polymer adsorbed have been determined. It will prove interesting to see what effect on the elastic term is produced by changing the segment density

Fig.9. Plots of the elastic interaction parameter S_{el}^{R} for random walk monoterminally adsorbed chains on spheres versus the distance parameter δ_0.

Lines: (1) ξ = 1.8, (2) ξ = 2.0, (3) ξ = 2.2, (4) ξ = 2.4, (5) ξ = 2.6.

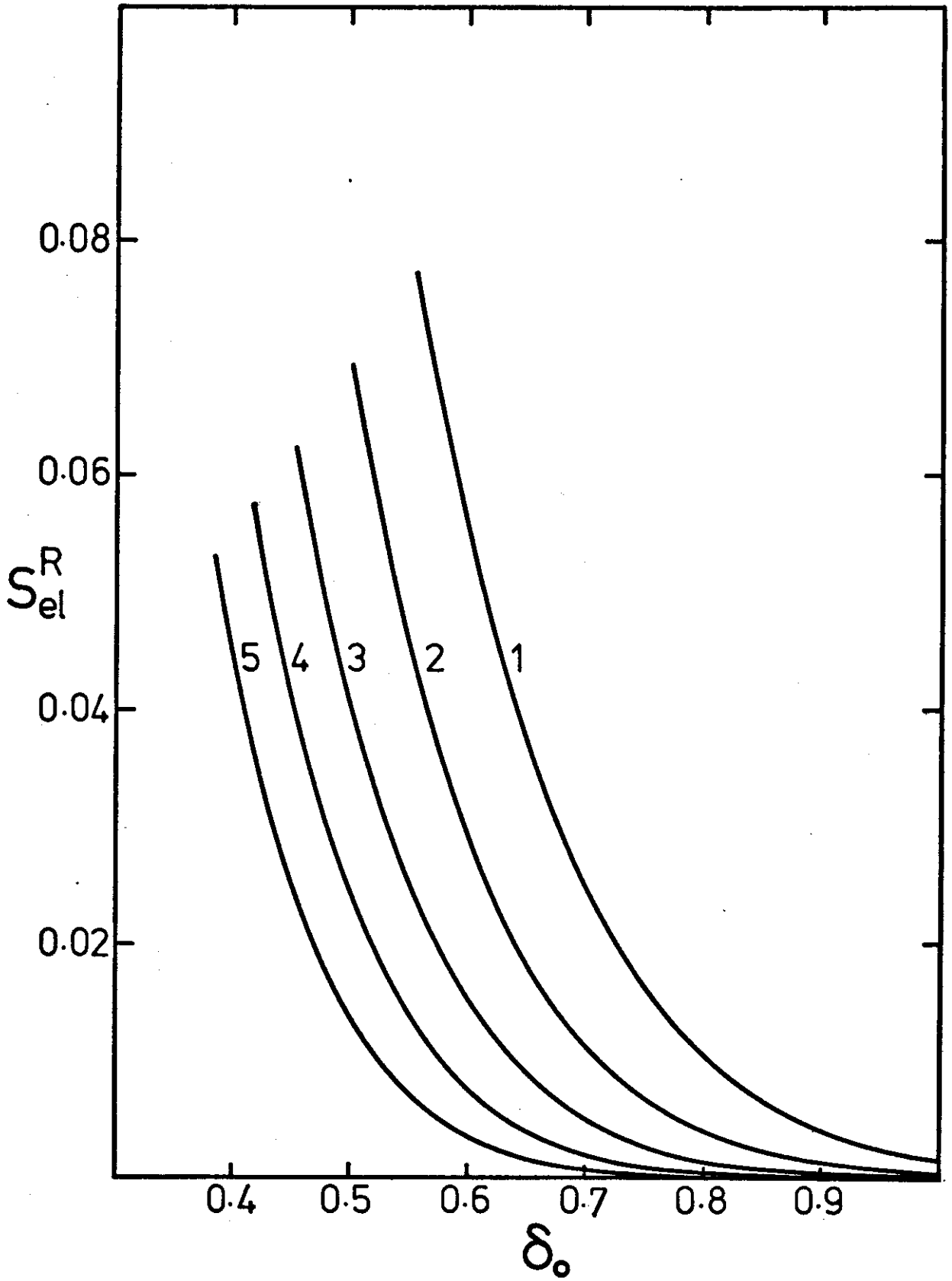
0·08
0·06
0·04
0·02
S_{el}^{R}
5
4
3
2
1
0·4
0·5
0·6
0·7
0·8
0·9
δ_o

distribution.

To begin, we know that our future calculations of the osmotic effect will be enormously simplified if we are permitted the use of a uniform segment density distribution. If, in fact, we find that the precise distribution is not needed, we will be justified in using two different models for the calculation of the total osmotic plus elastic interaction. We need not go to the extreme of using completely different models, but we must establish that our use of a "softened" uniform segment density distribution for the osmotic effect in section 6 does not conflict with our use of a "hard" uniform distribution for the elastic effect. Recall that we "softened" the distribution for the osmotic effect by making the <u>total</u> segment density between the two flat plates uniform. A "hard" distribution is merely a step-function (as used, for example, by Fischer (17), Ottewill and Walker (24) and Bagchi (25)).

The most obvious method of ensuring that the probability of finding a segment at any point in the stabilizer layer is constant, is to replace the adsorbate with a confined ideal gas. We can show, using the results of calculations by Edwards and Freed (77), that it is not unreasonable to replace each adsorbed <u>chain</u> by a hypothetical <u>point molecule</u> able to move over the volume originally available to the chain. Edwards and Freed found that the pressure which a highly confined polymer molecule exerts on the walls of a rectangular box is "like that of a perfect gas" of m molecules, where

$$m = \frac{\pi^2}{3}(\ell L' / V^{2/3}) \qquad \{50\}$$

and V is the volume of the box. Our polymer is adsorbed so that we may neglect any ideal contributions to the entropy (or pressure).

For real polymer molecules, we may use (as before) $\ell L' = \langle r^2 \rangle$. If we place the volume of the confining box V equal to that of a square box with sides $1.8\langle r^2 \rangle^{\frac{1}{2}}$, we find $m \simeq 1$. Smaller boxes would give larger values for m. Nevertheless, we see that our one-to-one correspondence of adsorbed chains to hypothetical ideal gas molecules is justifiable as a first approximation.

The change in the number of possible positions of our hypothetical point molecule is directly proportional to the change in available volume. Let the ratios of the dimensions of a volume element after deformation to those before deformation be δ_x, δ_y and δ_z. The available volume ratio is therefore:

$$\frac{V}{V_0} = \delta_x \delta_y \delta_z$$

$$= \delta_x \delta_{yz}^2 \quad ,$$

where $\delta_{yz} = \delta_y = \delta_z$ parallel to the surface. The change in entropy of the molecule is:

$$S_{el}^u = -k \ln \frac{V}{V_0} = -k \ln \delta_x \delta_{yz}^2 \quad . \qquad \{51\}$$

The dimensional change δ_x normal to the interface must be equal to the compressional ratio $d/L = \delta$, where L is the thickness of the stabilizer before contact with the second flat plate and d is the separation of the flat plates ($d \leq L$). The entropy change is therefore

$$\Delta S_{el}^u = -k \ln \delta \delta_{yz}^2 \qquad \{52\}$$

for one adsorbed chain.

Having obtained an expression relating the entropy of the confined molecule to the separation of the flat plates, we are confronted with two boundary conditions:

$$\Delta S_{el} = 0 \qquad \text{at} \qquad d = L \qquad \{53\}$$

and

$$\frac{\partial \Delta S_{el}}{\partial d} = 0 \qquad \text{at} \qquad d = L \quad . \qquad \{54\}$$

The first requires repulsion to commence when compression of the stabilizer commences. The second requires the stabilizer layer to be at equilibrium when no external forces are applied (we ignore solvent effects here, assuming them to be separable to a first approximation). Treatment of the adsorbed layer as a confined gas problem satisfies the uniform segment density condition but does not necessarily satisfy the above boundary conditions. There is, however, a convenient method of satisfying these conditions, provided we can make the assumption that lateral expansion of the volume available to the equivalent point molecule occurs during normal compression. We may assume that the entropy components due to dimensional changes of the volume available to the point molecule in the directions normal and parallel to the interface are uncorrelated.

Applying condition {53} to eq.{52} we have

$$\delta_{yz} = 1 \qquad \text{when} \quad \delta = 1 \quad . \qquad \{55\}$$

Applying condition {54} ,

$$-k \frac{\partial}{\partial d} \ln\delta\delta_{yz}^2 = -\frac{k}{L} \frac{\partial}{\partial \delta} \ln\delta\delta_{yz}^2$$

$$= -\frac{k}{L} \cdot \frac{1}{\delta\delta_{yz}^2} \left(\delta_{yz}^2 + 2\delta\delta_{yz} \frac{\partial \delta_{yz}}{\partial \delta}\right)$$

$$= 0 \quad \text{when} \quad \delta = 1 \ .$$

Therefore

$$\frac{\partial \delta_{yz}}{\partial \delta} = -\tfrac{1}{2} \quad \text{when} \quad \delta = 1 \ . \qquad \{56\}$$

The simplest expression for δ_{yz} which obeys eq.{55} and eq.{56} is

$$\delta_{yz} = \frac{3 - \delta}{2} \ . \qquad \{57\}$$

Since there is no justification for using higher order expressions, we shall use eq.{57}. Substitution into eq.{52} yields:

$$\Delta S_{el}^u = -k \ln\delta \left(\frac{3 - \delta}{2}\right)^2 \ . \qquad \{58\}$$

Therefore, the elastic free energy of repulsion is

$$\Delta G_{el}^u = -2kT\nu \ln\delta \left(\frac{3 - \delta}{2}\right)^2 \qquad \{59\}$$

$$= 2kT\nu R_{el}^u \qquad \{60\}$$

where

$$R_{el}^u = -\ln\delta \left(\frac{3 - \delta}{2}\right)^2 \ . \qquad \{61\}$$

Note that by allowing lateral expansion, we have apparently ignored the condition that the segment density remains uniform throughout the stabilizer layer. The layer becomes laterally discontinuous when adjacent polymer molecules overlap. However, we do not introduce this discontinuity into the free energy of mixing expression because it is merely an artifact of this

elastic model (the real chains need not spread at all). In addition, since each polymer molecule is assumed independent of every other polymer molecule in the elastic model, we see that in the final analysis, the stabilizer layer may be considered to be isotropic at all compressions.

Making use of the Derjaguin method (14), we find for the elastic repulsion between coated spheres:

$$\Delta V^{u}_{el} = 2\pi akT\nu L\int_{\delta_0}^{1} R^{u}_{el}\, d\delta$$

$$= 2\pi akT\nu L S^{u}_{el} \qquad \{62\}$$

where

$$S^{u}_{el} = \delta_0 \ln\delta_0 \left(\frac{3 - \delta_0}{2}\right)^{2} - 6\ln\frac{3 - \delta_0}{2} + 3(1 - \delta_0). \qquad \{63\}$$

The integral is terminated at $\delta_0 = 1$ because R^{u}_{el} does not remain mathematically zero at $\delta_0 > 1$ (in reality R^{u}_{el} must be zero at all $\delta_0 > 1$ unless we allow "bridging" to take place (13)).

7.3. Comparison with Flory's Elasticity Theory

At this stage it would be interesting to compare the random flight model and uniform segment density model with the linear deformation of free Gaussian chains.

Flory (42) has derived an approximate expression for the entropy of deformation of an unattached freely jointed chain:

$$\Delta S_{el}^{G} = -k\{(\delta_x^2 + \delta_y^2 + \delta_z^2 - 3)/2 \; - \; \ln\delta_x\delta_y\delta_z\}$$

where the superscript G indicates the Gaussian model and the δ_i retain their previous significance. Replacement of δ_y and δ_z each by δ_{yz} and application of conditions {53} and {54} yield:

$$\delta_{yz} = 1 \quad \text{for all } \delta$$

and

$$\Delta S_{el}^{G} = -k\{(\delta_x^2 - 1)/2 \; - \; \ln\delta_x\} \; . \qquad \{64\}$$

We now have a problem concerning the relationship between δ_x and the compression ratio δ. Monte Carlo calculations (56) indicate that for random flight chains between planar barriers δ_x is proportional to δ after a certain compressional stage is reached; however, as $\delta \to \infty$, $\delta_x \to 1$ and δ_x/δ asymptotically approaches zero. It seems unlikely, therefore, that we can place $\delta_x = \delta$ for a single Gaussian chain. Alternatively, we can consider the chain as one in a network of chains (42), in which case the compressional force will be transmitted equally to all parts of the chain. Uniform dimensional changes result and we may place $\delta_x = \delta$:

$$\Delta S_{el}^{G} = -k\{(\delta^2 - 1)/2 \; - \; \ln\delta\} \qquad \{65\}$$

or

$$\Delta G_{el}^{G} = 2kT\nu\{(\delta^2 - 1)/2 \; - \; \ln\delta\} = 2kT\nu R_{el}^{G} \qquad \{66\}$$

where

$$R_{el}^{G} = (\delta^2 - 1)/2 \; - \; \ln\delta \qquad \{67\}$$

for two surfaces, each having ν associated chains. Equation {66} was used by Smitham et al (48) to describe the elastic repulsion of sterically stabilized particles.

Again, extension to spheres is straightforward (14):

$$\Delta V_{el}^{G} = 2\pi a \nu kTL\ S_{el}^{G} \quad , \qquad \{68\}$$

where

$$S_{el}^{G} = \delta_0 \ln\delta_0 - \delta_0^3/6 - \delta_0/2 + 2/3 \quad . \qquad \{69\}$$

7.4. Simple Approximations and Comparison of Results

Before comparing the three models, we note that by expanding the logarithm in eq.{67} and integrating we can find simple quadratic and cubic approximations for the elastic repulsion parameters:

$$R_{el}^{A} = (1 - \delta)^2 \qquad \{70\}$$

and

$$S_{el}^{A} = (1 - \delta_0)^3/3 \quad , \qquad \{71\}$$

where the superscript distinguishes these quantities as approximations.

Figs.10 and 11 compare the distance dependences of the elastic repulsion parameters for flat plates and spheres respectively. The value of $\xi = 2.1$ was chosen for the random flight case to fit the other curves. This value for the extension parameter lies midway between the values calculated on the basis of number- and weight-average stabilizer molecular weights in section 9. We have assumed that $\langle M_w \rangle / \langle M_n \rangle = 2$; $\langle M_n \rangle$ and L are given in Table 2 (at the end of section 9) for three stabilizer polymers. A more accurate estimate of ξ awaits barrier layer thickness measurements using <u>monodisperse</u> stabilizer polymers adsorbed at one end only.

All models predict similar elastic behaviour. From a theoretical point

of view, the random flight model of Dolan and Edwards is to be preferred. In practice, however, there would be considerable difficulty in experimentally distinguishing the various models. As we pointed out previously, random flight statistics break down for small chains and the number of equivalent freely jointed links in a real chain is probably an order of magnitude less than the number of mer units (47,80). Therefore, if only to retain nominal self-consistency, we shall use the uniform segment density elastic model in conjunction with the uniform segment density mixing (or osmotic) model.

From these results and results for various osmotic models (41) we see that the choice of models does not seriously affect the quantitative predictions of the theory of steric stabilization provided that the barrier layer thickness and amount of adsorbed polymer are determined.

Rewriting equations {59} and {62} we have for flat plates:

$$\Delta G^{u}_{el} = \frac{-2RTL}{\bar{V}_2}\,\bar{v}\ln\delta\left(\frac{3-\delta}{2}\right)^2 \qquad \{72\}$$

and spheres:

$$\Delta V^{u}_{el} = 2\pi a\,\frac{RTL^2}{\bar{V}_2}\,\bar{v}\{\delta_0\ln\delta_0\left(\frac{3-\delta_0}{2}\right)^2 - 6\ln\frac{3-\delta_0}{2} + 3(1-\delta_0)\}\quad , \qquad \{73\}$$

where $\bar{v} = \frac{\nu\bar{V}_2}{N_A L}$

$\bar{V}_2$ is the molar volume of the adsorbed polymer

and N_A is Avogadro's number.

These results and those for the osmotic interaction will now be combined in a theory of the equilibrium disjoining pressure of concentrated sterically stabilized latices.

Fig.10. Elastic interaction parameter for flat plates R_{el} plotted against the reduced distance of separation δ.

Lines: (1) Uniform segment density model (R^{u}_{el}),

(2) Gaussian model (R^{G}_{el}),

(3) Random flight model ($\xi = 2.1$) (R^{R}_{el}),

(4) Quadratic approximation (R^{A}_{el}).

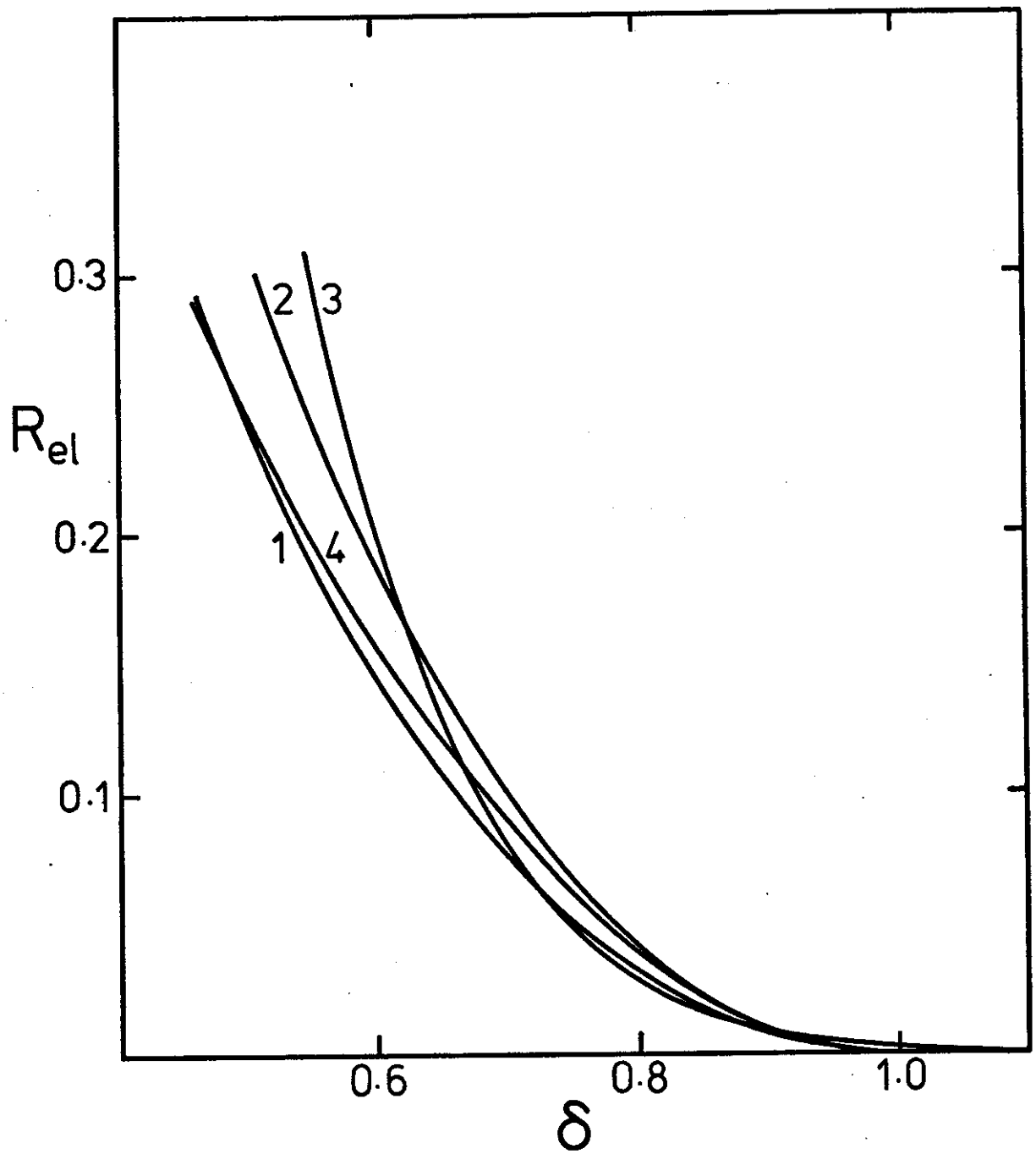
0·3
0·2
0·1
R_{el}
2
3
1
4
0·6
0·8
1·0
δ

Fig.11. Elastic interaction parameters for spheres S_{el} plotted against the reduced distance of separation δ_0.

Lines: (1) Uniform segment density model (S_{el}^{u}),

(2) Gaussian model (S_{el}^{G}),

(3) Random flight model ($\xi = 2.1$) (S_{el}^{R}),

(4) Cubic approximation (S_{el}^{A}).

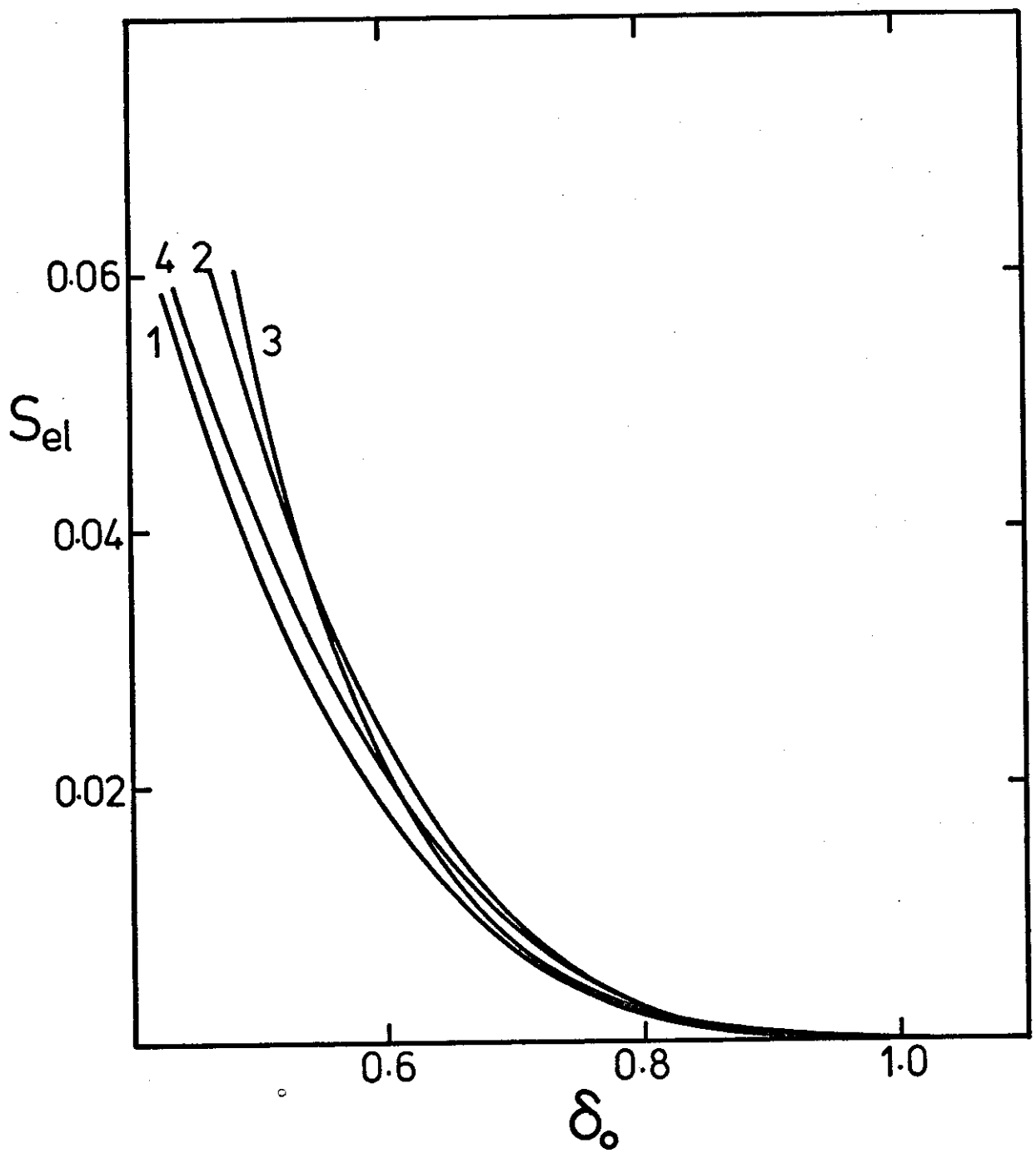
0.06
0.04
0.02
S_{el}
4
2
1
3
0.6
0.8
1.0
δ_o

8. EQUILIBRIUM DISJOINING PRESSURE OF CONCENTRATED LATICES

Experimental studies of the distance dependence of the interaction energy between sterically stabilized particles have been carried out by several authors (50-52,86) using a variety of methods. The most promising (and direct) method appears to be that of the measurement of the equilibrium disjoining pressure of a bulk latex as a function of latex volume (or volume fraction) at constant particle number (50,51). We shall now derive a simple relationship between this disjoining pressure and the separation of the core particles.

When the particles in a stable monodisperse latex are packed close enough to suppress Brownian motion, several workers (83,84,85,86) have found that the latex exhibits a predominantly close-packed structure. It will be assumed in the following treatment that all concentrated latices are close-packed with no defects (see appendix 1.3). At the walls of the container, the particles are considered to form an hexagonal array (85). The overall disordering effect of the surface of the container on the array should be insignificant when the radius of curvature of the container is many orders of magnitude greater than the particle radius. Therefore, the following derivation is equivalent to calculating the pressure on one side of a hypothetical plane inserted into the latex along a slip-plane. Accordingly, we assume that the area A occupied per particle at the wall (or hypothetical plane) is equal to that of a regular hexagon constructed about an inscribed circle of radius $(a + d_0/2)$, where a is the particle radius and d_0 is the surface separation of two adjacent particles:

$$A = 2\sqrt{3}(a + d_0/2)^2 \ . \qquad \{75\}$$

The force on each particle at the wall is transmitted equally to three others, which form the other three apices of a regular tetrahedron. The normal component of the force exerted by each of these three particles on the one at the wall is:

$$F_N = -F\cos\tau$$

where τ is the tetrahedral angle and F is the force along the line of the centres. The total force on the particle at the wall is therefore

$$3F_N = -3F\cos\tau$$

$$= F \quad \text{since } \cos\tau = -\frac{1}{3} \quad .$$

The force exerted per unit area by the latex on the container is simply F/A.

We know the total interaction energy between two sterically stabilized spheres is ΔV_T. The force is

$$F = -\frac{\partial \Delta V_T}{\partial d_0} \quad . \qquad \{76\}$$

We recall that ΔV_T can be obtained from the total interaction energy between flat plates ΔG_T by Derjaguin's method:

$$\Delta V_T = \pi a \int_{d_0}^{\infty} \Delta G_T(d)\,d(d) \quad .$$

Therefore:

$$F = -\frac{\partial}{\partial d_0}\left\{\pi a \int_{d_0}^{\infty} \Delta G_T(d)\,d(d)\right\} \qquad \{77\}$$

$$= \pi a \Delta G_T(d_0) \qquad \{78\}$$

and the total pressure on the walls of the container is

$$P_T = F/A = \frac{\pi a \Delta G_T(d_0)}{2\sqrt{3}(a + d_0/2)^2} \quad . \qquad \{79\}$$

It must be remembered that the derivation of this expression relies on the validity of the Derjaguin approximation and is therefore subject to the condition that the particle radius be considerably greater than the steric barrier thickness L or the range of the interaction. Under this condition and provided that the latex is stable in order for it to adopt a predominantly close-packed configuration, eq.{79} is a general expression for the disjoining pressure in a concentrated, monodisperse latex.

This pressure is the sum of four principal component pressures:

$$P_T = P_{os} + P_{el} + P_e + P_A \ ,$$

where P_{os} = excess osmotic pressure due to mixing of polymer ,

P_{el} = elastic pressure ,

P_e = electrostatic osmotic pressure. ,

P_A = van der Waals pressure of attraction.

The present theory deals with uncharged particles and stabilizers ($P_e = 0$). Additionally, we assume, for the time being, that the van der Waals attraction is negligible compared with the osmotic and elastic terms ($P_A \simeq 0$). There are two remaining contributions:

$$P_{os} = \frac{\pi a \Delta G_{os}(\delta_0)}{2\sqrt{3}(a + d_0/2)^2} \ , \qquad \{80\}$$

$$P_{el} = \frac{\pi a \Delta G_{el}(\delta_0)}{2\sqrt{3}(a + d_0/2)^2} \quad . \qquad \{81\}$$

Using eqs.{34} and {72} (uniform segment density model):

$$P^u_{os} = \frac{\pi a RTL}{\sqrt{3}(a + d_0/2)^2 \bar{V}_1} (\tfrac{1}{2} - \chi_1)\bar{v}^2(2/\delta_0 - 1)\{1 + \frac{\bar{v}}{3}(2/\delta_0 + 1)\} \qquad \{82\}$$

and

$$P^u_{el} = \frac{\pi a RTL\bar{v}}{\sqrt{3}(a + d_0/2)^2 \bar{V}_2} \ln \frac{4}{\delta_0(3 - \delta_0)^2} \quad . \qquad \{83\}$$

Therefore, the excess pressure of a concentrated uncharged latex due to the osmotic and elastic terms is:

$$P^u_T = \frac{\pi a RTL}{\sqrt{3}(a + d_0/2)^2 \bar{V}_1} (\tfrac{1}{2} - \chi_1)\bar{v}^2(2/\delta_0 - 1)\{1 + \frac{\bar{v}}{3}(2/\delta_0 + 1)\} + \bar{v}\frac{\bar{V}_1}{\bar{V}_2} \ln \frac{4}{\delta_0(3 - \delta_0)^2} \qquad \{84\}$$

when $\delta_0 < 1$, and

$$P^u_T = \frac{\pi a RTL}{\sqrt{3}(a + d_0/2)^2 \bar{V}_1} (\tfrac{1}{2} - \chi_1)\bar{v}^2(2/\delta_0 - 1)\{1 + \frac{\bar{v}}{3}(2/\delta_0 + 1)\} \qquad \{85\}$$

when $1 \leq \delta_0 \leq 2$.

These expressions require the following data:

1. particle radius (a)
2. distance of separation of particles (d_0)
3. molar volume of solvent ($\bar{V}_1$)
4. barrier layer thickness (L)
5. surface concentration of adsorbate (ω)

6. specific volume of adsorbate (v_{sp})

7. molecular weight of adsorbate (M)

where $\omega v_{sp}/L = \bar{v}$, $d_0/L = \delta_0$ and $Mv_{sp} = \bar{V}_2$.

In practice, δ_0 or d_0 must be calculated from the volume fraction of core particles. We include in appendix 1.3 a derivation of the relationship between the core particle volume fraction (ϕ_p) and the separation parameter (δ_0).

Also, in appendix 1.4, we perform a brief calculation justifying the neglect of van der Waals attraction in our disjoining pressure theory. The above proposed theories will now be tested using experimental results from the literature.

9. INTERPRETATION OF EXPERIMENTAL RESULTS REPORTED IN THE LITERATURE

Very little experimental work has been done on the distance dependence of the interaction between sterically stabilized colloidal particles. The results of four studies will be examined here in terms of our uniform segment density model. In general, comparisons between theory and these results are difficult to make because the systems studied are not readily describable in terms of any theoretical model so far proposed. The difficulties arise mainly from the experimental use of one or more of the following:

(1) short stabilizer chains

(2) very high segment densities

(3) polydisperse stabilizer chains

(4) polydisperse core particles .

Nevertheless, the values of the parameters required to fit the experimental data can be justified, to some extent, by comparison with values from independent sources.

9.1. Doroszkowski and Lambourne (52), using a surface balance technique, found the repulsion between polyacrylonitrile (PAN) spheres sterically stabilized by PS in toluene at 297 K. Fig.12, line 1, represents the experimental distance dependence of the repulsion. The authors computed the repulsion potential per particle by assuming hexagonal packing in the particulate monolayer. Electron microscopy studies substantiated this assumption.

We have chosen the barrier layer thickness L to be 14.5 nm, which is equal to the average contour length of the stabilizer (molecular weight = 6000).

This is consistent with Doroszkowski's and Lambourne's empirical estimation of the barrier layer thickness (15 nm), although later we shall discuss reasons for possible overestimation of this thickness. The surface concentration ω of PS stabilizer was measured chemically as 5.2×10^{-8} g cm^{-2}. This figure, together with the specific volume v_{sp} of PS (0.95 cm^{3}g^{-1}) and the barrier layer thickness, yields the average volume fraction of PS in the stabilizer layer:

$$\bar{v} = \omega v_{sp}/L = 0.034 \quad .$$

The only other parameters required are χ_1 and χ_2. Although we have shown that, for many systems, $\chi_2 \simeq 2\chi_1/3$, the system under consideration is a known exception. We have examined the experimental data of Schick et al (87) and Gandhi and Williams (88), who measured the osmotic pressures of moderately concentrated PS solutions in toluene. Our conclusion is that, within experimental error, χ is almost independent of concentration and has a small tendency to decrease with increasing concentration. Accordingly, we have chosen $\chi_2 = 0$. It is assumed that $(\frac{1}{3} - \chi_2)$ is much less sensitive to changes in molecular weight than is $(\frac{1}{2} - \chi_1)$, since χ_1 is close to $\frac{1}{2}$ and χ_2 far from $\frac{1}{3}$. The value of χ_1 has been obtained (41) from viscosity measurements on toluene solutions of PS having a similar molecular weight to that of the stabilizer used by Doroszkowski and Lambourne. The parameters found were:

$$\psi_1 = 0.07$$

$$\chi_1 = 0.47 = \tfrac{1}{2} - \psi_1(1 - \Theta/T) \quad ,$$

where Θ = 160 K (42), T = 297 K and ψ_1 is the entropy of dilution parameter (42). As we have not used the relationship $\chi_2 = 2\chi_1/3$ we must calculate the osmotic repulsion on the basis of eq.{35}. Accordingly:

$$V_{os}^{u} = 4\pi a \frac{RTL^2}{\bar{V}_1} \bar{v}^2 \left[(\tfrac{1}{2} - \chi_1)(\ln \frac{2}{\delta_0} + \frac{\delta_0}{2} - 1) + \frac{\bar{v}}{2}(\frac{1}{3} - \chi_2)(\frac{2}{\delta_0} + \frac{\delta_0}{2} - 2) \right] + O(\bar{v}^4). \quad \{86\}$$

When $d_0 < L$, we add the contribution from the elastic effect, as represented by eq.{73}.

The data for this system and the three systems to be discussed later are listed in Table 2. Fig.12 compares the predictions of our theory (line 1) and the experimental results of Doroszkowski and Lambourne. Agreement is excellent for separations greater than 10 nm, especially in view of the fact that virtually no adjustment of parameters is required. Line 2 is the result according to the denting model of Bagchi (25) and line 3 indicates the effect of ignoring the third virial coeffecient. The denting model overestimates the interaction energy by a factor of about two because the elastic term starts at $d_0 = 2L$, while neglect of the third virial coefficient (represented by $(\frac{1}{3} - \chi_2)$) underestimates the interaction energy at intermediate separations.

All theoretical predictions asymptotically approach infinity as $d_0 \to 0$. We suspect that the experimental points at close separations, as drawn on the graph, do not represent the true behaviour of the particulate monolayer. The experimental curve suggests that the repulsion increases steadily to a finite value on contact of the core particles, whereas the intervening stabilizer would have reached its solid state density at approximately 1 nm separation. Experiments on other systems (50,86) suggest that the repulsion does indeed rise almost vertically as the particles approach to a finite surface separation. One possible reason for the absence of a steep rise in the interaction curve from the surface balance experiments is that the monolayer may tend to expel

Fig.12. Interaction potential V_T versus the minimum surface separation d_0 of two PAN spheres stabilized by PS in toluene.

Dashed line and points: experimental results of Doroszkowski and Lambourne (52),

Lines: (1) theoretical calculation based upon data in Table 2 and eqs.{73} and {85},

(2) theoretical prediction of denting model (25),

(3) as for line 1, but with $\chi_2 = \frac{1}{3}$ (i.e., ignoring terms of $O(\bar{v}^3)$ and higher).

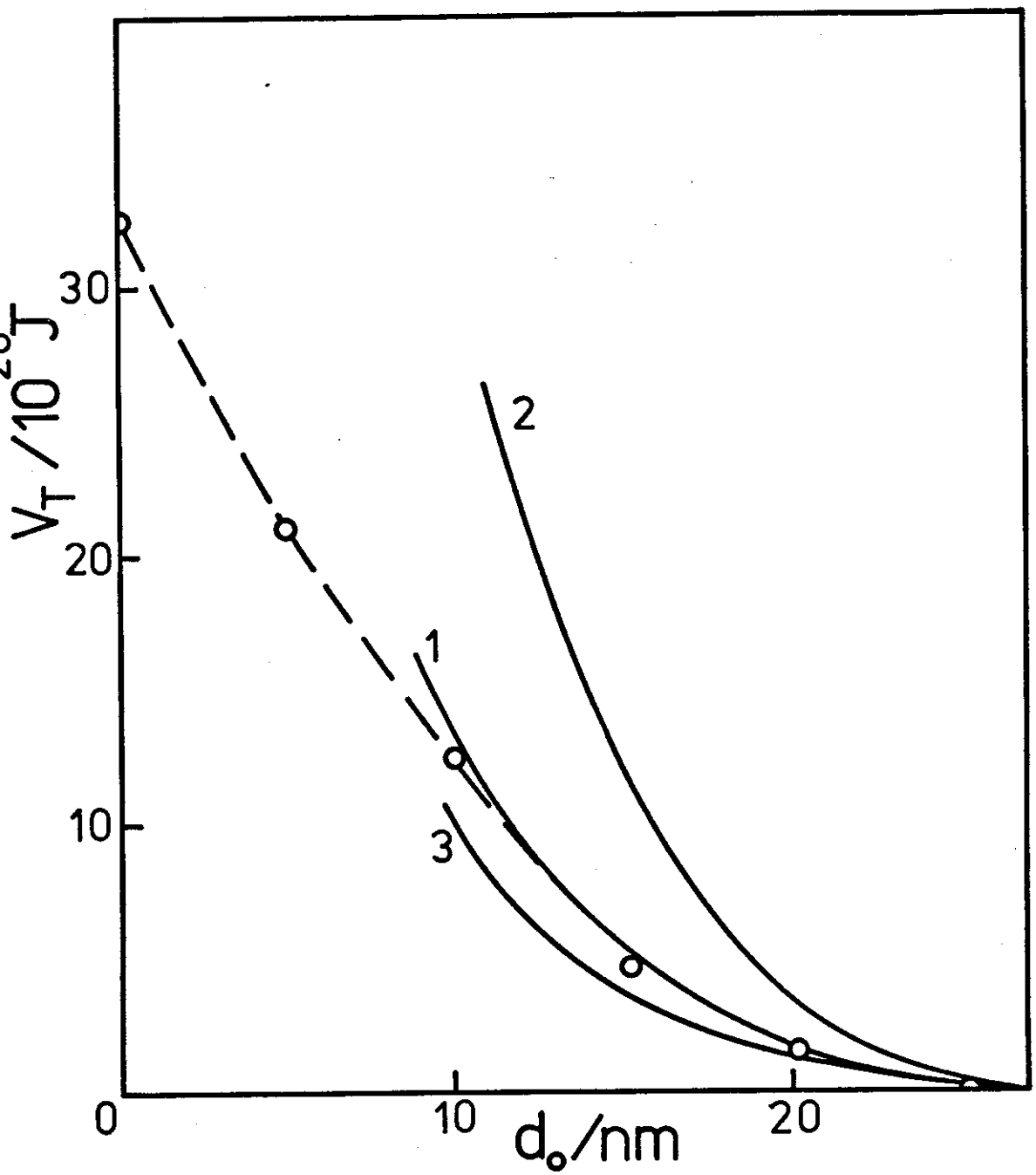
$V_T / 10^{-20} J$
30
20
10
0
10
20
d_o / nm
1
2
3

particles under high compressive forces, particularly since the monolayer units are spherical and the only force preventing upward displacement of a particle appears to be gravitational. The volume of the added dispersion in toluene was approximately 0.01 cm^3; the total area of the monolayer was of the order of 100 cm^2, therefore the thickness of the toluene layer was approximately 1000 nm, assuming negligible evaporation. No contact with the toluene/air interface by the particles (diameter 200 nm) is possible if the monolayer is supported at the water/toluene interface. Therefore, the toluene/air interface is unlikely to oppose the upward displacement of particles. The vertical component of the compressive force on each particle is small only while the centre of each particle remains close to the plane of centres. Even a small degree of polydispersity would result in large vertical forces at high compressions. Any particles significantly larger or smaller than the mean would probably be expelled from the layer rather easily. Unfortunately, the micrograph of the PS latex published in ref.52 is not sharp enough to permit a reasonable estimate of the particle size distribution. However, in a separate paper, Doroszkowski and Lambourne (40) published an electron micrograph of a compressed dispersion with the same degree of polydispersity as the one studied here (coefficient of variation ~6%). Several particles much larger than the mean are evident. The total area occupied by these large particles is approximately 5% of the area occupied by all other particles. Our calculations indicate that a 5% reduction in monolayer area caused by vertical expulsion of these particles would result in a 25% increase in the apparent barrier layer thickness (the true thickness being 20% less than the measured thickness). The onset of repulsion would involve these large particles, but they would not be accounted for at high compressions. Even the presence of only 1% of area due to large particles

could result in an overestimate of ~0.6 nm of the barrier layer thickness. This could be achieved by having only one particle in four hundred with a diameter twice that of the mean. The expulsion of particles having a diameter close to the mean would require much more energy than the expulsion of a particle with a diameter far from the mean. The lack of a vertical rise in the experimentally measured repulsion may be due to successive expulsion of particles different from, but approaching the mean.

An alternative explanation is that the point of complete barrier collapse may have been chosen at too great a distance of particle separation. Extrapolation of the pressure-area isotherms to zero pressure gives a reasonable estimate for the area per particle, however, the area under the isotherm (which is integrated to yield the energy of repulsion) must be extremely sensitive to the position of the asymptote cutting the area axis. A slight shift of this asymptote toward a smaller area would result in a very large increase in the calculated energy of repulsion at small distances.

For the above reasons, we believe that the surface balance technique is most useful for determining repulsive forces at large distances of separation, where the forces are comparatively small, but may be misleading at close separations, especially if the compressive energy can be dissipated by processes other than steric barrier collapse.

We have not as yet determined whether our theory predicts flocculation under worse than Θ-conditions for the stabilizing moieties. Doroszkowski and Lambourne (52) have examined a system comprised of PAN particles coated with

PS in cyclohexane at ~9 K below the Θ-temperature for free PS in cyclohexane (~306 K(59,75)). They found a residual repulsion between the particles even though the latex was seen to be flocculated (52). For the PS/cyclohexane system at the Θ-point, detailed information is available concerning the concentration and temperature dependence of χ (59,75). Koningsveld et al (59) have found that their results are best fitted by:

$$\chi = 0.2035 + 90.65/T + 0.3092v_2 + 0.1554v_2^2 ,$$

and Kuwahara et al found:

$$\chi = 0.2798 + 67.50/T + 0.3070v_2 + 0.2589v_2^2 .$$

Using the results of Koningsveld et al (59), we have:

$$\chi_1 = 0.2035 + 90.65/T ,$$

$$\chi_2 = 0.3092$$

and

$$\chi_3 = 0.1554 .$$

These parameters can be used in eq.{35} along with the data in Table 2. Note that L is smaller in cyclohexane near Θ ($\alpha \simeq 1$) than in toluene ($\alpha = 1.057$ (41)) by the factor α.

Fig.13 compares the prediction of our theory with the experimental results of Doroszkowski and Lambourne (52). The van der Waals attraction has been added in line 3. This attraction has little overall effect. The use of Kuwahara's expression for χ yields similar results to those in Fig.13. As with the PS/toluene system, the experimental curve approaches a finite value of repulsion as δ_0 approaches zero and we have mentioned possible explanations for this behaviour.

Fig.13. Interaction potential V_T versus minimum surface separation d_0 of two PAN spheres stabilized by PS in cyclohexane at ~8 K below Θ.

Lines: (1) experimental results of Doroszkowski and Lambourne,

(2) theoretical calculation based upon data in Table 2 and results of Koningsveld et al (59) using eqs.{35} and {73},

(3) as for line 2 but including the van der Waals attraction term with a Hamaker constant of 2.3×10^{-21} J. (see chap.IV).

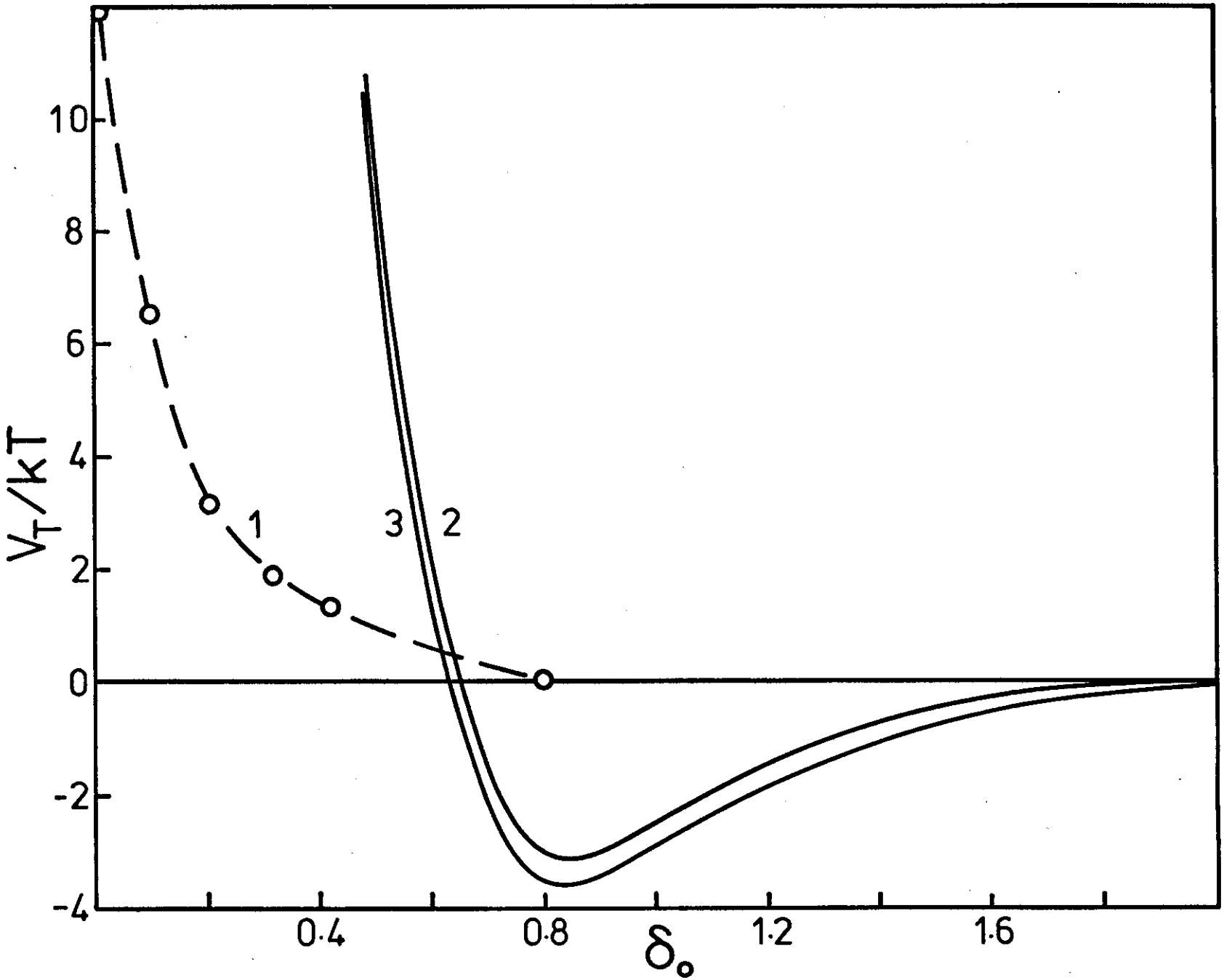
10
8
6
4
2
0
-2
-4
V_T/kT
1
3
2
0·4
0·8
1·2
1·6
δ_o

The depth of the minimum in the theoretical curve is almost 4kT, which is probably sufficient to cause the observed flocculation (52). We believe, however, that this depth may be underestimated. Kuwahara et al (75) have indicated that trace quantities of water in the cyclohexane may increase Θ by up to 2 K. Doroszkowski and Lambourne (52) spread the cyclohexane dispersion medium over water so that their system was probably saturated with water. It is possible that the value of Θ (under their experimental conditions) was at least 308 K and perhaps much higher. The energy minimum in Fig.13 would then be at least 5kT deep. In any case, in flocculated systems, close packing of spheres is not usually found (52,86). In view of this and other complications due to viscous interactions between stabilizer layers (41), the quantitative interpretation of the experimental results in Fig.13 is much more difficult than for stable systems.

It is worth noting that the magnitude of the osmotic interaction is inversely proportional to the solvent molar volume $\bar{V}_1$. In general, because of the relatively small intermolecular interactions involved, most non-aqueous solvents have much higher molar volumes than water in order to exist as liquids at ordinary temperatures. All other things being equal, we expect that aqueous latices ($\bar{V}_1 \simeq 18$ cm^3mol^{-1}) would flocculate much closer to Θ than non-aqueous latices.

9.2. Homola (51) measured the equilibrium swelling or disjoining pressure of concentrated PS latices stabilized by PEO in aqueous media. His technique was to measure directly, by means of a pressure transducer, the equilibrium pressure in a latex confined between a semi-permeable membrane and a mercury "piston". The pressure was applied by accurately raising the temperature of a silicone oil reservoir, which was connected directly to the mercury "piston", and the volume change resulting from thermal expansion was calculated from a previously determined calibration equation. The possible error in the calculation of the particle separation was estimated to be of the order of 1 nm.

One of the first points to be noted about Homola's results is that the pressure/volume curves show a fairly abrupt increase in the rate of pressure rise near the region of total stabilizer overlap. We would expect this phenomenon on the basis of our theoretical model (and other entropy plus solvency models): after the stabilizer layers have become fully interpenetrated, the osmotic pressure increase is supplemented by the large elastic effect. Fig.14 compares our fitted theoretical curve with Homola's results for a latex stabilized by PEO of mean molecular weight 2200. This latex was compressed at pH 3.0 under which conditions, Homola states that the zeta-potential of the particles was practically zero. The form of the distance dependence as predicted by our theory agrees very well with the measured distance dependence. The absolute magnitude of the interaction is also readily explicable in terms of a realistic choice of the interaction parameter χ_1, the only adjustable parameter.

Viscosity measurements have been performed (2) using moderately high molecular weight (100,000) PEO in water gave:

$$\psi_1 \simeq -0.07$$

and

$$\Theta \simeq 390 \text{ K} .$$

However, Flory has shown (42) that experimental values for the ratio $(\alpha^5-\alpha^3)/M^{\frac{1}{2}}$ decrease in magnitude with decreasing molecular weight (α is the intramolecular expansion factor and M is the molecular weight). This ratio is directly proportional to the entropy of dilution parameter ψ_1. The value of ψ_1 required to fit Homola's data is -0.026. A threefold decrease in the magnitude of ψ_1 appears to be quite reasonable on going from M = 100,000 to M = 2200. The value of χ_1 that we require is

$$\chi_1 = \tfrac{1}{2} - \psi_1(1 - \Theta/T)$$

$$\simeq 0.492 \quad \text{at} \quad T = 298 \text{ K}$$

and in the absence of any evidence to the contrary, we use $\chi_2 = 2\chi_1/3$. The value of L as indicated by the experimental results is ~9.0 nm, which is approximately half the average contour length of the stabilizer chains, and the weight of stabilizer per unit area ω was measured as ~1.5×10^{-7} g cm^{-2} (modified to account for the anchor polymer). From these figures and the specific volume of PEO ($v_{sp} = 0.885$) we can determine $\bar{v}$:

$$\bar{v} = \omega v_{sp}/L = 0.1475 .$$

The required data has been listed in Table 2. Application of eqs.{36} and {73} yields the theoretical curve depicted in Fig.14.

It appears that this three-dimensional compression method, although requiring more sophisticated apparatus, is preferable to the two-dimensional compression method of Doroszkowski and Lambourne. In principle, both methods

Fig.14. Disjoining pressure P_T of a PS latex stabilized by PEO in water as a function of the minimum surface separation d_0 of core particles.

Lines: (1) experimental results of Homola (51),

(2) theoretical curve calculated on the basis of the data in Table 2 and eqs.{84} and {85}.

Perfect close-packing is assumed.

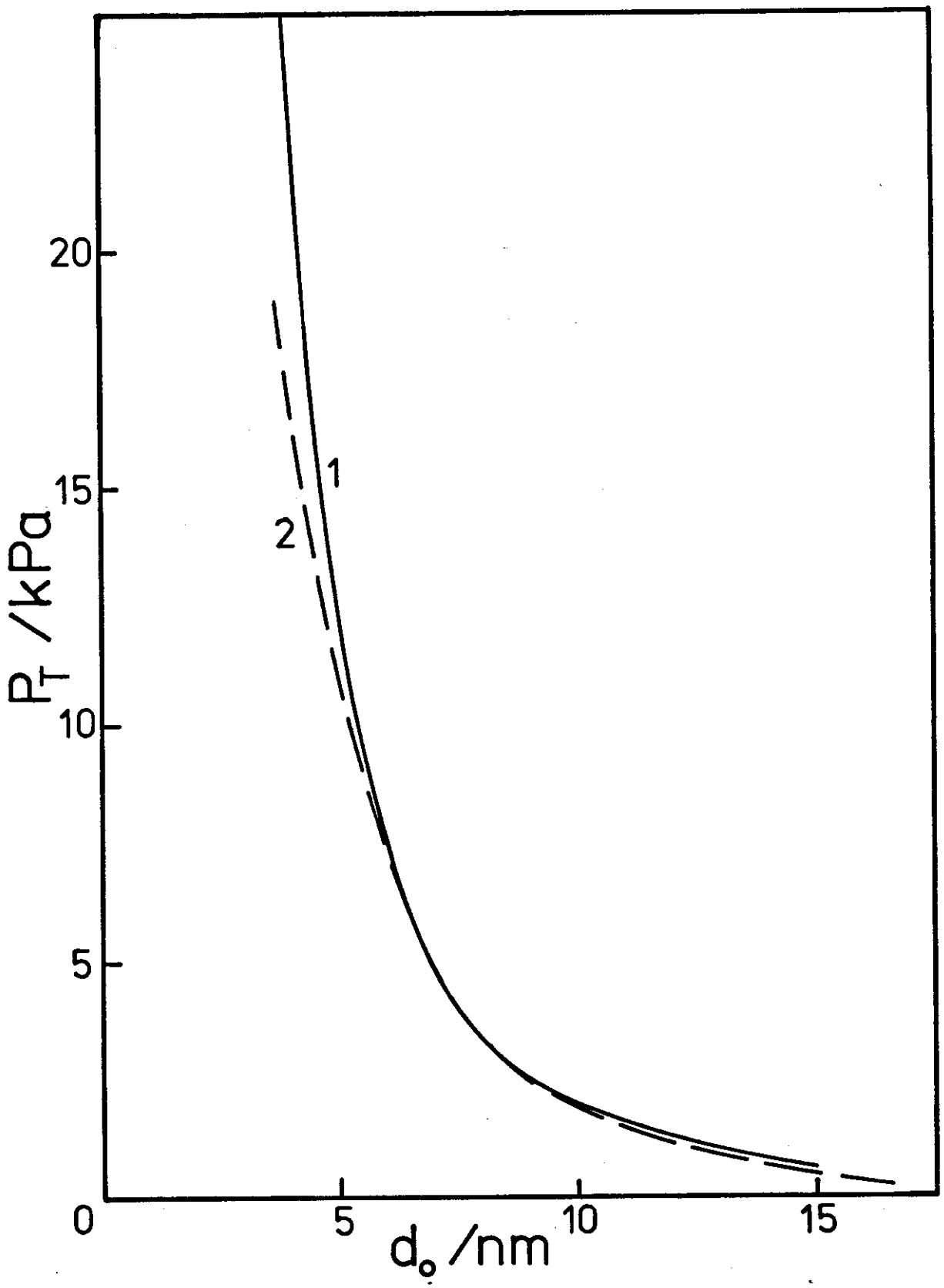
20
15
10
5
0
P_T /kPa
1
2
5
10
15
d_o /nm

should give the same results. In practice, the surface balance method is extremely sensitive to impurities, excess stabilizer, deviations from particle monodispersity and interpretation of the pressure/area curves. Admittedly, Homola's method requires an absence of excess stabilizer and requires particle monodispersity but apparently suffers much less if these conditions are not quite met. For example, if a few particles larger than the average are present in the three-dimensional latex, the worst that can happen is local disruption of the array and this disruption is likely to be fairly constant during compression. There is no opportunity for expulsion.

9.3. Cairns and Ottewill (50) were the first to use the three-dimensional compression method for the study of steric repulsion between latex particles stabilized by adsorbed polymer. Their method differed from that of Homola in that the independent variable was the pressure. The volume of the latex was monitored using a capacitance technique. Stabilizer used by Cairns and Ottewill - poly(12-hydroxystearate)(PHS) side chains on a poly(methyl methacrylate) (PMMA) backbone - appears to be the same as that used by Doroszkowski and Lambourne in one of their sets of surface balance experiments (40). Even the molecular weights correspond. Doroszkowski and Lambourne measured the surface concentration of their stabilizer as ~5 × 10^{-8} g cm^{-2}, which remained reasonably constant over a range of particle sizes from 140 nm to 610 nm diameter. In addition, the average thickness of the stabilizer barrier was measured (using the surface balance) to be ~13.0 nm, the range of thickness being 10.0-14.5 nm, where the lower value was measured using the most monodisperse latex (coefficient of variation 12.4%). They also cite a range of barrier thicknesses obtained by hydrodynamic measurements using similar polymers. This

range is 7.0 nm to 10.0 nm (40). Barsted et al (55), who obtained a hydrodynamic thickness of 6.2 nm using a very similar polymer, mention that viscosity measurements probably underestimate the true barrier layer thickness.

We have already discussed the possibility of overestimation of barrier thickness as obtained by the surface balance method using polydisperse particles. The particles used by Doroszkowski and Lambourne (40) were far from being monodisperse: the coefficient of variation ranged from 12.4% to 28%. The value we have chosen for L is a mean of the hydrodynamic thicknesses, L = 8.5 nm, which is slightly less than the average contour length of the stabilizer and nearly 40% larger than the value obtained by Barsted et al (55). Proceeding as before, we find the mean volume fraction of segments in the stabilizer layer:

$$\bar{v} = \omega v_{sp}/L \simeq 0.064 \ ,$$

where (1) $v_{sp} \simeq 1.09$.

It remains only to assign a value to χ_1 (again, we assume that $\chi_2 = 2\chi_1/3$). Napper (2) has determined the enthalpy and entropy of dilution parameters, κ_1 and ψ_1 respectively, for the similar system PHS in n-heptane:

$$\kappa_1 = 0.2$$

$$\psi_1 = 0.3 \ ,$$

which yield (42):

$$\chi_1 = \tfrac{1}{2} - \psi_1 + \kappa_1 = 0.4 \ .$$

Experimental studies of mixtures of n-alkanes with polyethylene (PE) (89), polyisobutylene (PIB) (90) and poly(dimethyl siloxane) (PDMS) (90) indicate

that solubility increases with increasing n-alkane chain length. From these observations we can infer that, in general, for polymer/n-alkane mixtures, χ_1 decreases with increasing n-alkane chain length since the free energy of mixing becomes less negative as χ_1 increases. Thus, we would expect for the PHS/dodecane system:

$$\chi_1 < 0.4 \quad .$$

We have chosen $\chi_1 = 0.3$ and 0.4 for our theoretical comparison with the results of Cairns and Ottewill.

Fig.15 assumes perfect close packing of monodisperse spheres, under which conditions the theoretical curve (line 2) asymptotically approaches $\phi_p = 0.740$, where ϕ_p is the volume fraction of particles in a latex. The volume fraction limit to which the experimental curve approaches (vertical line) was estimated from the pressure/volume fraction curve, including the condition that the spheres can approach no closer than 1.1 nm, which is the point at which the intervening stabilizer polymer reaches its solid state density. This limiting volume fraction is $\phi_0 = 0.578$.

We can make some allowance for deviations from perfect close packing in our theoretical model (see appendix 1.3). Substitution of $\phi_0 = 0.578$ into eq.{99} yields:

$$\phi_{pm} = 0.578(1 + d_0/2a)^{-3} \quad , \qquad \{87\}$$

where ϕ_{pm} is the measured volume fraction of particles. Fig.16 compares the theoretical and experimental results when eq.{87} is used to find the core particle volume fraction. Improvement over the fit in Fig.15 is significant; however, the theoretical curves appear much too extended. Further attempts to

Fig. 15. Comparison of experimental and theoretical disjoining pressure P_T versus the particle volume fraction ϕ_p plots for PMMA particles stabilized by PHS in dodecane.

Lines: (1) experimental results of Cairns and Ottewill (50),

(2) theoretical curve based on the data in Table 2 and eqs.{84} and {85} ($\chi_1 = 0.3$).

Perfect close-packing is assumed. The vertical line at $\phi_p = 0.578$ indicates the estimated point of core particle contact.

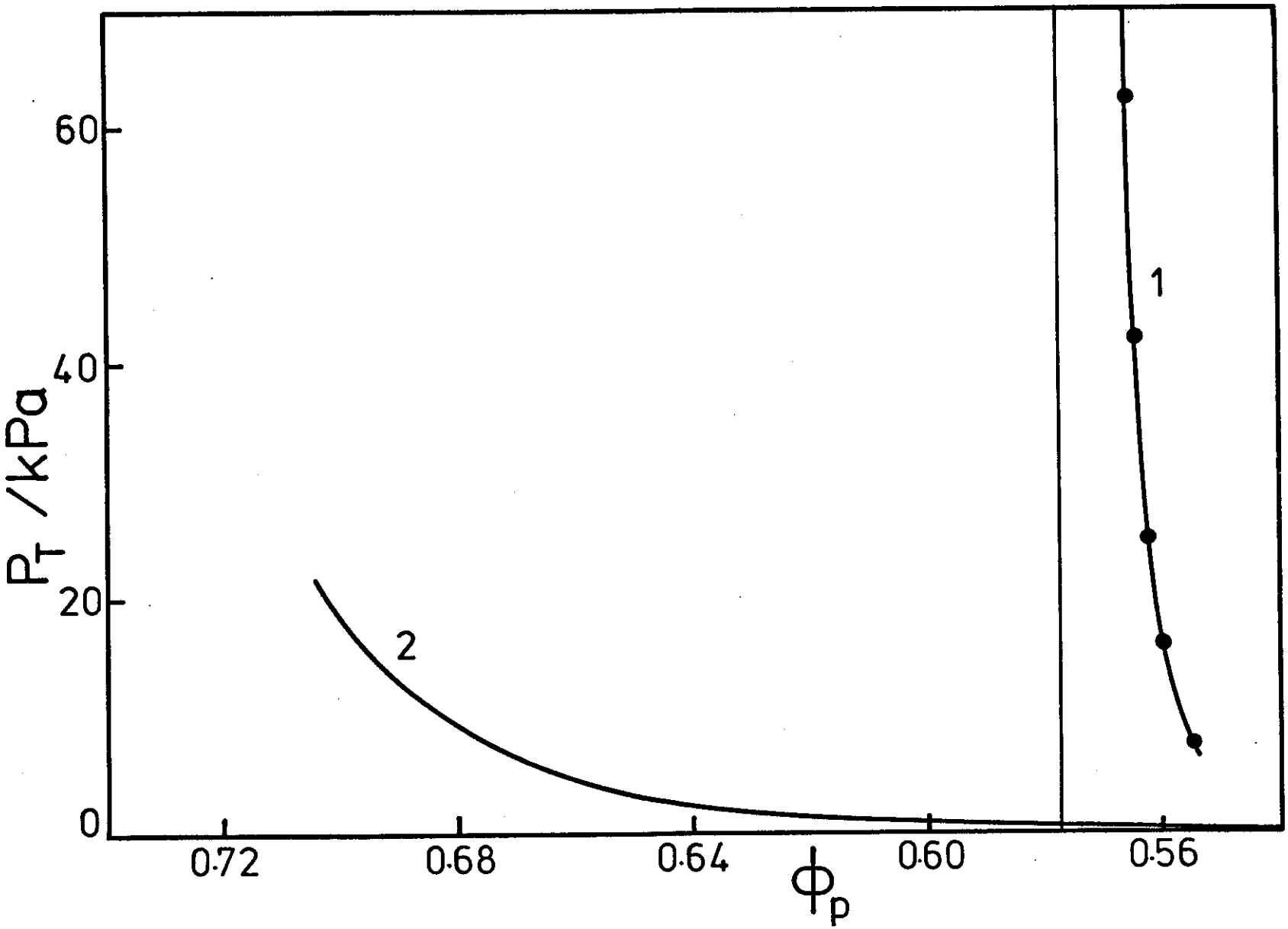
60
40
20
0
P_T /kPa
0.72
0.68
0.64
0.60
0.56
Φ_p
1
2

Fig.16. Comparison of experimental and theoretical disjoining pressure P_T versus particle volume fraction ϕ_p plots for PMMA particles stabilized by PHS in dodecane.

Lines: (1) experimental results of Cairns and Ottewill (50),

(2) theoretical curve based on data in Table 2 and eqs.{84} and {85} ($\chi_1 = 0.3$),

(3) as for line 2 but with $\chi_1 = 0.4$.

Perfect close-packing is not assumed.

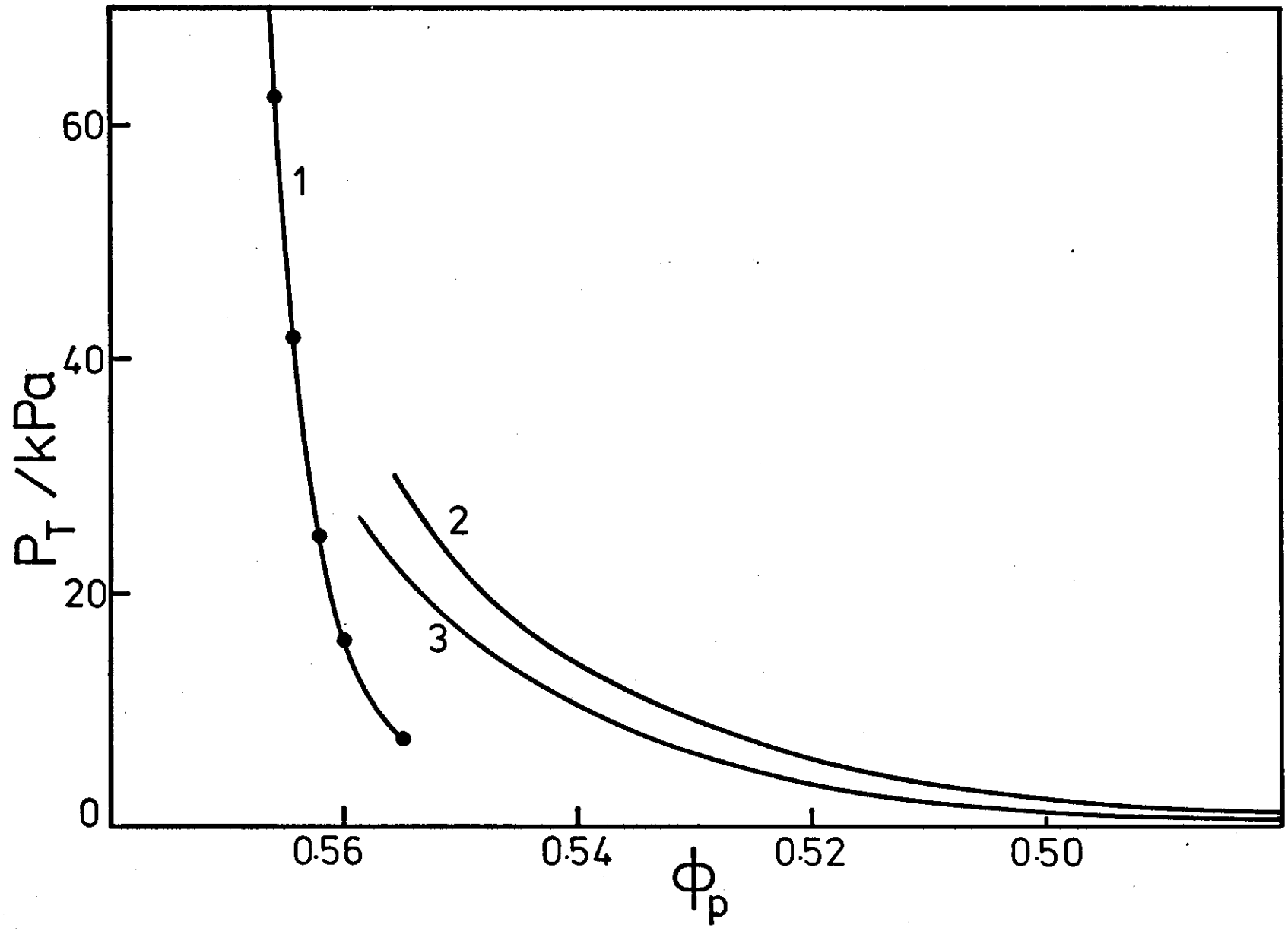
60
40
20
0
P_T /kPa
1
2
3
0·56
0·54
0·52
0·50
Φ_p

improve the fit result in unrealistic values for the barrier layer thickness (e.g., 1.6 nm). Indeed, the experimental points appear to span a particle separation range of only 0.1 nm according to eq.{98}.

One explanation of the discrepancy between theory and experiment is that the particles may have swollen slightly during the many weeks they were in contact with dodecane. We have already mentioned above that the solubility of many polymers in n-alkanes increases with increasing n-alkane chain length. An increase in the radius of the particles of ~5% would easily account for much of the difference between the observed and calculated results.

9.4. Andrews, Manev and Haydon (82) utilized the thinning behaviour of sterically stabilized optically black films to determine the distance dependence of the steric interaction. The films were formed in aqueous media from solutions of glyceryl mono-oleate in aliphatic hydrocarbons. Thinning was induced by the application of an electrical potential across the film and the thickness was measured by a capacitance technique. Only the n-decane film was studied in detail.

The results of Andrews et al cannot be satisfactorily interpreted using our model because:

i) the mean stabilizer concentration in the film was found to be 73%, which is approximately five times greater than the maximum allowable concentration,

ii) the edges of the film probably do not constitute impenetrable barriers as required by our model,

iii) the glyceryl mono-oleate stabilizer is extremely small: the oleate

chain containing only seventeen bonds or the equivalent of nine segments in a polyolefin chain.

The question arises as to whether the interaction is predominantly elastic or osmotic; even Born repulsion may be significant. Their relative importance is undetermined. We can only agree with Andrews et al when they conclude that the high compressibility of the film is probably due to the interaction of a very few of the oleate chains present. They infer from thickness measurements that the small number of chains which do interact are close to the fully extended state.

TABLE 2

SYSTEM PARAMETERS

Parameter	Doroszkowski and Lambourne *	Homola	Cairns and Ottewill
a/nm	100	170	77.5
L/nm	14.5 (13.7)	9.0	8.5
T/K	297	298	298
$\bar{V}_1$/cm^3 mol^{-1}	106 (110)	18	228
$\bar{V}_2$/cm^3 mol^{-1}	5700	1950	1760
M/g mol^{-1}	6000	2200	1600
ω/g cm^{-2}	5.2×10^{-8}	1.5×10^{-7}	5.0×10^{-8}
v_{sp}/cm^3 g^{-1}	0.94	0.885	1.09
$\bar{v}$	0.034 (0.036)	0.148	0.064
χ_1	0.47 (see text)	0.492	0.3 , 0.4
χ_2	0 (see text)	0.328	0.2 , 0.267

* Bracketed figures refer to latex in cyclohexane.

10. CONCLUSIONS

The need for experimental studies on model latices is evident from our comparison of theory with the few observations available. Model latices should have the following basic properties:

1. Monodisperse, spherical core particles.
2. Monodisperse stabilizer chains.
3. Moderate to high molecular weight stabilizer chains (e.g., $M \geq 10^5$).
4. Reasonably large a/L ratio (to ensure validity of the Derjaguin approximation).
5. Good stabilizer anchoring.
6. Uncharged particles and stabilizer (unless electrostatic effects are negligible, as in the presence of high ionic strength media).
7. No interactions between stabilizer segments and particle surface (apart from the intended anchor segment/surface "bond").
8. No tendency of the solvent medium to swell the particles.

In addition, it may be desirable for the latex to have certain properties which facilitate the observation of its behaviour. For example, if capacitance measurements are used to find the volume of the latex under compression (50), the particles should ideally have the same permittivity as the medium and stabilizer (although the stabilizer p ermittivity is much less critical - see end of chapter on van der Waals attraction). On the other hand, monitoring of the latex by light scattering methods requires that the particles and medium have different refractive indices (and permittivities). Finally, low molecular weight solvent media are preferable in order to obtain osmotic equilibrium

rapidly.

A typical model latex might be PAN particles (a = 300 nm) stabilized by PIB ($M = 10^5$) in benzene at $T \geq 298$ K. This latex would be well suited to the high frequency capacitance method of volume measurement, since the dielectric permittivities of the particles and medium are 2.304 and 2.244 respectively. Furthermore, the latex is easily cooled to the Θ-point (68) of PIB in benzene (297.5 K), allowing studies of latex stability near this critical point. One difficulty, which may be encountered during the preparation of this latex, is unwanted grafting during formation of the stabilizer. PIB has been found to hydrogen-abstract very easily in the presence of free-radical initiators (99,100), which would result in polydisperse stabilizer loops. An obvious solution would be to use anionic polymerization methods to form the stabilizer copolymer as an unbranched chain (e.g., poly(isobutylene-b-acrylonitrile)).

With regard to the small amount of evidence so far available, we have found that it supports our free energy of interaction theory and our disjoining pressure theory. Furthermore (and in some ways, more importantly), our theory predicts the experimentally observed correlation between the Θ-point and the critical flocculation point. From a practical point of view, the distance dependence of the interaction is often of secondary importance to the critical flocculation point. The steric interaction is usually so strong (in the absence of desorption) that the stability ratio is either 0 or 1; we need to know whether or not the latex is stable rather than how fast it flocculates. Therefore, theories which fail to predict the known critical flocculation point are either incompletely formulated (e.g., Bagchi (25), Dolan and Edwards (44)) or

require quantitative adjustment (e.g., Meier (12), HVO (13)). This is also the reason that the solvency theories, although incompletely formulated, are perhaps preferable to theories which introduce an elastic term without regard to its effect on the predicted critical flocculation point of model latices.

On the same subject, we note that it has been inferred (52) from the small repulsion observed by Doroszkowski and Lambourne for PS in cyclohexane below that stability in worse than Θ-solvents is possible. We agree that under extreme conditions we may obtain stability under conditions worse than the Θ-point for the stabilizer in free solution; however, the compression results of Doroszkowski and Lambourne are irrelevant in this regard. They state that the particles were <u>flocculated</u> during their measurements. Therefore, their results are not evidence for the possibility of stability in worse than Θ-solvents. In section 3 we suggested that stability be determined from the resistance to spontaneous aggregation in dilute latices, or, at least, not so concentrated that Brownian motion is stopped.

Several other misconceptions are evident in the literature. Osmond <u>et al</u> (91), for example, argue that Napper's (2) interpretation of stability (i.e., the origin of the terms "entropic" and "enthalpic" stabilization) is based upon the Fischer theory (17). They state that the Fischer theory is incorrect in ignoring interpenetrational configuration changes and that the small repulsion observed by Doroszkowski and Lambourne (52) between coated particles (flocculated) in a worse than Θ-solvent is evidence for the incorrectness of Fischer's theory.

Firstly, we have pointed out in the introduction to this chapter, the

origin of the terms "entropic" and "enthalpic" stabilization is independent of any theory of steric stabilization. They are derived from general thermodynamic principles (4) . (Note that the origin of these terms has nothing to do with the proposed correlation between the Θ-point of the stabilizer and the critical flocculation point.) Secondly, we believe that the neglect of the interpenetrational elastic effect is justifiable considering the approximations made in the Fischer theory (6,17); the results of Doroszkowski and Lambourne support this view indirectly. No repulsion was evident until the separation of particles was approximately equal to the barrier layer thickness (52,91), therefore, no evidence of an interpenetrational elastic repulsion was found. Hence, the available evidence (6) supports the qualitative aspects of Fischer's theory, which was not intended to account for configurational changes caused by compression of adsorbed chains between the latex particles.

The principle achievement of the Fischer theory was that it predicted the observed correlation between the Θ-point for the stabilizer and the critical flocculation point. Osmond et al regard this as "fortuitous". Their explanation (91) of flocculation in terms of a phase-separation process is virtually identical to that given earlier by Evans and Napper (27) and in no way invalidates the use of the Θ-point/critical flocculation point correlation as a test of the theory.

In their discussion of the solvency theories of steric stabilization, Osmond et al (91) state that the term $\frac{-k}{V_1}(1 - v_2)\ln(1 - v_2)\delta V$ (eq.{4} of this chapter) accounts for the number of ways of arranging solvent molecules and segments in the volume δV and they imply that the configurational entropy of

the polymer is partially accounted for in this term. In fact, the above term accounts for none of the configurational entropy of the polymer and refers solely to the ideal entropy gain when the solvent molecules are distributed throughout the greater volume of the solution; the polymer merely provides "extra space" for the solvent. We may derive the term as follows (42,92):

number of solvent molecules = n_1 ,

initial volume available to solvent molecules in pure solvent = V_i ,

final volume available to solvent molecules in the solution = V_f ,

gain in entropy of solvent when distributed over V_f = $kn_1 \ln(V_f/V_i)$

$= -kn_1 \ln v_1$

$= -kn_1 \ln(1 - v_2)$

where v_2 is the volume fraction of polymer in the solution

and v_1 is the volume fraction of solvent in the solution.

Number of solvent molecules in volume δV = $n_1 = \delta V(1 - v_2)/V_1$

where V_1 is the volume of a solvent molecule.

Therefore, the ideal entropy gain of the solvent = $\frac{-k\delta V}{V_1}(1 - v_2)\ln(1 - v_2)$.

Consequently, the objection that Osmond et al raise against the addition of a volume restriction term (12,91) to the osmotic interaction is not valid (i.e., eq.{4} contains no polymer configuration terms).

While it is true that none of the theories so far proposed gives a complete description of steric stabilization, we add that even methods based on Monte Carlo techniques (20,21) and random walk statistics (12,13,43,44) cannot be rigorously correct owing to their use of "production chains" (47) (see section 6 for a discussion of this point). A rigorous solution, therefore,

is not yet in sight. We believe that a complete description of the interactions between sterically stabilized particles cannot be formulated on the basis of equilibrium thermodynamics alone. Polymer relaxation, viscosity and other non-equilibrium effects must also be considered. The problem becomes even more difficult when applied to the multiple interactions of spheres, since adsorbed polymer configuration at a spherical surface is, as yet, an unsolved problem.

Appendix 1.1

FREE VOLUME THEORY AND STERIC STABILIZATION

As a result of our formulation of the theory of steric stabilization (osmotic contribution) in terms of the coefficients of χ_i of the series expansion:

$$\chi = \chi_1 + \chi_2 v_2 + \chi_3 v_2^2 + \ldots ,$$

we are not necessarily restricted by any polymer solution theory. Treatment of the χ_i parameters as experimental quantities ensures this independence (93). Therefore, regardless of the polymer solution theory chosen to predict χ from more fundamental quantities, we cannot expect an improvement in the predictions of the theory of steric stabilization over those obtained using an empirical χ. By using an empirical χ, however, we forfeit much of our understanding of the basic thermodynamic processes involved. It is often in the interest of the correct evolution of a theory to formulate the theory in terms of reasonably fundamental quantities.

We now briefly examine the possibility of using one of the modern theories of polymer solutions (e.g.,94,95) to predict the value of the interaction parameter χ. In keeping with the form of the expressions derived in our theory of steric stabilization, we seek to predict the χ_i parameters in the abovementioned power series (discussion will be limited to χ_1 and χ_2 of the series).

The most tractable free volume theory (FVT) to date is that due to Flory

(95). (Although we refer to the modern solution theories as free volume theories, we recognize the limited connotations of such a label (49).) A succinct resumé of this theory is given by Booth and Devoy (74); more detail is supplied in a series of papers by Eichinger and Flory (96,63,97,65) and by Höcker, Blake, Shih and Flory (98,70,72,64).

Following Flory (95), we shall use the segment fraction ϕ instead of the volume fraction in this appendix. For the present, we will not make a quantitative distinction between the χ values obtained on the basis of segment fractions and volume fractions. That a small difference exists has been pointed out by Flory (49). We require, therefore, χ_1 and χ_2 in:

$$\chi = \chi_1 + \chi_2\phi_2 + \ldots.$$

where ϕ_2 is the segment fraction of polymer in the solution.

Originally, Flory derived a series expansion, in powers of ϕ_2, for the reduced chemical potential of solvent in a mixture in which a single interaction energy parameter X_{12} was used (e.g.,95). Subsequently, it was found that an additional parameter Q_{12} was often required to account for the entropy associated with the exchange interaction (70,96). Modification of eq.{43} of ref.95 to account for Q_{12} and division by $RT\phi_2^2$ (where RT is the molar thermal energy unit) yields the reduced residual chemical potential of the solvent ($\equiv \chi$) as a power series in ϕ_2 (70,95):

$$\chi = \frac{p_1^*V_1^*}{RT\tilde{v}_1}\left(Y_{12} + \frac{A^2\alpha_1 T}{2}\right) - \frac{V_1^*Q_{12}}{R}\left(\frac{s_2}{s_1}\right)^2 + \frac{p_1^*V_1^*}{RT\tilde{v}_1}\left[2Y_{12}\left(1 - \frac{s_2}{s_1}\right) + \left\{2Y_{12} + \left(1 - \frac{p_2^*T_2^*}{p_1^*T_2^*}\right)A\right\}A\alpha_1 T\right.$$

$$\left. - \frac{2A^3\alpha_1 T}{9}\{3 + 2\alpha_1 T(1 + \alpha_1 T)\}\right]\phi_2 - \frac{2V_1^*Q_{12}}{R}\left(\frac{s_2}{s_1}\right)^2\left(1 - \frac{s_2}{s_1}\right)\phi_2 + O(\phi_2^2) \qquad \{87\}$$

where $Y_{12} = (\frac{s_2}{s_1})^2 X_{12}/p_1^*$

$A = (1 - \frac{T_1^* p_2^*}{T_2^* p_1^*}) - \frac{s_2}{s_1} X_{12}/p_1^*$

X_{12} = exchange energy parameter

p_i^* = characteristic pressure of component i (i = 1 for solvent
i = 2 for polymer)

T_i^* = characteristic temperature of component i

V_i^* = characteristic molar volume of solvent

$\tilde{v}_1$ = reduced volume of solvent

α_1 = thermal expansion coefficient of solvent

s_2/s_1 = segment surface ratio

T = absolute temperature

R = gas constant

ϕ_2 = segment fraction of polymer .

Evaluation of the above parameters has been extensively discussed by several authors (e.g.,74,96,98). From eq.{87} (70):

$$\chi_1 = (p_1^* V_1^*/\tilde{v}_1 RT)(Y_{12} + A^2\alpha_1 T/2) - V_1^* Q_{12}(s_2/s_1)^2/R \qquad \{88\}$$

and

$$\chi_2 = (p_1^* V_1^*/v_1 RT)\left[2Y_{12}(1 - s_2/s_1) + \{2Y_{12} + (1 - p_2^* T_1^*/p_1^* T_2^*)A\}A\alpha_1 T - (2/9)A^3\alpha_1 T\{3 + 2\alpha_1 T(1 + \alpha_1 T)\}\right] - 2V_1^* Q_{12}(s_2/s_1)^2(1 - s_2/s_1)/R \; . \qquad \{89\}$$

These expressions may only be used at low pressures owing to the use of an equation of state in the limit of zero pressure (95) in their derivation.

In addition to χ_1 and χ_2, we shall evaluate the entropy and enthalpy components of χ_1; i.e., Flory's entropy ψ_1 and enthalpy κ_1 of dilution parameters in the limit of infinite dilution (42,70):

$$\psi_1 - \kappa_1 = \tfrac{1}{2} - \chi_1$$

where

$$\psi_1 = \tfrac{1}{2} + (p_1^*V_1^*/RT\tilde{v}_1)\left[Y_{12}\alpha_1 T - (A^2\alpha_1 T/2)\{1 + \frac{4}{3}\alpha_1 T(1 + \alpha_1 T)\}\right] + V_1^*Q_{12}(s_2/s_1)^2/R \qquad \{90\}$$

and

$$\kappa_1 = (p_1^*V_1^*/RT\tilde{v}_1)(1 + \alpha_1 T)\{Y_{12} - \frac{2}{3}A^2\alpha_1^2T^2\} \; . \qquad \{91\}$$

Tables 3 and 4 list the requisite data for several solvents and polymers; this data is used to construct Tables 5 and 6 for several polymer/solvent mixtures. Also required for the mixtures are X_{12}, Q_{12} and s_2/s_1. Rather than have s_2/s_1 as an adjustable parameter (66), we will use values from the literature which have been calculated by the methods of Flory; e.g., the "sphere-cylinder" approximation (70,74). When the solvent molecules can be approximated by spheres and the polymer chain by a cylinder, we can formulate (after a little algebra) the segment surface ratio as:

$$s_2/s_1 = 2.13V_1^{*1/3}(\ell/M_m v_{sp2}^*)^{1/2} \; , \qquad \{92\}$$

where

ℓ is the crystallographic repeat distance per monomer unit (nm)

M_m is the molecular weight of a mer unit (g mol^{-1})

v_{sp2}^* is the characteristic specific volume of the polymer (cm^3 g^{-1})

and V_1^* is the molar volume of the solvent (cm^3 mol^{-1}).

The only adjustable parameters are now X_{12} and Q_{12}.

TABLE 3

Data for Pure Solvents

Solvent	T/K	p_1^* J. cm^{-3}	T*/K	V_1^* cm^3 mol^{-1}	$\tilde{v}_1$	α_1 10^{-3} K^{-1}	refs.
cyclohexane	298	530	4717	84.3	1.2906	1.217	64
benzene	298	628	4709	69.2	1.2917	1.223	63
methyl ethyl ketone	298	582	4557	68.9	1.3075	1.308	70
chlorobenzene	293	600	5320	82.5	1.2356	0.957	66
ethylbenzene	298	551	5176	98.4	1.2515	1.019	72
n-pentane	298	406	4158	85.4	1.3607	1.61	65

TABLE 4

Data for Pure Polymers

Polymer	T/K	p_2^* J. cm^{-3}	T_2^*/K	v_{sp2}^* $cm^3\ g^{-1}$	M_m g mol^{-1}	ℓ/nm	refs.
PS	298	547	7420	0.8098	104	0.25	70,98
PIB	298	519	6775	0.9493	56	0.23	63,73
PDMS	298	341	5528	0.8395	74	0.29	66
PDMS	293	343	5494	0.8381	74	0.29	66

TABLE 5

Results for Mixtures Fitted to Experimental κ_1 and χ_1

System	T/K	s_2/s_1	X_{12} J. cm^{-3}	Q_{12} J. cm^{-3} K^{-1}	κ_1	χ_1	χ_2	refs.
PS/cyclohexane	298	0.50	45.8	0.0304	0.225	0.505	0.325	75
PS/methyl ethyl ketone	298	0.48	26.0	-0.0424	-0.029	0.486	0.312	70
PS/ethylbenzene	298	0.53	8.5	-0.0295	-0.02	0.40	0.206	72
PIB/benzene	298	0.58	38.0	-0.0393	0.30	0.500	0.423	68
PIB/n-pentane	298	0.53	35.0	0.0778	-0.10	0.486	-0.092	65
PDMS/chlorobenzene	293	0.64	11.4	-0.0854	0.156	0.475	0.343	66,67
PDMS/benzene	298	0.60	19.4	-0.107	0.20	0.481	0.392	66,71

TABLE 6

Results for Mixtures Based on Literature Values of X_{12} and Q_{12}

System	T/K	s_2/s_1	X_{12} J. cm^{-3}	Q_{12} J. cm^{-3} K^{-1}	κ_1	χ_1	χ_2	refs.
PS/cyclohexane	298	0.50	42.0	0.023	0.188	0.505	0.312	64
PS/methyl ethyl ketone	298	0.48	26.0	-0.038	-0.026	0.481	0.303	70
PS/ethylbenzene	298	0.53	8.8	-0.029	-0.017	0.398	0.205	72
PIB/benzene	298	0.58	42.0	0	0.342	0.418	0.357	63
PIB/n-pentane	298	0.53	11.7	0	-0.412	0.648	-0.171	65
PDMS/chlorobenzene	293	0.64	11.0	-0.064	0.158	0.384	0.277	66
PDMS/benzene	298	0.60	22.0	-0.042	0.228	0.481	0.254	66

In Table 5, we have taken the measured values of κ_1 and χ_1 and calculated the X_{12} and Q_{12} exchange parameters according to eqs.{91} and {88}. From these results, χ_2 was calculated (eq.{89}). The average concentration of polymer on the surface of a sterically stabilized latex is generally of the order of 10% (see section 9). Values of X_{12} and Q_{12} fitted to the experimental data near $\phi_2 = 0.5$ (71) may, therefore, yield misleading results. For this reason we have chosen to fit the exchange parameters to the experimental data in the limit of infinite dilution. ψ_1 has not been listed as it can readily be obtained from

$$\psi_1 = \tfrac{1}{2} + \kappa_1 - \chi_1 \ .$$

Table 6 was constructed from values of X_{12} and Q_{12} reported in the literature. Values for these parameters may vary significantly depending on the relative importance each author places on various experimental data (e.g., whether X_{12} should be found from excess volume of mixing data (74) or excess enthalpy of mixing data (71)).

We chose the systems listed in Tables 5 and 6 as examples for which the semi-empirical approximation $\chi_2 \simeq 2\chi_1/3$ was found to hold (section 5.2.). The value of the ratio χ_1/χ_2 in all cases should therefore be near 1.5. Excluding the system PIB/n-pentane, the average value of χ_1/χ_2 in Table 5 is 1.5 ± 0.3 and in Table 6 it is 1.6 ± 0.3.

Contrary to the experimental results (65), the value of χ for the PIB/n-pentane system is predicted to be almost independent of polymer concentration at low ϕ_2 values. In fact, a small tendency for χ to decrease with increasing ϕ_2 is predicted. In addition, as is pointed out in ref.65, the theoretical

value of χ_1 (Table 6) is much too high and incorrectly predicts limited miscibility in this system ($\chi_1 > 0.5$). Adjustments of the parameters according to experimental χ_1 and κ_1 values (Table 5) corrects this by greatly increasing X_{12} (11.7 → 35.0 J. cm^{-3}). Improvement in χ_2 is marginal, however, and the value of Q_{12} required seems unrealistically large (65).

One very important prediction of the theory is that κ_1 and ψ_1 for the PIB/n-pentane system are both negative. This appears to be an unequivocal prediction which cannot be made in terms of the lattice theory of polymer solutions (42). We discuss this point further in chapter II.

The method of evaluating the s_2/s_1 parameter is somewhat artificial in that polymer and solvent molecules are considered to be geometric solids. However, a much more sophisticated treatment of s_2/s_1 is probably unwarranted in view of the other assumptions in the theory (e.g., the adoption of a $(3,\infty)$ intermolecular pair potential (49) and the use of a volume-independent exchange entropy (96)). Much closer agreement with experiment could have been obtained for several of the systems is s_2/s_1 had been made an arbitrary adjustable parameter. Although the concentration dependence of χ can be strongly dependent on s_2/s_1 (96), arbitrary parameters should be avoided in order that logical comparisons be made between different systems.

Free volume theory appears, in most cases, to give a satisfactory description of the above systems. For our purposes,however, the theory is not particularly suitable in its present form. There are two main reasons for this conclusion. First, steric stabilization theory contains the parameters $(\frac{1}{2} - \chi_1)$ and $(\frac{1}{3} - \chi_2)$ which are far more sensitive to changes in s_2/s_1, Q_{12}

and X_{12} than are χ_1 or χ_2 when $\chi_1 \simeq \frac{1}{2}$ and $\chi_2 \simeq \frac{1}{3}$. These latter conditions are of particluar interest in the theory of steric stabilization since they usually prevail near the critical flocculation point (27). For example, in Table 5, the system PS/cyclohexane at 298 K has $\chi_1 = 0.505$ and $\chi_2 = 0.325$ or $(\frac{1}{2} - \chi_1) = -0.005$ and $(\frac{1}{3} - \chi_2) = 0.008$. A 10% change in χ_2 would lead to a change of 0.03 in $(\frac{1}{3} - \chi_2)$. Consequently, even the sign of $(\frac{1}{3} - \chi_2)$ is uncertain when $\chi_2 \simeq \frac{1}{3}$.

Second, before the theoretical values of χ_1 and χ_2 can be calculated from <u>fitted</u> X_{12} and Q_{12} parameters, the values of χ_1 and κ_1 must be <u>measured</u>. This involves measuring the concentration dependence of χ (or at least the initial slope of the χ versus concentration plot). From a practical point of view, therefore, the use of a polymer solution theory in steric stabilization theory is superfluous.

Instead of using polymer solution theory to predict the parameters required in steric stabilization theory, we should, perhaps, use these theories independently. In this way, the theory of steric stabilization would benefit from the thermodynamic insight afforded by the FVT without suffering from its quantitative deficiencies.

Appendix 1.2

THE "EXACT" OSMOTIC INTERACTION

χ is best defined as the reduced residual chemical potential of the solvent in a solution (49). This definition releases us from the restriction that χ be treated as a difference in reduced contact free energies.

To the accuracy of experimental measurement, χ is defined by:

$$\left(\frac{\mu_1 - \mu_1^{\phi}}{RT}\right)^E = \ln(1 - v_2) + v_2 + \chi v_2^2 \qquad \{93\}$$

where $\left(\frac{\mu_1 - \mu_1^{\phi}}{RT}\right)^E$ is the experimental excess relative chemical potential of the solvent as obtained <u>via</u> activity measurements. The usual methods of determining solvent activity include osmotic pressure measurements for low to moderate polymer concentrations (68) and vapour pressure measurements for high polymer concentrations (62).

From eqs.{ 4 } and {10} in section 4, we have for the excess free energy of mixing polymer and solvent in volume element δV:

$$\delta(\Delta G_M^E) = \frac{kT\delta V}{V_1}\{(1 - v_2)\ln(1 - v_2) + v_2 \sum_{i=1}^{\infty} \frac{\chi_i}{i}(1 - v_2^i) \quad , \qquad \{94\}$$

where we have assumed that it is possible to replace the experimental values of χ by a polynomial (power series) approximation without losing accuracy. We do not expand the logarithm at this point; therefore, even simple non-uniform segment density distribution functions will cause this expression {94} to be

unmanageable. We proceed by applying eq.{94} to the uniform segment density model. The osmotic free energy of interaction of flat plates (cf. eq.{32}) becomes:

$$\Delta G^{u}_{os} = \frac{RTL}{\bar{V}_1}\left[\delta(1 - \frac{2\bar{v}}{\delta})\ln(1 - \frac{2\bar{v}}{\delta}) - 2(1 - \bar{v})\ln(1 - \bar{v}) + 2\bar{v}\sum_{i=1}^{\infty}\frac{\chi_i\bar{v}^i}{i}\{1 - (\frac{2}{\delta})^i\}\right]. \quad \{95\}$$

Integration with respect to δ leads us to the osmotic interaction between equal spheres (cf. eq.{35}):

$$\Delta V^{u}_{os} = \pi a\frac{RTL^2}{\bar{V}_1}\left[2(\delta_0 - 1 - \bar{v})(1 - \bar{v})\ln(1 - \bar{v}) - \frac{\delta_0^2}{2}(1 - \frac{2\bar{v}}{\delta_0})^2\ln(1 - \frac{2\bar{v}}{\delta_0}) + 2\bar{v}^2\ln\frac{2}{\delta_0}\right.$$
$$\left. + \bar{v}(\delta_0 - 2) - 4\bar{v}^2\left(\chi_1(\ln\frac{2}{\delta_0} + \frac{\delta_0}{2} - 1) + \sum_{i=2}^{\infty}\frac{\chi_i\bar{v}^{i-1}}{i(i-1)}\{(\frac{2}{\delta_0})^{i-1} + (i-1)\frac{\delta_0}{2} - i\}\right)\right] \quad \{96\}$$

Note that eqs.{95} and {96} are equivalent to eqs.{32} and {35} only if we take the summations over i to infinity. In practice, a power series approximation will have only a few terms and the sets of equations do not coincide. Although the above equations {95} and {96} are more "exact" than eqs.{32} and {35} within the framework of our segment density model, the difference between them is small at the polymer concentrations considered. Only when very high concentrations are reached do eqs.{95} and {96} have an advantage; in the limit as $\bar{v} \to 1$, ΔG^{u}_{os} and ΔV^{u}_{os} both approach ∞, which means that the finite real volume of the polymer is accounted for.

We cannot realistically approach this extreme in our theory partially because of the elastic term, which must be invalid at high concentrations owing

to the real volume of the polymer.

Appendix 1.3

RELATIONSHIP BETWEEN PARTICLE VOLUME FRACTION AND SEPARATION IN CLOSE-PACKED ARRAYS OF MONODISPERSE SPHERES

In either hexagonally or cubic close-packed arrays, each sphere has twelve equidistant nearest neighbours; six in one plane and three on each side of this plane. We require the frequency of occurrence of spheres in three mutually perpendicular directions in order to calculate the number of spheres per unit volume.

Let ℓ be the distance between the centres of two adjacent spheres. The volume fraction of particles can readily be found using the dimensions of a regular tetrahedron of side ℓ (see Fig. 17). Any two adjacent rows are separated by a perpendicular distance of $\frac{\sqrt{3}}{2}\ell$ and any two layers by $\sqrt{2/3}\,\ell$. The number of spheres per unit volume, N, is

$$N = \frac{1}{\ell} \times \frac{2}{\sqrt{3}\,\ell} \times \frac{\sqrt{3}}{\sqrt{2}\,\ell}$$

$$= \frac{\sqrt{2}}{\ell^3} \quad .$$

Placing $\ell = 2a + d_0$, we find

$$N = \frac{\sqrt{2}}{(2a + d_0)^3} \quad .$$

Multiplication by the volume per sphere gives, for the volume fraction of spheres (core particles):

$$\phi_p = \frac{4\sqrt{2}\,\pi a}{3(2a + d_0)^3}$$

or $$\phi_p = \frac{\pi}{3\sqrt{2}} (1 + d_0/2a)^{-3} \ . \qquad \{97\}$$

In terms of the distance parameter δ_0, we have:

$$\delta_0 = \frac{2a}{L}\left[\left(\frac{\pi}{3\sqrt{2}\,\phi_p}\right)^{1/3} - 1\right] \ . \qquad \{98\}$$

When $d_0 = 0$ in eq.{97}, $\phi_p = \pi/(3\sqrt{2}) \simeq 0.74$. This is the maximum volume fraction of particles possible in a perfect close-packed array of monodisperse spherical particles. If a latex is predominately close-packed but has some "dead space", the measured volume fraction will be underestimated. We can allow, to some extent, for faults in the latex structure by using:

$$\phi_{pm} = \phi_0(1 + d_0/2a)^{-3} \ , \qquad \{99\}$$

where ϕ_0 is the maximum volume fraction of particles estimated by extrapolation of experimental results to $d_0 = 0$ and ϕ_{pm} is the measured apparent volume fraction of particles. Corresponding changes in A have a much smaller effect on the final interaction equations; consequently, we need not alter eq.{75}.

Fig.17. Dimensions of a regular tetrahedron used to find the relationship between the particle volume fraction ϕ_p and the distance (or reduced distance) of separation d_0 (or δ_0) in a perfectly close-packed array of spherical particles.

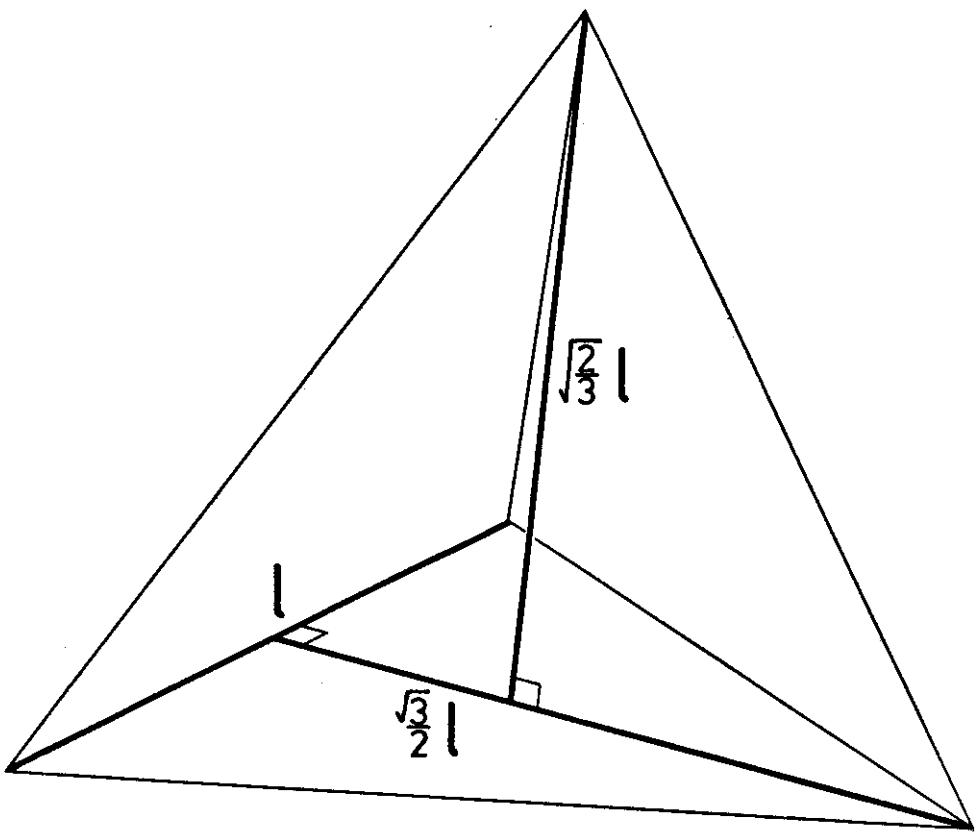
$\sqrt{\frac{2}{3}}\,l$
l
$\frac{\sqrt{3}}{2}\,l$

Appendix 1.4

INFLUENCE OF VAN DER WAALS ATTRACTION ON DISJOINING PRESSURE OF CONCENTRATED LATICES

An estimate of the relative magnitude of the van der Waals attraction shows that it is negligibly small. Let the attraction energy between two spheres be approximated by:

$$G_A = \frac{-aH}{12d}$$

where H is the Hamaker "constant". This expression is not very accurate (see chapter on van der Waals attraction); however, for our present purposes, accuracy is not required. Differentiation gives us the force of attraction:

$$F_A = \frac{-\partial \Delta G_A}{\partial d_0} = \frac{-aH}{12d_0^2}$$

and division by the area over which this force acts yields the pressure:

$$P_A = F/A = \frac{-aH}{12\sqrt{3}\, d_0^2 (a + d_0/2)^2} .$$

Note that the pressure is inversely proportional to the particle radius, whereas the attraction energy and force are directly proportional to the particle radius.

We show in the van der Waals attraction chapter that H, for polymer latices, is of the order of thermal energy (kT). A typical particle radius would be ~100 nm. Comparison of Table 7 with, say, Fig.14 indicates that the van der Waals pressure is approximately two orders of magnitude smaller than the measured repulsion.

TABLE 7

Van der Waals attraction pressure for a typical latex of radius 100 nm and with H = kT.

d_0/nm	P_A/kPa
12	-0.01
10	-0.02
8	-0.03
6	-0.05
4	-0.12

11. REFERENCES

1. Napper,D.H., Trans. Faraday Soc., 64, 1701 (1968).
2. Napper,D.H., J. Colloid and Interface Sci., 32, 106 (1970).
3. Napper,D.H., J. Colloid and Interface Sci., 29, 168 (1969).
4. Napper,D.H. and Netshey,A., J. Colloid and Interface Sci., 37, 528 (1971).
5. Evans,R., Davison,J.B. and Napper,D.H., J. Polymer Sci., B10, 449 (1972).
6. Evans,R. and Napper,D.H., Kolloid-Z-Z. Polym., 251, 409 (1973).
7. Napper,D.H. and Hunter,R.J., MTP Int. Rev. Sci., Series 1, 7, 280 (1972).
8. Napper,D.H., Kolloid-Z-Z. Polym., 234, 1149 (1969).
9. Smitham,J.B. and Napper,D.H., "Elastic Stabilization in Polymer Melts", Kolloid-Z-Z. Polym., accepted for publication (1976).
10. Smitham,J.B. and Napper,D.H., "Steric Stabilization in Polymer Melts", submitted for publication.
11. Napper,D.H., J. Colloid and Interface Sci., 33, 384 (1969).
12. Meier,D.J., J. Phys. Chem., 71, 1861 (1967).
13. Hesselink,F.Th., Vrij,A. and Overbeek,J.Th.G., J. Phys. Chem., 75, 2094 (1971).
14. Derjaguin,B.V., Kolloid-Z., 69, 155 (1934).
    Also:Kruyt,H.R.(ed.),"Colloid Science", Vol 2,(Elsevier, Amsterdam, 1952).
15. Mackor,E.L., J. Colloid Sci., 6, 942 (1951).
16. Mackor,E.L. and van der Waals,J.H., J. Colloid Sci., 7, 535 (1952).
17. Fischer,E.W., Kolloid-Z., 160, 120 (1958).
18. Jäckel,K., Kolloid-Z., 197, 143 (1964).
19. Clayfield,E.J. and Lumb,E.C., Disc. Faraday Soc., 42, 314 (1966).
20. Clayfield,E.J. and Lumb,E.C., J. Colloid and Interface Sci., 22, 269 (1966).

21. Clayfield,E.J. and Lumb,E.C., J. Colloid and Interface Sci., 22, 285 (1966).

22. Clayfield,E.J. and Lumb,E.C., Macromolecules, 1, 133 (1968).

23. Clayfield,E.J. and Lumb,E.C., J. Colloid and Interface Sci., 49, 489 (1974).

24. Ottewill,R.H. and Walker,T.W., Kolloid-Z-Z. Polym., 227, 108 (1968).

25. Bagchi,P., J. Colloid and Interface Sci., 47, 86 (1974).

26. Bagchi,P., J. Colloid and Interface Sci., 47, 100 (1974).

27. Evans,R. and Napper,D.H., Kolloid-Z-Z. Polym., 251, 329 (1973).

28. Hesselink,F.Th., J. Phys Chem., 73, 3488 (1969).

29. Hesselink,F.Th., J. Phys.Chem., 75, 65 (1971).

30. Evans,R. and Napper,D.H., J. Colloid and Interface Sci., 51, 552 (1975).

31. Evans,R. and Napper,D.H., J. Colloid and Interface Sci., 52, 260 (1975).

32. Evans,R., B.Sc. Hons. Thesis, Sydney University (1972).

33. Heller,W. and Pugh,T.L., J. Chem Phys., 22, 1778 (1954).

34. Heller,W., Pure Appl. Chem., 12, 249 (1966).

35. Molau, G.E., Kolloid-Z-Z. Polym., 238, 493 (1970).

36. Molau,G.E., J. Polymer Sci., A, 3, 1267 (1965).

37. Molau,G.E., J. Polymer Sci., A, 3, 4235 (1965).

38. Stromberg,R.R., Tutas,D.J. and Passaglia,E., J. Phys. Chem., 69, 3955 (1965).

39. Dobbie,J.W., Evans,R., Gibson,D.V., Smitham,J.B. and Napper,D.H., J. Colloid and Interface Sci., 45, 557 (1973).

40. Doroszkowski,A. and Lambourne,R., J. Polymer Sci., C, 34, 253 (1971).

41. Smitham,J.B., Evans,R. and Napper,D.H., Trans. Faraday Soc., 71, 285 (1975).

42. Flory,P.J., "Principles of Polymer Chemistry" (Cornell, Ithaca, 1953).

43. Dolan,A.K. and Edwards,S.F., Proc. Roy. Soc. Lond., A337, 509 (1974).

44. Dolan,A.K. and Edwards,S.F., Proc. Roy. Soc. Lond., A343, 427 (1974).

45. Hartree,D.R., Proc. Camb. Phil. Soc., 24, 89 (1928).

46. Edwards,S.F., Proc. Phys. Soc., 85, 613 (1965).

47. Yamakawa,H., "Modern Theory of Polymer Solutions", (Harper and Row, New York, 1971).

48. Evans,R., Smitham,J.B. and Napper,D.H., Kolloid-Z-Z. Polym., accepted for publication . (1975).

49. Flory,P.J., Disc. Faraday Soc., 49, 7 (1970).

50. Cairns,R.J.R. and Ottewill,R.H., Abstract for ACS Symposium , preprint 34, 555 (1974).

51. Homola,A., Ph.D. Thesis (Part V), McGill University, Montreal, Canada (1974).

52. Doroszkowski,A. and Lambourne,R., J. Colloid and Interface Sci., 43, 97 (1973).

53. Di Marzio,E.A. and McCrackin,F.L., J. Chem Phys., 43, 539 (1965).

54. Ottewill,R.H. and Walker,T.W., Kolloid-Z-Z. Polym., 227, 108 (1968).

55. Barsted,S.J., Nowakowska,L.J., Wagstaff,I. and Walbridge,D.J., Trans. Faraday Soc., 67, 3598 (1971).

56. Smitham,J.B. and Napper,D.H., "Monte Carlo Simulation of a Random Flight Chain in a Restricted Environment", submitted for publication.

57. Nash,L.K., "Elements of Statistical Thermodynamics", (Addison-Wesley, Menlo Park, 1968).

58. Koningsveld,R. and Staverman,A.J., J. Polymer Sci., A2, 6, 325 (1968).

59. Koningsveld,R., Kleintjens,L.A. and Schultz,A.R., J. Polymer Sci., A2, 8, 1261 (1970).

60. Stockmayer,W.H. and Casassa,E.F., J. Chem. Phys., 20, 1560 (1952).

61. McMillan,Jr.,W.G. and Mayer,J.E., J. Chem Phys., 13, 276 (1945).

62. Krigbaum,W.R. and Geymer,D.O., J. Amer. Chem. Soc., 81, 1859 (1959).

63. Eichinger,B.E. and Flory,P.J., Trans Faraday Soc., 64, 2053 (1968).

64. Höcker,H., Shih,H. and Flory,P.J., Trans. Faraday Soc., 67, 2275 (1971).

65. Eichinger,B.E. and Flory,P.J., Trans. Faraday Soc., 64, 2066 (1968).

66. Shih,H. and Flory,P.J., Macromolecules, 5, 761 (1972).

67. Kuwahara,N., Okazawa,T. and Kaneko,M., J. Polymer Sci., C, 23, 543 (1968).

68. Flory,P.J. and Daoust,H., J. Polymer Sci., 25, 429 (1957).

69. Gaeckle,D., Kao,W., Patterson,D. and Rinfret,M., Trans. Faraday Soc., I, 69, 1849 (1973).

70. Flory,P.J. and Höcker,H., Trans. Faraday Soc., 67, 2258 (1971).

71. Chahal,R.S., Kao,W. and Patterson,D., Trans. Faraday Soc., I, 69, 1834 (1973).

72. Höcker,H. and Flory,P.J., Trans. Faraday Soc., 67, 2270 (1971).

73. Flory,P.J., Ellenson,J.L. and Eichinger,B.E., Macromolecules, 1, 279 (1968).

74. Booth,C. and Devoy,C.J., Polymer, 12, 309 (1971).

75. Kuwahara,N., Nakata,M. and Kaneko,M., Polymer, 14, 415 (1973).

76. Vincent,B., J. Colloid and Interface Sci., 42, 270 (1973).

77. Edwards,S.F. and Freed,K.F., J. Phys. A(Gen. Phys.), Ser. 2, 2, 145 (1969).

78. White,J.W., in "Polymer Science", (Jenkins,A.D., ed., North-Holland, Amsterdam, 1972).

79. Markoff,A.A., "Wahrscheinlichkeitsrechnung", Leipzig (1912).

80. Flory,P.J., "Statistical Mechanics of Chain Molecules", (Interscience, New York, 1969).

81. Abramowitz,M. and Stegun,I.A., "Handbook of Mathematical Functions", (Nat. Bur. Stand., Washington, 1970).

82. Andrews,D.M., Manev,E.D. and Haydon,D.A., Spec. Disc. Faraday Soc.,

1, 46 (1970).

83. Hiltner,P.A. and Krieger,I.M., J. Phys. Chem., 73, 2386 (1969).

84. Hiltner,P.A., Papir,Y.S. and Krieger,I.M., J. Phys. Chem., 75, 1881 (1971).

85. Kose,A., Ozaki,M., Takano,K., Kobayashi,Y. and Hachisu,S., J. Colloid and Interface Sci., 44, 330 (1973).

86. Barclay,L., Harrington,A. and Ottewill,R.H., Kolloid-Z-Z. Polym., 250 655 (1972).

87. Schick,M.J., Doty,P. and Zimm,B.H., J. Amer. Chem. Soc., 71, 530 (1950).

88. Gandhi,K.S. and Williams,M.C., J. Polymer Sci., C, 35, 211 (1971).

89. Flory,P.J., Orwoll,R.A. and Vrij,A., J. Amer. Chem. Soc., 86, 3515 (1964).

90. Zeman,L., Biros,J. and Patterson,D., J. Phys. Chem., 76, 1206 (1972).

91. Osmond,D.W.J., Vincent,B. and Waite,F.A., Kolloid-Z-Z. Polym., 253, 666 (1975).

92. Moore,W.J., "Physical Chemistry", 4th ed., (Longmans, London, 1965).

93. Orofino,T.A. and Flory,P.J., J. Chem. Phys., 26, 1067 (1957).

94. Patterson,D., Macromolecules, 2, 672 (1969).

95. Flory,P.J., J. Amer. Chem. Soc., 87, 1833 (1965).

96. Eichinger,B.E. and Flory,P.J., Trans. Faraday Soc., 64, 2035 (1968).

97. Eichinger,B.E. and Flory,P.J., Trans. Faraday Soc., 64, 2061 (1968).

98. Höcker,H., Blake,G.J. and Flory,P.J., Trans. Faraday Soc., 67, 2251 (1971).

99. Beuche,F., J. Colloid and Interface Sci., 41, 374 (1972).

100. Osmond,D.W.J. and Walbridge,D.J., J. Polymer Sci., C, 30, 381 (1970).

CHAPTER II

THE EFFECT OF PRESSURE ON STERICALLY STABILIZED LATICES

1. INTRODUCTION

At the beginning of the first chapter, we discussed the thermal methods of flocculating sterically stabilized latices. Thermal flocculation behaviour enabled us to classify sterically stabilized latices as enthalpic, entropic or combined enthalpic-entropic (1). (See chap.I, Fig.1.) This classification is based upon the thermodynamic conditions (2) under which the free energy of interaction ΔG between the latex particles is reduced to zero:

$$\Delta G = \Delta H - T\Delta S = 0$$

where ΔH and ΔS are the enthalpy and entropy changes associated with the mutual approach of latex particles during flocculation. If we now rewrite the above expression by recalling that

$$\Delta H = \Delta E + P\Delta V$$

at constant temperature T and pressure P, we have, at the critical flocculation point:

$$\Delta G = \Delta E + P\Delta V - T\Delta S = 0, \qquad \{1\}$$

where ΔE and ΔV are the changes in internal energy and volume associated with flocculation. (ΔV is not to be confused with the interaction energy between spheres in chapter I.) It is clear from Fig.1 that a latex may be flocculated by increasing the pressure only if ΔV is negative, irrespective of whether the latex is entropically or enthalpically stabilized. The arrows indicate the direction of increasing pressure. At atmospheric pressure we assume that $\Delta H \simeq \Delta E$. The sign of ΔV is shown on each arrow. We emphasise that such diagrams are strictly valid only in the immediate vicinity of the $\Delta G = 0$ line (2) where it may be assumed that ΔE, ΔV and ΔS are independent of T and P. Large changes in T and P are likely to affect ΔE, ΔV and ΔS and they should be re-

Fig.1. Stability diagrams for sterically stabilized dispersions - effect of increasing pressure from P = 0. (Stability is possible only above the $\Delta G = 0$ diagonal.) Signs on the arrows are those of the volume change ΔV associated with flocculation. Distance from the $\Delta G = 0$ line is greatly exaggerated.

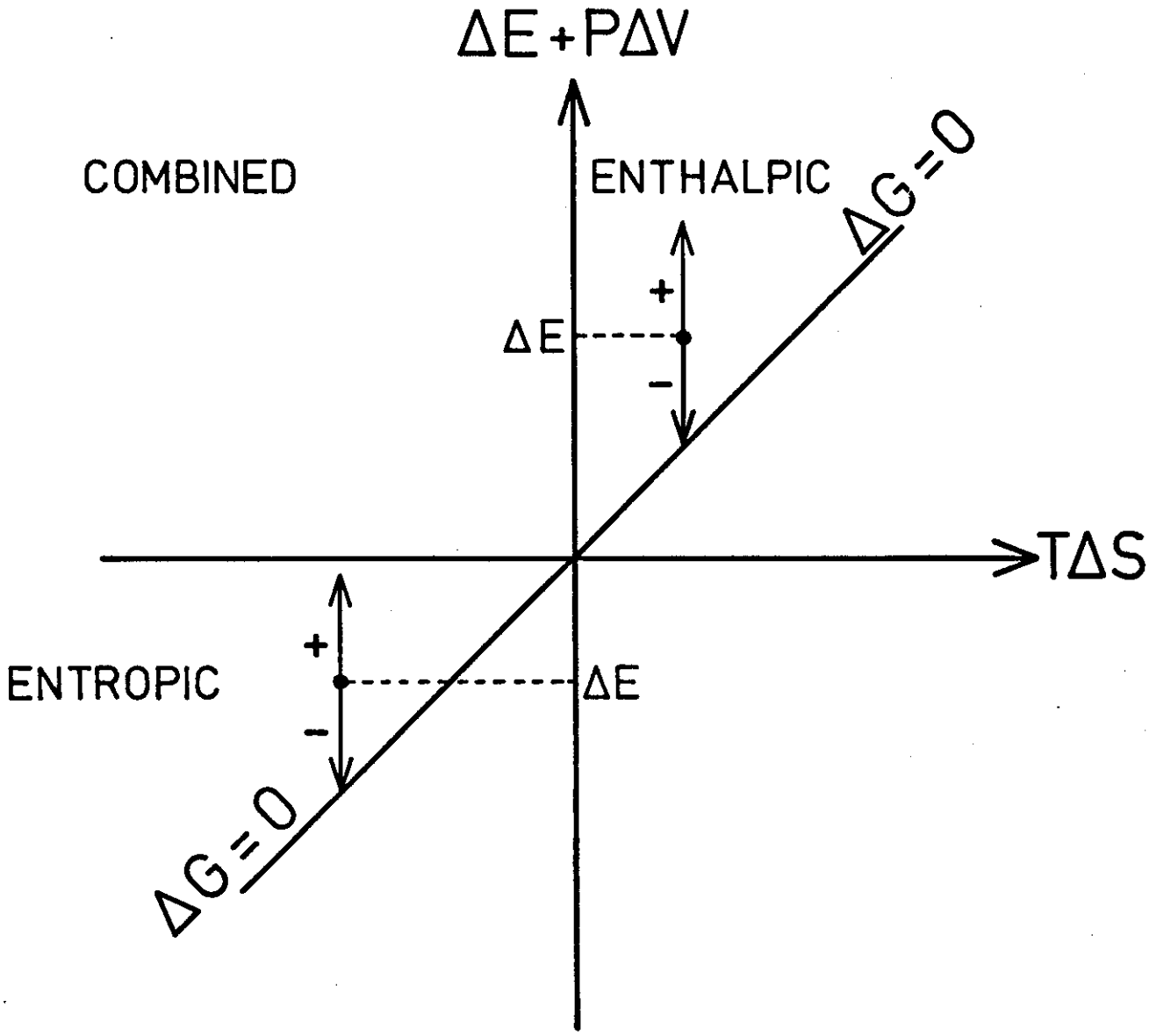
ΔE+PΔV
COMBINED
ENTHALPIC
ΔG=0
+
ΔE
−
TΔS
ENTROPIC
+
−
ΔE
ΔG=0

evaluated under the different conditions.

In the following sections, we will concentrate on two main points. First, there appears to be no valid thermodynamic reason why enthalpic stabilization and entropic stabilization should be observed only in aqueous and non-aqueous media respectively (3). Ottewill (4) has pointed out that entropic stability is dominant in non-aqueous media and enthalpic stability occurs most often in aqueous media. We have indicated exceptions to this rule and have presented the flocculation behaviour of the "exceptional" latices (5,6). Enthalpic stabilization in non-aqueous media will be discussed in section 3. This topic has been incorporated into the "pressure" chapter because enthalpic stabilization in non-aqueous media is expected to occur above the normal boiling point of the solvent medium. Observation of this phenomenon must therefore be made at pressures exceeding 1 atmosphere.

The second point concerns the correlation between the critical flocculation point of a latex and the Θ-point for the stabilizer in free solution. We have investigated the effect of pressure on this correlation and our results are presented in section 4. The remainder of the chapter consists mainly of a qualitative examination of the effect of pressure on the systems studied and sterically stabilized latices in general.

2. PRESSURE APPARATUS

The initial experiments were performed using equipment built by the C.S.I.R.O. Subsequently, a basically similar system was constructed in these laboratories. The main difference between the two sets of apparatus is that the original pressure bomb had to be heated with an external heating mantle while the temperature of the modified bomb was controlled by pumping fluid through channels drilled inside the bomb. Results obtained with the original apparatus were found to agree with those obtained using the apparatus described below.

A cross-section of the high pressure bomb is shown in Fig.2. Not shown are the holes drilled through the bomb to allow the circulation of water (or other fluids) from a temperature regulated bath. This bath was a Haake type F 4391, which could be used to cool as well as heat the bomb. The connections for the temperature regulating fluid can be seen in Plate 1. A separate hole drilled into the top of the bomb held a thermometer. The pressure cell was a glass syringe modified by the removal of the flange and subsequent sealing of the nozzle. The end of the plunger served as a piston to isolate the test sample from the hydraulic medium, while maintaining pressure equilibrium. This cell was immersed in the hydraulic fluid (a clear paraffin oil) in the cell compartment (Fig.2). Pressure was applied with an Enerpac P228 manual pump *via* a high pressure line consisting mostly of Sno-trik stainless steel tubing and valves, although some Enerpac fittings were used.

Three Bourdon-type guages were required to cover the pressure range from

Fig.2. Cross-section of high pressure bomb (300 MPa)

(1) Bomb (stainless steel, height: 14.6 cm)

(2) Window nut (R-5 high tensile steel)

(3) O-ring seal

(4) window support (stainless steel)

(5) glass window

(6) cell chamber

(7) optically flat surfaces

(8) second window assembly (not shown)

(9) sealing plug (stainless steel)

(10) lock nut (R-5 high tensile steel)

(11) lock nut for pressure-line connection

Based on CSIRO design.

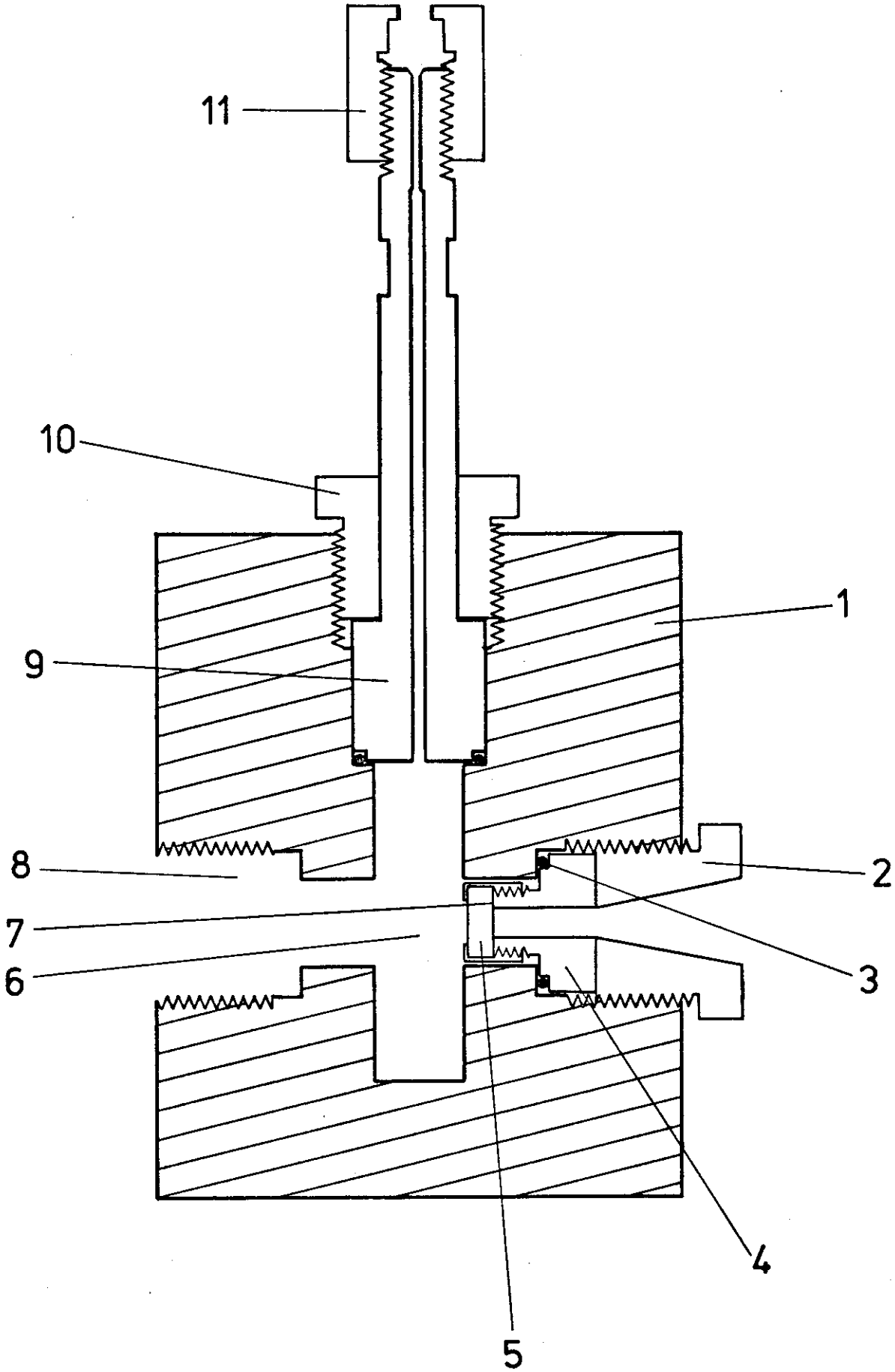
11
10
1
9
8
2
7
3
6
4
5

Plate 1. High pressure apparatus. Note the glass pressure cell beside the bomb.

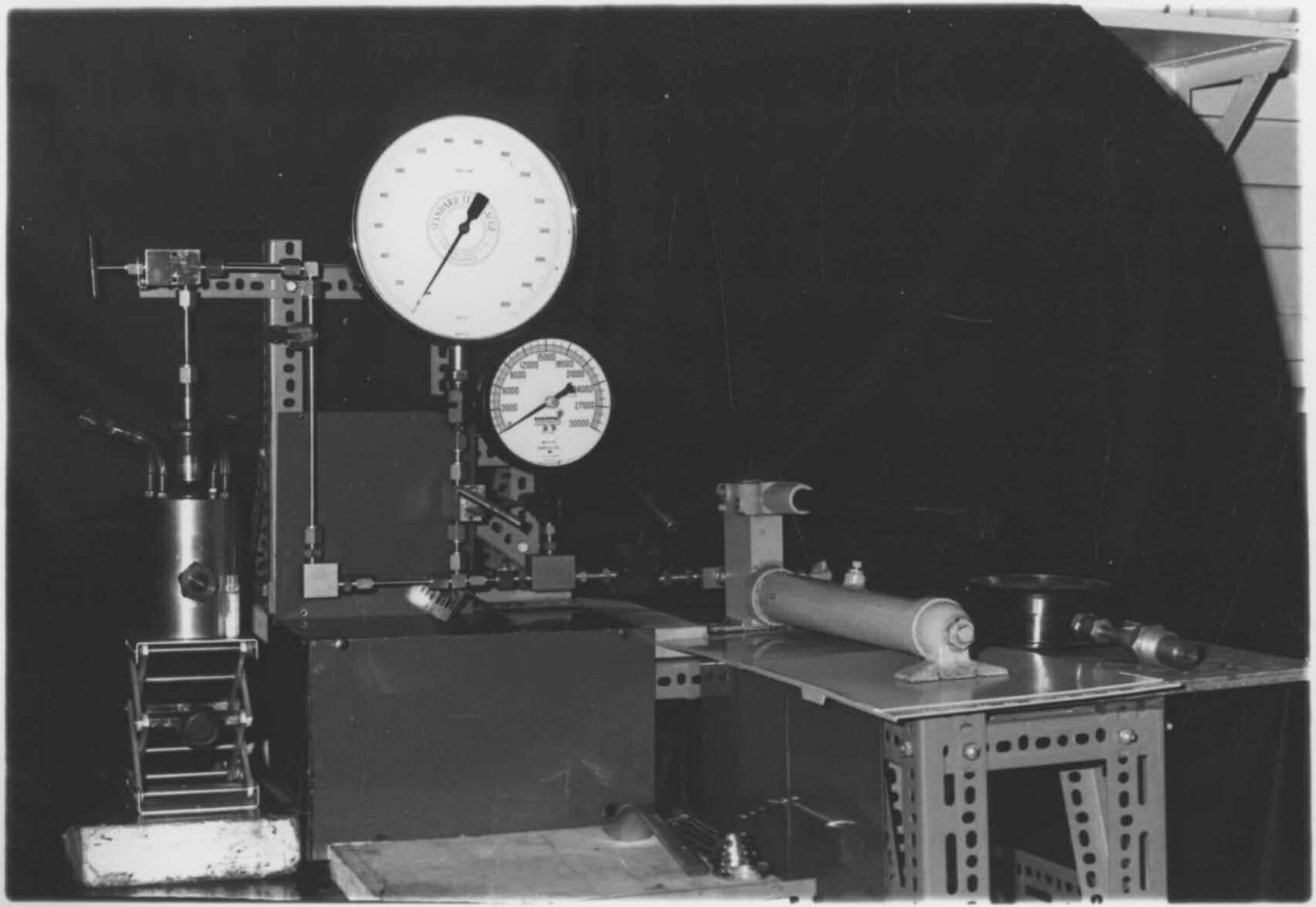

atmospheric pressure to 200 MPa. For high pressures, an Enerpac model 31-302 test guage was used; for intermediate pressures (up to 20 MPa) a Budenburg standard test guage was used. Low pressures (up to 2 MPa) were measured with a Budenburg guage. (1 MPa = 10.1325 atm. (7)).

3. ENTHALPIC STABILIZATION IN NON-AQUEOUS MEDIA

3.1. Experimental

Two samples of polyisobutylene (PIB) were kindly supplied by Essochem Australia Ltd. The higher molecular weight sample was Esso Butyl Rubber grade 035 containing nominally 0.8 mole% unsaturation (isoprene). The lower molecular weight sample, Vistamex grade LM MH, contained negligible unsaturation. Viscosity average molecular weights were determined in benzene at the Θ-temperature (297 K), allowing the use of the following Mark-Houwink equation (8):

$$[\eta]/\mathrm{dl\ g^{-1}} = 1.07 \times 10^{-3} \langle M_v \rangle^{\frac{1}{2}} \quad .$$

The molecular weights found were $(1.5 \pm 0.1) \times 10^5$ and $(2.3 \pm 0.2) \times 10^4$.

Acrylonitrile and benzoyl peroxide were Fluka purum grade. The 2-methylbutane was BDH laboratory reagent.

Amphipathic stabilizers were prepared,for example, be heating the grade 035 PIB (2 g), dissolved in n-heptane (38 g), with acrylonitrile (0.2 g) at 60°C for 20 hours in the presence of benzoyl peroxide initiator (0.1 g). The copolymer, poly(isobutylene-g-acrylonitrile), was isolated by pouring the reaction mixture into ice-cold ether, decanting the supernatant and drying the precipitate under vacuum.

The sterically stabilized polyacrylonitrile (PAN) latex was prepared by polymerizing acrylonitrile (2 g) in n-heptane (100 cm^3) in the presence of

dissolved stabilizer (2 g) and benzoyl peroxide initiator at 70°C The latex was formed after several hours. Excess stabilizer was removed by repeated centrifugation and redispersion in 2-methylbutane. The weight average particle radius (determined turbidimetrically) for the latex stabilized by the higher molecular weight PIB was 53 nm; that for the latex stabilized by the lower molecular weight PIB was 47 nm.

Since the phase separation of PIB in 2-methylbutane occurs above the normal boiling point of the solution, the experiments were carried out using sealed tubes and the pressure bomb described earlier. (The normal boiling point of 2-methylbutane is 301 K (7)). The pressure of the system was closely approximated by the vapour pressure of 2-methylbutane, which was calculated (for the tubes and bomb) from (7):

$$\log_{10}(P/\text{mm Hg}) = -(1.4139 \times 10^3)/(T/K) + 7.54468 \ .$$

All measurements were corrected to the hypothetical state of P = 0 (9-11). This was done by employing the pressure dependence of the lower critical solution temperature (LCST) of PIB in 2-methylbutane as found by Allen and Baker (9) and Gaeckle and Patterson (10). They found that the LCST increases by approximately 0.05 K MPa^{-1} and our experiments confirmed this small dependence.

3.2. Results and Discussion

The phase diagram for the separation of the higher molecular weight PIB in 2-methylbutane is shown in Fig.3a. These measurements were performed in

Fig.3. (a) Phase diagram for PIB ($<M_v>$ = 1.5 × 10^5) in 2-methylbutane.

(b) Cornet and van Ballegooijen plot to determine the Θ-temperature:

filled circles - sealed tubes

open circles - pressure bomb.

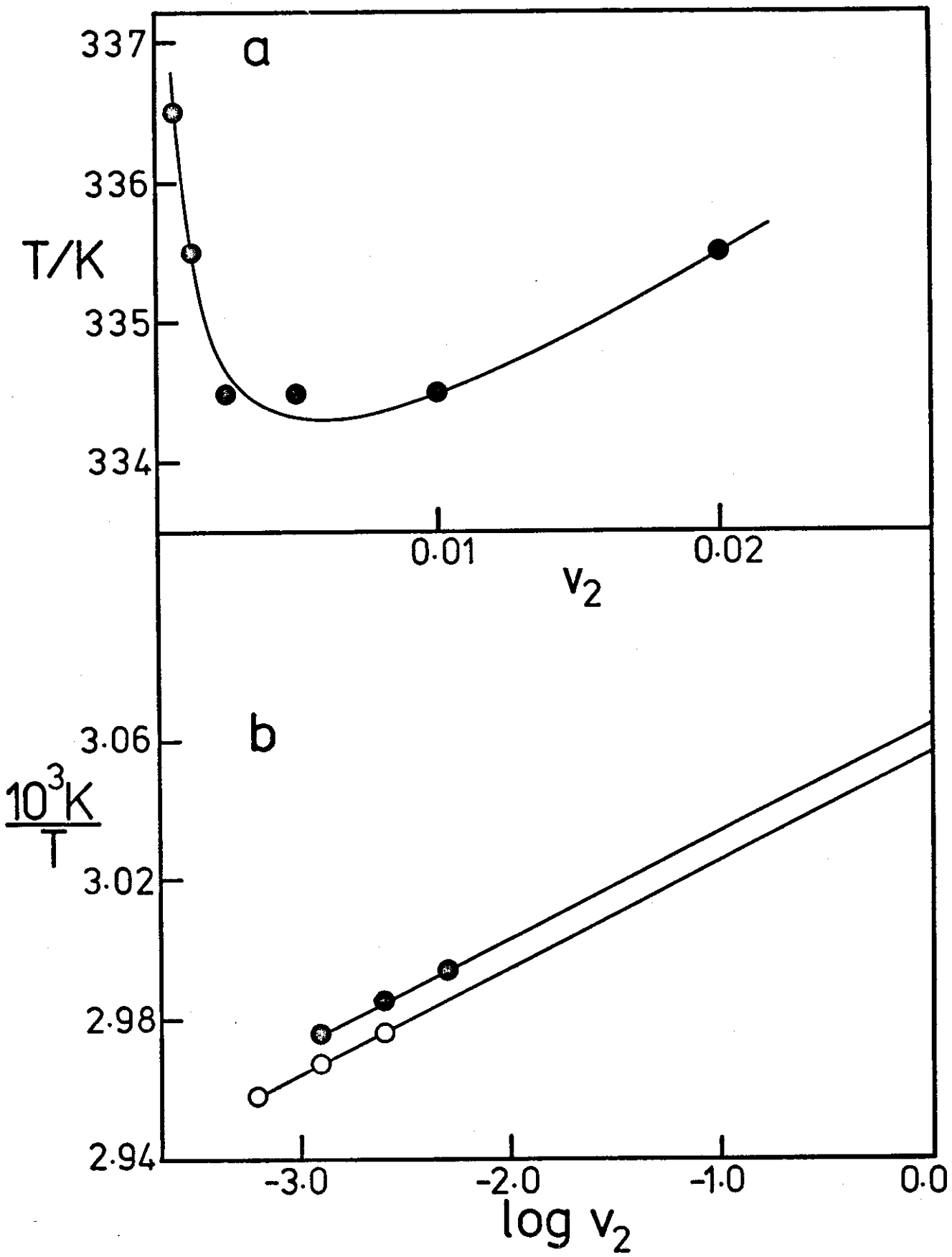
a
337
336
335
334
T/K
0.01
0.02
v_2
b
3.06
3.02
2.98
2.94
$\frac{10^3 K}{T}$
-3.0
-2.0
-1.0
0.0
log v_2

the pressure bomb. As expected, the solution exhibited an LSCT, signifying that the entropy and enthalpy of dilution parameters for this system are both negative (12), at least in the vicinity of the LCST. Negative values for these parameters indicate that dispersions stabilized by PIB in 2-methylbutane should be enthalpically stabilized (1). Extrapolation of the phase separation data (13) yields the Θ-temperature of PIB in 2-methylbutane (Fig.3b). The values of Θ obtained were 325 ± 2 K (sealed tubes) and 326 ± 2 K (pressure bomb). Gaeckle and Patterson found a slightly lower value of Θ (316 K) using a fully saturated sample of PIB. We were unable to measure Θ for our fully saturated sample because of the high temperatures required to induce phase separation. The difference in the values of Θ as obtained by us and by Gaeckle and Patterson may have been due to differences in the method of measurement. Additionally, different degrees of branching and/or unsaturation may have contributed to the discrepancy. The purity of the 2-methylbutane is unlikely to have been the scource of the discrepancy, since the addition of 5% n-pentane (the most probable impurity) increased Θ by only ~0.5 K.

The PAN latex stabilized by the higher molecular weight PIB flocculated on heating to 325 ± 1 K in both the sealed tube and the pressure bomb. The latex stabilized by the lower molecular weight PIB also flocculated on heating to 325 ± 1 K. These critical flocculation temperatures coincide with the measured Θ-temperature for free PIB in 2-methylbutane.

With the preparation of these enthalpically stabilized latices in 2-methylbutane, we have completed the demonstation that both entropic and enthalpic stabilization should be evident in both aqueous and non-aqueous media. A

summary of all the well characterized sterically stabilized dispersions prepared to date is presented in Table 1.

Classical polymer solution theories such as the Flory-Huggins theory (14,15) are unable to predict the phenomenon of enthalpic stabilization. The principal reason is that theories based on the lattice model for polymer solutions ignore the differences in free volume between the solvent and polymer (12). It is this free volume difference which has been found to be primarily responsible for the existence of an LCST (16). Furthermore, it is believed (17) that most polymer solutions have an LCST in the vicinity of the gas-liquid critical point of the pure solvent. The LCST's extrapolated to the limit of infinite molecular weight polymer have been found for many systems (18,19) to lie in the range 73-99% of the pure solvent critical temperature (all temperatures being expressed in absolute units). Of course, these extrapolated LCST's are the Θ-temperatures of the systems. We shall distinguish the Θ-temperatures associated with upper and lower critical solution temperatures by labelling them Θ_H and Θ_S respectively. The subscripts refer to the fact that near each Θ-temperature, the infinite molecular weight polymer remains in solution by virtue of dominant enthalpic and entropic effects respectively.

TABLE 1

Classification of Sterically Stabilized Dispersions

Stabilizer	Dispersion Medium		Type	Refs.
	Type	Example		
PLMA	Non-aqueous	n-heptane	Entropic	36
PHS	Non-aqueous	n-heptane	Entropic	36
PS	Non-aqueous	Toluene	Entropic	37
PEO	Non-aqueous	Methanol	Entropic	2
PIB	Non-aqueous	2-methylbutane	Enthalpic	6
PEO	Aqueous	0.48 M $MgSO_4$	Enthalpic	20,38
PVOH	Aqueous	2 M NaCl	Enthalpic	24
PMAA	Aqueous	0.02 M HCl	Enthalpic	5
PAA	Aqueous	0.2 M HCl	Entropic	5
PAAm	Aqueous	2.1 M $(NH_4)_2SO_4$	Entropic	5
PVOH	Mixed	Dioxan/water	Combined	24
PEO	Mixed	Methanol/water	Combined	2

4. A CORRELATION BETWEEN CRITICAL FLOCCULATION PRESSURES AND Θ-PRESSURES

4.1. Experimental

The preparation of poly(ethylene oxide) (PEO) stabilized latices has been described previously (20). The disperse phase was poly(vinyl acetate) (PVA) and the dispersion medium was water. Viscosity average molecular weights $\langle M_v \rangle$ were determined as in ref.20. The PEO used for the determination of Θ-conditions had $\langle M_v \rangle = 2.08 \times 10^5$; that used to stabilize the latices had $\langle M_v \rangle = 1.0 \times 10^4$, except for those latices subject to pressures in excess of 80 MPa, when $\langle M_v \rangle$ was increased to 2.08×10^5.

Glass windows in the bomb allowed the contents of the cell to be monitored visually. Small differences in the visually determined onset of flocculation and phase separation were detected at atmospheric pressure for samples inside and outside the bomb. This apparently arose from the decreased sensitivity of observations inside the bomb; all measurements taken inside the bomb were corrected for these differences.

Two methods were used to find the points of phase separation and flocculation. The first involved changing the temperature at constant pressure at such a rate as to maintain thermal equilibrium in the bomb. Rates of less than 0.1 K min^{-1} were required. A less time-consuming method was to induce the transition by changing the pressure at constant temperature. In this way, reproducibility could be checked by performing several pressure cycles.

4.2. Results

The Θ-temperatures at various pressures up to 150 MPa were obtained for PEO in 0.41m $MgSO_4$ solution by the extrapolation procedure of Cornet and Ballegooijen (13). (The electrolyte concentration is expressed on the pressure independent molal scale.) Phase separation was found to occur on heating and/or on raising the pressure. The phase separation curves are depicted in Fig.4. The linear extrapolation plots for finding Θ_H are shown in Fig.5. As the pressure increases, the Θ-temperature decreases. This result indicates that aqueous latices stabilized by PEO should become less stable with increasing pressure.

The critical flocculation pressures of the latices were found by increasing the pressure at constant temperature until an abrupt increase in turbidity signified the onset of flocculation. This pressure-induced flocculation was found to be reversible below 80 MPa. Above 80 MPa some irreversibility was apparent, even when PEO of much higher molecular weight ($\langle M_v \rangle = 2.08 \times 10^5$) was used as the stabilizer.

The close correlation between the Θ-pressures and critical flocculation pressures is evident in Fig.4. These results reinforce and extend the thesis (20) that the limit of stability of most sterically stabilized latices (21,22) correlates closely with the attainment of Θ-conditions for the stabilizer polymer.

Fig.4 Plots of phase separation pressure, Θ-pressure and critical flocculation pressure as a function of temperature. Curves 1-4 show phase separation pressures for polymer volume fractions: (1) 2.5×10^{-3}, (2) 5×10^{-3}, (3) 1×10^{-2}, (4) 2×10^{-2}. Curves 5 and 6 show the Θ-pressure and critical flocculation pressure respectively.

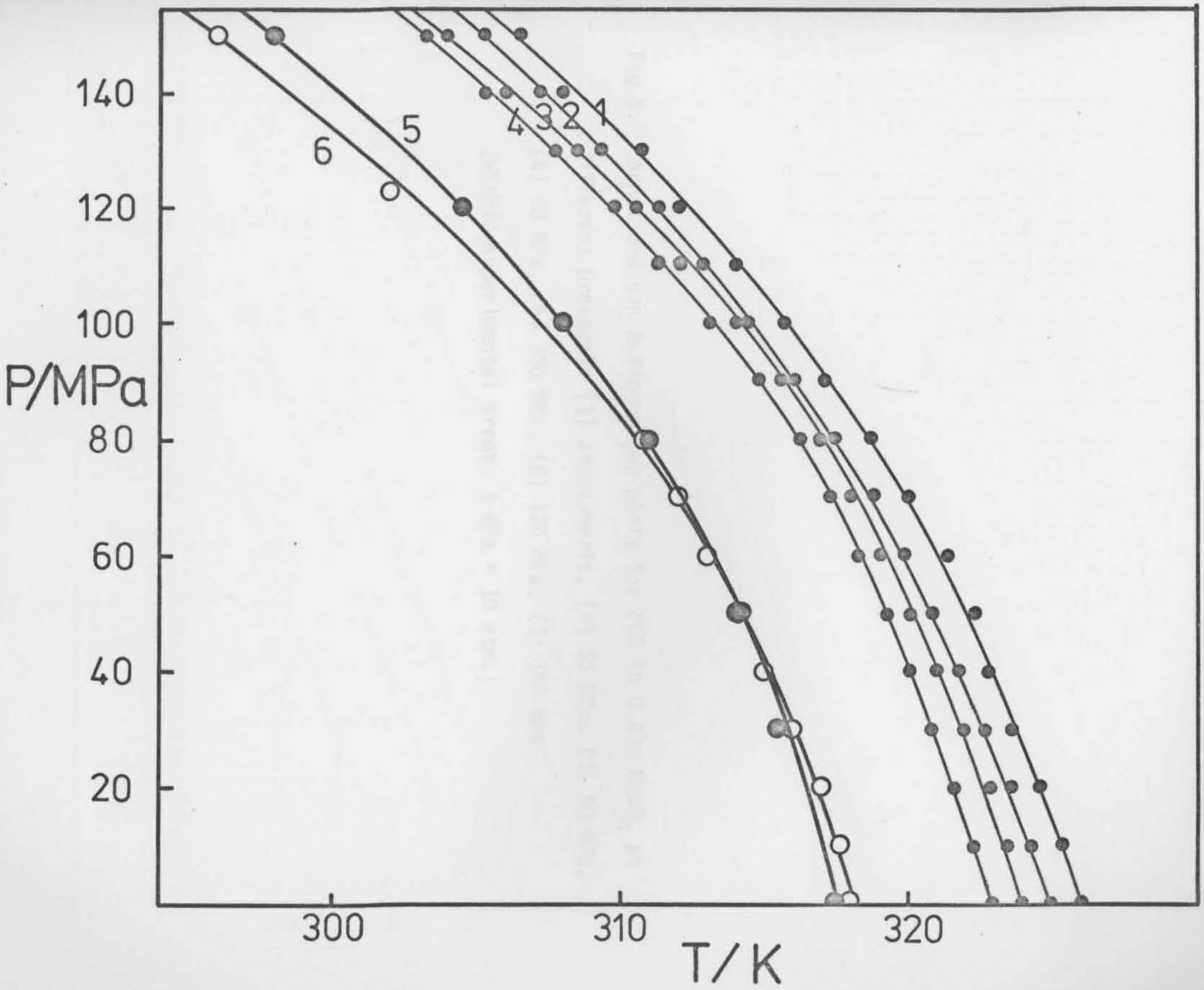
140
120
100
P/MPa
80
60
40
20
300
310
320
T/K
1
2
3
4
5
6

Fig.5. Cornet and van Ballegooijen plots for PEO in 0.41m $MgSO_4$ at different pressure: (1) atmospheric, (2) 30 MPa, (3) 50 MPa, (4) 80 MPa, (5) 100 MPa, (6) 120 MPa, (7) 150 MPa. (Within experimental error, 1 MPa = 10 atm.)

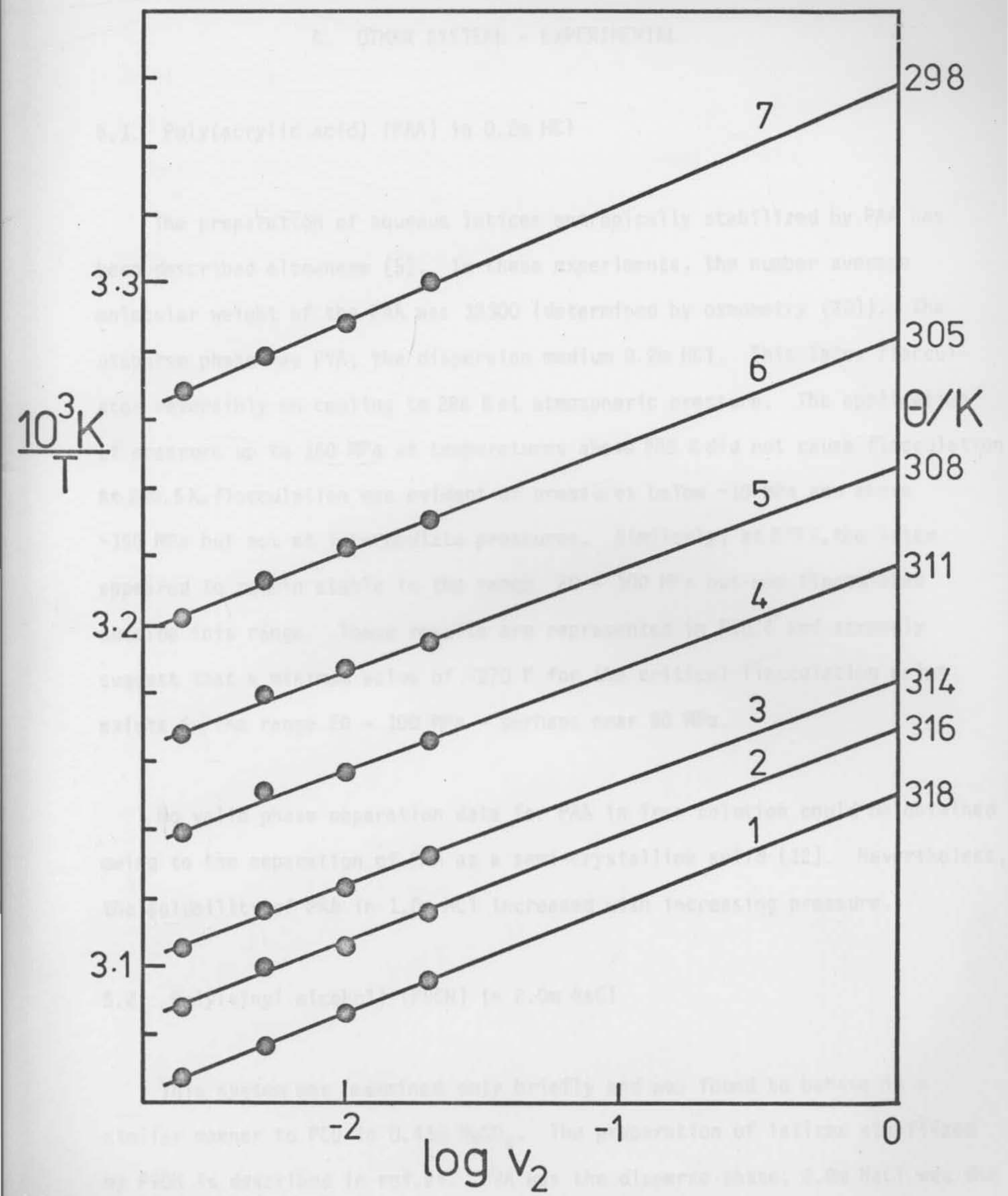
298
7
3.3
305
6
$\frac{10^3 K}{T}$
Θ/K
308
5
311
4
3.2
314
3
316
2
318
1
3.1
-2
-1
0
log v_2

5. OTHER SYSTEMS - EXPERIMENTAL

5.1. Poly(acrylic acid) (PAA) in 0.2m HCl

The preparation of aqueous latices entropically stabilized by PAA has been described elsewhere (5). In these experiments, the number average molecular weight of the PAA was 19300 (determined by osmometry (23)). The disperse phase was PVA; the dispersion medium 0.2m HCl. This latex flocculated reversibly on cooling to 288 K at atmospheric pressure. The application of pressure up to 160 MPa at temperatures above 288 K did not cause flocculation. At 280.5 K, flocculation was evident at pressures below ~10 MPa and above ~150 MPa but not at intermediate pressures. Similarly, at 273 K, the latex appeared to remain stable in the range 20 - 100 MPa but was flocculated outside this range. These results are represented in Fig.6 and strongly suggest that a minimum value of ~270 K for the critical flocculation point exists in the range 20 - 100 MPa - perhaps near 50 MPa.

No valid phase separation data for PAA in free solution could be obtained owing to the separation of PAA as a semi-crystalline solid (12). Nevertheless, the solubility of PAA in 1.0m HCl increased with increasing pressure.

5.2. Poly(vinyl alcohol) (PVOH) in 2.0m NaCl

This system was examined only briefly and was found to behave in a similar manner to PEO in 0.41m $MgSO_4$. The preparation of latices stabilized by PVOH is described in ref.24. PVA was the disperse phase; 2.0m NaCl was the

dispersion medium. The molecular weight of the PVOH was 26000 (25). Fig.7 indicates the effect of pressure on the critical flocculation point of this enthalpically stabilized latex. Although the pressure dependence is of the same form as that for the PEO/0.41m $MgSO_4$ system, the sensitivity of the PVOH/2.0m NaCl system to pressure is considerably less.

Fig.6. Pressure and temperature dependence of the critical flocculation point of a PVA latex stabilized by PAA ($\langle M_n \rangle$ = 19300) in 0.2m HCl.

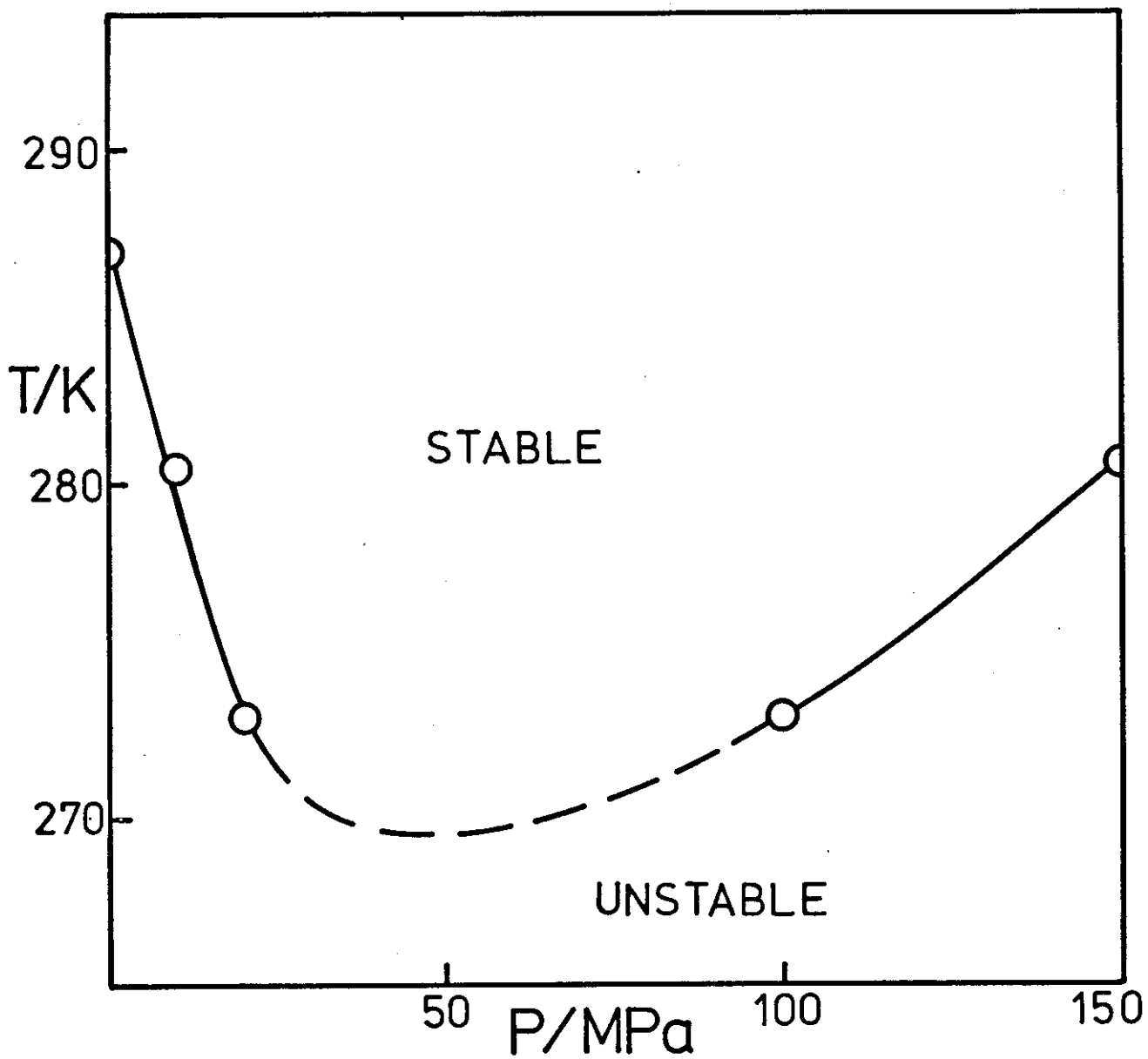
290
T/K
280
270
STABLE
UNSTABLE
50
P/MPa
100
150

Fig.7. Pressure and temperature dependence of the critical flocculation point of a PVA latex stabilized by PVOH (<M> = 26000) in 2.0m NaCl.

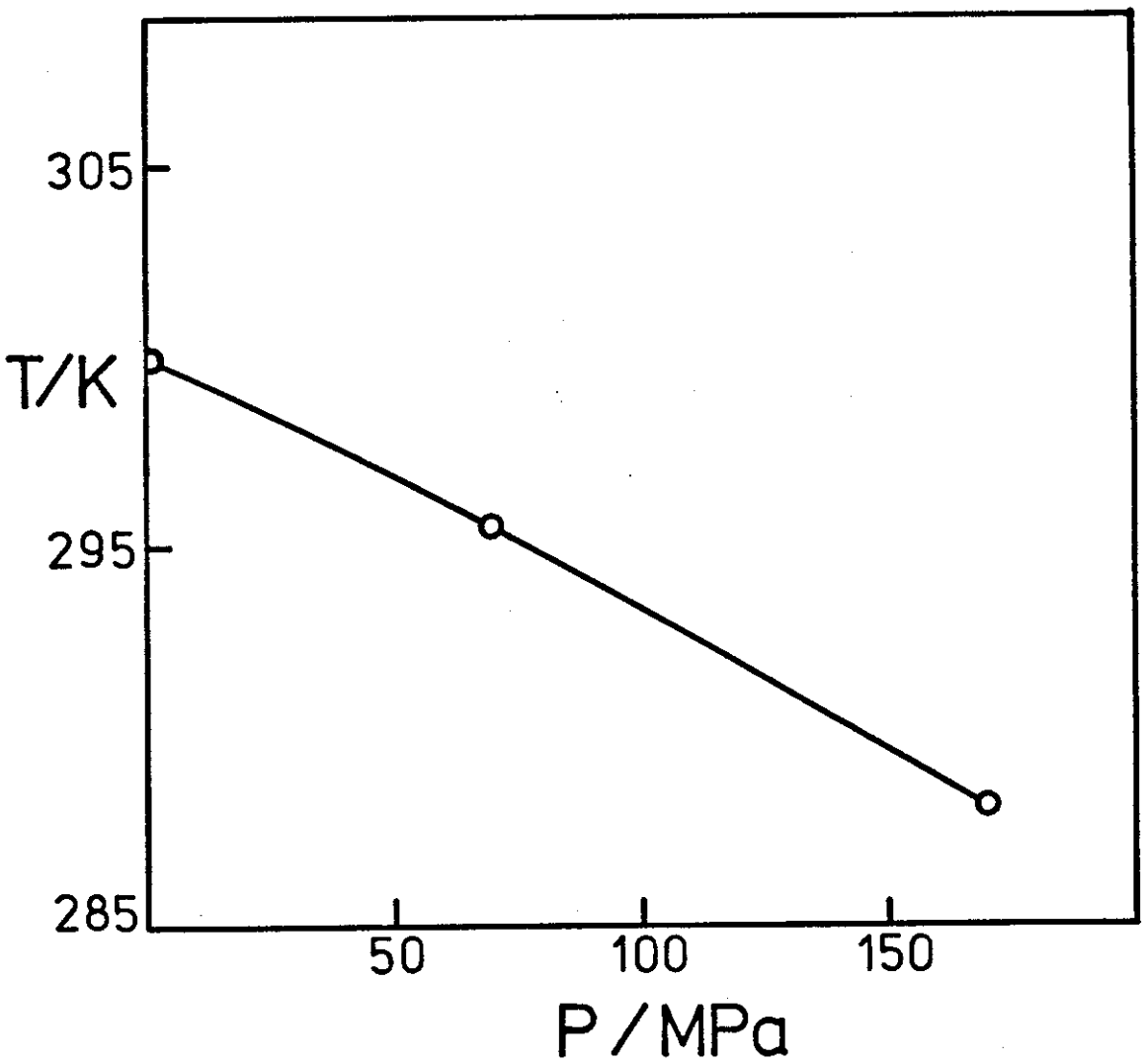
305
T/K
295
285
50
100
150
P / MPa

6. GENERAL DISCUSSION

If flocculation can be considered a phase transition process (22), we would expect the Clausius-Clapeyron relationship to hold (26):

$$\frac{\partial P}{\partial T} = \frac{\Delta S}{\Delta V} = \frac{\Delta H}{T\Delta V} \quad , \qquad \{2\}$$

where ΔS and ΔV are the entropy and volume changes associated with the flocculation process. The above relationship is obtained by differentiating expression {1}:

$$\Delta G = \Delta E + P\Delta V - T\Delta S = 0$$

with respect to temperature (see introduction to this chapter). Note from Fig.1 that near the critical flocculation point ($\Delta G = 0$) a sterically stabilized latex must be either entropically or enthalpically stabilized. In other words, if the critical flocculation point is to be observable, ΔH and ΔS must be of the same sign. Combined entropic-enthalpic latices cannot be flocculated. We can predict the signs of ΔH, ΔE, ΔV and ΔS from the flocculation behaviour of the latex.

Consider, for example, the aqueous latices stabilized by PEO (section 4). Flocculation on heating indicates that these latices are enthalpically stabilized near the critical flocculation point (2). Therefore ΔH and ΔS are both positive. We know from our high pressure experiments that $\frac{\partial P}{\partial T}$ is negative. When an aqueous latex stabilized by PEO flocculates, we expect a decrease in overall volume to accompany the transition. We have mixed PEO of molecular weight 400 with water (50% v/v) and found that the mixing process is exothermic and is accompanied by a decrease in total volume (~2%). This is in agreement with the results of a more detailed study made by Malcolm and Rowlinson (27).

The negative enthalpy change on dilution (exothermic process) is consistent with a positive enthalpy change on flocculation, since flocculation involves an overall increase in concentration of PEO in the latex stabilizer layer. However, a negative value of ΔV for both dilution and flocculation may, at first, seem inconsistent. Fig.8 illustrates the general form of excess volume of mixing (V_M^E) versus polymer concentration (v_2) curves when V_M^E is negative (e.g., for the PEO/water system).

The maximum value of $|V_M^E|$ is typically near $v_2 = 0.5$ (e.g.,28,29,30), although some asymmetry is often apparent (e.g., $|V_M^E|_{max}$ for PEO in water occurs near $v_2 = 0.7$ (27)). Point A indicates the excess volume of mixing when the stabilizer is initially dissolved in the solvent medium, resulting in a stable latex. The flocculation process involves an increase in average stabilizer concentration due to overlap and/or compression of the stabilizer layers. Point B indicates the excess volume of mixing of the adsorbed stabilizer with solvent medium in a flocculated latex. Obviously, flocculation (A → B) involves a decrease in overall latex volume as we predicted from eq.{2}.

The average volume fraction of polymer in the stabilizer layer of a sterically stabilized latex is generally much less than 0.5 (see chap.I, section 9, Table 2). It seems unlikely, therefore, that a latex can be prepared which, on flocculation, suffers a change in volume opposite in sign to that of V_M^E (Fig.8, C → D).

So far we have found the signs of $\Delta H(+)$, $\Delta S(+)$ and $\Delta V(-)$ for the flocculation of aqueous latices stabilized by PEO. Since ΔV is negative and ΔH is

Fig.8. Excess volume of mixing V_M^E as a function of polymer volume fraction v_2 when V_M^E is negative (PEO/water system (27)).

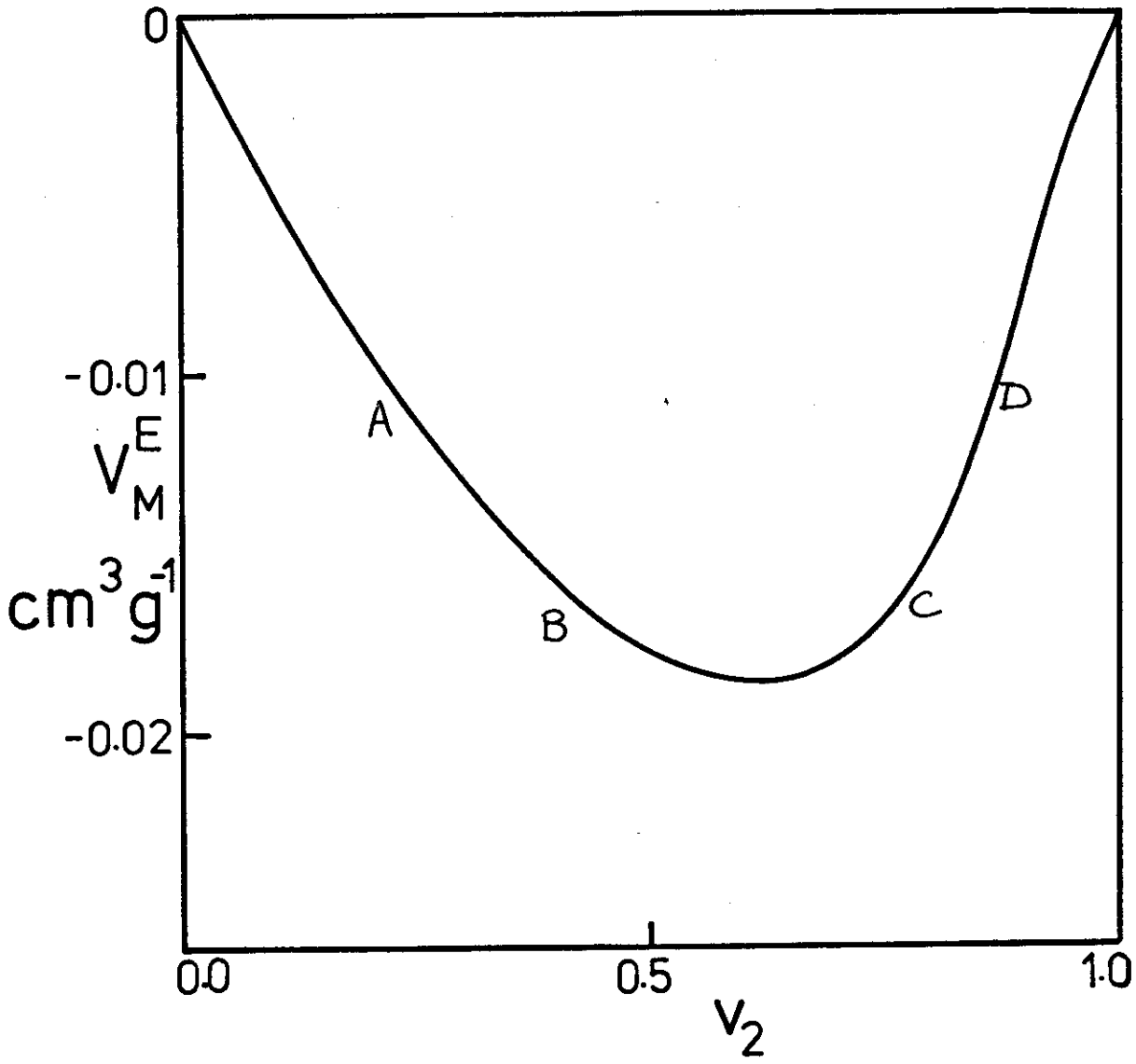
0
-0.01
-0.02
V_M^E
$cm^3 g^{-1}$
A
B
C
D
0.0
0.5
1.0
V_2

positive, ΔE must be positive (eq.{1}). Similarly, the signs of the thermodynamic functions can be found for all the systems we have studied. These signs are listed in Table 2. Whether the latex is enthalpic or entropic is also indicated.

The unusual behaviour of the PAA/0.2m HCl system under pressure deserves further comment. Taniguchi et al (31) have shown that the solubility of PMMA is enhanced by increasing the pressure. They explain this increase in solubility by pointing out that the dissociation of the polyacid is accompanied by a decrease in volume (32); therefore, the dissociation is promoted by increasing the pressure. Hydration of the ionized groups results in increased solubility (31). Similar ionization behaviour is expected for PAA under pressure, since the volume change accompanying ionization of many carboxylic acids has been found to be negative (33). We suggest, therefore, that the minimum in Fig.6 may be due to the competition between the negative ΔV effect and the ionization effect. The latter presumably becomes dominant above about 50 MPa. This explanation may be tested at a later date by investigating the pH dependence of the phenomenon. We expect the minimum to move to higher pressures and temperatures with decreasing pH.

Although we have not as yet been able to demonstrate both enthalpic and entropic stabilization in a single solvent medium, we expect such behaviour to be possible on the basis of modern polymer solution theories (16,34). As we mentioned earlier, these theories predict that all polymer solutions should exhibit an LCST near the critical point of the pure solvent. Any solution which exhibits a UCST, therefore, should have an accessible Θ_H and Θ_S provided a large enough range of temperature and pressure is scanned.

TABLE 2

Signs of Thermodynamic Functions Near the Critical Flocculation Point

System Stabiiizer/medium	$\frac{\partial P}{\partial T}$	ΔV	ΔE	ΔH	ΔS	type
PEO/0.41m $MgSO_4$	-	-	+	+	+	enthalpic
PIB/2-methylbutane	+	+	+	+	+	enthalpic
PAA/0.2m HCl (low P)	-	+	-	-	-	entropic
PAA/0.2m HCl (~50 MPa)	∞	0	-	-	-	entropic
PAA/0.2m HCl (high P)	+	-	unknown	-	-	entropic
PVOH/2.0m NaCl	-	-	+	+	+	enthalpic

Note that the sign of ΔE cannot be determined in the case of PAA/0.2m HCl at high pressure. The signs of the other quantities do not constitute sufficient data.

Finally, we note that our results conflict with the theory proposed by Lechner et al (35), which predicts that for all high polymer solutions, Θ increases with increasing pressure. We found the opposite effect in the PEO/0.41m $MgSO_4$ system and we expect a similar trend in Θ_H for PVOH/0.2m NaCl and in Θ_S for PAA/0.2m HCl (at low pressures).

7. REFERENCES

1. Napper,D.H. and Hunter,R.J., MTP Int. Rev. Sci., Series II, 7 (1975).
2. Napper,D.H. and Netschey,A., J. Colloid and Interface Sci., 37, 528 (1971).
3. Osmond,D.W.J., Vincent,B. and Waite,F.A., Kolloid-Z-Z. Polym., 253, 676 (1975).
4. Ottewill,R.H., Ann. Rep. Prog. Chem., (Chem. Soc. Lond.), A66, 212 (1969).
5. Evans,R., Davison,J.B. and Napper,D.H., J. Polymer Sci., B10, 449 (1972).
6. Evans,R. and Napper,D.H., J. Colloid and Interface Sci., 52, 260 (1975).
7. "Handbook of Chemistry and Physics", 54th ed., CRC Press, Cleveland (1973).
8. Brandrup,J. and Immergut,E.H., (eds.), "Polymer Handbook", Wiley-Interscience, New York, (1966).
9. Allen,G. and Baker,C.H., Polymer, 6, 181 (1965).
10. Gaeckle,D. and Patterson,D., Macromolecules, 5, 136 (1972).
11. Zeman,L., Biros,J., Delmas,G. and Patterson,D., J. Phys. Chem., 76, 1206 (1972).
12. Flory,P.J., "The Principles of Polymer Chemistry", Cornell University Press, Ithaca, New York (1953).
13. Cornet,C.F. and van Ballegooijen,H., Polymer, 7, 293 (1966).
14. Huggins,M.L., J. Chem. Phys., 9, 440 (1941).
15. Flory,P.J., J. Chem. Phys., 9, 660 (1941).
16. Patterson,D., Macromolecules, 2, 672 (1969).
17. Freeman,P.I. and Rowlinson,J.S., Polymer, 1, 20 (1960).
18. Patterson,D., Delmas,G. and Somcynsky,T., Polymer, 8, 503 (1967).
19. Bardin,J.M. and Patterson,D., Polymer, 10, 247 (1969).

20. Napper,D.H., J. Colloid and Interface Sci., 32, 102 (1970).

21. Dobbie,J.W., Evans,R., Gibson,D.V., Smitham,J.B. and Napper,D.H., J. Colloid and Interface Sci., 45, 557 (1973).

22. Evans,R. and Napper,D.H., Kolloid-Z-Z. Polym., 251, 329 (1973).

23. Davison,J.B., M.Sc. Thesis, Sydney University (1971).

24. Napper,D.H., Kolloid-Z-Z. Polym., 234, 1149 (1969).

25. Went,P.M., B.Sc.Hons. Thesis, Sydney University (1974).

26. Moore,W.J., "Physical Chemistry", 4th ed., Longmans, London (1965).

27. Malcolm,G.N. and Rowlinson,J.S., Trans. Faraday Soc., 53, 921 (1957).

28. Flory,P.J. and Höcker,H., Trans Faraday Soc., 67, 2258 (1971).

29. Höcker,H. and Flory,P.J., Trans. Faraday Soc., 67, 2270 (1971).

30. Höcker,H., Shih,H. and Flory,P.J., Trans. Faraday Soc., 67, 2275 (1971).

31. Taniguchi,Y., Suzuki,K. and Enomoto,T., J. Colloid and Interface Sci., 46, 511 (1974).

32. Suzuki,K. and Taniguchi,Y., J. Polymer Sci., A2, 8, 1679 (1970).

33. Kauzmann,W.,Bodanszky,A.,Rasper,J., J. Amer. Chem. Soc., 84, 1777 (1962).

34. Flory,P.J., Disc. Faraday Soc., 49, 7 (1970).

35. Lechner,M.D., Schulz,G.V. and Wolf,B.A., J. Colloid and Interface Sci., 39, 462 (1972).

36. Napper,D.H., Trans Faraday Soc., 64, 1701 (1968).

37. Doroszkowski,A. and Lambourne,R., J. Colloid and Interface Sci., 43, 97 (1973).

38. Napper,D.H., J. Colloid and Interface Sci., 29, 168 (1969).

CHAPTER III

FLOCCULATION OF LATICES BY LOW MOLECULAR WEIGHT POLYMERS

1. INTRODUCTION

High molecular weight polyelectrolytes are well known as flocculants for electrostatically stabilized dispersions (e.g., Table 1 of ref.1). It is thought that they cause flocculation by each chain adsorbing onto two or more particles (bridging mechanism), thus restricting Brownian movement (1-7). Gregory (4,8) has demonstrated that low molecular weight cationic polymers are effective flocculants for negatively charged polystyrene (PS) latices. He gives an explanation in terms of non-uniform charge distribution effects which result in overall electrostatic attraction near the optimum flocculant concentration.

We have found (9) that efficient flocculation of latices with suitable surface groups can be achieved using low molecular weight non-ionic polymers (viscosity average molecular weight $M_v \geq 10^3$ to 10^4).

We begin this chapter by presenting the results of a preliminary qualitative investigation into the flocculation behaviour of various latex/polymer systems. One system will then be examined in more detail using a rapid mixing technique devised by Ottewill and Sirs (10). The results will be compared with those obtained by flocculation with barium nitrate and discussed in terms of two proposed mechanisms.

2. QUALITATIVE FLOCCULATION STUDIES

2.1. Materials

Flocculants and Stabilizers

Polymer abbreviations are listed at the beginning of this thesis. Apart from PAA and PMAA, which were prepared by a heterogeneous polymerization procedure (11,12), the polymer samples were obtained from the following sources:

PEO	Union Carbide (Australia)
PPO	Shell Chemicals (Australia)
PVOH	Ajax Chemicals
PVP	GAF (N.S.W.)

The steric stabilizers were prepared according to procedures given in the following references:

poly(ethylene oxide-b-vinyl acetate)	(13)
poly(acrylic acid-g-vinyl acetate)	(14)
poly(vinyl alcohol-g-vinyl acetate)	(15)

Latices

"High carboxyl" PS latices were prepared by the method of Ottewill and Shaw (9,16). All other latices were prepared by the heterogeneous polymerization of vinyl acetate in the presence of stabilizer copolymer using potassium persulphate initiator at 50^{0}C in water. Excess stabilizer was removed by centrifugation and redispersion in water.

The particle size of the "high carboxyl" PS latex used in the kinetic

studies was determined by measuring the dry weight and latex turbidity. A weight average particle radius of 31 nm was found. The polymer molecular weight (usually viscosity average) will be indicated, where necessary, as a suffix to the polymer abbreviation.

2.2. Polystyrene Latices with Surface Acid Groups

It was found (9) that small PS latices prepared by the method of Ottewill and Shaw (16) could be flocculated by trace amounts of low (and high) molecular weight PEO at a sufficiently low pH. Even PEO of molecular weight as low as 4000 induced flocculation. The presence of surface acid groups on these PS particles has been demonstrated by several authors (17-21). These acid groups have been found to be mostly carboxylic, although some sulphonic acid residues may be produced by the action of persulphate initiators (e.g.,17,21). The flocculation behaviour of low carboxyl PS latices (20), prepared at low temperatures (< 30°C) in the absence of oxygen, was not affected by the presence of PEO. In addition to this sensitivity to small amounts of PEO, it was found (20) that small "high carboxyl" latices, typically of a few hundred Ångströms radius, exhibit unusually high stability in aqueous media of high ionic strength (e.g., 0.5 M NaCl) and flocculate on cooling in these media.

This may be attributed to a polymeric oxidation product formed during the initial stages of particle formation (20). This polymer would contain many of the surface carboxyl groups and would sterically stabilize (entropically) the small particles. It was not found possible to grow larger particles (radius ~100 nm) with the same steric stability properties. Perhaps the stabilizer

polymer became buried in the particles as they grew. These large particles were found to be unstable in 0.05 M NaCl.

Oxidised surfactant can be discounted as the scource of the steric stability of these latices because very small (a few hundred Ångströms) entropically stabilized PS latices have been produced in these laboratories without the use of surfactants (e.g., by refluxing low concentrations of styrene ($\gtrsim$ 0.5%) in water with potassium persulphate). In fact, latices which appear to remain stable for many hours in 0.2 M NaCl can be prepared without surfactant or initiator by stirring low concentrations of styrene in water at high temperatures (e.g.,80^{o}C) for several hours. Stability is probably a result of the oxidation by residual oxygen in the water. One latex prepared by this method had an average radius of 90-100 nm (determined by turbidimetry).

Isolation of the unknown stabilizer was attempted by rapidly stirring a 2% styrene emulsion stabilized by aerosol OTN (0.05%) in water at 80^{o}C and frequently adding aliquots of potassium persulphate solution. The emulsion changed colour and broke as oxidation proceeded (white → yellow → green → brown) over ~30 minutes. A sticky brown product settled out and was redissolved in water then extensively dialyzed to remove salts, soap, monomer and any other low molecular weight substances. The brown solution contained a significant quantity of stable latex particles which were removed by centrifugation, leaving a clear, brown, surface-active solution. This solution probably contained many polymeric species in various stages of oxidation, making structural analysis impractical. Elemental analysis (by C.S.I.R.O. Microanalytical Laboratory, Melbourne) yielded the following proportions for carbon, hydrogen,

oxygen and sulphur, which together comprised 98% by weight of the product:

$$C : H : O : S \simeq 35 : 29 : 11 : 1$$

Assuming that the sulphur is in the form of sulphate, we still have an oxygen to carbon ratio of 1:5.

It appears, therefore, that there may be sufficient carboxylation to form a water soluble polymer during the initial stages of polymerization.

The solution exhibited the following properties:

i) pH ≃ 2.7.

ii) Phase separation on cooling in ~1 M NaCl solution.

iii) Precipitation with PEO only when acidified (0.2 M HCl) and redissolved on the addition of sodium hydroxide.

iv) Flocculation of PEO stabilized latices in the presence of acid.

v) When added to a purely electrostatically stabilized PVA latex, the latex, which was initially unstable in 0.01 M NaCl, remained stable in 0.4 M NaCl for about twelve hours after treatment.

vi) The above treated latex flocculated almost irreversibly in 0.4 M NaCl on cooling to ~10°C. This irreversibility was probably due to poor anchoring (13).

vii) Addition of acidified PEO solutions to the treated latex resulted in flocculation.

All of the above evidence indicates that the brown solution contains the same polymer which is responsible for the steric stabilization of small highly carboxylated PS latices as prepared by the method of Ottewill and Shaw.

This initial attempt at isolating the steric stabilizer, although crude, does provide further evidence of its existence. Another approach would be to prepare water-soluble polymers which may conceivably have a similar structure to the "unknown" and to determine which of these polymers behaves most like the "unknown".

We will show in section 3.4 of this chapter, that the proposed steric stabilizer on high carboxyl latices facilitates explanation of their flocculation behaviour in the presence of PEO at low pH.

2.3. Sterically Stabilized Latices

Based upon evidence given above and elsewhere (20), we shall henceforth assume that small "high carboxyl" PS latices are sterically stabilized by polyacids. Bailey *et al* (22,23) and Saito and Taniguchi (24,25) have presented much evidence for strong hydrogen (H) bonding interactions between the carboxyl groups of polymeric acids and the ether oxygens of PEO. If H-bonding is responsible for the observed flocculation behaviour of "high carboxyl" PS latices, we would expect to see similar behaviour with many other latex/flocculant systems specifically chosen for their potential H-bonding capabilities. Table 1 lists the additional systems in which flocculation was observed. It is expected that stabilizer and flocculant are interchangeable in general.

Strong H-bonded complexes between polymer pairs listed in Table 1 have been reported in the following references:

	(22,23,24)	PAA - PEO
	(22)	PMAA - PEO
	(24)	PAA - polyalcohols
	(26)	PAA - PVP .
Also:	(27)	PMAA - PVP .

We found that poly(propylene oxide) (PPO) could be used as the H-bonding base in place of PEO.

2.4. Effect of Urea

Urea (carbamide) is a well known protein denaturant (28,29). The denaturation mechanism appears to be rather complex, involving alteration of the water structure and competition for H-bonding sites (30-34). We are concerned primarily with the H-bonding ability of urea. It was expected that urea would have the same effect on flocculant-particle H-bonds as on the intramolecular H-bonds of proteins. Urea is known to form complexes with PEO (35) and with carboxylic acids (34).

Two dispersions of PS stabilized by PEO 23000 were prepared: one in 0.1 M HCl and the other in 0.1 M HCl/10 M urea. To each of these stable latices was added an equal quantity of PAA 19300 (~50 ppm). The dispersion without urea flocculated in seconds while that with urea remained stable. Subsequent addition of water to the latex protected by urea resulted in immediate flocculation.

TABLE 1

Aqueous Latex/Flocculant Systems at Low pH

Flocculant	Stabilizer	Particle
PAA 19300	PEO 23000	PVA
PAA 19300	PVOH 56000	PVA
PEO 23000	PAA 19300	PVA
PMAA 20000	PEO 23000	PVA
PMAA 20000	PVOH 56000	PVA
PVOH 56000	PAA 19300	PVA
PVP 25000	PAA 19300	PVA
PPO 2000	PAA 19300	PVA

It is proposed that the urea preferentially H-bonds to the PAA carboxyl groups and the PEO ether oxygens, preventing the formation of a PEO - PAA complex. As we have mentioned previously, Bailey et al (22) found that mixtures of PAA and PEO form an insoluble H-bonded complex at sufficiently low pH ($\lesssim 4$) in water. They concluded from their experiments that the addition of urea to the complex in aqueous solution is not effective in breaking up the complex. However, only 1 M urea was used, and our experiments on the PEO - PAA complex revealed that considerably higher urea concentrations do break up the complex at low pH. A mixture of 2½% PEO 23000 and 2½% PAA 19300 in 0.25 M HCl is turbid owing to phase separation of the PEO - PAA complex. Addition of solid urea to a concentration of ~4 M results in a completely clear solution, indicating dissolution of the complex. Dilution of this clear solution with water again causes phase separation (or precipitation, if the molecular weight of either or both of the components is high).

Similar behaviour was observed in the PAA/PVOH, PAA/PVP and PAA/PPO systems. Precipitation of the polymeric complex could be prevented or reversed by the addition of urea or by raising the pH.

Latices stabilized by PVOH, for example, were found to be stable in aqueous urea and these protected latices could not be flocculated by the addition of PAA. In this case, less than 1 M urea was effective.

Although urea is a strong H-bonding agent, it is not strongly self-associating in aqueous media (31,36) and any weak association can be explained in terms of dipole interactions (36). We would not expect, therefore, that

adsorbed urea molecules in the above systems could H-bond with each other and cause flocculation or complex formation. Instead, they appear to render the H-bonding sites inactive.

Having examined the qualitative behaviour of several particle/flocculant systems, we now consider the possible flocculation mechanisms.

2.5. Flocculation Mechanisms

Two distinct mechanisms are believed to be responsible for the flocculation behaviour of sterically stabilized latices in the presence of polymeric flocculants. Both rely on specific interactions between the stabilizer polymer and the flocculant. The evidence indicates that H-bonding is the basic interaction responsible in the latices considered here.

Consider, for example, the flocculation by PEO of a latex stabilized by PAA (at low pH). When the molecular weight of the PEO is very high, relatively few segments should adsorb, via H-bonds, onto the particles in the first few seconds after mixing. We would expect many of the segments to extend well into the medium, adsorbing onto and "trapping" one or more other particles. This is the "normal" bridging mechanism associated with high molecular weight flocculants (e.g.,1,2,37). At the other extreme, when low molecular weight PEO is used, diffusion is much more rapid. There are, we believe, two distinct possibilities in this case.

The first is that the PEO adsorbs onto the outer surface of the PAA

stabilizer layer by H-bonding through a significant fraction (but not all) of its ether oxygens. In this way, the latex has a fraction θ of its surface randomly coated with PEO. Flocculation is caused by H-bond bridging when the PEO and PAA areas come into contact during Brownian encounters. This is the type of bridging mechanism most often associated with low molecular weight flocculants (9,38), although high molecular weight flocculants behave in the same way if the particle size is large enough (1) or if alternative mixing procedures are used to allow equilibrium adsorption to take place in the absence of flocculation (39).

The second mechanism will be termed the complexing mechanism. It relies on the fact that the particles are sterically stabilized and that the flocculant complexes stoichiometrically with the stabilizer (e.g.,22,26,27). (We assume here that such a complex can also form between PEO and the stabilizer on "high carboxyl" latices.) In contrast with the high molecular weight PEO, short flocculant chains would have a much better chance of being entirely adsorbed onto the PAA stabilizer in a time shorter than the particle collision time. In other words, a stoichiometric PEO - PAA polymeric complex, as described by Bailey et al (22), should form on the particle surface. At low pH ($\lesssim$ 4) this complex is insoluble in water (22); therefore, if enough low molecular weight PEO is used to complex with most of the PAA stabilizer at low pH, the latex must flocculate (in the absence of electrostatic effects).

Both of the above mechanisms are probably active during flocculation but it seems likely that the bridging mechanism predominates for high molecular weight flocculants and the complexing mechanism for very low molecular weight flocculants.

Before examining the more quantitative aspects of flocculation, we report an interesting phenomenon which was observed during an attempt at flocculating a PEO stabilized latex and a PAA stabilized latex together (heteroflocculation).

Two sterically stabilized latices, one coated with PEO 23000 and the other coated with PAA 19300, were centrifuged and redispersed until the supernatant from each latex no longer contained enough free polymer to flocculate the other latex (three times each at ~75000 × g for one hour). A significant difference in particle size was visually evident; the size of the PAA stabilized latex being the greater. When these latices were mixed in 0.2 M HCl, only a slight turbidity was observed. This mixture was then divided into two parts. To one part, PAA 19300 was added; to the other, PEO 23000 was added. Flocculation occurred only in the part to which PAA was added.

One possible explanation for the observed behaviour is that, upon mixing the latices, several PEO stabilized latex particles attach to each PAA stabilized particle to form small flocs which are sterically stabilized by PEO. Subsequent addition of PAA flocculates these composite particles while the addition of PEO has no effect. Differences in latex concentration as well as particle size may have contributed to this phenomenon.

The particular PEO stabilized latex had, in this instance, to be freshly centrifuged before use as some desorption of the stabilizer was evident after several hours (indicating the need for stronger anchoring).

We next report the results of flocculation rate studies on "high carboxyl" PS latices. This system was chosen because PS latices prepared by the method of Ottewill and Shaw (9,16),and similar methods, are used, for example, in the experimental determination of the Hamaker constant for PS in water (48). The existence of a steric contribution to the stability of "high carboxyl" latices has been demonstrated by Smitham et al (20). The assumption that such latices are solely electrostatically stabilized can no longer be made. Apart from a general interest in this system, a further reason for using "high carboxyl" latices is that no excess stabilizer could be detected in the supernatant liquid after the particles were removed (i.e. the supernatant was incapable of affecting the stability of an acidified PEO stabilizer latex). This obviated the centrifugation which is usually required to remove excess stabilizer.

3. FLOCCULATION RATE STUDIES

3.1. Apparatus

A slightly modified version of the rapid mixing apparatus described by Ottewill and Sirs (10) was designed to be used in a Varian Techtron 635 spectrophotometer. Automatic recording was performed on a National chart recorder (model 135A-1). The mixing apparatus (Plate 2) provided its own light-tight seal and simultaneously operated the photomultiplier micro-switch at the rim of the cell compartment opening. We found that a return spring on the plunger increased the operating efficiency considerably and obviated the need for a supporting clip (10). Considerable experimentation was required to find the optimum dimensions for the mixing "cube": if the cube fits too tightly in the cell the solution may be ejected out of the cell and if the cube is too small its contents may not be completely mixed.

3.2. Method

1. The turbidity of the latex is measured with respect to that of pure water at the sodium D line (589 nm). Turbidity τ = optical density $\times$ ln10.
2. A constant volume of latex (3.00 cm^3) of known concentration is placed in each of two matched 1 cm cells.
3. A constant volume of flocculant solution of known concentration is metered into the mixing cube with a micrometer syringe. The solution is divided approximately equally among the four holes.

Plate 2. Rapid mixing apparatus disassembled and assembled. The mixing cube is made of Teflon and is threaded onto a stainless steel shaft.

4. The apparatus is assembled and placed in position in the spectrophotometer; the chart recorder and spectrophotometer are zeroed with the apparatus and reference latex in place.

5. The plunger is slowly depressed until the mixing cube is below the meniscus of the latex (indicated by a mark on the plunger shaft). This greatly reduces the possibility of expulsion of material from the cell. No reaction should be noticeable on the chart recorder at this stage.

6. Immediately, the plunger is depressed and released rapidly, completing the mixing process. Some practice may be required to find the most rapid mixing possible without loss of solution. Mixing times are generally less than 1 second (including instrumental response times).

Good reproducibility was obtained after a little practice; all runs were performed in triplicate as a check on reproducibility. By mixing known concentrations of potassium chromate solutions with water we found the mixing efficiency to be consistently better than 97%. The wavelength used for this mixing test was 275 nm (10).

3.3. Theory

Lichtenbelt et al (40,41) have derived an expression for the rate constant k_{11}, which characterises the rate of formation of doublets from single particles in a flocculating latex:

$$k_{11} = \frac{1}{N_1 \tau_0} \left(\frac{\partial \tau}{\partial t}\right)_0 / \left(\frac{c_2}{2c_1} - 1\right) , \qquad \{1\}$$

where τ is the turbidity of the latex at time t, N_1 is the initial number conc-

entration of the particles, c_1 and c_2 are the extiction cross-sections of a singlet and doublet respectively and the subscript 0 refers to the limit as $t \to 0$.

Equation {1} applies to the flocculation of latices by simple salts. According to the bridging theory of Smellie and La Mer (42), if polymers are used as the flocculant, the rate should be modified by the factor $\theta(1 - \theta)$, where θ is the fraction of the latex covered by flocculant. When $\theta = 0$ or 1 (i.e., no flocculant or full coverage) the flocculation rate is predicted to be zero. At $\theta = 0.5$ we have $\theta(1 - \theta) = 0.25$ and the maximum flocculation rate is only one quarter of that possible with simple electrolytes.

Unfortunately, we found that our "high carboxyl" PS latex was too stable to electrolytes to permit the determination of k_{11} for rapid flocculation. The concentration of flocculant in the mixing cube had to be thirty to sixty times the desired final concentration and, apart from solubility problems, the high viscosity of the salt solutions prevented efficient rapid mixing.

There should be an important observable difference between the two flocculation mechanisms discussed in section 2.5. The bridging mechanism is theoretically subject to the condition that the rate of flocculation is proportional to $\theta(1 - \theta)$ (as mentioned above). The complexing mechanism, on the other hand, would lead to a maximum rate near $\theta = 1$ and zero rate at $\theta = 0$. Additionally, we can visualize a second layer of flocculant forming over the insoluble complex to restabilize the latex. Therefore, we may find zero or low flocculation rate near $\theta = 2$. The simplest expression which reflects these flocculation

characteristics is:

$$\text{rate} \propto \theta(2 - \theta) \quad .$$

Of course, whether the flocculant has any effect on the latex after complex formation is complete has not been tested. It seems likely that once the stoichiometric quantity of flocculant has been added, further additions will have relatively little effect on the latex stability. Therefore, from the shapes of the rate versus flocculant concentration curves and the values of the maximum flocculation rates, it should be possible to determine whether the complexing mechanism or the bridging mechanism is dominant. The theoretical maximum rate due to the complexing mechanism is four times that due to the bridging machanism and the surface coverage at the maximum rate should be approximately 1.0 and 0.5 respectively.

These arguments apply only to low molecular weight flocculant unless the particle size is very large. There is no provision in the theory for a dramatic increase in the effective collision cross-section of the particles due to the adsorption of high molecular weight flocculant. Trains of segments may extend into the medium for many particle radii (37), interfering with Brownian motion long before particle-particle contact is possible. In most cases, we have used low molecular weight flocculant (PEO 5500, PEO 23000) but in one set of experiments, the molecular weight was varied up to 10^6. Equation {1} will be used for all calculations of k_{11} bearing in mind that quantitative deviations from the expected behaviour for high molecular weight flocculants may arise, in part, from a progressive failure of eq.{1}. The results will be presented as a fraction of the von Smoluchowski theoretical maximum flocculation rate constant (e.g.,10):

$$k_{11}^{max} = 10.8 \times 10^{-12} \text{ cm}^3\text{s}^{-1} \quad \text{at } 293 \text{ K} . \qquad \{2\}$$

3.4. Results and Discussion

The value of the optical constant, $\frac{c_2}{2c_1} - 1$, in eq.{1} was estimated from the results of Lichtenbelt et al (40). For a particle radius of 31 nm (determined turbidimetrically),

$$\frac{c_2}{2c_1} - 1 \simeq 0.8 .$$

The particle number concentration N_1 was found, on the basis of dry weight and turbidity measurements, to be 1.37×10^{12} cm^{-3}. At this concentration the value of τ_0 was 0.0677. Substituting these values into eq.{1} we have:

$$k_{11} = 1.35 \times 10^{-11} \left(\frac{\partial \tau}{\partial t}\right) , \qquad \{3\}$$

or, expressing the result in terms of the ratio R of the measured rate constant to the von Smoluchowski rapid flocculation rate constant (eq.{2}):

$$R = \frac{k_{11}}{k_{11}^{max}} = 1.25 \left(\frac{\partial \tau}{\partial t}\right)_0 . \qquad \{4\}$$

The experiments were performed at room temperature (20 ± 2°C). Because the flocculation times of the latices were found to be only of the order of seconds, the highest rates reported here may be underestimated. The dead-time of the apparatus is of the order of 1 second, thus difficulty was experienced in extrapolating to zero time.

A typical form of the dependence of flocculation rate on flocculant conc-

entration is given in Fig.1. The flocculant is PEO 5500 and the medium 0.3 M HCl. As expected (e.g.,1) there is a maximum in the rate curve. The position of this maximum corresponds to a complete surface coverage of ~(2-3) × 10^{-7} g cm^{-2}, which is of the same order of magnitude obtained by Homola (43) for low molecular weight PEO on PS particles (chapter 1). Homola determined the surface coverage by adding known quantities of stabilizer and measuring the dry weight remaining after removing the particles by centrifugation.

The results in Fig.1 are depicted in a different form in Fig.2. Also shown (line 2) are the results of flocculation by PEO 23000 in 0.2 M HCl. Note that the PEO concentration axis is linear. The dotted lines indicate the theoretically expected behaviour assuming that the rate is approximately proportional to $\theta(1 - \theta)$ (bridging model) and that flocculant adsorption is rapid and complete. It appears that the curves behave as expected until approximately 50% more than the optimum flocculant concentration is added, then the restabilizing effect diminishes dramatically. The slopes of the restabilization (right hand side) section of the curves are 1-2 orders of magnitude less than those of the initial destabilization sections. This effect can be attributed, in part, to the relatively poor stabilizing properties of unanchored PEO (44). Corresponding curves obtained by Gregory (8) for the flocculation of PS latices by low molecular weight cationic flocculants are much more symmetrical. This symmetry is probably due to an approximately symmetrical charge reversal from negative (particles) to positive (cationic flocculant).

Similar curves to ours have been found by La Mer and Healy (1), Gregory (4), Williams and Ottewill (6). They also found it more convenient to plot

Fig.1. Relative flocculation rate R versus the logarithm of the flocculant concentration for a "high carboxyl" PS latex flocculated with PEO 5500.

Acid concentration = 0.3 M

$$N_1 = 1.37 \times 10^{12} \text{ cm}^{-3}$$

$$\tau_0 = 0.0677$$

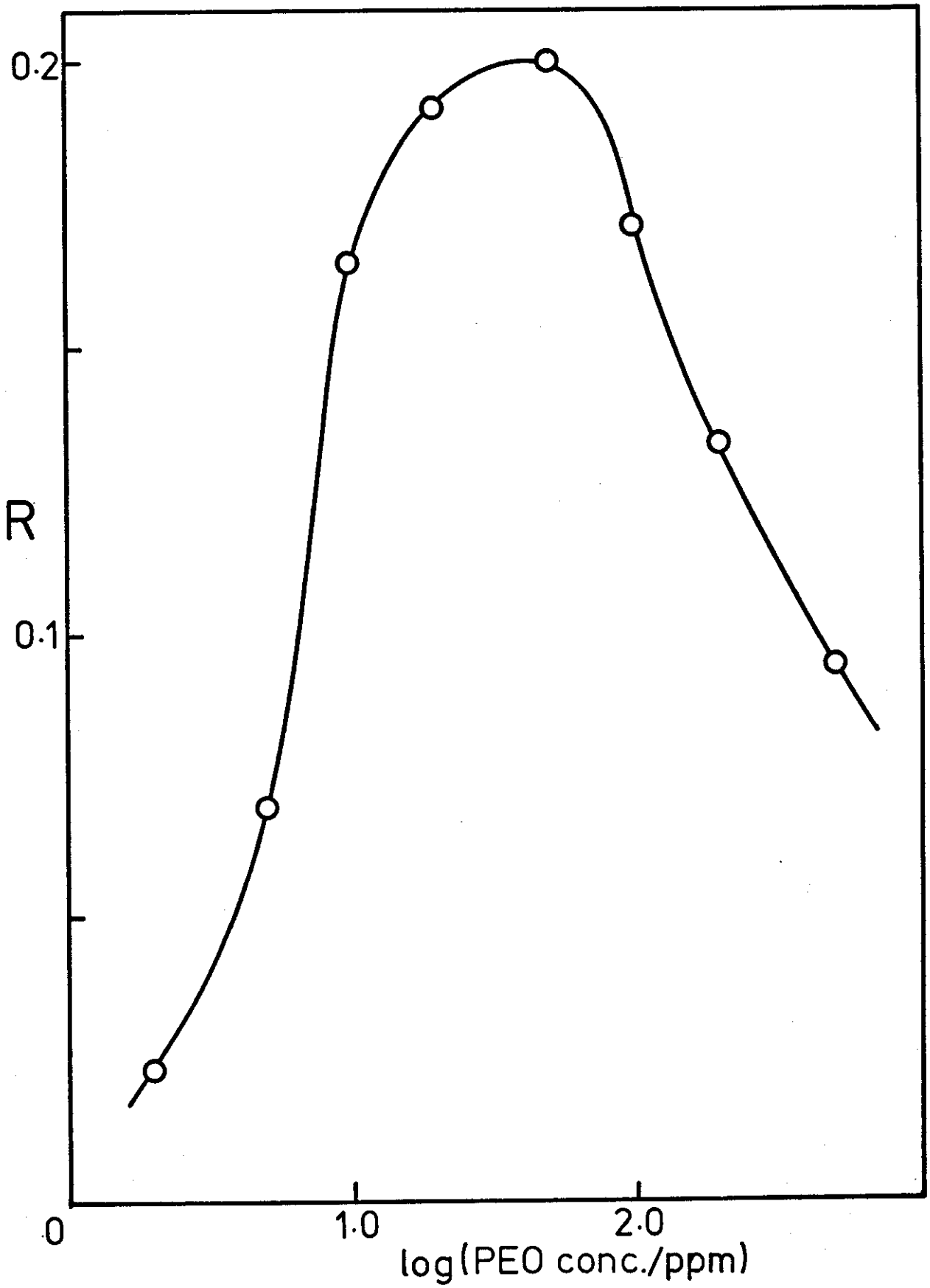
0·2
R
0·1
0
1·0
2·0
log(PEO conc./ppm)

Fig.2. Relative flocculation rate R versus flocculation concentration for a "high carboxyl" PS latex flocculated with PEO.

Lines: (1) PEO 5500 , 0.3 M HCl

(2) PEO 23000 , 0.2 M HCl .

$N_1 = 1.37 \times 10^{12}$ cm^{-3}

$\tau_0 = 0.0677$

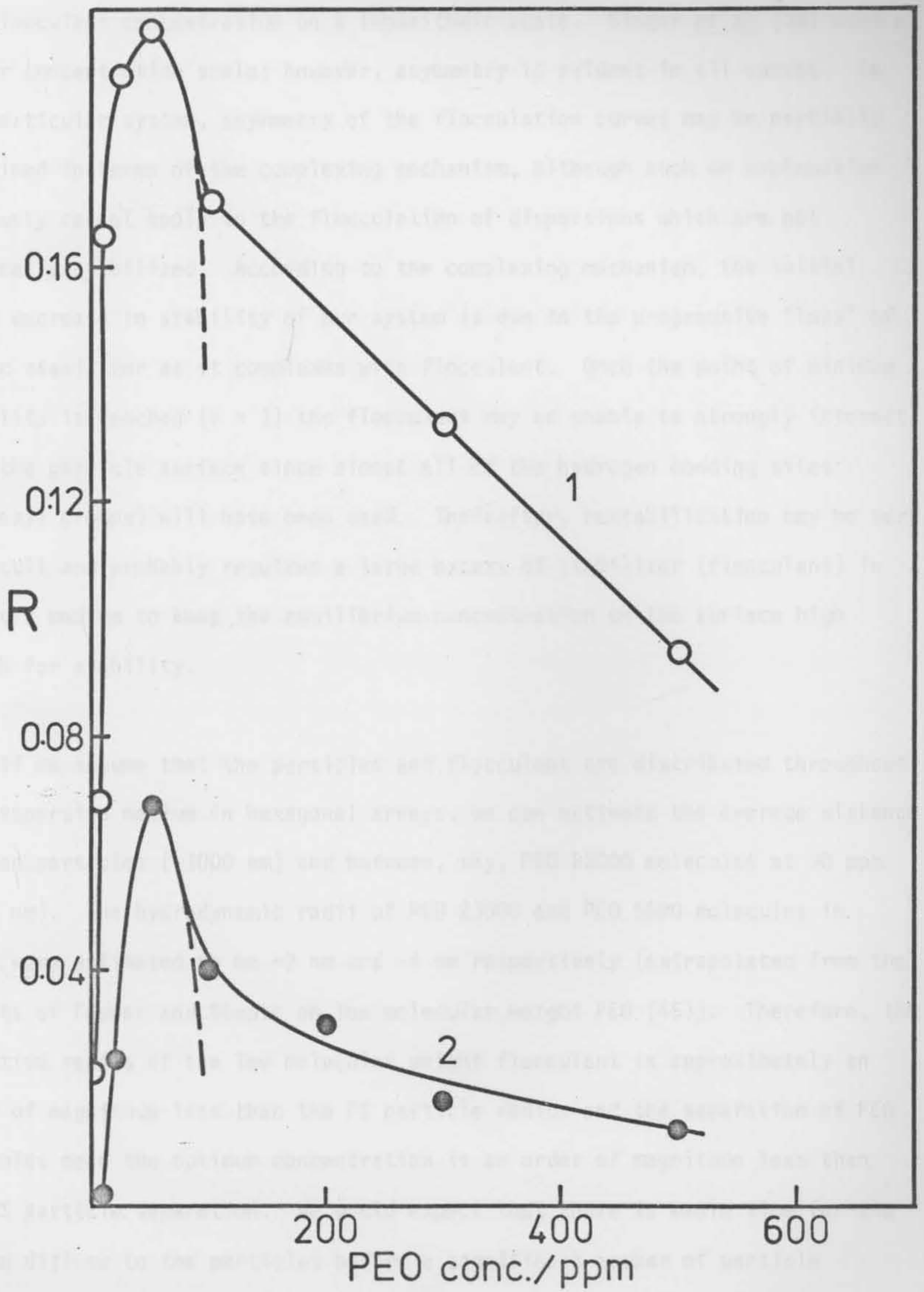
0·16
0·12
R
0·08
0·04
1
2
200
400
600
PEO conc./ppm

the flocculant concentration on a logarithmic scale. Singer et al (38) used a linear concentration scale; however, asymmetry is evident in all curves. In our particular system, asymmetry of the flocculation curves may be partially explained in terms of the complexing mechanism, although such an explanation obviously cannot apply to the flocculation of dispersions which are not sterically stabilized. According to the complexing mechanism, the initial rapid decrease in stability of our system is due to the progressive "loss" of steric stabilizer as it complexes with flocculant. Once the point of minimum stability is reached ($\theta \simeq 1$) the flocculant may be unable to strongly interact with the particle surface since almost all of the hydrogen bonding sites (carboxyl groups) will have been used. Thereafter, restabilization may be very difficult and probably requires a large excess of stabilizer (flocculant) in the bulk medium to keep the equilibrium concentration on the surface high enough for stability.

If we assume that the particles and flocculant are distributed throughout the dispersion medium in hexagonal arrays, we can estimate the average distance between particles (~1000 nm) and between, say, PEO 23000 molecules at 30 ppm (~100 nm). The hydrodynamic radii of PEO 23000 and PEO 5500 molecules in water were estimated to be ~2 nm and ~4 nm respectively (extrapolated from the results of Couper and Stepto on low molecular weight PEO (45)). Therefore, the effective radius of the low molecular weight flocculant is approximately an order of magnitude less than the PS particle radius and the separation of PEO molecules near the optimum concentration is an order of magnitude less than the PS particle separation. We would expect that there is ample time for the PEO to diffuse to the particles before a significant number of particle

collisions occur. The question arises, however, as to whether complex formation can be assumed to be at equilibrium before flocculation is significant.

In order to test this assumption, we changed the order of mixing acid and flocculant. At the concentrations of acid employed (~0.2 M), the surface carboxyls are considered to be fully protonated ($pK_a \simeq 4$-5 (17-20)). The acid serves two main purposes: one is to protonate the surface carboxyls and allow hydrogen bonding to occur, the other is to suppress any electrostatic effects due to surface charges. In 0.2 M HCl, we calculate (chapter IV, section 4.3.) a double layer thickness of approximately 0.7 nm. If, instead, we mix the latex and flocculant together in 0.18 M NaCl and wait a few minutes before adding 0.02 M HCl, we should have equilibrium flocculant adsorption as well as the same degree of double layer compression and virtually complete carboxyl protonation. The advantage of this method is that we need not assume that flocculant adsorption is much more rapid than particle flocculation. We only require that protonation of the carboxyl groups is rapid relative to the flocculation rate. This is a very reasonable assumption in view of the rapid reaction rates of simple oppositely charged ions in solution (e.g.,46).

Fig. 3 illustrates the effect of allowing the flocculant time to come to equilibrium at the latex surface. It is important to note from the work of Bailey et al (22), that the PEO - PAA complexes formed in acid solution are not completely dissociated at higher pH values. The PAA and PEO still tend to associate at high pH but remain in solution. We visualize a similar occurrence with sterically stabilized latices and H-bonding flocculants. Addition of PEO, for example, to a latex stabilized by PAA at high pH should result in the form-

Fig.3. Relative flocculation rate R versus flocculant concentration for a "high carboxyl" PS latex flocculated with PEO 23000.
Lines: (1) latex first mixed with 0.18 M NaCl + PEO 23000 then, after 5 min., flocculation induced with 0.02 M HCl.
(2) normal mixing procedure; PEO 23000, 0.2 M HCl.
$N_1 = 1.37 \times 10^{12}$ cm^{-3}
$\tau_0 = 0.0677$

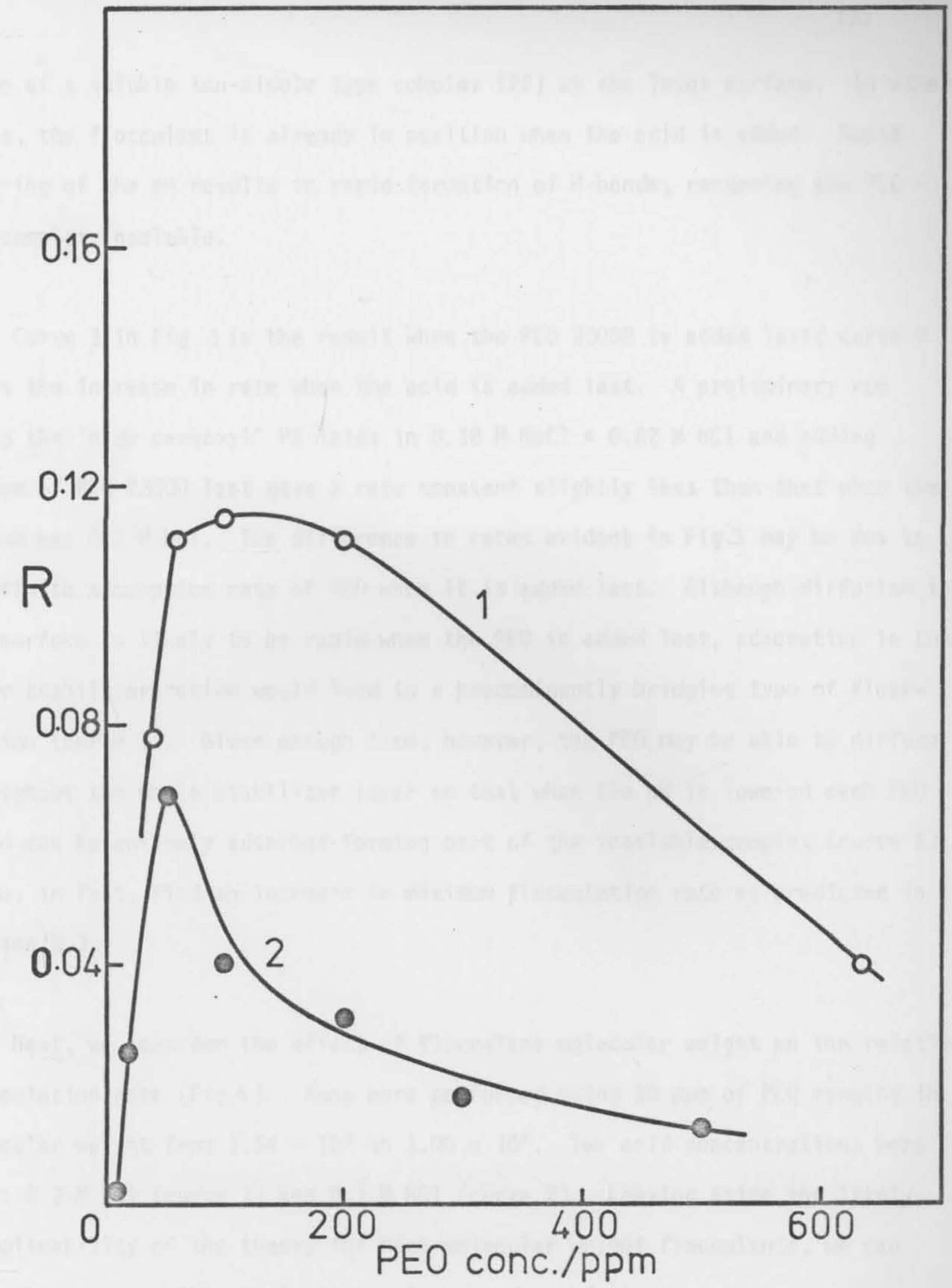
0·16
0·12
0·08
0·04
0
R
1
2
0
200
400
600
PEO conc./ppm

ation of a soluble ion-dipole type complex (22) at the latex surface. In other words, the flocculant is already in position when the acid is added. Rapid lowering of the pH results in rapid formation of H-bonds, rendering the PEO - PAA complex insoluble.

Curve 1 in Fig. 3 is the result when the PEO 23000 is added last; curve 2 shows the increase in rate when the acid is added last. A preliminary run using the "high carboxyl" PS latex in 0.18 M NaCl + 0.02 M HCl and adding 20 ppm of PEO 23000 last gave a rate constant slightly less than that when the medium was 0.2 M HCl. The difference in rates evident in Fig.3 may be due to the finite adsorption rate of PEO when it is added last. Although diffusion to the surface is likely to be rapid when the PEO is added last, adsorption in the outer stabilizer region would lead to a predominantly bridging type of flocculation (curve 1). Given enough time, however, the PEO may be able to diffuse throughout the whole stabilizer layer so that when the pH is lowered each PEO chain can be entirely adsorbed forming part of the insoluble complex (curve 2). We do, in fact, find an increase in maximum flocculation rate as predicted in section 3.3.

Next, we consider the effect of flocculant molecular weight on the relative flocculation rate (Fig.4). Runs were performed using 20 ppm of PEO ranging in molecular weight from 1.54×10^3 to 1.00×10^6. Two acid concentrations were used: 0.3 M HCl (curve 1) and 0.1 M HCl (curve 2). Leaving aside the likely inapplicability of the theory for high molecular weight flocculants, we can suggest a few possible explanations for the form of these curves.

i) There is a fairly abrupt rise in rate as the PEO molecular weight increases.

Fig.4. Relative flocculation rate R versus logarithm of flocculant molecular weight for a "high carboxyl" PS latex flocculated with PEO.

Lines: (1) in 0.3 M HCl

(2) in 0.1 M HCl .

PEO concentration = 20ppm

$N_1 = 1.37 \times 10^{12}$ cm^{-3}

$\tau_0 = 0.0677$

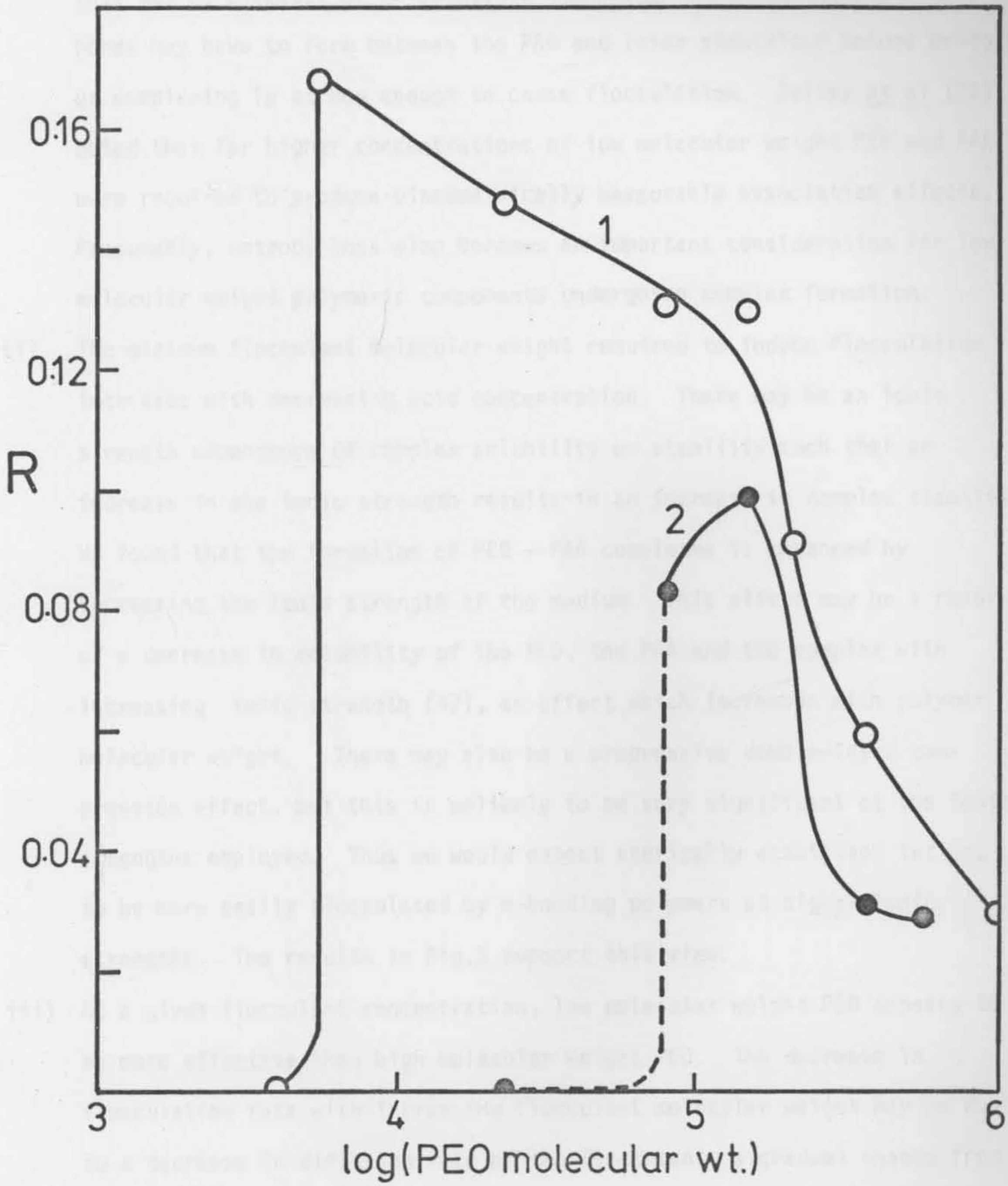
0·16
0·12
R
0·08
0·04
1
2
3
4
5
6
log(PEO molecular wt.)

This may be a result of co-operative H-bonding: a minimum number of H-bonds may have to form between the PEO and latex stabilizer before bridging or complexing is strong enough to cause flocculation. Bailey et al (22) noted that far higher concentrations of low molecular weight PEO and PAA were required to produce viscometrically measurable association effects. Presumably, entropy loss also becomes an important consideration for low molecular weight polymeric components undergoing complex formation.

ii) The minimum flocculant molecular weight required to induce flocculation increases with decreasing acid concentration. There may be an ionic strength dependence of complex solubility or stability such that an increase in the ionic strength results in an increase in complex stability. We found that the formation of PEO - PAA complexes is enhanced by increasing the ionic strength of the medium. This effect may be a result of a decrease in solubility of the PEO, the PAA and the complex with increasing ionic strength (47), an effect which increases with polymer molecular weight. There may also be a progressive double-layer compression effect, but this is unlikely to be very significant at the ionic strengths employed. Thus we would expect sterically stabilized latices to be more easily flocculated by H-bonding polymers at higher ionic strengths. The results in Fig.5 support this view.

iii) At a given flocculant concentration, low molecular weight PEO appears to be more effective than high molecular weight PEO. The decrease in flocculation rate with increasing flocculant molecular weight may be due to a decrease in diffusion rate of the flocculant, a gradual change from the complexing mechanism to the bridging mechanism and/or progressive failure of eq.{1} to describe the flocculation rate (e.g., flocculation

rate should be a function of flocculant concentration if adsorption cannot be considered "instantaneous").

Fig.5. Dependence of relative flocculation rate R on acid concentration for a "high carboxyl" PS latex flocculated with PEO 6000.

$N_1 = 1.37 \times 10^{12} cm^{-3}$

$\tau_0 = 0.0677$

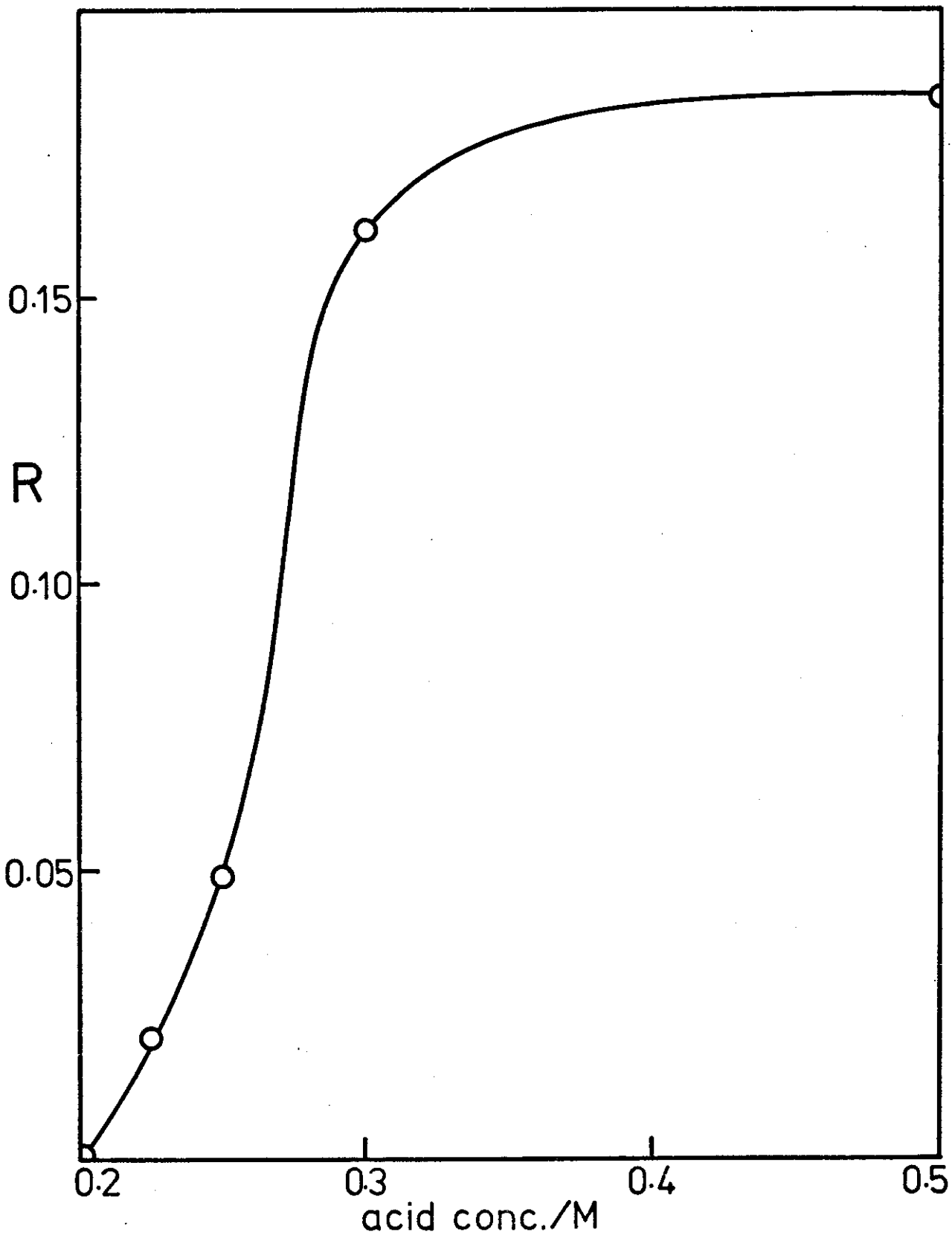
0·15
R
0·10
0·05
0·2
0·3
0·4
0·5
acid conc./M

4. CONCLUSIONS

These preliminary results indicate that low molecular weight non-ionic polymers can be effective as flocculants of appropriate sterically stabilized latices or latices which have suitable surface groups. An analogy may be drawn between flocculation by these non-ionic flocculants and that by polyelectrolytes. Gregory (4) has pointed out that, while high molecular weight polyelectrolytes probably act *via* a combination of bridging and charge reduction mechanisms, low molecular weight polyelectrolytes are effective solely by virtue of their charge cancellation capability. In comparison, we believe that high molecular weight non-ionic polymers flocculate sterically stabilized latices *via* a combination of bridging and complexing mechanisms, whereas low molecular weight non-ionic polymers, under suitable conditions, seem to be effective by virtue of their complexing capabilities. The analogy is between the charge reduction effect in electrostatically stabilized latices and the stabilizer solubility reduction effect in sterically stabilized latices. This investigation was carried out on "high carboxyl" PS latices because of interest in their unusual stability properties. As model latices for flocculation kinetic studies, however, it would be more desirable to use larger (~100 nm) monodisperse latices sterically stabilized, for example, by PAA.

Future studies of the complexing flocculation mechanism will include the possibility of flocculation in non-aqueous systems. Bailey *et al* (49) found that PEO could be quantitatively removed from benzene solution by the addition of dispersed urea due to the formation of an insoluble complex. Accordingly, we expect that urea would be a flocculant for PEO stabilized latices in benzene.

We have found that PVP 25000 and PAA 19300 form strong gel-like complexes in ethanol. PEO 23000 and PAA 19300 also interact to form a complex in this solvent. Thus there exists the possibility of flocculating sterically stabilized latices dispersed in ethanol.

It would be interesting to combine the effects of H-bonding and electrostatic attraction in sterically stabilized systems: charge-neutralization and stabilizer-complexing (or bridging) may be engineered to occur at the same time, eliminating both electrostatic and steric stabilization scources (e.g., by using random copolymers of ethylene oxide and quaternary ammonium compounds at low pH to flocculate negatively charged latices coated with PAA).

5. REFERENCES

1. La Mer,V.K. and Healy,T.W., Rev. Pure Appl. Chem., 13, 112 (1963).
2. Napper,D.H. and Hunter,R.J., MTP Int. Rev. Sci., Phys. Chem. Series 1, 7, 294 (1972).
3. Ries,jun.,H.E. and Meyers,B.L., Science, N.Y., 160, 1449 (1968).
4. Gregory,J., Trans. Faraday Soc., 65, 2260 (1969).
5. Ries,jun.,H.E., Nature,226, 72 (1970).
6. Williams,D.J.A. and Ottewill,R.H., Kolloid-Z-Z. Polym., 243, 141 (1971).
7. Crees,O.L., Proc. Roy. Aust. Chem. Inst., 39, 333 (1972).
8. Gregory,J., J. Colloid and Interface Sci., 42, 448 (1973).
9. Evans,R. and Napper,D.H., Nature, 246, 34 (1973).
10. Ottewill,R.H. and Sirs,J.A., Photoelectric Spectrometry Group Bulletin, 10, 262 (1957).
11. Davison,J.B., M.Sc. Thesis, Sydney University, 1971.
12. Alexandrowicz,Z., J. Polymer Sci., 40, 91 (1959).
13. Napper,D.H., J. Colloid and Interface Sci., 32, 106 (1970).
14. Evans,R., Davison,J.B. and Napper,D.H., J. Polymer Sci., B10, 449 (1972).
15. Napper,D.H., Kolloid-Z-Z. Polym., 234, 1149 (1969).
16. Ottewill,R.H. and Shaw,J.N., Kolloid-Z-Z. Polym., 215, 161 (1967).
17. Ottewill,R.H. and Shaw,J.N., Kolloid-Z-Z. Polym., 218, 34 (1967).
18. Shaw,J.N. and Marshall,M.C., J. Polymer Sci. A-1, 6, 449 (1968).
19. Shaw,J.N., J. Polymer Sci., C27, 237 (1969).
20. Smitham,J.B., Gibson,D.V. and Napper,D.H., J. Colloid and Interface Sci., 45, 211 (1973).
21. Stone-Masui,J. and Watillon,A., J. Colloid and Interface Sci., 52, 479 (1975).

22. Bailey,F.E., Lundberg,R.D. and Callard,R.W., J. Polymer Sci., A, 2, 845 (1964).

23. Bailey,F.E. and Koleske,J.V., "Nonionic Surfactants" (ed. Schick,M.J.), 1, 819 (Dekker, N.Y., 1967).

24. Saito,S. and Taniguchi,T., Kolloid-Z-Z. Polym., 248, 1039 (1971).

25. Saito,S. and Taniguchi,T. J. Colloid and Interface Sci., 44, 114 (1973).

26. Boyer-Kawenoki,F., Comptes Rendus, 263, 203 (1966).

27. Bimendina,L.A., Roganov,V.V. and Bekturov,E.A., J. Polymer Sci., C, 44, 65 (1974).

28. Neurath,H., Greenstein,J.P., Putnam,F.W. and Erickson,J.O., Chem. Revs., 34, 157 (1944).

29. (a) Kauzmann,W. and Simpson,R.B., J. Amer. Chem. Soc., 75, 5145 (1953).

(b) Frensdorff,H.K., Watson,M.T. and Kauzmann,W., J. Amer. Chem. Soc., 75, 5157, 5167 (1953).

30. Frank,H.S. and Franks,F., J. Chem. Phys., 48, 4746 (1968).

31. Hammes,G.G. and Schimmel,P.R., J. Amer. Chem. Soc., 89, 442 (1967).

32. Rupley,J.A., J. Phys. Chem., 68, 2002 (1964).

33. Robinson,D.R. and Jencks,W.P., J. Amer. Chem. Soc., 87, 2462 (1965).

34. Kim,H., J. Solution Chem., 3, 271 (1974).

35. Bailey,F.E.,Jr. and France,H.G., J. Polymer Sci., 49, 397 (1961).

36. Kresheck,G.C., J. Phys. Chem., 73, 2441 (1969).

37. Walles,W.E., J. Colloid and Interface Sci., 27, 797 (1968).

38. Singer,J.M., Vekemans,F.C.A., Lichtenbelt,J.W.Th., Hesselink,F.Th. and Wiersema,P.H., J. Colloid and Interface Sci., 45, 608 (1973).

39. Fleer,G.J. and Lyklema,J., J. Colloid and Interface Sci., 46, 1 (1974).

40. Lichtenbelt,J.W.Th., Ras,H.J.M.C. and Wiersema,P.H., J. Colloid and Interface Sci., 46, 522 (1974).

41. Lichtenbelt,J.W.Th., Pathmamanoharan,C. and Wiersema,P.H., J. Colloid and Interface Sci., 49, 281 (1974).

42. Smellie,Jr.,R.H. and La Mer,V.K., J. Colloid and Interface Sci., 13, 589 (1958).

43. Homola,A., Ph.D. Thesis (Part V), McGill University, Montreal, Canada (1974).

44. Evans,R. and Napper,D.H., Kolloid-Z-Z. Polym., 251, 409 (1973).

45. Couper,A. and Stepto,R.F.T., Trans. Faraday Soc., 65, 2486 (1969).

46. Frost,A.A., and Pearson,R.G., "Kinetics and Mechanism", 2nd ed., (John Wiley and Sons, London, 1961).

47. Napper, D.H., J. Colloid and Interface Sci., 33, 384 (1969).

48. Visser,J., Advan. Colloid and Interface Sci., 3, 331 (1972).

49. Bailey,F.E.,Jr. and France,H.G., J. Polymer Sci., 49, 397 (1961).

CHAPTER IV

VAN DER WAALS ATTRACTION

1. INTRODUCTION

Most theories of steric stabilization to date have been formulated with a van der Waals attraction term. This term has traditionally been estimated on the basis of the pairwise additivity approach of Hamaker (1) and London (2). The shortcomings of the Hamaker approach have long been recognized (e.g.,3-7) and may be enumerated as follows:

i) The London dispersion interactions were assumed to be pairwise additive, i.e., the frequency and strength of each atomic "oscillator" were taken to be unaffected by neighbouring oscillators. This is a zero-order approximation which is valid only for rarefied gases.

ii) Only electromagnetic correlations at UV frequencies were thought to produce the attraction potential.

iii) The presence of intervening dielectrics was allowed for by various operations (3,4,6) performed on the self-attraction potentials of the particles and medium in vacuo.

Although attempts have been made to correct all three deficiencies (e.g.,3-5), the result is understandably rather inelegant and subject to dispute.

In 1956 Lifshitz (7,8) developed his macroscopic continuum theory which overcomes most of the difficulties of the classical theory. He showed

that electrodynamic correlations over the entire dielectric absorption spectrum are responsible for the attraction between like media and he properly treated the problem of intervening and surrounding dielectrics with regard to their modification of the electrodynamic correlations. The many-body problem is conveniently circumvented by the assumption that the interacting media are continuous.

The geometry of the system and the macroscopic dielectric absorption properties of the media are the only data required in the calculation of the van der Waals interactions within the system.

Where the pairwise additivity approach fails, the Lifshitz theory proves its worth; especially in the light of its interpretation and extension by Ninham and Parsegian and coworkers (9-18).

2. THEORY

Symbols used:

T = absolute temperature

a = particle radius

d = minimum surface separation of particles

n = refractive index

I = ionization potential

v = volume fraction

L = layer thickness

H = Hamaker function

δ = d/a

ω = absorption frequency

ξ = eigenfrequency

ε = relative dielectric permittivity

κ = inverse Debye length

2.1. Equation for Spheres

Mitchell and Ninham (15), using Lifshitz theory and a first order perturbation approach, have derived an approximate formula for the unretarded free energy of interaction between spherical particles in a dispersion medium. For particles of equal composition and radii we have, at close approach:

$$G = \frac{kT}{8\eta^2} \sum_{j=0}^{\infty}{}' \{ \int_0^{\infty} x\ln(1 - \Delta_j^2 e^{-x})dx + 4\eta^2(1 - \Delta_j)\ln\eta\ln(1 - \Delta_j^2)\} \qquad \{1\}$$

$$+ \text{unknown higher terms,}$$

where

$$\eta = \ln\{(\delta^2/4 + \delta)^{\frac{1}{2}} + (\delta^2/4 + \delta + 1)^{\frac{1}{2}}\}$$

and

$$\Delta_j = (\varepsilon_p - \varepsilon_m)/(\varepsilon_p + \varepsilon_m).$$

The subscripts p and m refer to the particles and medium respectively and the prime on the summation implies that the term for the eigenvalue j=0 must be divided by two because it is a zero-point energy term.

The lower bound on δ is determined by the assumption that the particles and medium are continuous: the particle separation must be greater than molecular dimensions. Ninham (19) has suggested that eq.{1} is only valid if the perturbation term is less than, say, one third of the leading term for each frequency. As discussed below, this limits δ to $\lesssim 0.02$ in systems for which Δ_j is large (~1). When Δ_j is small for all j, the perturbation term is small even when $\delta > 0.5$. It must be remembered, however, that eq.{1} is a non-retarded approximation and as such cannot be applied to systems in which the particle separation is greater than a few hundred Ångströms (16,17). Therfore, apart from the limits imposed by the perturbation approach, an absolute upper limit of 0.10 will be placed on δ. In a typical latex (1000 Å) this corresponds to a separation of 100 Å. This limit is by no means restrictive in steric stabilization problems since the attraction potential is reduced to the order of thermal energy (kT) before $\delta = 0.05$, as will be shown.

Tabor and Winterton (47) have found experimentally that near d=100 Å there is a change in the distance dependence of the attraction.

2.2 Dielectric Permittivity

Ninham and Parsegian have demonstrated that for materials of similar density, the whole dielectric dispersion spectra do not have to be known accurately to obtain reasonable results (9). The spectra may be approximated by the principal absorption frequencies of the media at which most of the energy transfer occurs.

The absorption properties of, and therefore the van der Waals forces between bodies can be formulated entirely in terms of their complex dielectric permittivities; more specifically, that part of the permittivity which describes absorption:

$$\varepsilon(\omega) = \varepsilon' - i\varepsilon'',$$

where ε' is the measured dielectric permittivity and ε'' describes absorption at the frequency ω. ($i = \sqrt{-1}$).

The flux density in a dielectric resulting from an applied alternating field would, in general, differ in phase from that of the field. This phase lag is due to the inertia of polarization which, when the frequency is high enough, cannot follow the field. Thus there is a relaxation of the measured permittivity (14).

The dielectric spectrum in the Ninham and Parsegian approach is approximated by three representative absorption peaks (9), each being composed of one or more peaks, suitably weighted and assigned a single absorption frequency:

$$\varepsilon(\omega) = \frac{\Delta\varepsilon_{MW}}{1 - i\,\omega/\omega_{MW}} + \frac{\Delta\varepsilon_{IR}}{1 - \omega^2/\omega_{IR}^2} + \frac{\Delta\varepsilon_{UV}}{1 - \omega^2/\omega_{UV}^2} + 1 \qquad \{2\}$$

where the last term, 1, is the relative dielectric permittivity of free space and the other three are increments due to Debye microwave relaxation (first term), vibrational relaxation (second term) and Lorentz electronic relaxation (third term). The $\Delta\varepsilon$'s are the changes in relative dielectric permittivity due to each relaxation.

The absorption characteristics are related to the phase difference between the applied field and the molecular or electronic polarization. Phase shifts are most conveniently represented as rotations on an Argand diagram, which means that if $\varepsilon(\omega)$ is evaluated on the complex frequency plane, all the absorption characteristics are represented on the imaginary axis. Therefore, putting $\omega = i\xi$ we have from eq.{2} the pure absorption spectrum:

$$\varepsilon(i\xi) = \varepsilon = \frac{\varepsilon_0 - \varepsilon_D}{1 + \xi/\omega_{MW}} + \frac{\varepsilon_D - n^2}{1 + \xi^2/\omega_{IR}^2} + \frac{n^2 - 1}{1 + \xi^2/\omega_{UV}^2} + 1 \qquad \{3\}$$

which is a monotonically decreasing function of ξ.

The allowed values of the eigenfrequency are given by

$$(\xi/\text{rad s}^{-1}) = 8.2256 \times 10^{11}(T/K)j,$$

where

$$j = 0,1,2,....$$

Equation {3} indicates that with increasing frequency, relaxation first occurs with a drop in permittivity from the static value ε_0 to a smaller value ε_D during Debye relaxation. Then follows a decrease from ε_D to a smaller value in the visible range, which, because of its electronic nature, obeys Maxwell's relationship $\varepsilon = n^2$. When the frequency becomes so high that even the electrons can no longer follow the field, ultraviolet relaxation occurs and the permittivity drops from n^2 to the value of free space, 1.

The original formulations of ε by Ninham and Parsegian (e.g.,9) included an X-ray contribution which was assumed to originate from the electronic oscillations at the plasma frequency of the dielectric. Apart from the fact that such high frequency oscillations will be strongly damped at relatively small separations, it does not seem reasonable to expect significant contributions from the plasma frequency oscillations of non-conductors. This term is important for metals but eq.{1} cannot be used since $\Delta_j = 1$ for lower values of j. Furthermore, calculations involving metals must include retardation (16).

The evaluation of the absorption equation may be further simplified by introducing the ionization potential of the material which is an experimentally more accessible parameter than the ultaviolet relaxation frequency:

$$(\omega_{UV}/\text{rad s}^{-1}) = 1.519 \times 10^{15}(I/\text{eV})$$

where I is the ionization potential in eV. Furthermore, in all cases to be considered here,

$$\xi/\omega_{MW} >> 1, \qquad \text{for } j > 0.$$

Substituting the expressions for ξ and ω_{UV} into eq.{3} we have

$$\varepsilon = \frac{\varepsilon_0 - \varepsilon_D}{1 + 8.226 \times 10^{11}\, Tj/\omega_{MW}} + \frac{\varepsilon_D - n^2}{1 + 6.767 \times 10^{23}\, T^2 j^2/\omega_{IR}^2} + \frac{n^2 - 1}{1 + 2.931 \times 10^{-7}\, T^2 j^2/I^2} + 1 \qquad \{4\}$$

(Note: it seems to be very common in the literature to refer to ε as the dielectric susceptibility (e.g.,16) when in fact it is the relative permittivity. Dielectric susceptibility χ_e is related to ε by:

$$\varepsilon = 1 + \chi_e \quad (20).$$

The dielectric susceptibility of vacuum is zero so that if

$$\Delta_j = \frac{\chi_e(p) - \chi_e(m)}{\chi_e(p) + \chi_e(m)} \quad ,$$

where p and m refer to the particles and medium respectively, we would have $\Delta_j = 1$ for all substances at all frequencies in air or vacuum. In fact:

$$\Delta_j = \frac{\chi_e(p) - \chi_e(m)}{2 + \chi_e(p) + \chi_e(m)} \quad .)$$

3. DATA

3.1. Ionization Potentials

Owing to the relatively large number of eigenfrequencies required to evaluate the ultraviolet contribution to the permittivity, the results are most sensitive to the choice of the ultraviolet relaxation frequency or ionization potential.

As a first approximation, the ionization potentials of polymers have been equated to the ionization potentials of small molecules structurally similar to the repeating mer units (e.g.,16). For polystyrene (PS), for example, we could use ethyl benzene, isopropyl benzene or toluene, all of which have similar well documented ionization potentials (28). However, for the same reasons that the pairwise additivity approach fails in the calculation of dispersion energies, we cannot use gaseous ionization potentials for solids and liquids.

In general, many-body effects in condensed media reduce the overall electromagnetic interactions within atoms and, as a result, reduce the ionization potentials. A correction must be applied to the initially chosen gaseous ionization potential to allow for the presence of many-body interactions. The correction term is the polarization energy P for a single charge in a dielectric medium. Thus (21,22)

$$I_C = I_G + P$$

where the subscripts C and G refer to condensed and gas phase.

Lyons and Mackie (21,22) have shown that for many crystals and some liquids

$$P/eV = -1.5 \pm 0.5$$

It seems likely that in liquids the greater mobility of molecules would tend to make this value more negative since the molecules can orient their maximum polarizability axes to point at the charge, although this effect is partially neutralized by thermal motion. It has been suggested that P may be as large as 7.0 eV (23) but direct measurements by Siegbahn have been recently performed on formaldehyde (24,25) which would be expected to exhibit a large polarization energy. The results show that the principal ultraviolet relaxation energy is reduced by 1.6 eV on going from the gaseous to the liquid state. In light of such evidence, it seems reasonable to expect the ionization potential of liquid water to be 11.0 eV (26) although direct empirical confirmation may be difficult to obtain owing to experimental problems (24).

Fujihira and Inokuchi (27) have measured the ionization potential of polyethylene (PE) directly as 8.5 eV. The above procedure (24) predicts this result because the ionization potentials of n-alkanes asymptotically approach 10.0 eV with increasing chain length, as shown in Table 1.

The dependence of the ionization potential on chain length is another problem which is very difficult to overcome because apparently no work has been done on the ionization of oligomers. Estimates must be made which involve considerable uncertainty. For instance, the cognate compound

TABLE 1

Ionization Potentials of n-alkanes (23)

No. of carbons	I_G/eV
1	13.0
2	11.7
3	11.1
4	10.6
5	10.4
6	10.2
7	10.1
8	10.4
9	10.2
10	10.2

TABLE 2

Ionization Potentials of Polymers

Cognate Compound	I_G/eV	Polymer	I_C/eV
ethylbenzene	8.8	PS	7.0
isopropylbenzene	8.4		
toluene	8.8		
isopropyl acetate	10.0	PVA	8.5
ethyl acetate	10.1		
methyl isobutanoate	10.0	PMMA	8.5
acetonitrile	11.8	PAN	8.5
propionitrile	11.7		
diethyl ether	9.6	PEO	7.0

TABLE 3

Ionization Potentials of Liquids

Liquid	I_C/eV
water	11.0
n-heptane	8.5
toluene	7.3
cyclohexane	8.5
benzene	7.8

for poly(ethylene oxide) (PEO) would be diethyl ether which has an ionization potential of 9.6 eV (28). Assuming a similar trend to that in n-alkanes and adding the polarization energy, we find for liquid or solid PEO an ionization potential of approximately 7.0 eV. A similar treatment for polyacrylonitrile (PAN) yields about 8.5 eV.

For polymers which have easily ionizable side groups (e.g.,poly(methyl methacrylate) (PMMA)) the effects of polymerization will be ignored.

Table 2 shows the ionization potentials of the polymers studied and those of the corressponding compounds from which the polymer values were estimated (26,28).

Table 3 lists the estimated I_c values for all other compounds studied (28) after correction for condensed state.

3.2. Dielectric Constants and Microwave Relaxation

The zero frequency dielectric permittivity of polymers is often strongly dependent on temperature; particularly near the melting point. This arises from the large changes in rotational freedom in this domain. The relative permittivity of PEO, for example, increases sharply from ~4 to ~24 when the temperature is raised to its melting point near 60°C (29). PS on the other hand exhibits no significant relaxation in the microwave region at the temperatures considered in this study (33). Poly(vinyl acetate) (PVA) has a dielectric constant of ~7.8 at 25°C and ~100 at 85°C, the increase being due

to melting (28). Since the dispersion energies between particles are dependent on the difference in dielectric properties of the particles and dispersion medium, the choice of dielectric constant for most substances is not critical when water is part of the system, unless the substance has a very high dielectric constant such as that for PEO or PVA.

When moderate concentrations of salts are present in the aqueous phase the microwave contribution to van der Waals interactions may be effectively damped (30,31). This effect will be considered in more detail in a later section.

3.3 Complete Dielectric Data

Table 4 lists all the data used in the subsequent calculations of van der Waals attraction energies (26,28,32). The computations were performed with the aid of a Cyber 72-26 computer and an H.P.55 programmable calculator. It is very important to realize that each set of dielectric data used in the calculations represents an exact model system.

The results are "exact" to the extent of the applicability of eq.{1}; however this does not mean that the results represent the true behaviour of the real systems. The names of polymers and liquids are assigned as a matter of convenience and the greatest approximations may lie in equating the model with the real system. For example, PVA and PEO absorb strongly in the infrared but no permittivity data could be found; therefore, these names were applied to <u>model</u> polymers which do not relax in the infrared.

We found that the results are very insensitive to the microwave relaxation frequency; any value less than $\sim 10^{11}$ causes the Debye term to be negligible for $j > 0$.

TABLE 4

Dielectric Data Used in Computations

Substance	ε_0	ε_D	n	I_C/eV	ω_{MW}/rad s^{-1}
air (vacuum)	1.0	1.0	1.0	-	-
water (288 K)	82.0	5.2	1.3333	11.0	1.06×10^{11}
water (298 K)	78.3	5.2	1.3325	11.0	1.06×10^{11}
water (323 K)	69.9	5.2	1.329	11.0	1.06×10^{11}
water (348 K)	61.4	5.2	1.324	11.0	1.06×10^{11}
0.2 M HCl (287 K)	80.0	5.2	1.3356	11.0	1.06×10^{11}
0.39 M $MgSO_4$ (318 K)	67.4	5.2	1.3382	11.0	1.06×10^{11}
2.0 M NaCl (298 K)	56.5	5.2	1.3513	11.0	1.06×10^{11}
2.1 M $(NH_4)_2SO_4$ (298 K)	55.4	5.2	1.3704	11.0	1.06×10^{11}
n-heptane	1.932	1.932	1.39	8.5	-
toluene	2.238	2.238	1.496	7.3	-
benzene	2.244	2.244	1.498	7.8	-
cyclohexane	2.034	2.034	1.426	8.5	-
PS	2.544	2.544	1.595	7.0	-
PVA	7.8	2.152	1.467	8.5	10^6
PMMA	3.35	2.25	1.50	8.5	10^2
PAN	6.5	2.304	1.518	8.5	10^6
PEO (liquid)	24.0	2.154	1.468	7.0	10^3

The average infrared-visible relaxation frequency of water is 5.66×10^{14} rad s^{-1} (9). Where no value is entered any number other than zero may be used since the numerator in Δ_0 will be zero.

4. RESULTS AND DISCUSSION

4.1. The Hamaker Function

In order to facilitate the presentation of results, a Hamaker function is defined as:

$$H = -G/F \qquad \{5\}$$

where F is a geometric factor originally derived by Hamaker for spheres (1). This factor is defined by

$$F = \frac{1}{6}\left(\left(\frac{2}{\delta^2 + 4\delta} + \frac{2}{\delta^2 + 4\delta + 4}\right) + \ln\left(\frac{\delta^2 + 4\delta}{\delta^2 + 4\delta + 4}\right)\right). \qquad \{6\}$$

In equation {1} the approximation $\eta^2 = \delta$ is valid in the interval $0 \leq \delta \leq 0.2$ with an accuracy of better than 2%. Making this substitution we find from eq.{1}:

$$G = \frac{kT}{8\delta} \sum_{j=0}^{\infty} \left\{ \int_0^{\infty} x\ln(1 - \Delta_j^2 e^{-x})dx + 2\delta\ln\delta(1 - \Delta_j)\ln(1 - \Delta_j^2)\right\} \qquad \{7\}$$

$$= \alpha\left(\frac{1}{\delta} + \beta\ln\left(\frac{1}{\delta}\right)\right) \qquad \{8\}$$

where α and β are independent of δ. Applying eq.{6},

$$H = -\alpha\left(\frac{1}{\delta F} - \beta\frac{\ln\delta}{F}\right). \qquad \{9\}$$

Both $\frac{1}{\delta F}$ and $\frac{\ln\delta}{F}$ are, to a good approximation, linear functions of δ in

TABLE 5

Successive Approximations for F When δ is Small

δ	Exact F	$F=\frac{1}{12\delta}(1+2\delta\ln\delta)$	$F = \frac{1}{12\delta}$
0.005	15.85	15.78	16.67
0.010	7.63	7.57	8.33
0.015	4.92	4.86	5.56
0.020	3.57	3.51	4.17
0.025	2.78	2.72	3.33
0.030	2.25	2.19	2.78
0.035	1.88	1.82	2.38
0.040	1.60	1.55	2.08
0.045	1.39	1.34	1.85
0.050	1.22	1.17	1.67
0.055	1.08	1.03	1.52
0.060	0.97	0.92	1.39
	Maximum error	5% at 0.060	43% at 0.060

Fig.1. Plots of $(1/\delta F)$ and $(\ln\delta)/F$ versus the distance parameter δ.

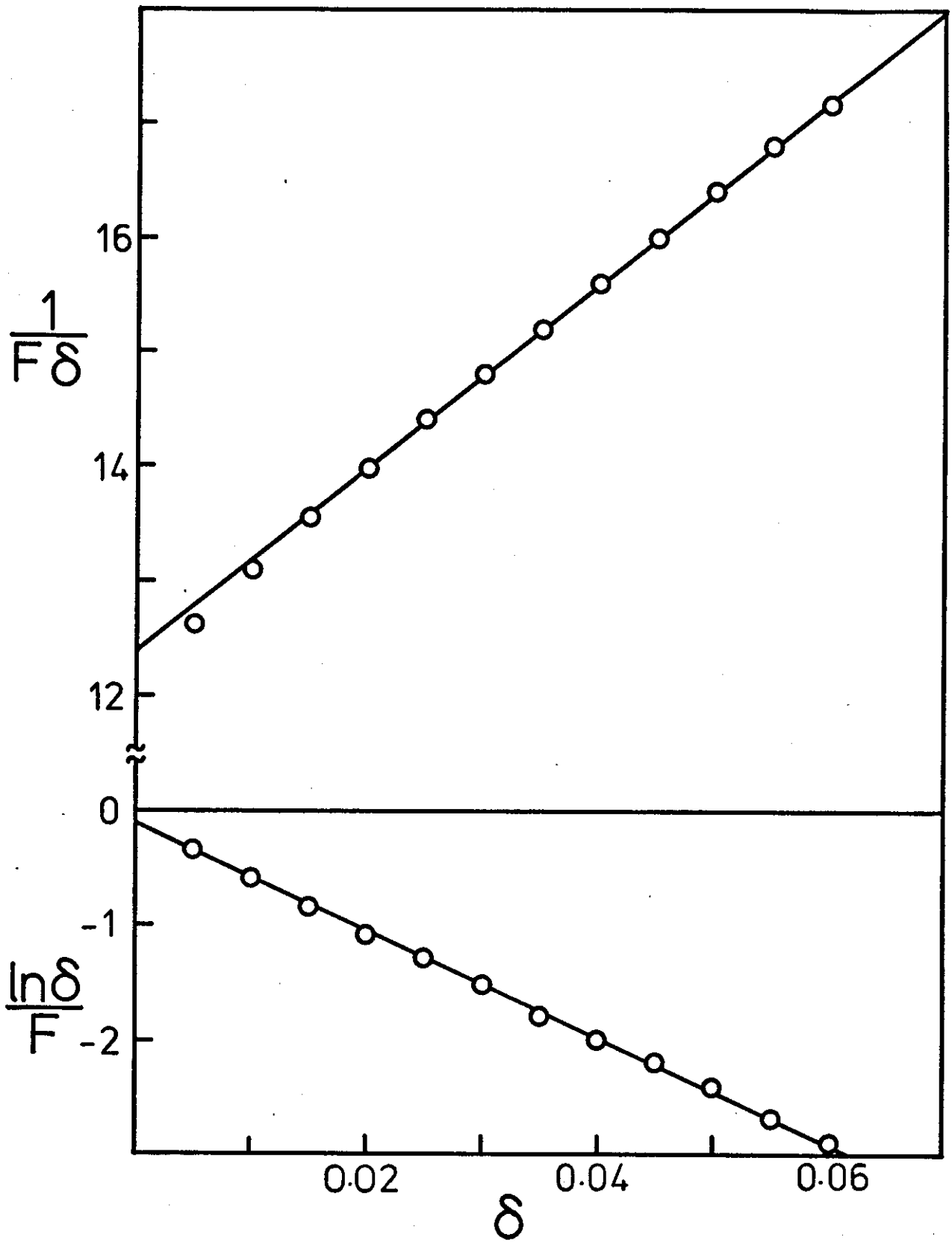
16
14
12
1/Fδ
0
-1
-2
lnδ/F
0·02
0·04
0·06
δ

the range $0.005 < \delta < 0.1$ as shown in Fig.1. The equations of the lines of best fit for these two functions are

$$-\frac{\ln\delta}{F} = 0.175 + 45.7\delta \qquad \{10\}$$

and

$$\frac{1}{\delta F} = 12.4 + 79.0\delta \qquad \{11\}$$

in the designated interval. The functions are actually sigmoidal in this range with very shallow oscillations about the straight line. Although the approximation breaks down for $\delta < 0.005$, the separation of particle surfaces at this value of δ for 1000 Å particles is of the order of 5 Å and the continuum approach ceases to be valid.

Linear combinations of the functions shown in Fig.1. and which yield H must be linear; therefore it is concluded that for close approach of spheres, the Hamaker function H should be a linear function of δ.

4.2. Sensitivity to Dielectric Data

The microwave contribution to the van der Waals attraction is obtained using one eigenfrequency ($j = 0$). The infrared-visible contribution requires a summation over approximately fifteen eigenvalues (30) and the ultraviolet contribution requires up to several hundred eigenvalues. On first sight it would seem that the order of increasing sensitivity to dielectric data is microwave < infrared-visible < ultraviolet contribution. Aqueous systems are unusual in that the microwave contribution can be as much as half of the

total interaction owing to the very large dielectric constant of water. Fig.2 displays computed Hamaker functions for PS in water at four different temperatures, with and without the microwave contribution. As expected, all Hamaker functions computed were found to be linear functions of δ to a good approximation. Note that when $\delta = 0$ the microwave contribution is almost equal to the sum of all other contributions, and that the dependence of H on δ seems to be due entirely to the microwave term. If one ignores the $j = 0$ term, a constant H is found.

The perturbation approximation breaks down rapidly for Hamaker functions with large slopes. For this reason the distance dependence of H must not be taken as quantitative for large δ. The main benefit of having a linear dependence is that all systems can be compared via a "contact Hamaker constant" obtained by extrapolating to $\delta = 0$. The continuum theory breaks down at contact but the mathematical comparison is still valid.

The temperature dependence of the microwave term is due mainly to the corresponding temperature dependence of the dielectric constant. For PS in water the dependence for $j = 0$ (24) is less than 0.5%/K. A similar trend is found for $H_{j\neq 0}$ where the change in the Hamaker constant is due to the temperature dependence of the refractive index. A change in the dielectric constant of 25% has about the same effect on H as a change in the refractive index of less than 1% (in the PS/water system).

Fig.3 illustrates the dependence of H on the value of the dielectric permittivity of water after Debye relaxation. The system is PS in water.

Fig.2. Plots of the Hamaker function H versus the distance parameter δ for PS in water. Lines: (a) with microwave, (b) without microwave, (1) T = 288 K, (2) T = 298 K, (3) T = 323 K, (4) T = 348 K.

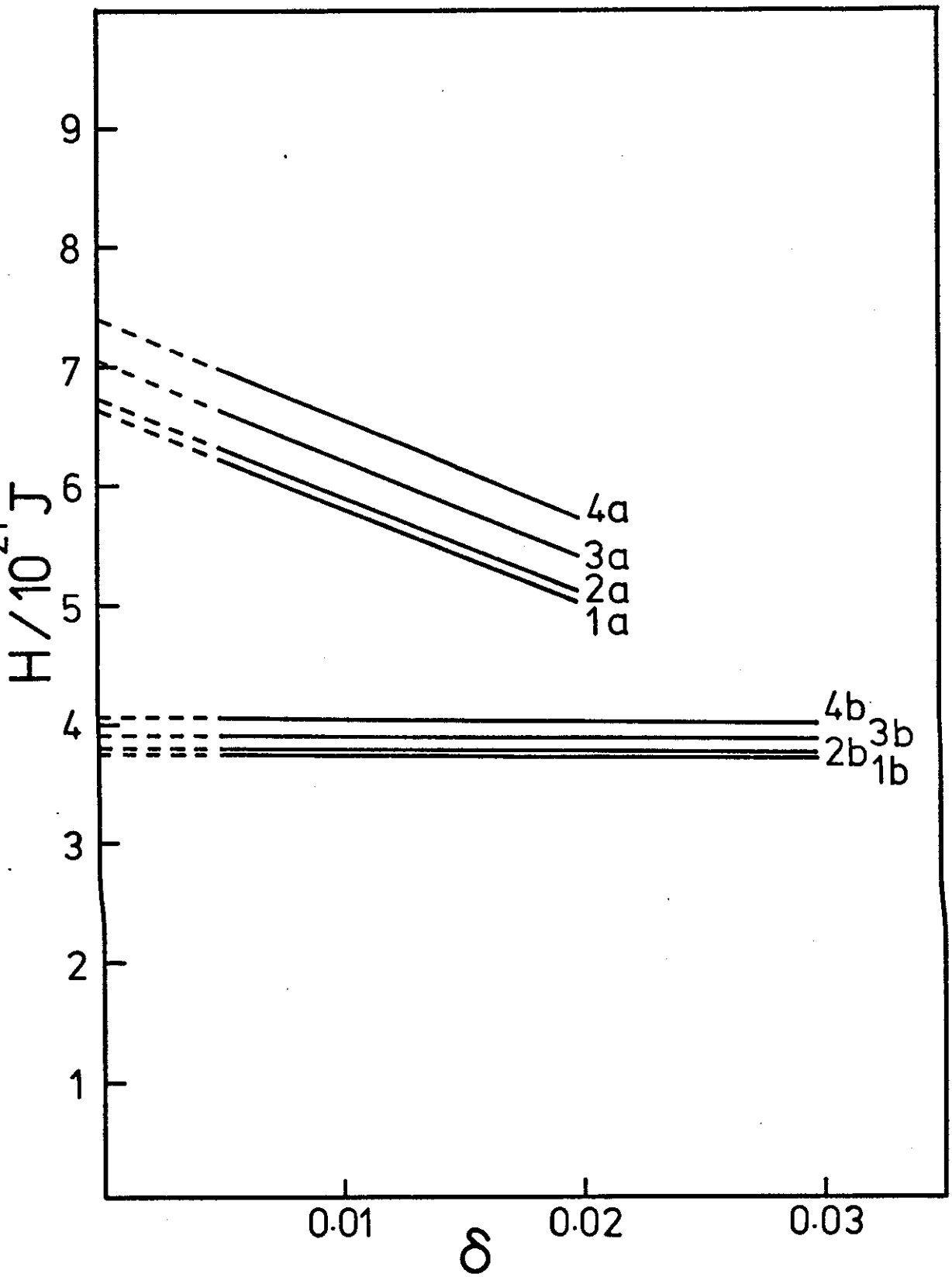
9
8
7
6
5
4
3
2
1
H / 10^-21 J
4a
3a
2a
1a
4b
3b
2b
1b
0·01
0·02
0·03
δ

Fig.3. Plots of the Hamaker function H versus the distance parameter δ for PS in water at 298 K. Lines: (1) $\varepsilon_D = 1.7756$, (2) $\varepsilon_D = 5.7$, (3) $\varepsilon_D = 3.0$, (4) $\varepsilon_D = 5.2$, (5) $\varepsilon_D = 4.5$.

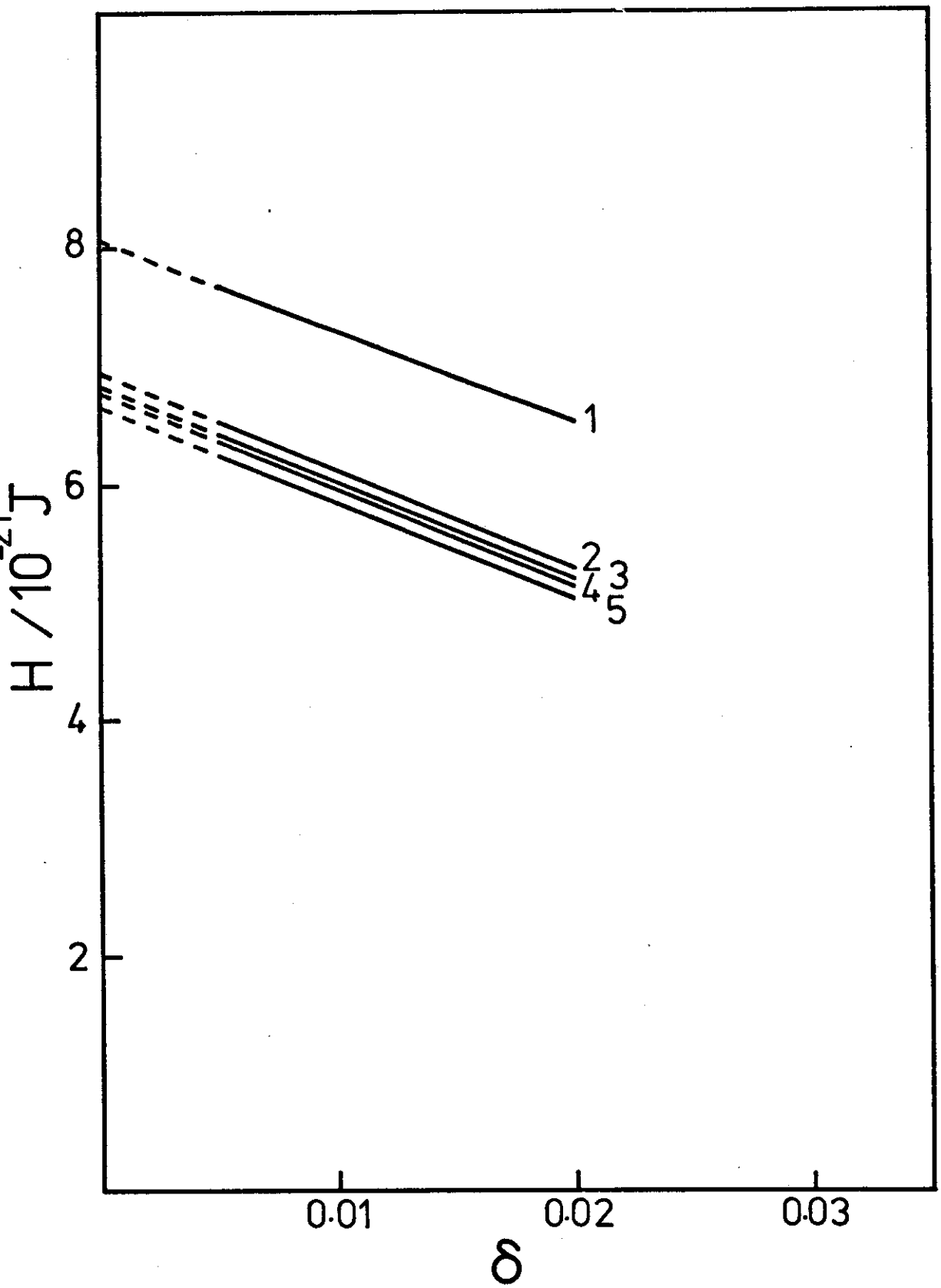
8
6
4
2
H /10^-21 J
1
2
3
4
5
0·01
0·02
0·03
δ

Note that neglect of the infrared relaxation of water (line 1) results in a rather large increase in H. As ε_D is increased, H passes through a minimum then increases. The range $4.5 < \varepsilon_D < 5.7$ covers most of the experimental measurements of ε_D (34), hence the error involved in the choice of this parameter is less than 2% (see Fig.4).

The choice of ionization potential or ultraviolet relaxation frequency may be very important as can be seen in Figs.5 and 6. It is interesting to note in Fig.5 that our reduction of the ionization potential of water in the gas phase, 12.6 eV, to that of liquid water, 11.0 eV, has produced a negligible effect on H. This is merely a fortunate coincidence that can be explained in terms of the difference in absorption properties of the particles and medium. Given all data except the ionization potential of water, the overall difference in absorption between PS and water (and hence the attraction) can be minimised by the appropriate choice of the ionization potential. Such arbitrary variations can only be performed on the model, of course, but the principle applies also to variations in experimental dielectric measurements. Both positive and negative variations of the ionization potential from this value will increase the attraction because the attraction is dependent on the square of the dielectric differences (through Δ_j^2). Both values of 11.0 eV and 12.6 eV for the ionization potential of water are near this minimum. This also explains the shape of the curve in Fig.4. In general, the independent variation of any single dielectric parameter will give rise to the behaviour typified in Fig.4, although in most situations only one arm of the curve will be seen.

Fig.4. Plot of the Hamaker function H extrapolated to $\delta = 0$ versus the microwave permittivity ε_D of water for PS in water at 298 K.

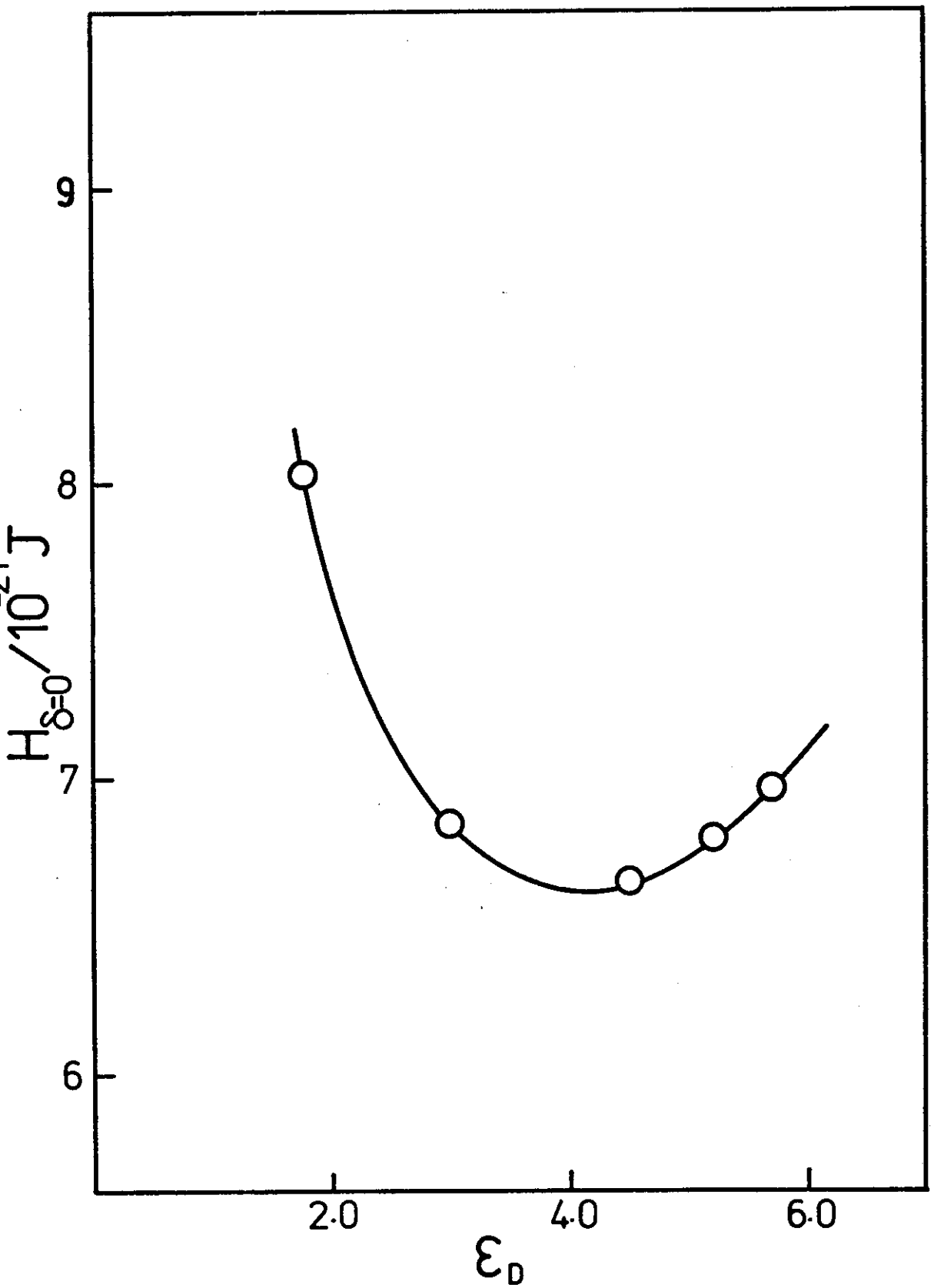
9
8
7
6
$H_{\delta=0}/10^{-21}$ J
2·0
4·0
6·0
ε_D

Fig.5. Plots of the Hamaker function H versus the distance parameter δ for PS in water at 298 K. Lines: (1) I_m = 12.62 eV, (2) I_m = 11.0 eV, (3) I_m = 9.0 eV.

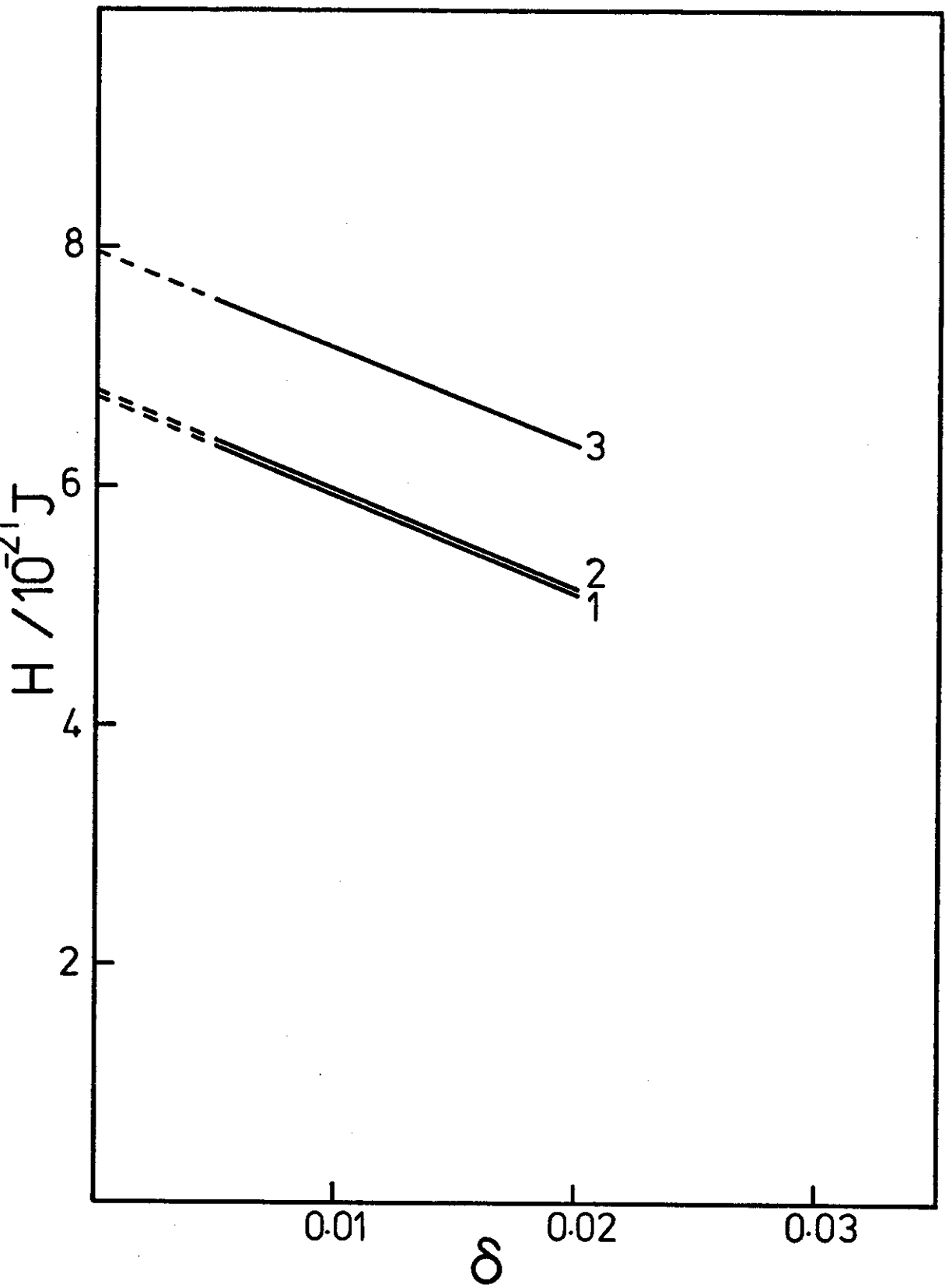
8
6
4
2
H /10^-21 J
3
2
1
0·01
0·02
0·03
δ

Fig.6. Plots of the Hamaker function H versus the distance parameter δ for PAN in toluene at 298 K. Lines: (1) I_p = 8.5 eV, (2) I_p = 9.0 eV, (3) I_p = 10.0 eV, (4) I_p = 11.5 eV.

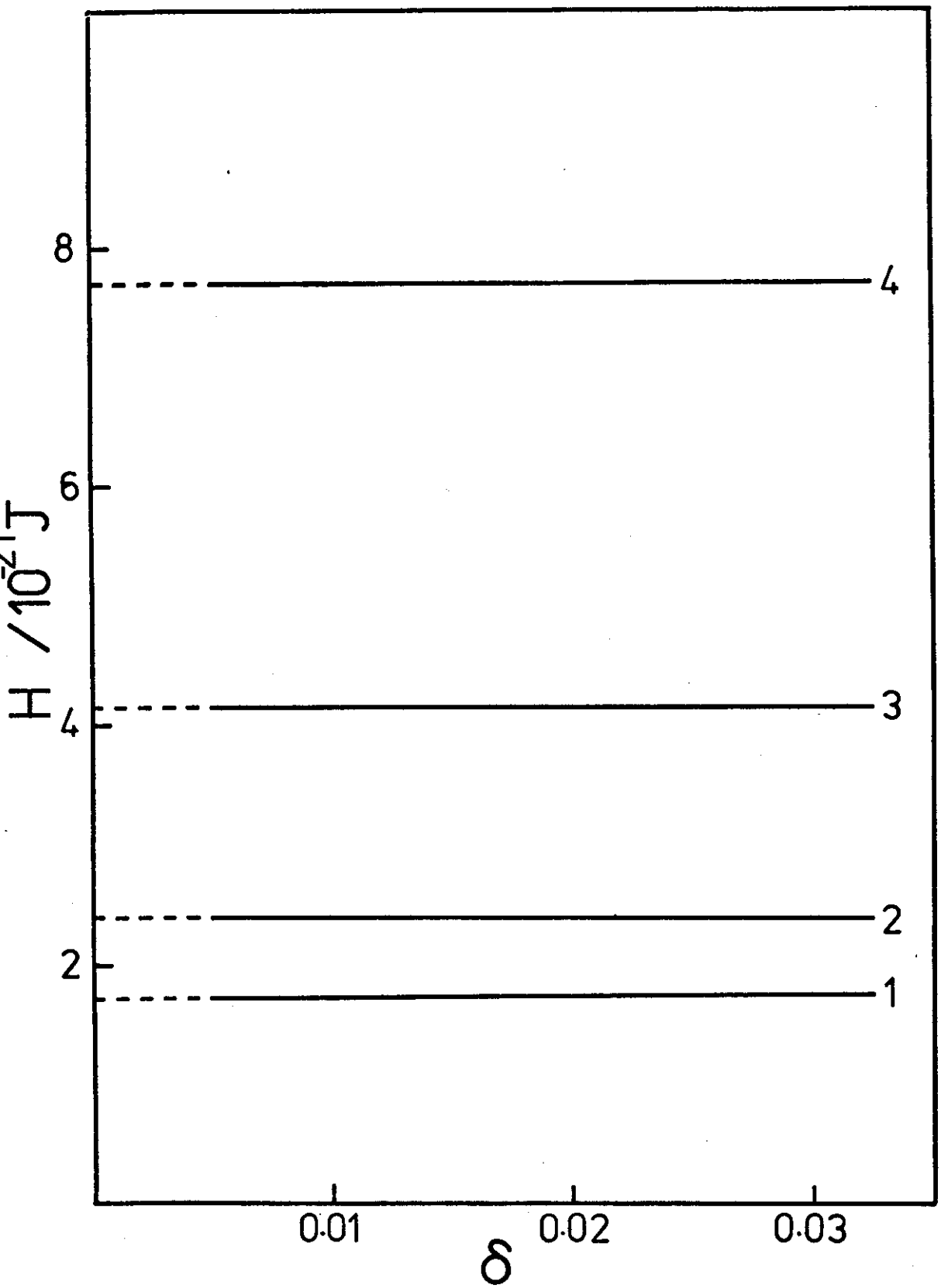
8
6
4
2
H /10^-21 J
4
3
2
1
0·01
0·02
0·03
δ

The high sensitivity of H to the ionization potential is also made clear in Fig.6 which refers to the system PAN in toluene at 298 K. Because of the small dielectric constants involved, the microwave term is small and H is essentailly constant. Reduction of the ionization potential of PAN from 11.5 eV, the approximate I_G of acetonitrile, to 10.0 eV, the estimated I_C for acetonitrile, results in a 46% decrease in H. Allowing for polymerization the I_C value for PAN becomes approximately 8.5 eV and H is reduced by a further 60%. (See Fig.7 for the dependence of H on this ionization potential.) This example illustrates the need for tables of direct measurements of solid and liquid state ionization potentials or work functions. Meanwhile, Lifshitz theory can only be expected to yield results within a factor of two or three of the "exact" values, which is still very much better than can be achieved using classical theory.

Examples of the dependence of the non-zero frequency contribution to H on refractive index are given in Figs.8 and 9. The systems are PS in water and PVA in water respectively. The refractive index of the water in Fig.8 has been changed by changing the temperature or the salt concentration or both; and in Fig.9 it has been arbitrarily varied. The microwave term has been omitted because of complications due to damping by ions which would mask the behaviour indicated. Note that a few percent increase in the refractive index of the water results in a large decrease in attraction. Again, it should be stressed that this sensitivity is not necessarily found in all systems; the values merely happen to lie well to the left of the minimum on the steeply sloping portion of a curve similar to that in Fig.4. At higher values of the refractive index, the sensitivity is greatly decreased because

Fig.7. Plot of the Hamaker function H versus the ionization potential of PAN for PAN in toluene at 298 K.

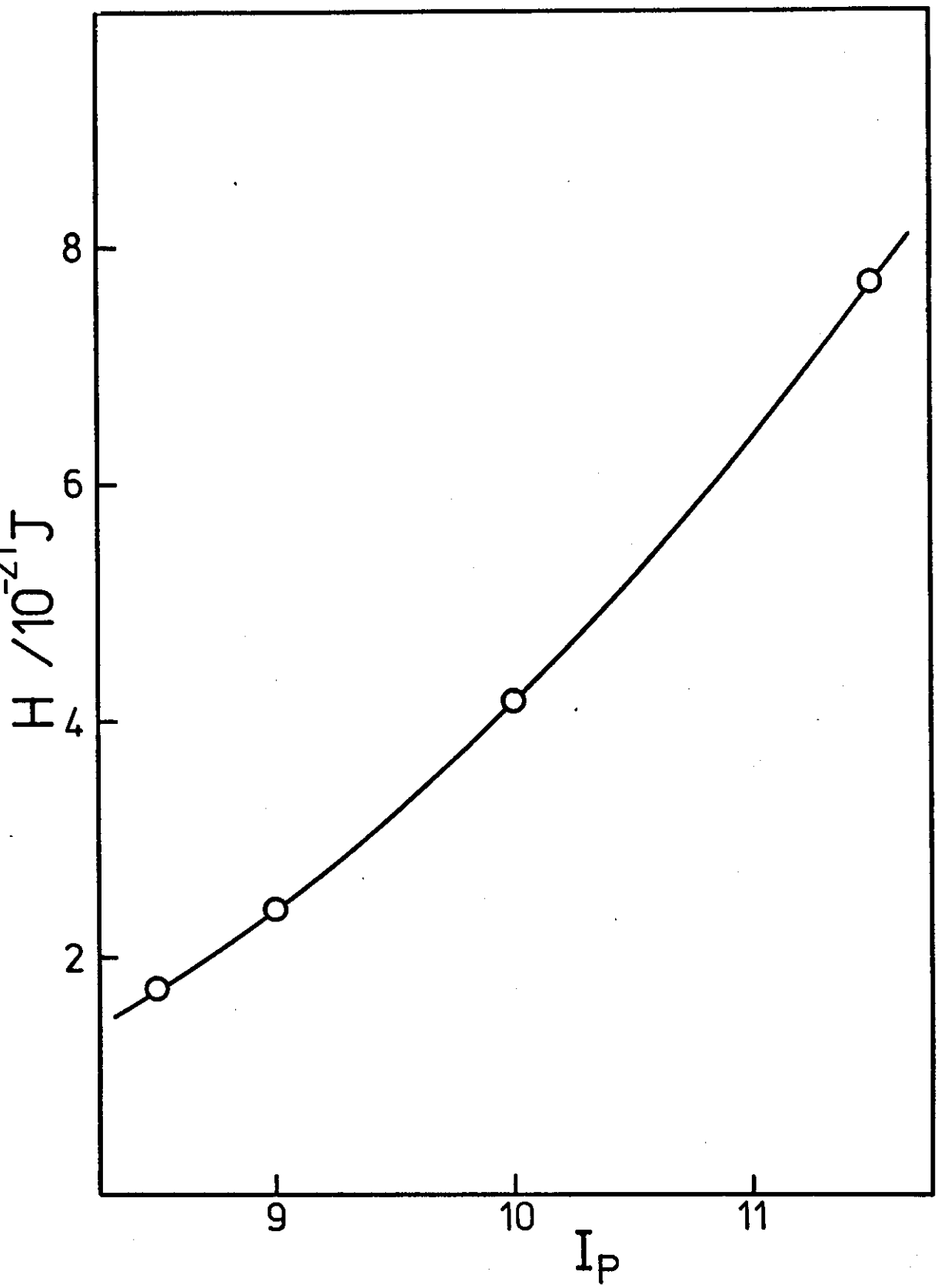
8
6
4
2
H /10^-21 J
9
10
11
I_P

Fig.8. Plot of the Hamaker function without the microwave term $H_{j\neq 0}$ versus the refractive index of the medium for PS at various temperatures in various salt solutions.

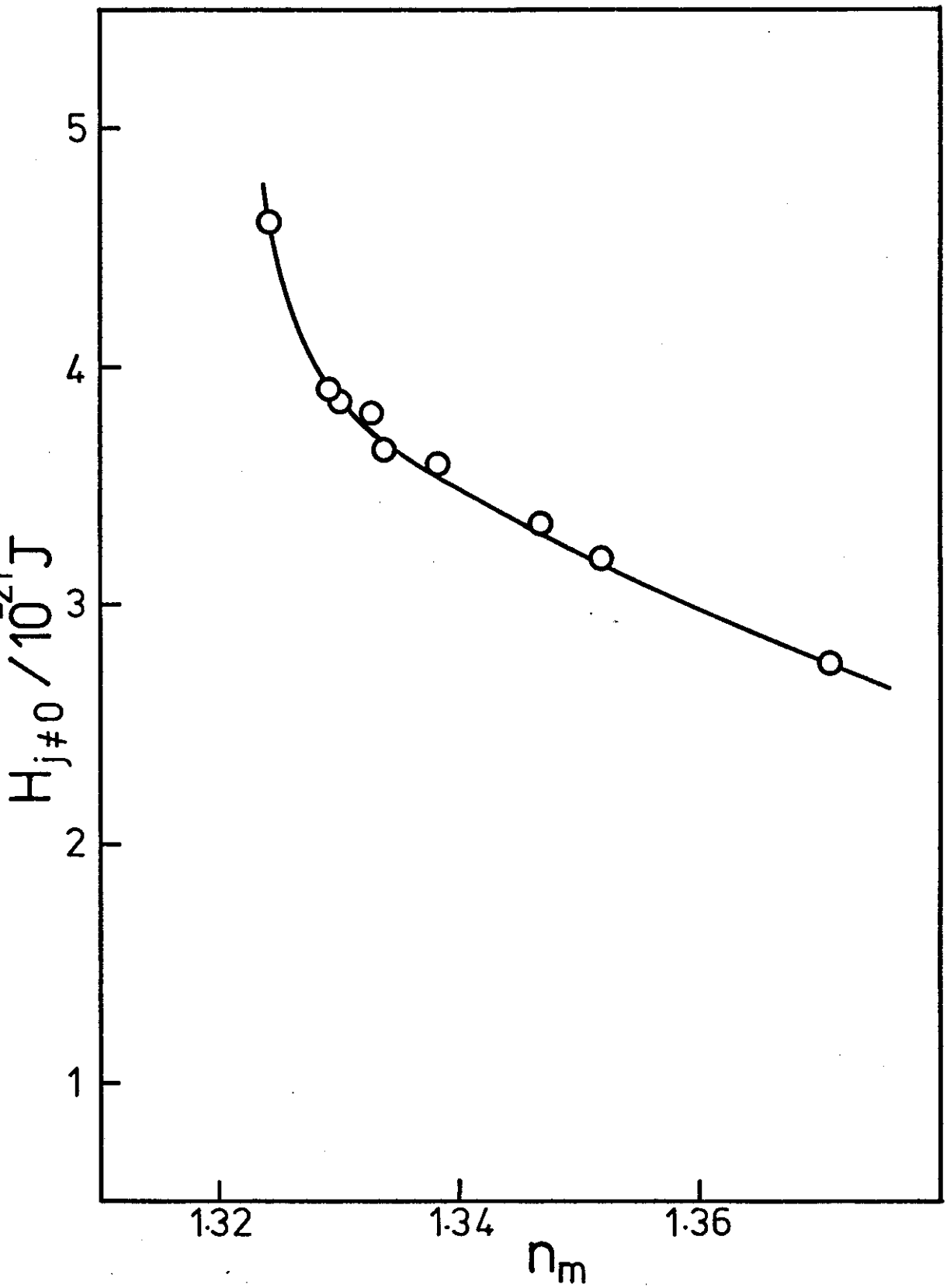
5
4
3
2
1
$H_{j\neq 0} / 10^{-21}$ J
1·32
1·34
1·36
n_m

Fig.9. Plot of the Hamaker function without the microwave term $H_{j\neq 0}$ versus the refractive index of the medium for PVA in water.

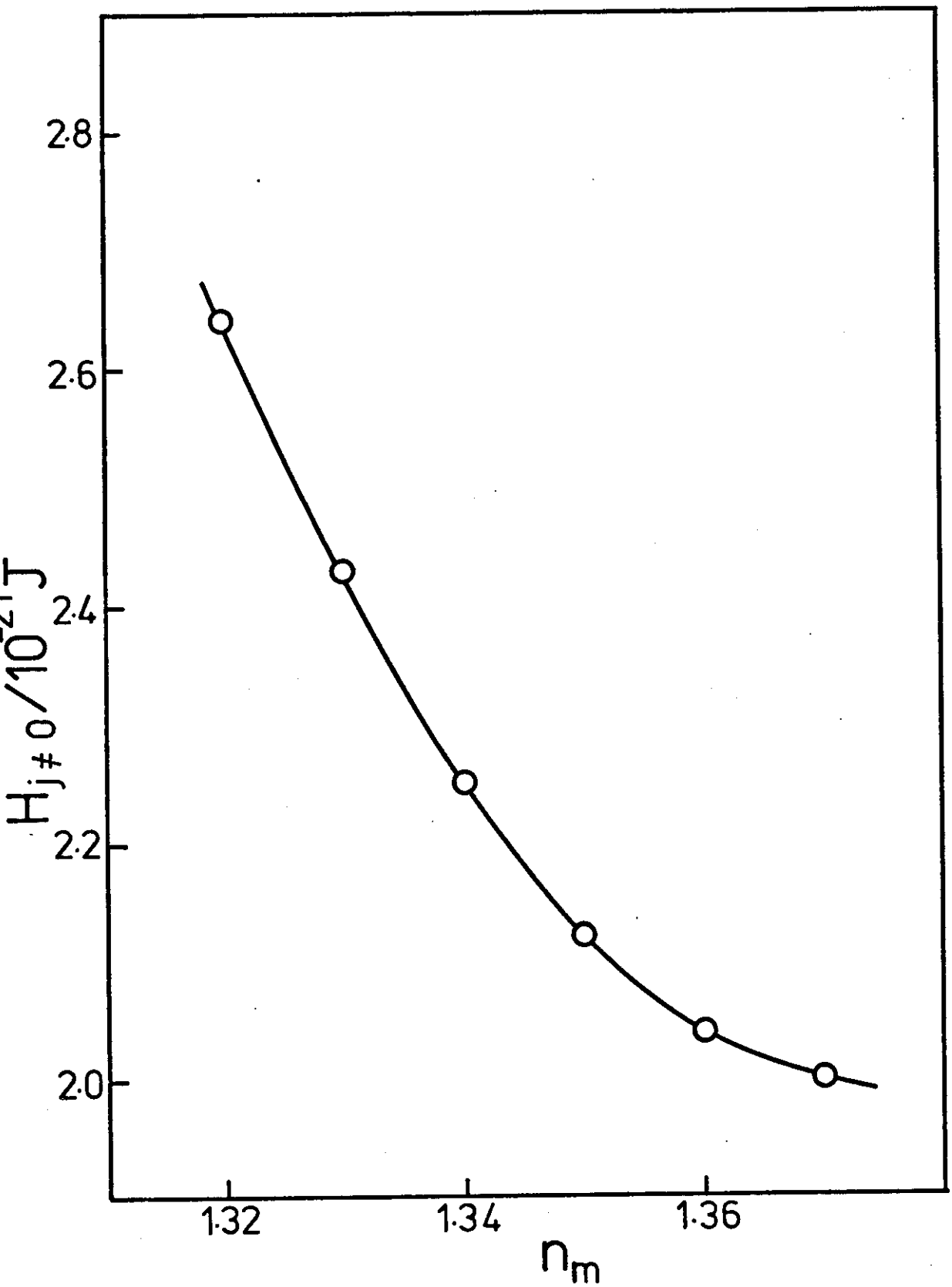
2·8
2·6
2·4
2·2
2·0
$H_{j\neq 0}/10^{-21}$ J
1·32
1·34
1·36
n_m

the refractive indices of particles and medium become more similar. The minimum in H does not necessarily coincide with the equality of the refractive indices; the same applies to any of the dielectric parameters.

The sensitivity of the final attraction energies to the dielectric data is different for each system considered. If all dielectric parameters are found to lie near minima of curves such as in Fig.4, reasonable confidence can be placed on the calculated attraction even if approximate data are supplied. When the results are as sensitive as those in Fig.7, very accurate data must be supplied and even the premise that the total absorption behaviour in the ultraviolet can be characterised by the ionization potential should be re-examined.

At present, significant increases in accuracy are obtained only at prohibitive increases in complexity.

A similar study of interacting spheres by Smith et al (16) was published at the same time as this work (26). They compared the results of Mitchell and Ninham (15) to a "fitted Hamaker constant" at $\delta = 4 \times 10^{-5}$. This procedure seems unrealistic as the particle radius required to give $d > 5$ Å is $a > 1.25 \times 10^5$ Å, which is too large to be considered colloidal in the traditional sense (35,36). Apart from this detail, Smith et al come to similar general conclusions to those in ref.26; large deviations from pairwise additivity occur when Δ_j is large and good agreement with pairwise additivity is obtained when Δ_j is small.

Their use of gaseous ionization potentials leads to a Hamaker constant of ~12 × 10^{-21} J. for PS in water, which is about twice the "generally accepted value" of 5 × 10^{-21} J. (37). Our value extrapolated to contact (26) ranges from ~4 × 10^{-21} J. to ~7 × 10^{-21} J. depending on how much the microwave term is damped (see section 4.3. on ionic damping). Visser (6) has tabulated a large range of experimental Hamaker constants; perhaps the best value for PS lies in the range (3-6) × 10^{-21} J.. This is consistent with our computed range.

4.3. Practical Aqueous Systems - Ionic Damping

In aqueous systems dissolved salts affect the zero frequency term in two ways. The first is through alteration of the dielectric constant of the aqueous phase (17). The dielectric constant falls by approximately 14% when the ionic strength is increased to 1. This effect will be neglected hereafter in view of the second, much greater damping factor introduced by ionic relaxation.

The damping factor for spheres has been derived in ref.31 and can be written:

$$D = \frac{\sum_{n=1}^{\infty} \Delta_0^{2n} \exp(-2\kappa dn)/n^3}{\sum_{n=1}^{\infty} \Delta_0^{2n}/n^3}$$

where κ is the inverse Debye length and d the surface separation of the two particles. For most aqueous systems $|\Delta_0| \sim 1$ and

$$D \simeq \sum_{n=1}^{\infty} \exp(-2\kappa dn)/n^3$$

$$\simeq e^{-2\kappa d} + \text{negligibly small terms} . \quad \{12\}$$

The microwave term must be multiplied by this factor. The value of κ can be found from:

$$(\kappa/\text{Å}^{-1}) = 0.327\ I_s^{\frac{1}{2}} \quad . \quad \{13\}$$

where I_s = the ionic strength.

At 10 Å, $d = 3.27\ I_s^{\frac{1}{2}}$. Table 6 shows the effect of the ionic strength on the damping factor.

In studies of steric stabilization, conditions causing incipient flocculation in aqueous systems almost always involve the presence of dissolved salts. Examples of aqueous media used in the work on steric stabilization in this thesis include 0.2 M hydrochloric acid, 0.39 M magnesium sulphate, 2 M sodium chloride and 2.1 M ammonium sulphate. The damping factor for an ionic strength of the order of 1 is such that the microwave term may be neglected in all steric stabilization studies of such aqueous systems near the flocculation point. Away from the flocculation point van der Waals forces are usually negligible compared with the large forces produced by the polymer layers on the interacting particles (see chapter on steric stabilization).

In Fig.10 we see the effect of ionic damping for PS spheres in the four aqueous media mentioned above, at temperatures whose significance is dealt with in the chapter on steric stabilization.

TABLE 6

Microwave Damping Factor in Electrolyte Solutions

I_s	D(10 Å)	D(20 Å)
0.05	0.23	0.05
0.10	0.13	0.02
0.14 *	0.09	0.01
0.20	0.05	$\sim 10^{-3}$
0.50	0.01	$\sim 10^{-4}$
1.00	$\sim 10^{-3}$	$\sim 10^{-6}$
2.00	$\sim 10^{-4}$	$\sim 10^{-8}$
4.00	$\sim 10^{-6}$	$\sim 10^{-12}$

* physiological saline (38,39)

Fig. 10. Plots of the Hamaker function H versus the distance parameter δ for PS in aqueous ionic media. Lines: (1) 0.2 M HCl at 287 K, (2) 0.39 M $MgSO_4$ at 318 K, (3) 2 M NaCl at 298 K, (4) 2.1 M $(NH_4)_2SO_4$ at 298 K.

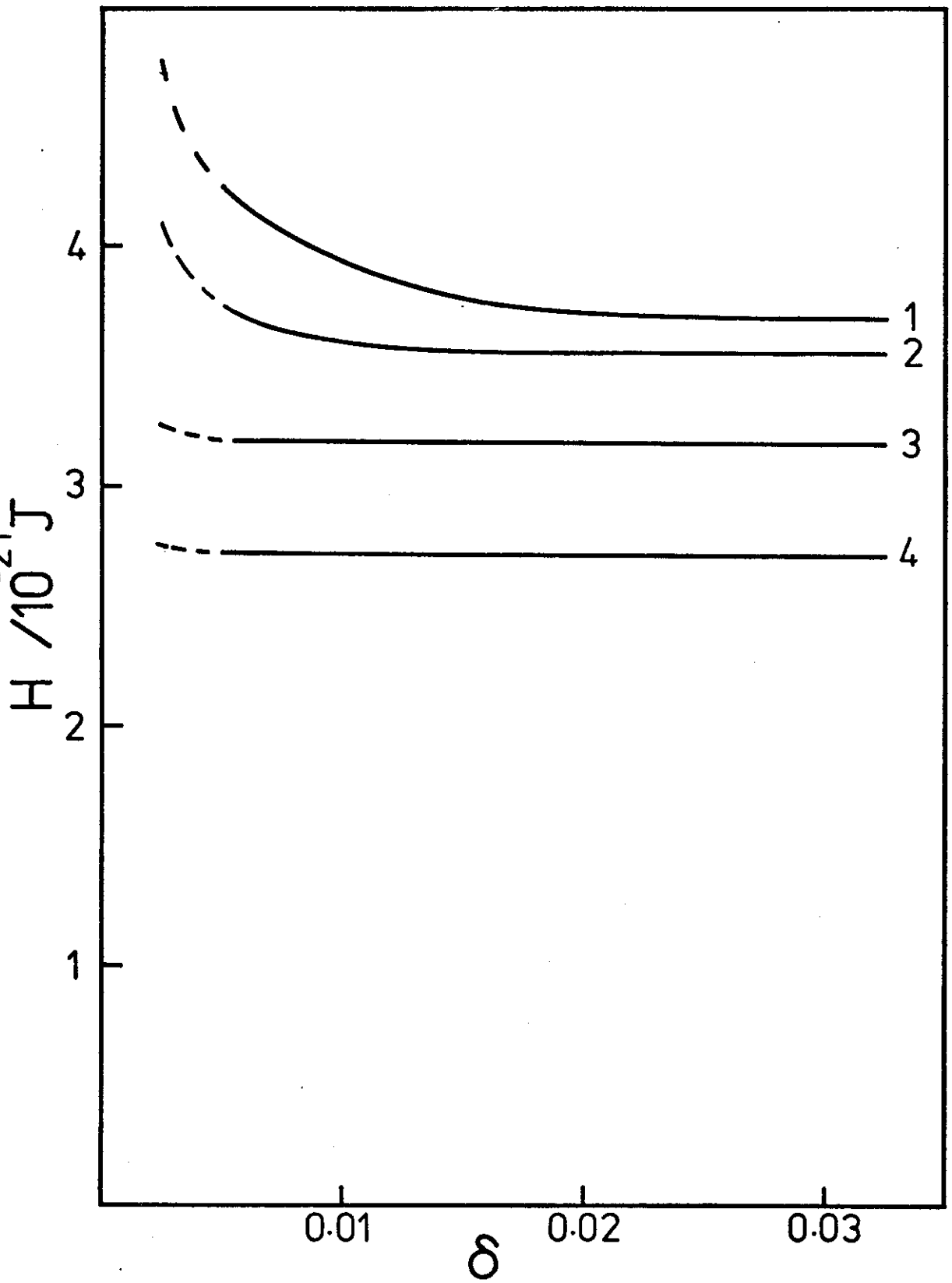
H /10^-21 J
4
3
2
1
0·01
0·02
0·03
δ
1
2
3
4

A very common method of determining the Hamaker constant experimentally is by flocculation studies involving ions in the aqueous medium. When comparing theoretical and empirical results it is important to bear this damping effect in mind. Lips and Willis (40) claim to have detected experimentally the damping effect of electrolyte on the Hamaker constant of PS latices. They find that the Hamaker constant increases with decreasing salt concentration in the aqueous phase.

4.4. Hamaker Constants and Complementary Systems

The Hamaker function is virtually constant (i.e., independent of δ) for all systems which exhibit small Δ_j^2 for all j. From eq.{7}, for small Δ_j^2:

$$\int_0^\infty x\ln(1 - \Delta_j^2 e^{-x})dx \simeq -\Delta_j^2 \int_0^\infty xe^{-x}dx \simeq -\Delta_j^2$$

and

$$(1 - \Delta_j)\ln(1 - \Delta_j^2) \simeq -\Delta_j^2.$$

Separating the zero and non-zero frequency contributions:

$$G_{j\neq 0} \simeq \frac{-kT}{8\delta} \sum_{j=1}^{\infty} \Delta_j^2(1 + 2\delta\ln\delta) \qquad \{14\}$$

$$G_{j=0} = \frac{kT}{16\delta} \left(\int_0^\infty x\ln(1 - \Delta_0^2 e^{-x})dx + 2(1 - \Delta_0)\ln(1 - \Delta_0^2)\delta\ln\delta \right) \qquad \{15\}$$

For $\delta \leq 0.05$:

$$H = -6G/\left(\frac{2}{\delta^2 + 4\delta} + \frac{2}{\delta^2 + 4\delta + 4} + \ln\frac{\delta^2 + 4\delta}{\delta^2 + 4\delta + 4}\right)$$

$$\simeq -12G\delta/(1 + 2\delta\ln\delta) \qquad \{16\}$$

Therefore, from eq.{14}:

$$H_{j\neq 0} \simeq \frac{3}{2} kT \sum_{j=1}^{\infty} \Delta_j^2 \qquad \{17\}$$

If Δ_0^2 is also small, as in non-polar systems, the zero frequency term need not be separated and we find

$$H \simeq \frac{3}{2} kT \sum_{j=0}^{\infty}{}' \Delta_j^2 \qquad \{18\}$$

The constancy of H as indicated by eq.{17} and eq.{18} is demonstrated using the full eq.{7} in Figs.11 and 12. The former shows the dependence of H on δ for several polymer/water systems, with and without the microwave term; the latter shows five non-aqueous systems in which the zero frequency term is included.

In the limit as $\delta \to 0$, eq.{7} reduces to

$$G_{\delta\to 0} = \frac{kT}{8\delta} \sum_{j=0}^{\infty}{}' \int_0^{\infty} x \ln(1 - \Delta_j^2 e^{-x}) dx$$

Similarly, F reduces to:

$$F_{\delta\to 0} = \frac{1}{12\delta}$$

Therefore

$$H_{\delta=0} = -\frac{G_{\delta\to 0}}{F_{\delta\to 0}} = -\frac{3}{2} kT \sum_{j=0}^{\infty}{}' \int_0^{\infty} x \ln(1 - \Delta_j^2 e^{-x}) dx \qquad \{19\}$$

This may be simplified by introducing the approximation

Fig.11. Plots of the Hamaker function H versus the distance parameter δ for spheres in water at 298 K. Lines: (a) with microwave, (b) without microwave, (1) PS, (2) PAN, (3) PMMA, (4) n-heptane, (5) PVA .

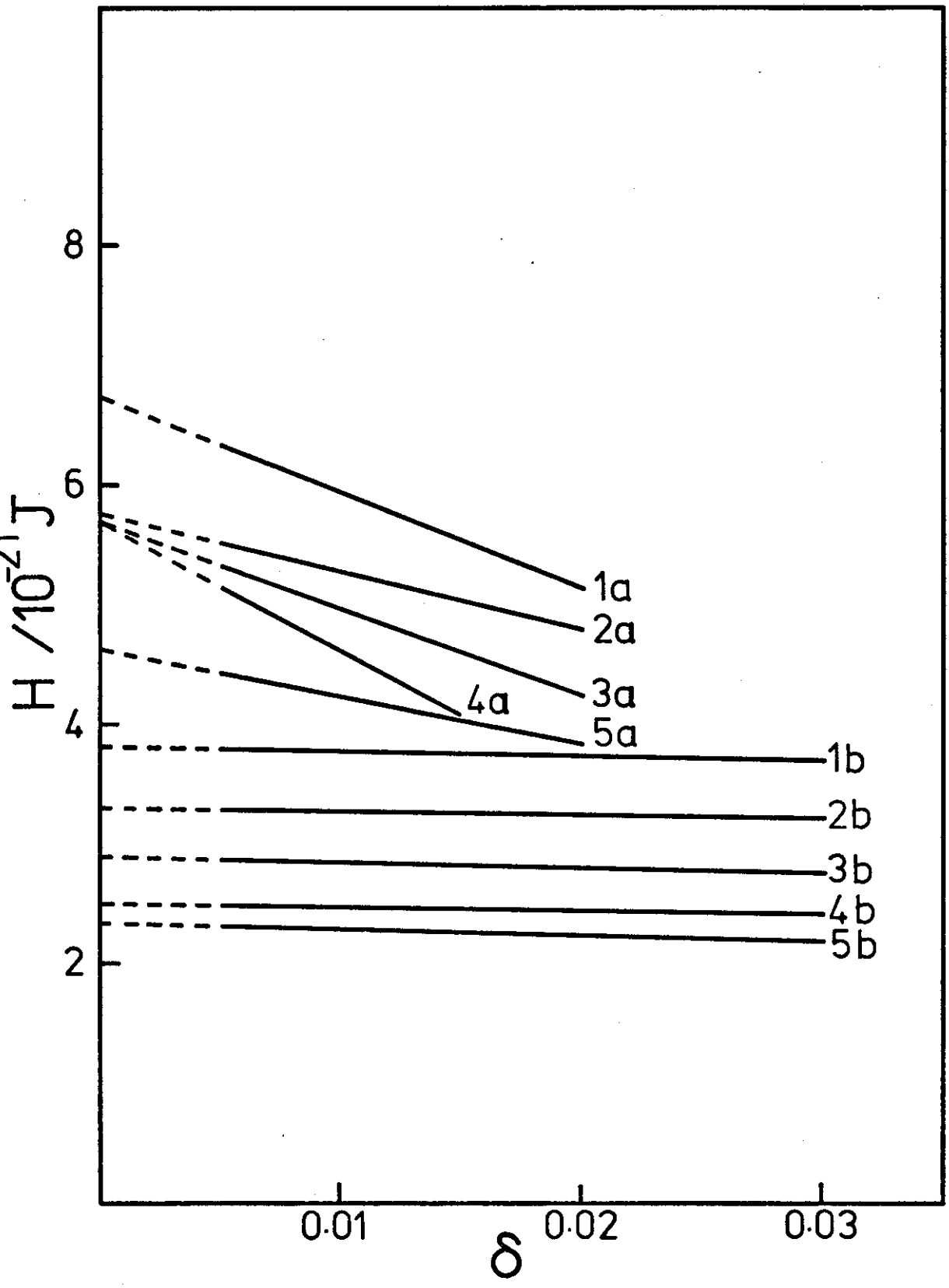
8
6
4
2
H /10^-21 J
1a
2a
3a
4a
5a
1b
2b
3b
4b
5b
0·01
0·02
0·03
δ

Fig.12. Plots of the Hamaker function H versus the distance parameter δ for some non-aqueous systems. Lines: (1) PS in n-heptane, (2) PAN in cyclohexane, (3) PMMA in n-heptane, (4) PAN in toluene, (5) PAN in benzene .

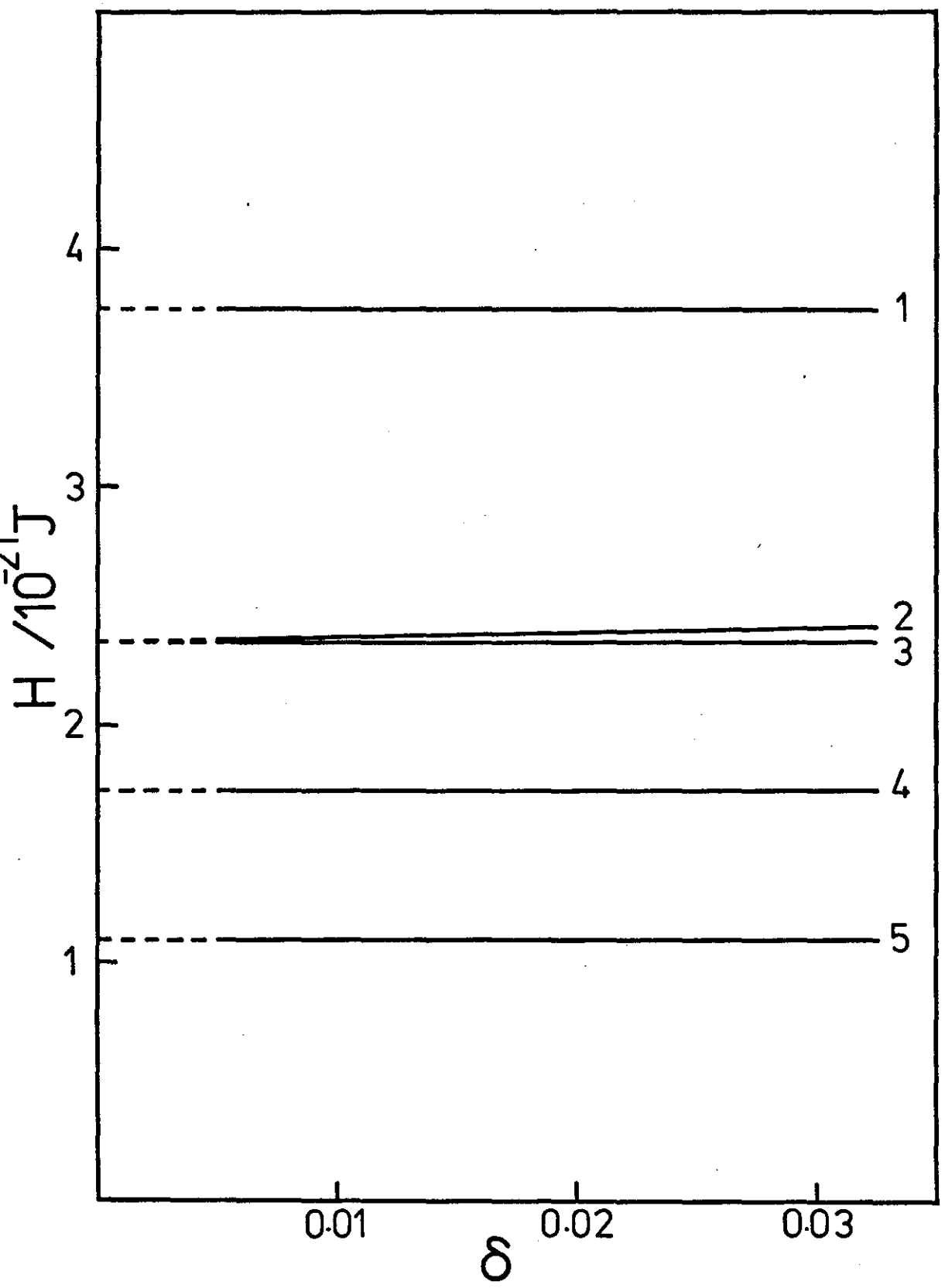
4
3
2
1
H /10^-21 J
1
2
3
4
5
0·01
0·02
0·03
δ

Fig.13. Upper curve: $Y_j = \Delta_j^2(1 + \Delta_j^2/5)$.

Lower curve: $Y_j = -\int_0^\infty x\ln(1 - \Delta_j^2 e^{-x})dx$.

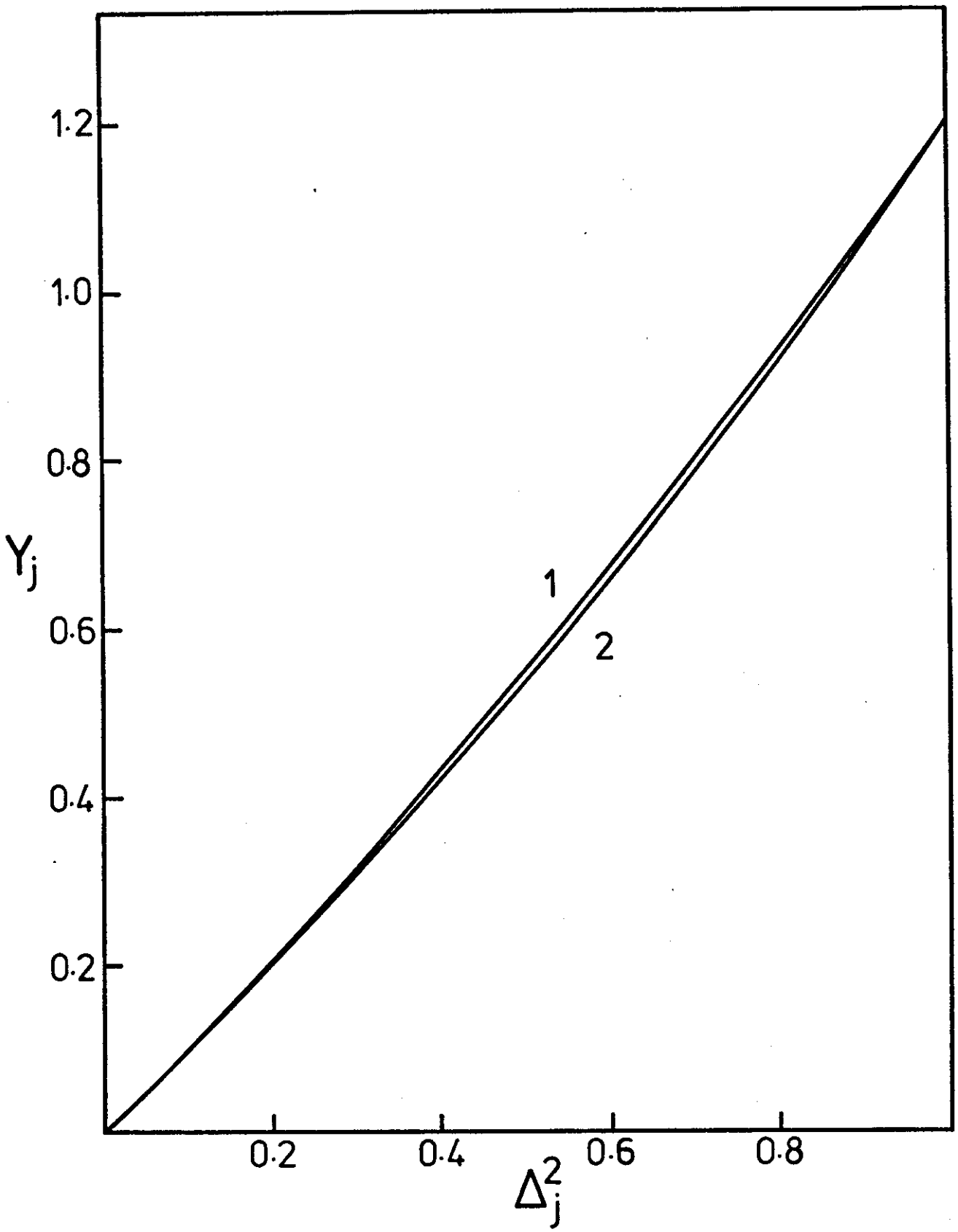
1.2
1.0
0.8
Y_j
0.6
0.4
0.2
1
2
0.2
0.4
0.6
0.8
Δ_j^2

Fig.14. Plots of the Hamaker function H versus the distance parameter δ for complementary aqueous systems at 298 K. Lines: (1) water in PS, (2) PS in water, (3) water in n-heptane, (4) n-heptane in water, (5) water in PAN, (6) PAN in water.

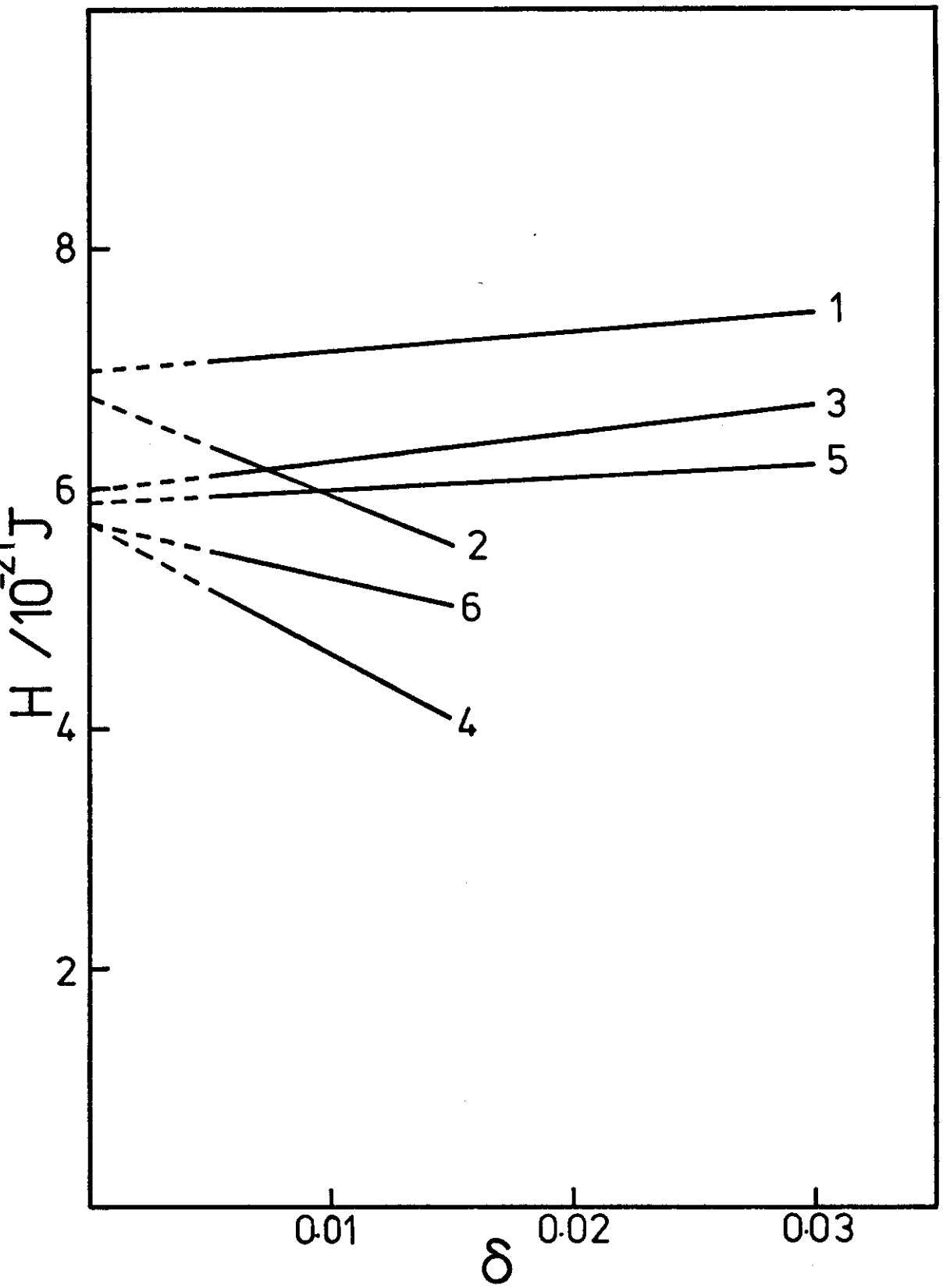
8
6
4
2
$H_4 / 10^{-21} J$
1
2
3
4
5
6
0·01
0·02
0·03
δ

Fig. 15. Plots of the Hamaker function H versus the distance parameter δ for complementary aerosols and foams at 298 K. Lines: (1) PS in air, (2) air in PS, (3) water in air, (4) air in water, (5) n-heptane in air, (6) air in n-heptane.

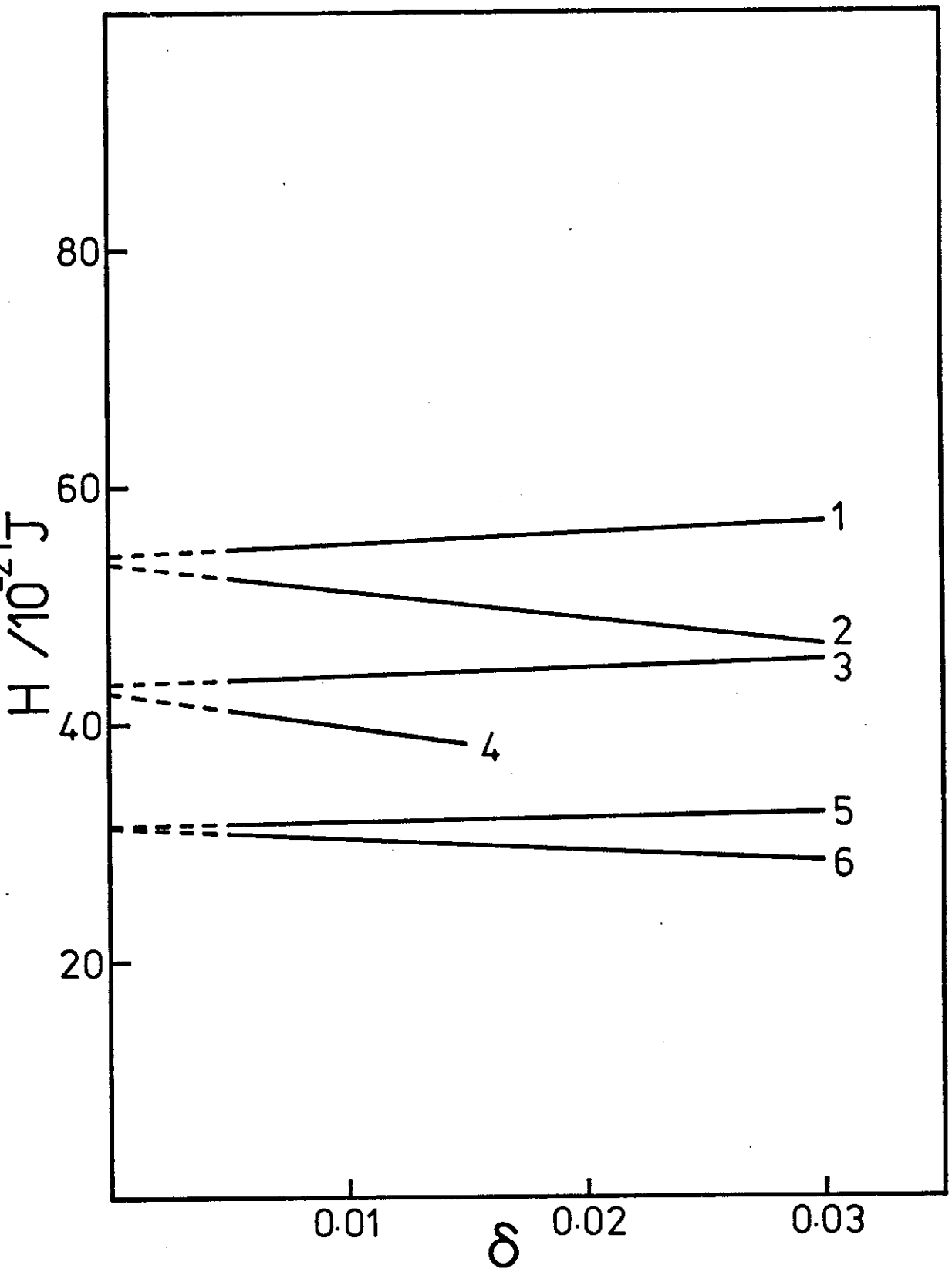
80
60
40
20
H /10^-21 J
1
2
3
4
5
6
0·01
0·02
0·03
δ

Fig.16. Plots of the Hamaker function $H_{j\neq 0}$ versus the distance parameter δ for complementary aqueous systems at 298 K without the microwave contribution. Lines as in Fig.14: (1) water in PS, (2) PS in water, (3) water in n-heptane, (4) n-heptane in water, (5) water in PAN, (6) PAN in water.

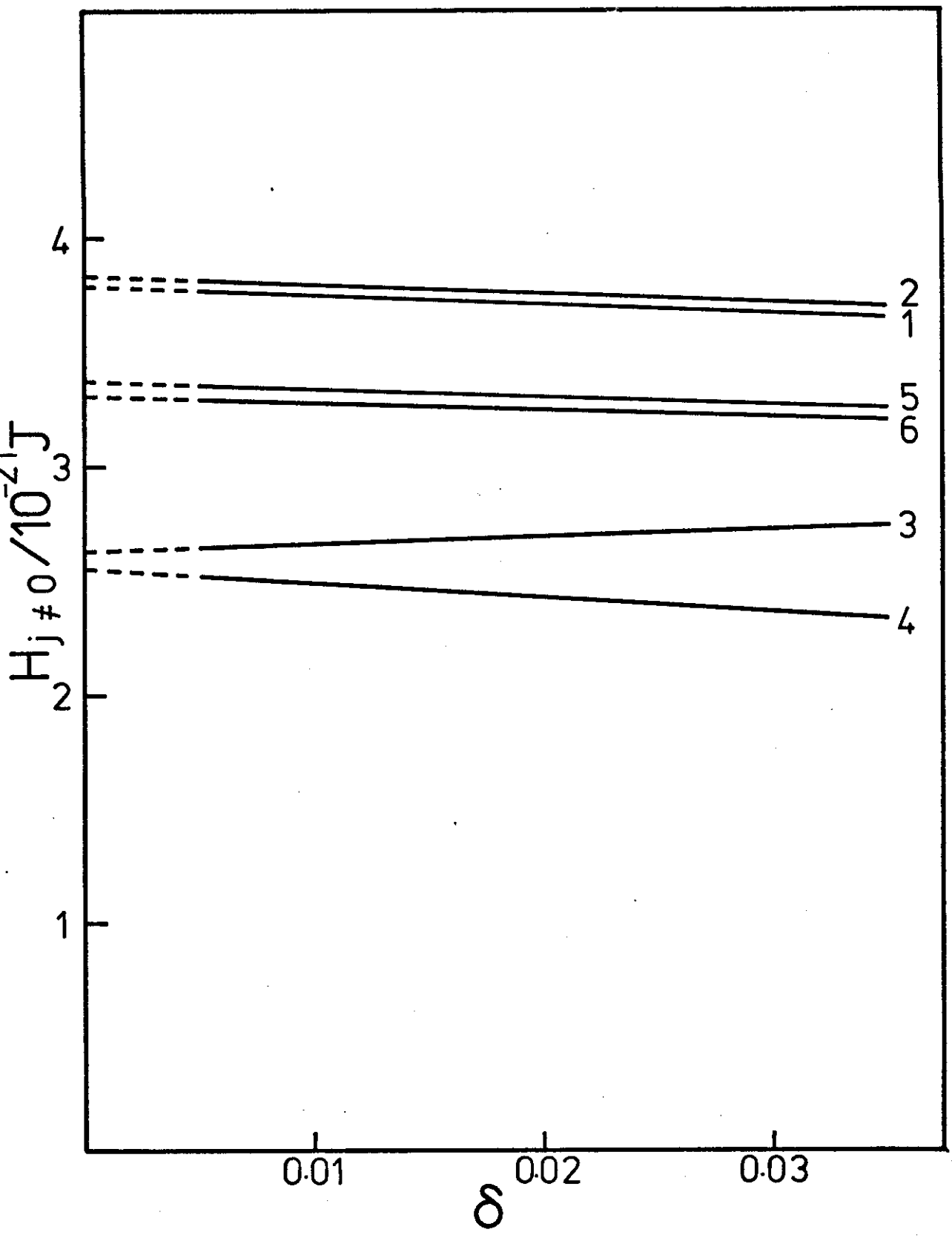
4
3
2
1
$H_{j\neq 0}/10^{-21}J$
2
1
5
6
3
4
0·01
0·02
0·03
δ

$$Y_j = -\int_0^\infty x\ln(1 - \Delta_j^2 e^{-x})dx$$

$$\simeq \Delta_j^2(1 + \Delta_j^2/5) \qquad \{20\}$$

which was checked numerically and found to be accurate to better than 2½% for all Δ_j. Both expressions are plotted in Fig.13 as functions of Δ_j^2. We have:

$$H_{\delta=0} \simeq \frac{3}{2} kT \sum_{j=0}^{\infty}{}' \Delta_j^2(1 + \Delta_j^2/5) \qquad \{21\}$$

where $H_{\delta=0}$ will be called the "contact Hamaker constant". This expression indicates that the value of $H_{\delta=0}$ is unaffected if the system is reversed, i.e., if the dielectric properties of the particles and medium are interchanged to give the complementary system. Because the linearity of H does not hold down to very small separations, the computed H functions for complementary systems do not always extrapolate to the same $H_{\delta=0}$ or contact Hamaker constant. However, as can be seen in Figs.14 and 15, the contact Hamaker constants measured by extrapolating are within 5% of each other. The values obtained from eq.{21} are midway between the extrapolated values.

Most of the discrepancy is caused by the microwave term as Fig.16 indicates.

4.5. An Approximation for the Contact Hamaker Constant

The contact Hamaker constant is defined here as the hypothetical value of H in the limit $\delta \to 0$. As was mentioned previously, the continuum theory is not valid at $d \leq 5$ Å; other (short-range) forces operate in this domain (43).

It is, however, very convenient to use $\delta = 0$ as the unique reference point for the comparison of all Hamaker functions.

In most cases $|\Delta_{j\neq 0}| \lesssim 0.5$ (latices, emulsions, aerosols and foams). From eq.{21} we may write

$$H_{\delta=0} \simeq \frac{3}{4} kT\Delta_0^2(1 + \Delta_0^2/5) + \frac{3}{2} kT \sum_{j=1}^{\infty} \Delta_j^2 \qquad \{22\}$$

where Δ_0 may not be small.

If relaxation in the infrared can be ignored (e.g., for n-alkanes, non-polar polymers, air) a crude approximation for the contact Hamaker constant can be found:

$$H_{\delta=0} \simeq \frac{3}{4} kT\Delta_0^2(1 + \Delta_0^2/5) + \frac{3}{2} kTj\Delta^2 \qquad \{23\}$$

where $$\Delta = \frac{n_p^2 - n_m^2}{n_p^2 + n_m^2} .$$

Using

$$\xi = \frac{2\pi kT}{h} j \simeq 8.2256 \times 10^{11} Tj .$$

and

$$\omega_{UV} = 1.519 \times 10^{11} I_C$$

we can find j at $\xi = \omega_{UV}$ as:

$$j = \frac{1.519 \times 10^{15} I_C}{8.2256 \times 10^{11} T} = \frac{1847 I_C}{T}$$

Therefore:

$$H_{\delta=0} \simeq \frac{3}{4} kT\Delta_0^2(1 + \Delta_0^2/5) + 2770kI_C\Delta^2 \qquad \{24\}$$

(note the temperature independence of the finite frequency component). A mean of the ionization potentials may be used for I_C.

Table 7 lists some "exact" and approximate contact Hamaker constants. The above equation is intended only as a rough guide in the absence of a programmable calculator or computer and only for systems in which there is little infrared relaxation.

Neglecting the microwave term we find for systems which relax only in the ultraviolet (e.g., PS in alkanes, PS in air, PE in alkanes):

$$H \simeq 3.8 \times 10^{-13} \left(\frac{n_p^2 - n_m^2}{n_p^2 + n_m^2}\right)^2 I_C = 3.8 \times 10^{-13} \Delta^2 I_C \qquad \{25\}$$

4.6. The Slope of the Hamaker Function

From eqs.{9,10,11} we can easily find the approximate slope $\frac{\partial H}{\partial \delta}$. Differentiating eqs.{10,11} we have

$$\frac{\partial}{\partial \delta}\left(\frac{\ln \delta}{F}\right) = -45.7$$

and

$$\frac{\partial}{\partial \delta}\left(\frac{1}{\delta F}\right) = 79.0 \ .$$

Thus

$$\frac{\partial H}{\partial \delta} = -\alpha(79.0 + 45.7\beta) = -79.0\alpha - 45.7\alpha\beta.$$

TABLE 7

"Exact" and Approximate Contact Hamaker Constants

System	"exact" $H_{\delta=0}/10^{-21}$ J. (eq.{19})	"approx" $H_{\delta=0}/10^{-21}$ J. (eq.{24})
PAN/toluene	1.7	0.83
PAN/benzene	1.2	0.82
PAN/cyclohexane	2.3	2.1
PAN/PS	1.0	1.3
PS/heptane	3.7	5.6
PS/PEO (60°C)	4.6	4.4
PS/PEO (45°C)	4.3	4.3
PMMA/heptane	2.3	2.1
PS/air	54	51
heptane/air	31	33

where

$$\alpha = \frac{kT}{8}\sum_{j=0}^{\infty}{}' \int_0^{\infty} x\ln(1 - \Delta_j e^{-x})dx = -\frac{kT}{8}\sum_{j=0}^{\infty}{}' Y_j$$

and

$$\alpha\beta = -\frac{kT}{4}\sum_{j=0}^{\infty}{}'(1 - \Delta_j)\ln(1 - \Delta_j^2) .$$

The microwave contribution is primarily responsible for large slopes (24) so we may neglect $j > 0$ as a first approximation:

$$\alpha_0 = -\frac{kT}{16} Y_0 \simeq -\frac{kT}{16}\Delta_0^2(1 + \Delta_0^2/5) ,$$

$$\alpha_0\beta_0 = -\frac{kT}{8}(1 - \Delta_0)\ln(1 - \Delta_0^2)$$

and

$$\frac{\partial H}{\partial \delta} \simeq -79.0\alpha_0 - 45.7\alpha_0\beta_0 .$$

For PS in water,

$$\Delta_0 = -0.94$$

$$\alpha_0 = -0.065\ kT$$

$$\alpha_0\beta_0 = 0.522\ kT .$$

Therefore

$$\frac{\partial H}{\partial \delta} \simeq -18.7\ kT$$

which agrees well with the slope -19.2 kT obtained from computations on the full equations {6} and {7}. This procedure is useful when estimating the initial slope of H for condensed systems whose components differ greatly in dielectric constant.

For condensed systems in which the components have similar dielectric constants (small or large), Δ_j is usually small for all j and we may use the approximations:

$$\alpha \simeq - \frac{kT}{8} \sum_{j=0}^{\infty}{}' \Delta_j^2$$

$$\alpha\beta \simeq \frac{kT}{4} \sum_{j=0}^{\infty}{}' \Delta_j^2$$

and

$$\frac{\partial H}{\partial \delta} \simeq 9.875\ kT \sum_{j=0}^{\infty}{}' \Delta_j^2 - 11.425\ kT \sum_{j=0}^{\infty}{}' \Delta_j^2$$

$$\simeq 1.55\ kT \sum_{j=0}^{\infty}{}' \Delta_j^2$$

where $\sum_{j=0}^{\infty}{}' \Delta_j^2$ is generally less than 1 (~0.6 for PS in n-heptane). In such cases, the slope is ~kT which is negligible over the range of δ in which the equations are applicable (usually $\delta \lesssim 0.03$).

Finally, for aerosols and foams, $\sum_{j=0}^{\infty}{}' \Delta_j^2$ may be as large as 8. However, because the contact value $H_{\delta=0}$ is very large, we find that the slope has relatively little effect over the allowed range of δ (Fig.15).

It is concluded therefore, that the slope of H is important only for condensed systems in which Δ_0 is large.

4.7. Sterically Stabilized Particles

It has been shown theoretically (41-44) that the presence of adsorbate between interacting particles can alter the van der Waals attraction. Vold (41) treats the coating as an impenetrable spherical shell and assumes the interaction energy becomes infinitely negative on contact of the adsorbed layer. Vincent (43) uses the treatment developed by Vold for the interaction before adsorbate contact and a composite Hamaker constant after overlap of the adsorbate. He predicts a large discontinuity in the attraction potential which is attributed to the initial contact of the adsorbate. Such a discontinuity seems to be physically unreasonable and indicates that the surface of the adsorbed layer cannot be treated in a similar manner to that of the particle.

Vold and Vincent both used the Hamaker theory. It will be shown below that Vincent's result (or at least the general form) is a limiting case of the corresponding result derived using Lifshitz theory.

In essence, the procedure used by Vincent is to calculate a composite Hamaker constant for the adsorbate/medium mixture in the region between the particles. Only the case where $d \leq 2L$ will be considered, where d is the separation of the particle surfaces and L is the adsorbate layer thickness. A constant segment density model is assumed in the first instance.

If we denote the volume fraction of adsorbate between the particles by v then Vincent obtained the following expression for the composite Hamaker

constant:

$$H_{comp} = (vH_2^{\frac{1}{2}} + (1 - v)H_1^{\frac{1}{2}})^2 \quad \{26\}$$

where H_2 is the Hamaker constant of the pure adsorbate and H_1 is that of the pure medium.

The distance dependence of H_{comp} is obtained through:

$$v = \frac{2L\bar{v}}{d} \quad \{27\}$$

where $\bar{v}$ is the mean volume fraction of adsorbate in each stabilizer layer when $d \geq 2L$ (i.e., before overlap).

Having presented the basic Vincent equation {26} we now approach the problem from the macroscopic viewpoint.

It is proposed that the intervening polymer (adsorbate) solution has adsorption characteristics which are linear combinations of those of the component solvent and polymer:

$$\varepsilon = v\varepsilon_2 + (1 - v)\varepsilon_1 \quad \{28\}$$

where ε_2 is the measured dielectric permittivity of the polymer and ε_1 is that of the solvent medium. This equation has been tested on the additivity of the visible absorption of sucrose solutions using data from the "Handbook of Physics and Chemistry" (28). The results are shown in Table 8 and Fig.17; for this system, at least, linearity is excellent.

TABLE 8

Relative Permittivities of Aqueous Sucrose Solutions

Weight fraction of sucrose(w_2)	Relative solution density(ρ)	Refractive index (n)	Calculated volume fraction of sucrose (v_2)	Permittivity of solution ($\varepsilon = n^2$)
0.0	1.0000	1.3330	0.0000	1.7769
0.1	1.0381	1.3479	0.0657	1.8168
0.2	1.0810	1.3639	0.1366	1.8602
0.3	1.1270	1.3811	0.2133	1.9074
0.4	1.1765	1.3997	0.2967	1.9592
0.5	1.2295	1.4200	0.3875	2.0164
0.6	1.2864	1.4418	0.4869	2.0788
0.7	1.3472	1.4651	0.5962	2.1465
0.8	1.4117	1.4901	0.7168	2.2204
1.0	1.5805	1.5481 (extrapolated)	1.0000	2.3965 (extrapolated)

v_2 is calculated from w_2 and the pure component densities, assuming volume additivity.

Fig. 17. Plot of volume fraction of sucrose in water versus the relative permittivity of the solution (from Table 8). Extrapolation to $v_2 = 1$ yields 1.548 for the refractive index of pure sugar. This value lies within those measured along the three optical axes of the crystal (1.5376, 1.5651, 1.5705). Correlation coefficient = 0.99999.

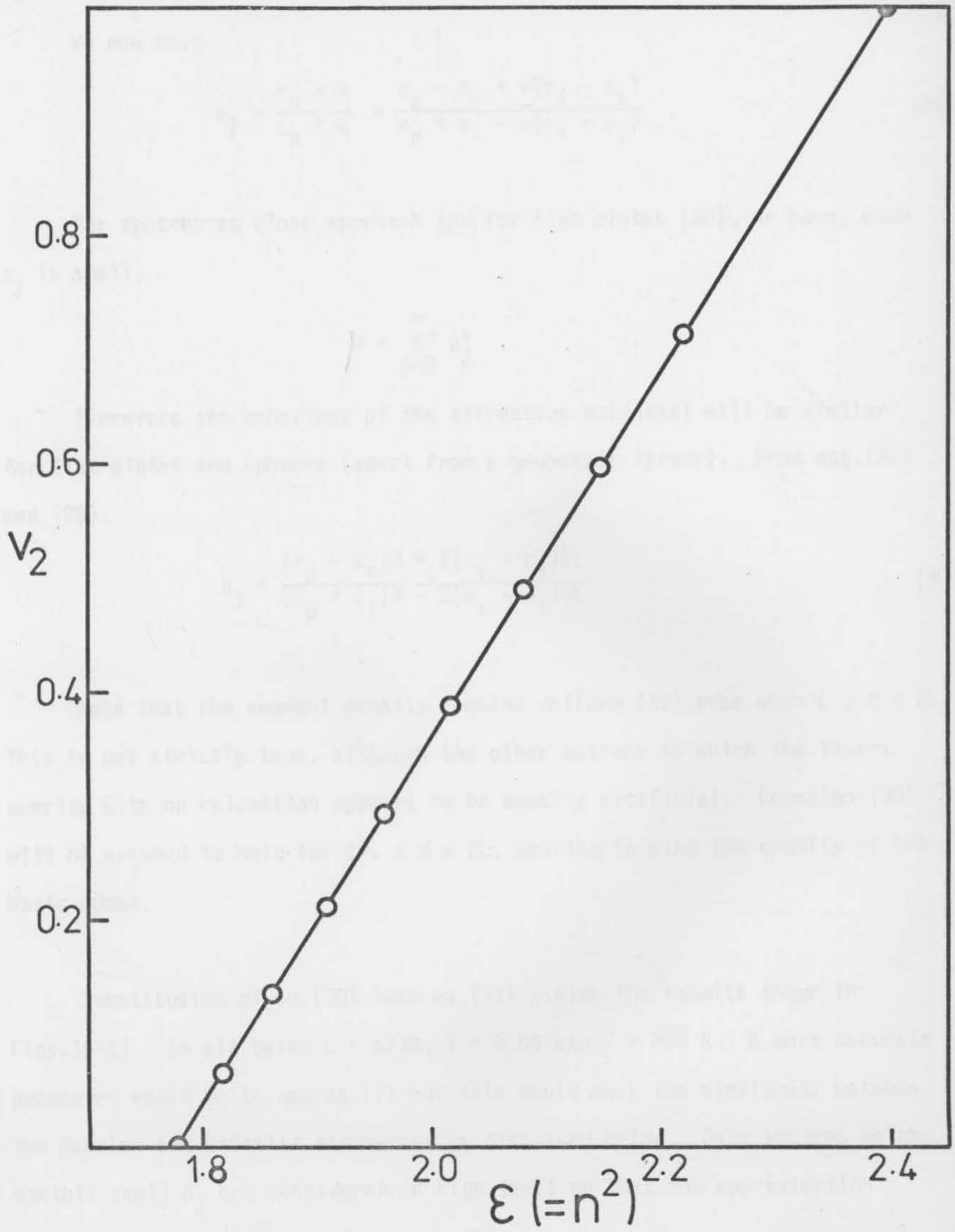
0.8
0.6
V_2
0.4
0.2
1.8
2.0
2.2
2.4
$\varepsilon\ (=n^2)$

We now have

$$\Delta_j = \frac{\varepsilon_p - \varepsilon}{\varepsilon_p + \varepsilon} = \frac{\varepsilon_p - \varepsilon_1 + v(\varepsilon_1 - \varepsilon_2)}{\varepsilon_p + \varepsilon_1 - v(\varepsilon_1 - \varepsilon_2)} \quad . \qquad \{29\}$$

For spheres at close approach and for flat plates (30), we have, when Δ_j is small,

$$H \propto \sum_{j=0}^{\infty}{}' \Delta_j^2 \quad .$$

Therefore the behaviour of the attraction potential will be similar for flat plates and spheres (apart from a geometric factor). From eqs.{27} and {29},

$$\Delta_j = \frac{(\varepsilon_p - \varepsilon_1)d + 2(\varepsilon_1 - \varepsilon_2)\bar{v}L}{(\varepsilon_p + \varepsilon_1)d - 2(\varepsilon_1 - \varepsilon_2)\bar{v}L} \quad . \qquad \{30\}$$

Note that the segment density remains uniform (43) even when $L \leq d \leq 2L$. This is not strictly true, although the other extreme in which the layers overlap with no relaxation appears to be equally artificial. Equation {30} will be assumed to hold for $2\bar{v}L \leq d \leq 2L$, bearing in mind the crudity of the basic model.

Substitution of eq.{30} into eq.{21} yields the results shown in Figs.18-21. In all cases $L = a/10$, $\bar{v} = 0.05$ and $T = 298$ K. A more accurate procedure would be to use eq.{7} but this would mask the similarity between the Hamaker and Lifshitz approaches as discussed below. Only systems which exhibit small Δ_j are considered in Figs.18-21 so that the approximation made by using eq.{21} is not unreasonable.

Fig. 18. Plot of the Hamaker function $H_{j\neq 0}$ versus the distance parameter δ for PS coated with PEO in water at 298 K without the microwave contribution. $L = a/10$, $v_{\infty} = 0.05$,
$H_{j\neq 0}$ (PS in water) $= 3.75 \times 10^{-21}$ J.
$H_{j\neq 0}$ (PS in PEO) $= 2.17 \times 10^{-21}$ J.

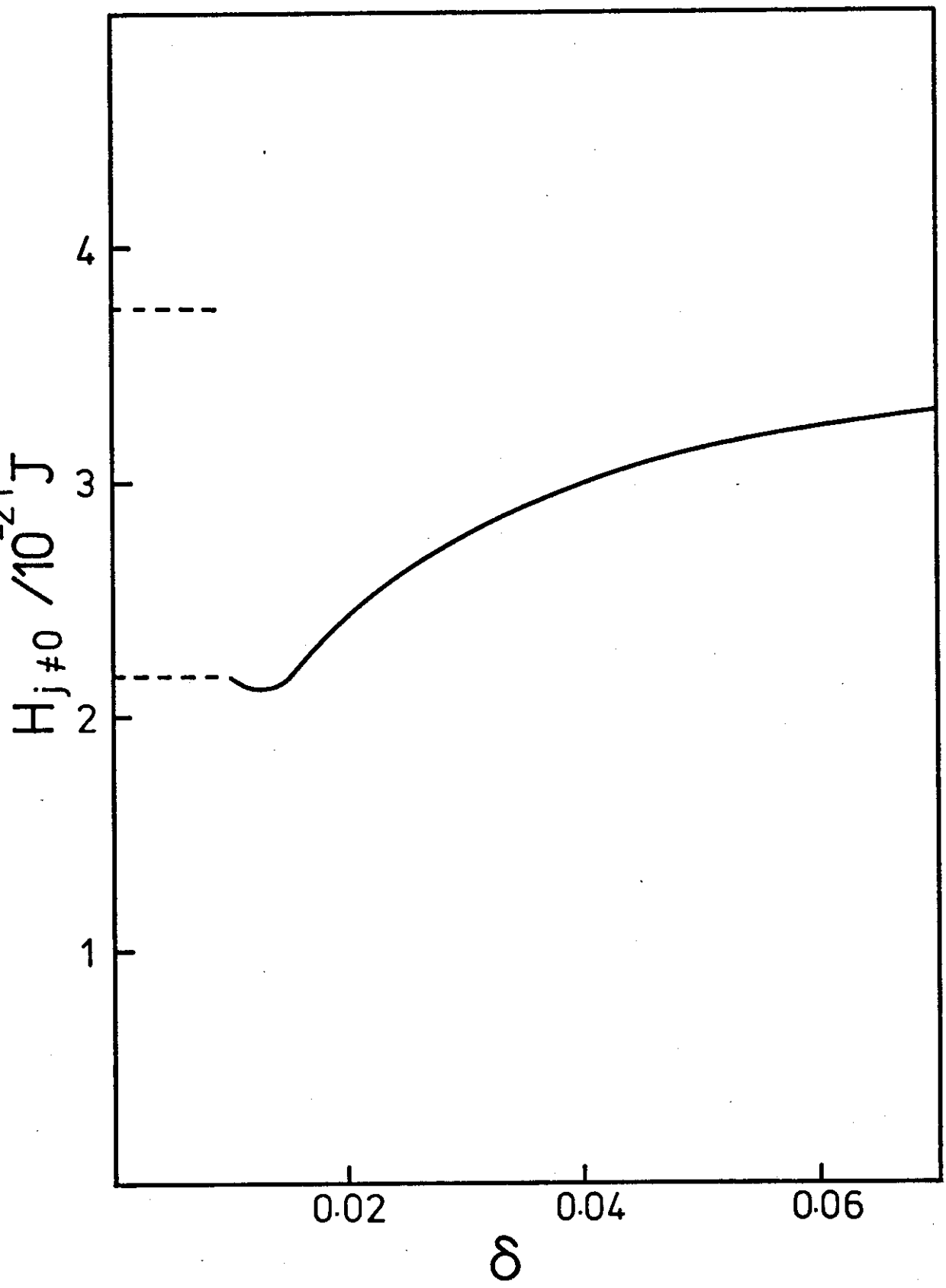
4
3
2
1
$H_{j\neq 0}$ /10^{-21} J
0.02
0.04
0.06
δ

Fig.19. Plot of the Hamaker function H versus the distance parameter δ for PAN coated with PS in cyclohexane at 307 K. L = a/10, v_∞ = 0.05.
H(PAN in cyclohexane) = 2.35×10^{-21} J.
H(PAN in PS) = 1.05×10^{-21} J.

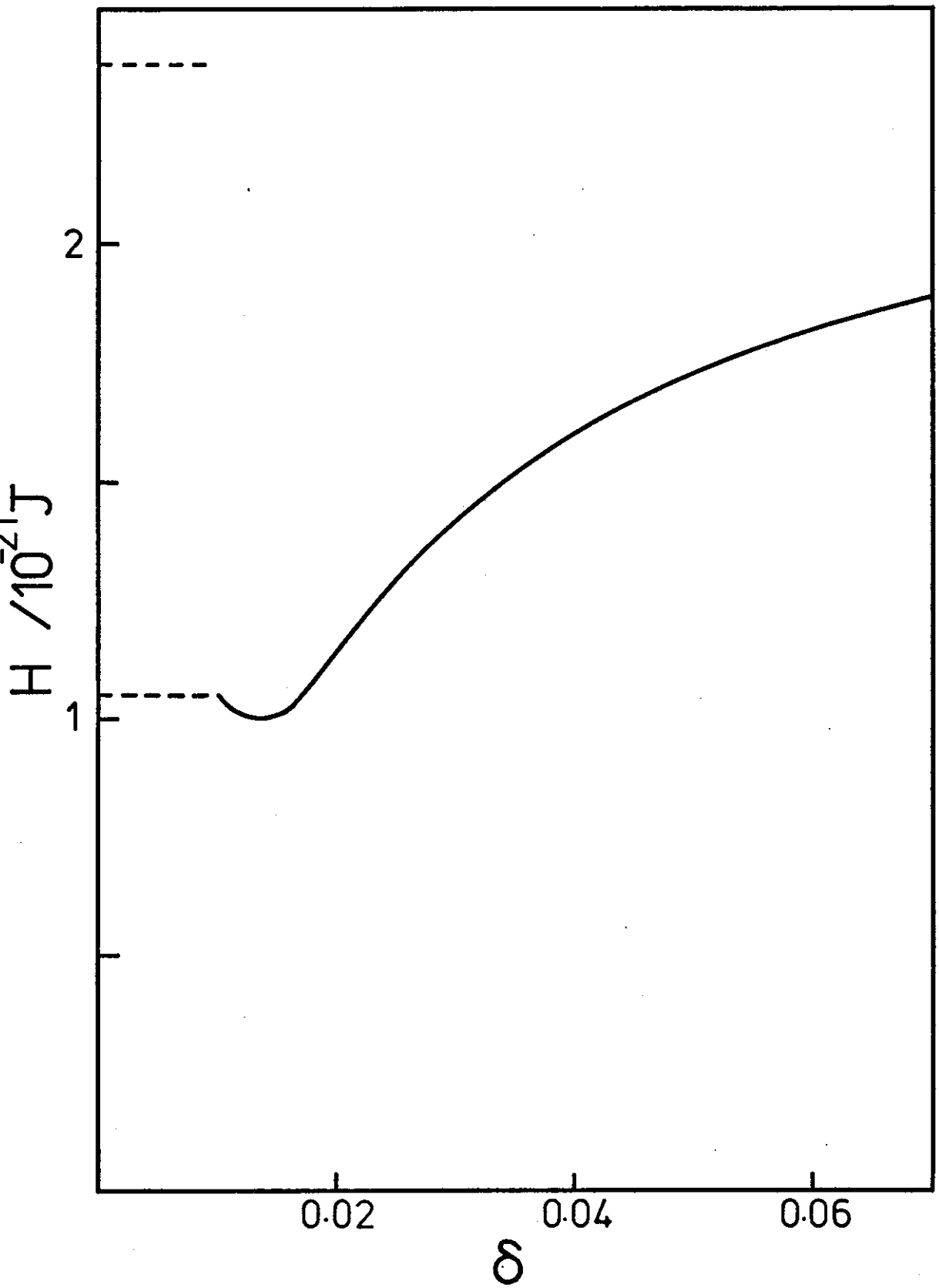
H /10^-21 J
2
1
0·02
0·04
0·06
δ

Fig.20. Plot of the Hamaker function $H_{j\neq 0}$ versus the distance parameter δ for n-heptane coated with PEO in water at 298 K without the microwave contribution. $L = a/10$, $v_{\infty} = 0.05$.
$H_{j\neq 0}$(n-heptane in water) = 2.57×10^{-21} J.
$H_{j\neq 0}$(n-heptane in PEO) = 0.4×10^{-21} J.

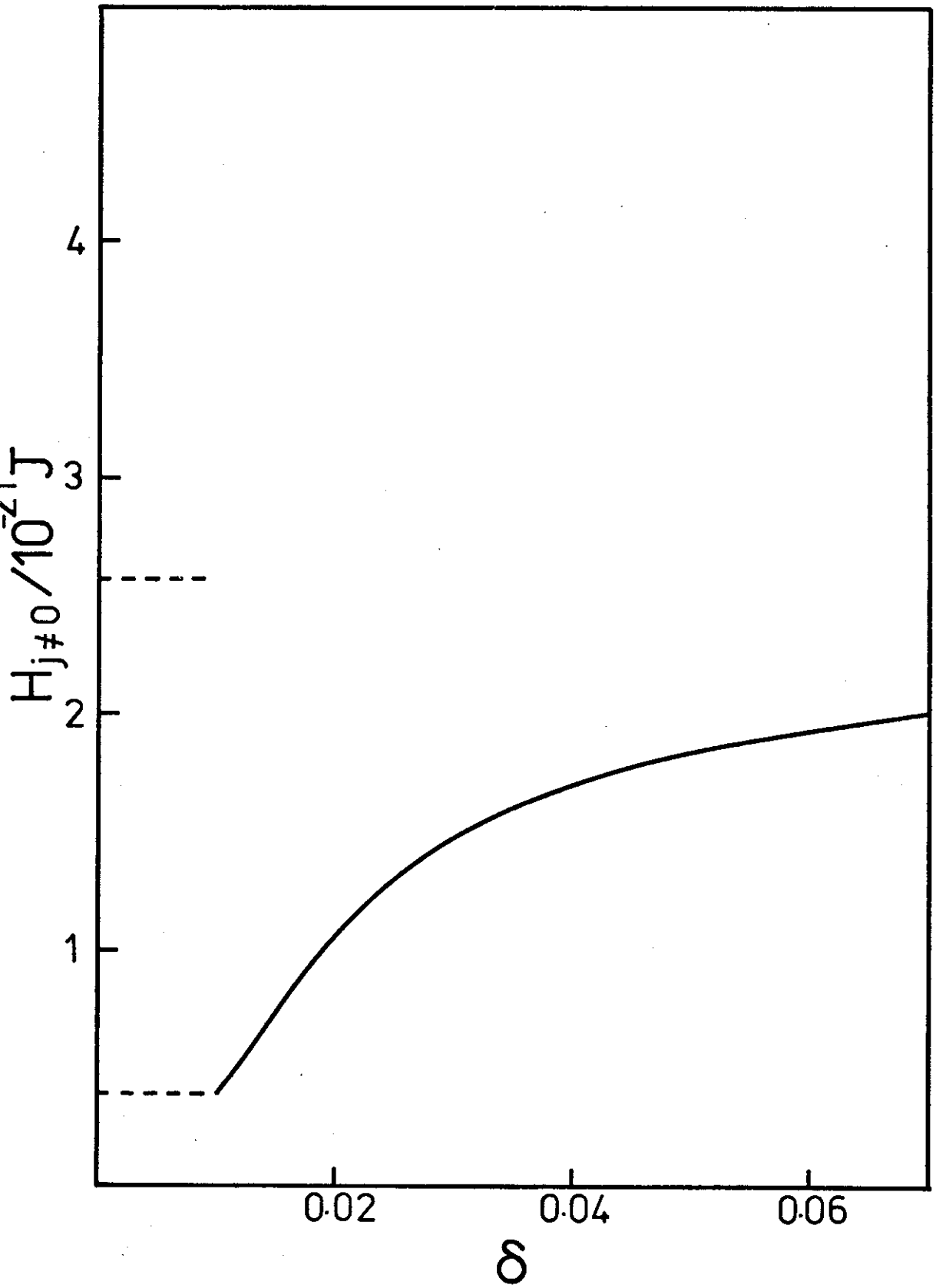
4
3
2
1
$H_{j\neq 0}/10^{-21}$ J
0·02
0·04
0·06
δ

Fig.21. Plot of the Hamaker function $H_{j\neq 0}$ versus the distance parameter δ for PAN coated with PEO in benzene at 298 K without the microwave contribution. $L = a/10$, $v_\infty = 0.05$.

$H_{j\neq 0}$(PAN in benzene) = 0.4×10^{-21} J.

$H_{j\neq 0}$(PAN in PEO) = 2.1×10^{-21} J.

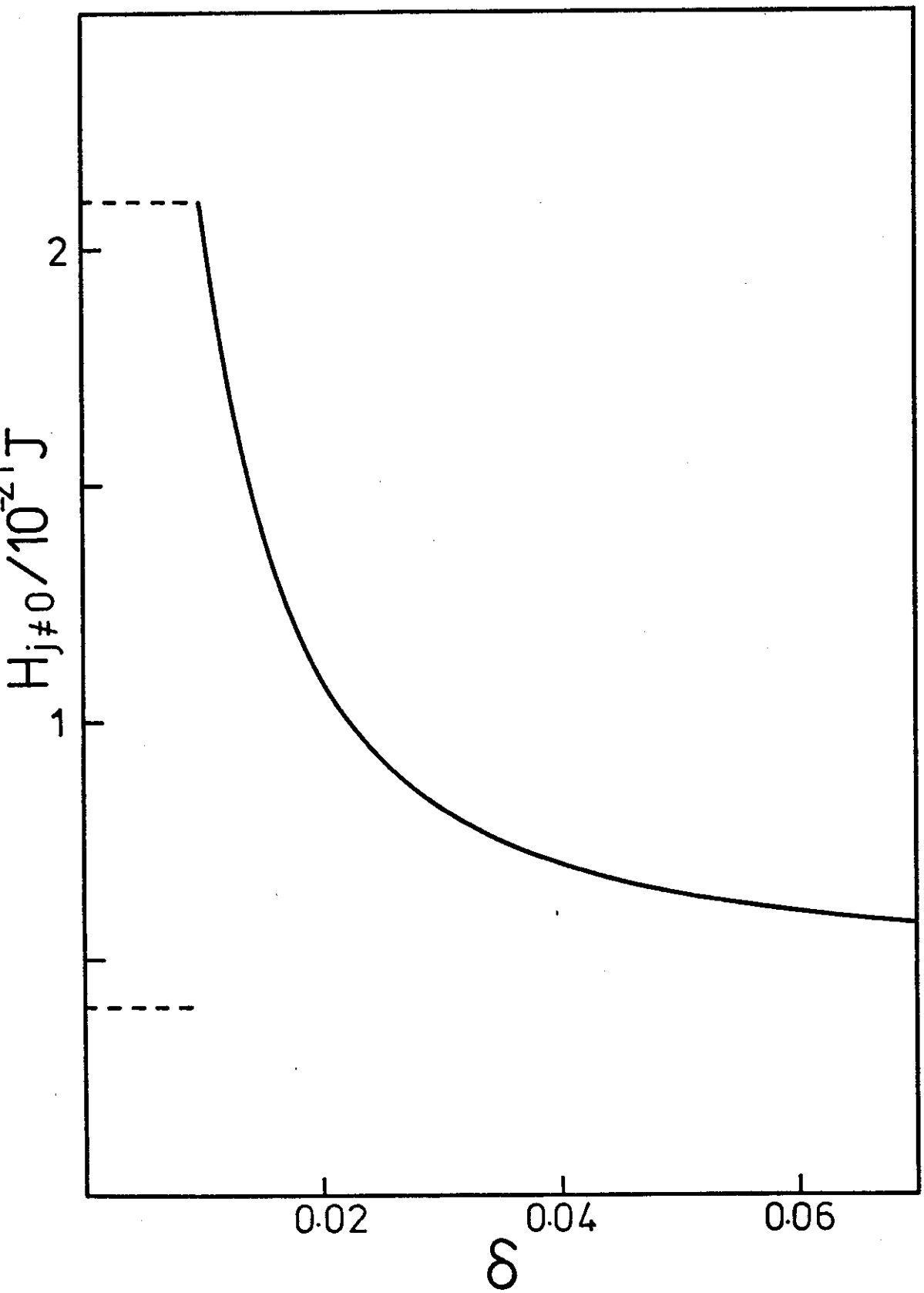
2
1
$H_{j\neq 0}/10^{-21}$ J
0·02
0·04
0·06
δ

Note that in Figs.18 and 19 a minimum occurs in H where the attraction between the particles in the composite medium is less than the attraction in either pure component. This phenomenon is related to the "Vold effect" (41,42). The same curves could be generated by keeping the distance of separation of the particles constant and varying the dielectric permittivity of the medium monotonically from that of pure solvent to that of pure adsorbate. The minimum occurs when the differences between the dielectric permittivity spectra of the composite medium and the particles are minimal. Total cancellation is extremely unlikely in real situations owing to the complexities of such spectra. Osmond et al (42) define the Vold effect as that reduction in van der Waals attraction, at constant particle separation, which can be produced by the addition of an adsorbed layer. They explain the reduction by invoking the analogy of the cancellation of buoyancy in a gravitational field by the appropriate combination of floats and sinkers. The situation represented in Figs.18 and 19 may be illustrated using a similar analogy except that neutral buoyancy is achieved when the density of a composite medium is the same as the density of the body. This situation is realized only if the density of the body lies between those of the components of the medium. Using this analogy, we may infer that the average dielectric permittivity of PAN lies between those of cyclohexane and PS (Fig.19) and the average non-zero frequency dielectric permittivity of PS lies between those of water and PEO (Fig.18). The appropriate conditions are never achieved for the systems represented in Figs.20 and 21. Strictly speaking, the Vold effect concerns only particles with adsorbed layers. It is one example of the general reduction in attraction (at constant separation) accompanying any process which causes the dielectric properties of the particle and medium to become

more similar.

According to classical theory, the Hamaker constant of particles imbedded in the composite medium is given by:

$$H_{Vinc} = (H_p^{\frac{1}{2}} - H_{comp}^{\frac{1}{2}})^2 \ ,$$

where the subscript Vinc indicates the use of the Vincent approach. From eq.{26}:

$$H_{Vinc} = (H_p^{\frac{1}{2}} - vH_1^{\frac{1}{2}} - (1-v)H_2^{\frac{1}{2}})^2. \qquad \{31\}$$

Comparison of this Hamaker constant with that obtained using eq.{29} (non-additive approach) is simplified if we restrict the following discussion to a single frequency component. The microwave term serves this purpose well since it is separable. Furthermore, eq.{31}will be reformulated in terms of the Lifshitz parameter Δ. Dropping the subscripts, eq.{21} may be crudely approximated by

$$H = \frac{3}{4} kT\Delta^2 \ . \qquad \{32\}$$

Therefore, eq.{31} can be written as:

$$\begin{aligned} \Delta_{Vinc} &= \Delta_p - v\Delta_2 - (1 - v)\Delta_1 \\ &= \Delta_p - \Delta_1 + v(\Delta_1 - \Delta_2) \ . \end{aligned} \qquad \{33\}$$

Note the similarity in form between eq.{33} and the numerator in eq.{29}.

From eq.{33}:

$$\Delta_{Vinc} = \frac{\varepsilon_p - 1}{\varepsilon_p + 1} - \frac{\varepsilon_1 - 1}{\varepsilon_1 + 1} + v\left(\frac{\varepsilon_1 - 1}{\varepsilon_1 + 1} - \frac{\varepsilon_2 - 1}{\varepsilon_2 + 1}\right) \qquad \{34\}$$

where the ε's are the dielectric constants.

From eq.{29}:

$$\Delta_{Lif} = \frac{\varepsilon_p - \varepsilon_1 + v(\varepsilon_1 - \varepsilon_2)}{\varepsilon_p + \varepsilon_1 - v(\varepsilon_1 - \varepsilon_2)} \quad . \qquad \{35\}$$

This is the result according to the continuum approach; the Δ function of the system is not derived from those of its component materials as it is in eq.{34}.

The comparative results for the zero frequency contact Hamaker constants of PS coated with PEO in water are shown in Table 9 (ε_p = 2.544, ε_1 = 78.3, ε_2 = 24.0). The additive approach yields results which are consistently too small by a factor of approximately three for this system. In general, $|\Delta_{Vinc}| < |\Delta_{Lif}|$ when any $\varepsilon > 1$.

For mixtures across a vacuum, we place $\varepsilon_p = 1$ in eqs.{34} and {35}:

$$|\Delta_{Vinc}| = \frac{\varepsilon - 1}{\varepsilon + 1} + v \frac{2\lambda}{(\varepsilon + 1)(\varepsilon + 1 + \lambda)} \qquad \{36\}$$

$$|\Delta_{Lif}| = \frac{\varepsilon - 1}{\varepsilon + 1} + v \frac{2\lambda}{(\varepsilon + 1)(\varepsilon + 1 + \lambda v)} \qquad \{37\}$$

where $\lambda = \varepsilon_1 - \varepsilon_2$ and $\varepsilon = \varepsilon_1$.

The similarity is now obvious. As $\lambda \to 0$, $|\Delta_{Vinc}| \to |\Delta_{Lif}|$ for a given v. In other words, disagreement between the two theories increases as the dielectric properties of the components in the mixture diverge.

TABLE 9

Comparison of Additive (Vincent/Hamaker) and Non-additive (Lifshitz) Approaches for Coated Particles

System: PS coated with PEO in water at 298 K (microwave term only).

v	$H_{Vinc}/10^{-21}$ J.	$H_{Lif}/10^{-21}$ J.	H_{Vinc}/H_{Lif}
0	0.896	2.708	0.33
0.1	0.878	2.682	0.33
0.2	0.860	2.652	0.32
0.3	0.843	2.617	0.32
0.4	0.825	2.576	0.32
0.5	0.808	2.527	0.32
0.6	0.790	2.468	0.32
0.7	0.773	2.395	0.32
0.8	0.757	2.302	0.33
0.9	0.740	2.181	0.34
1.0	0.724	2.015	0.36

v is the volume fraction of PEO between the particles

$\varepsilon_p = 2.544$, $\varepsilon_2 = 24$, $\varepsilon_1 = 78.3$.

TABLE 10

Composite Hamaker Constants for Mixtures Across a Vacuum

(microwave term only)

v	$H_{comp}/10^{-21}$ J.		Additive/Non-additive
	Additive approach	Non-additive approach	
0	0.34	0.34	1.00
0.1	0.49	2.05	0.24
0.2	0.66	2.46	0.27
0.3	0.85	2.63	0.32
0.4	1.07	2.73	0.39
0.5	1.32	2.80	0.47
0.6	1.59	2.84	0.56
0.7	1.89	2.87	0.66
0.8	2.21	2.90	0.76
0.9	2.56	2.92	0.88
1.0	2.93	2.93	1.00

v is the volume fraction of the higher permittivity component

$\varepsilon = \varepsilon_1 = 2$, $\varepsilon_2 = 80$, $\lambda = 78$.

Fig.22. Plots of the zero frequency composite Hamaker constant of a mixture across a vacuum versus the volume fraction v of the high permittivity component.
Lines: (1) Non-additive approach, (2) Additive approach.
$\varepsilon_2 = 2$, $\lambda = 78$, $T = 298$ K.

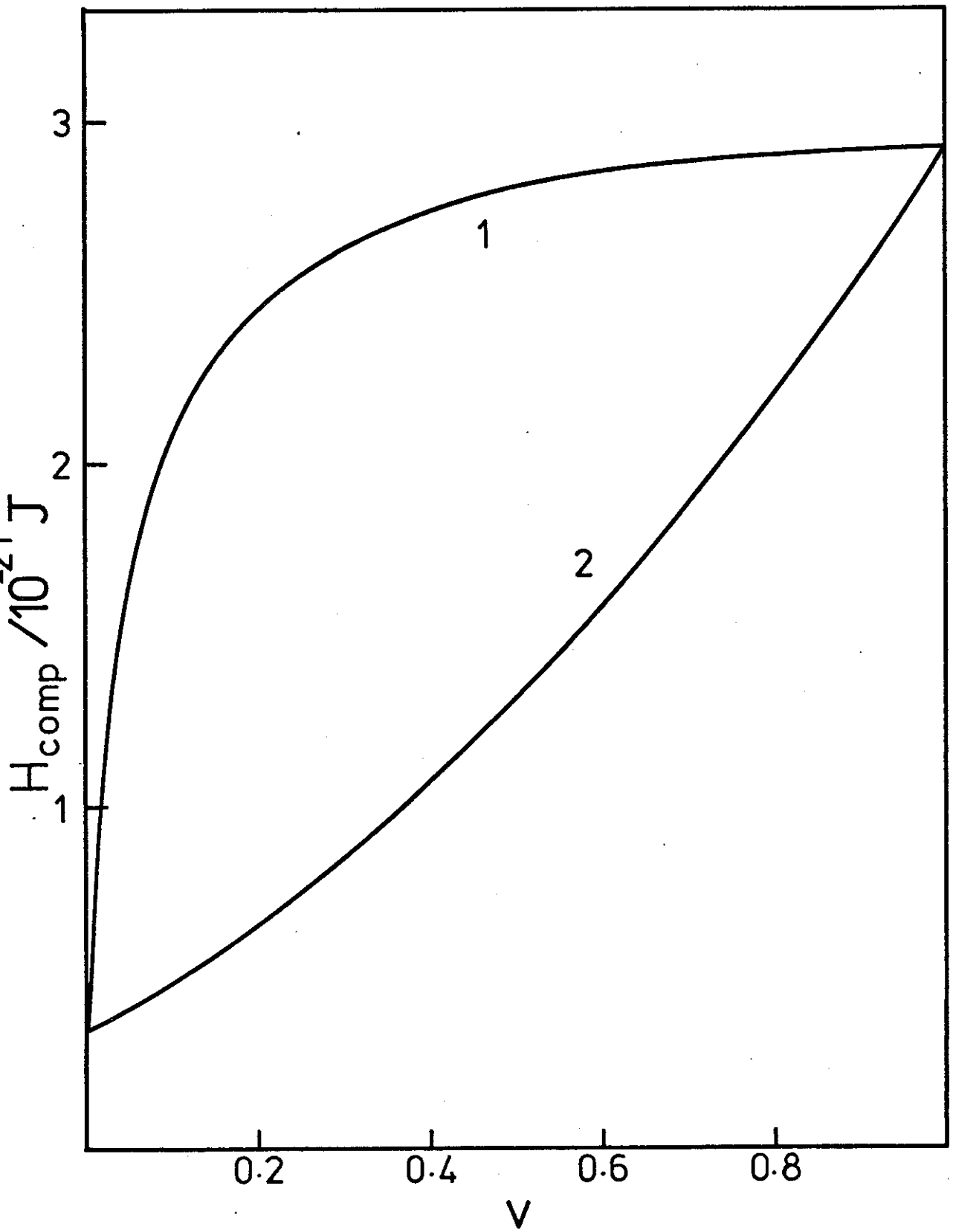
3
2
1
H_{comp} /10^{-21} J
1
2
0·2
0·4
0·6
0·8
V

The approximate composite Hamaker functions at zero frequency can be obtained by substituting eqs.{36} and {37} into

$$H_{comp} \simeq \frac{3}{4} kT\Delta^2 \ .$$

Placing $\varepsilon_2 = 80$ and $\varepsilon_1 = 2$ (large λ) we can illustrate the major qualitative difference between the additive and non-additive approaches (Table 10, Fig.22). In the additive approach, the composite Hamaker constant lies close to the mean of its components. In contrast, the non-additive composite Hamaker constant is heavily biased toward that of the material of higher dielectric constant. The situation is reminiscent of number and weight average quantities.

In conclusion, it must be emphasised that the foregoing crude approximations are intended only to point up the qualitative similarities and differences between the Hamaker and Lifshitz approaches as applied to mixtures. There have been recent advances made in the treatment of inhomogeneous dielectrics (15,45,46) which should prove useful in dealing with non-uniform surface coatings using Lifshitz theory. In this field the basic conceptual simplicity of the continuum approach will be invaluable.

4.8. Free Energy of Attraction

The results of this work are concluded with typical examples of the attraction energy for systems relevant to the studies of steric stabilization presented in chapter I. The system PAN in cyclohexane is shown in Fig.23

with and without PS coating at 307 K. The results in Fig.24 are for PS coated by PEO in 0.39 M magnesium sulphate solution at 318 K. Note that the energies involved are only of the order of kT(~4 × 10^{-21} J.). Curves 1 are of classical Hamaker shape or can be fitted to classical theory because the H functions are almost independent of δ. Curves 2 can only be found using the assumption that the Hamaker function is dependent on the combination of dielectric properties of the mixed medium. It is assumed that the coating polymers do not interact strongly with the medium. This ensures the additivity in eq.{26} for the model systems but not necessarily for real systems such as PEO in water.

Fig.23. Plots of the free energy G versus the distance parameter δ for PAN in cyclohexane at 307 K. Lines: (1) without coating, (2) with PS coating. $L = a/10$, $\tilde{v} = 0.05$.

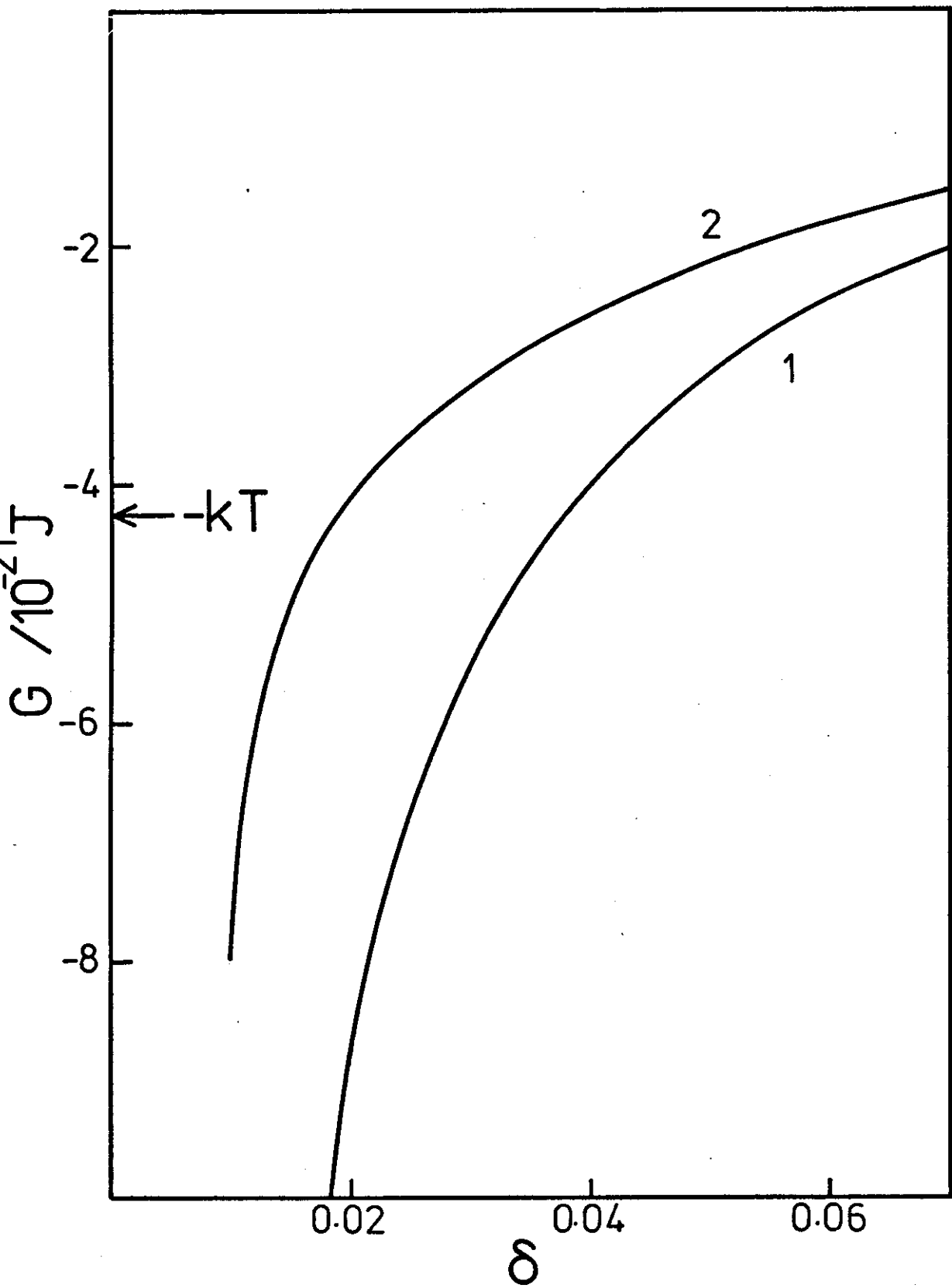
-2
-4
-6
-8
G /10^-21 J
-kT
2
1
0·02
0·04
0·06
δ

Fig.24. Plots of the free energy G versus the distance parameter δ for PS in 0.39 M magnesium sulphate solution at 318 K. Lines: (1) without coating, (2) with PEO coating. $L = a/10$, $v_\infty = 0.05$.

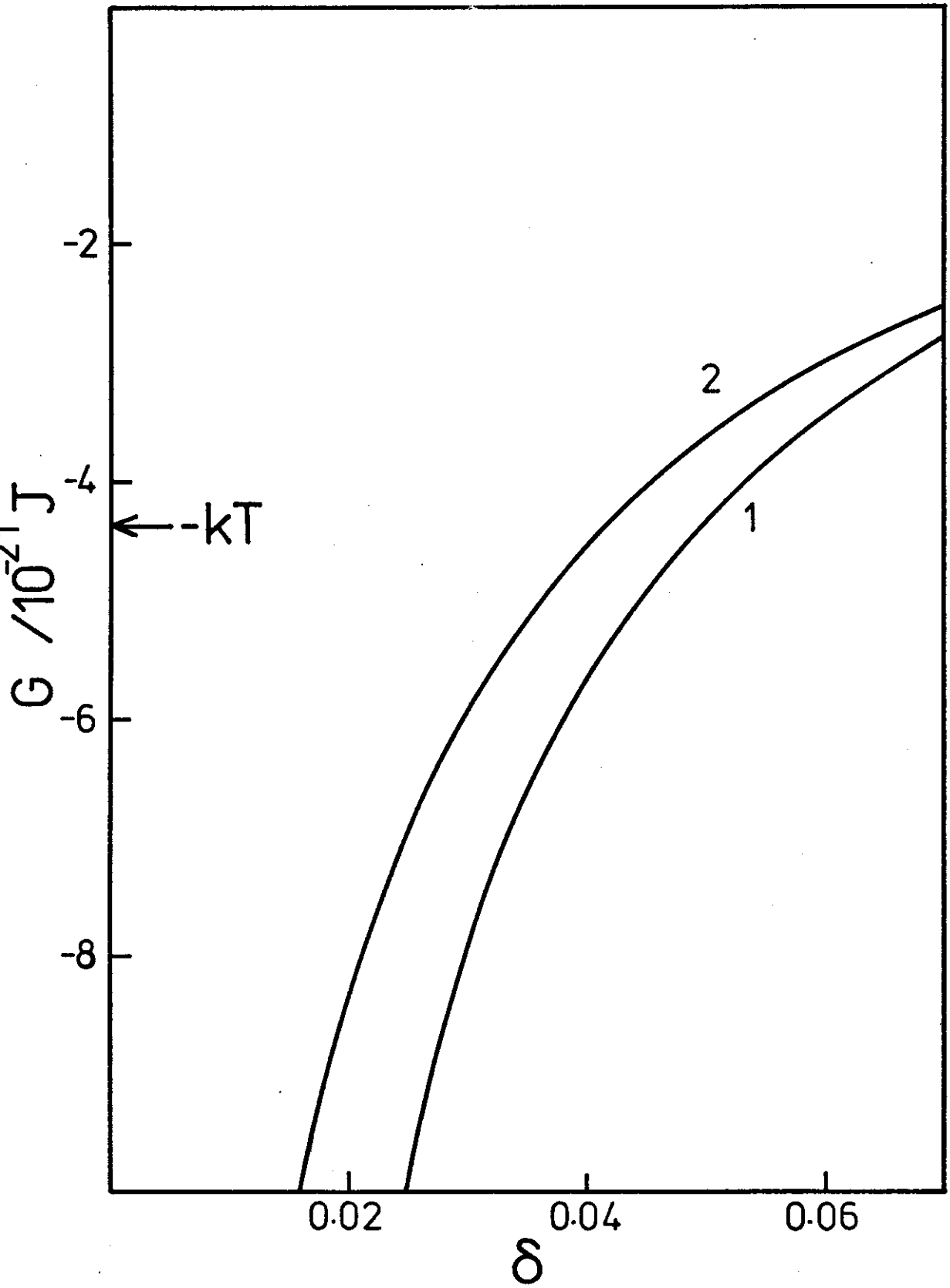
-2
-4
-6
-8
G /10⁻²¹ J
←-kT
2
1
0·02
0·04
0·06
δ

5. CONCLUSIONS

For several years, there has been a great deal of discussion on the dramatic qualitative difference between classical Hamaker theory and the macroscopic Lifshitz theory. Much importance is placed on the long-range microwave contribution and its role in biological systems. Apart from the greater range of the interaction energy afforded by a decrease in retardation of infrared and near ultraviolet correlations, there seems to be very little qualitative difference between the theories. Most practical aqueous systems contain ions which destroy the source of greatest difference: the microwave term.

The greatest merit of the modern approach is its ability to predict the magnitude of the attraction much more accurately than could the classical approach. In particular, it allows correctly for the intervening dielectric.

As an example of the ambiguity possible with the Hamaker theory we note that some workers, when calculating the Hamaker constant, allow for the intervening material by dividing by its dielectric permittivity (3). Others multiply by a factor of 1.5-2.0 (4). Such an approach can lead to a factor of four difference between calculated Hamaker constants for, say, PS in water. Arbitrary decisions of this nature are not possible with Lifshitz theory because all relevant physical effects can be properly included in the formulation.

Lifshitz theory has increased the accuracy of the predictions of van der Waals interaction energies to the extent where even a major breakthrough in the characterization of the permittivity will make a comparatively small improvement.

This work was undertaken to assess the importance of the van der Waals attraction in colloidal systems, with particular reference to sterically stabilized latices. It is concluded that in most cases this attraction is negligible compared with the large interactions between stabilizer layers on sterically stabilized particles unless the particles are very large and the adsorbed chain very short.

6. REFERENCES

1. Hamaker,H.C., Physica, 4, 1058 (1937).
2. London,F., Z. Phys., 63, 245 (1930).
3. Verwey,E.W.J. and Overbeek,J.Th.G., "Theory of Stability of Lyophobic Colloids", Elsevier, Amsterdam (1948).
4. Krupp,H., Schnabel,W. and Walter,G., J. Colloid and Interface Sci., 39, 421 (1972).
5. Krupp,H., Advan. Colloid and Interface Sci., 1, 111 (1967).
6. Visser,J., Advan. Colloid and Interface Sci., 3, 331 (1972).
7. Lifshitz,E.M., Sov. Phys. JETP, 2, 73 (1956).
8. Dzyaloshinskii,I.E., Lifshitz,E.M. and Pitaevskii,I.P., Advan. Phys., 10, 165 (1961).
9. Ninham,B.W. and Parsegian,V.A., Biophys. J., 10, 646 (1970).
10. Parsegian,V.A. and Ninham,B.W., Biophys. J., 10, 664 (1970).
11. Ninham,B.W. and Parsegian,V.A., J. Chem. Phys., 52, 4578 (1970).
12. Ninham,B.W. and Parsegian,V.A., J. Chem. Phys., 53, 3398 (1970).
13. Ninham,B.W., Parsegian,V.A. and Weiss,G.H., J. Stat. Phys., 2, 323, (1970).
14. Parsegian,V.A. and Ninham,B.W., J. Colloid and Interface Sci., 37, 332 (1971).
15. Mitchell,D.J. and Ninham,B.W., J. Chem. Phys., 56, 1117 (1972).
16. Smith,E.R., Mitchell,D.J. and Ninham,B.W., J. Colloid and Interface Sci., 45, 55 (1973).
17. Richmond,P., Ninham,B.W. and Ottewill,R.H., J. Colloid and Interface Sci., 45, 69 (1973).
18. Parsegian,V.A. and Gingell,D., "Recent Advances in Adhesion", Gordon and Breach, London (1973).

19. Ninham,B.W., private communication.

20. Feynman,R.P., "Lectures in Physics", Vol 2.,(Addison-Wesley, London, 1965).

21. Lyons,L.E. and Mackie,J.C., Proc. Chem. Soc., 71, (1962).

22. Lyons,L.E. and Mackie,J.C., Nature (London), 197, 589 (1963).

23. Gutman,F. and Lyons,L.E., "Organic Semiconductors", Chap. 6, John Wiley, New York (1967).

24. Siegbahn,K., J. Electron Spectroscopy and Related Phenomena, 5, 3 (1974).

25. Siegbahn,H. and Siegbahn,K., J. Electron Spectroscopy and Related Phenomena, 2, 319 (1973).

26. Evans,R. and Napper,D.H., J. Colloid and Interface Sci., 45, 138 (1973).

27. Fujihira,M. and Inokuchi,H., Chem Phys. Letters, 17, 544 (1972).

28. "Handbook of Physics and Chemistry" 54th ed. (1973).

29. Pochan,J.M. and Crystal,R.G., "Dielectric Properties of Polymers", Plenum Press, New York (1972).

30. Parsegian,V.A., Annual Rev. Biophys. and Engineering, 2, 221 (1973).

31. Barnes,C., "Dispersion Forces Between Macroscopic Bodies", Ph.D. Thesis, Australian National University (1975).

32. Brandrup,J. and Immergut,E.H., eds., "Polymer Handbook", Interscience, New York (1966).

33. "Tables of Dielectric Materials", Vols I and II, Massachusetts Institute of Technology (1944).

34. Eisenberg,D. and Kauzmann,W., "The Structure and Properties of Water", Chap. 4, Oxford University Press, New York (1969).

35. Napper,D.H. and Hunter,R.J., MTP Int. Rev. Sci., Series I, 7, Chap. 8 (1972).

36. Napper,D.H. and Hunter,R.J., MTP Int. Rev. Sci., Series II, 7, Chap. 3 (1975).

37. Ottewill,R.H. and Walker,T., Kolloid-Z-Z. Polym., 227, 108 (1968).

38. Parsegian,V.A., Annual Review of Biophysics and Engineering, 2, 221 (1973).

39. Cantarow,A. and Schepartz,B., "Biochemistry", W.B. Saunders Co., Philadelphia (1954).

40. Lips,A. and Willis,E., J. Chem. Soc. Faraday I, 69, 1226 (1973).

41. Vold,M.J., J. Colloid and Interface Sci., 16, 1 (1961).

42. Osmond,D.J.W., Vincent,B. and Waite,F.A., J. Colloid and Interface Sci., 42, 262 (1973).

43. Vincent,B., J. Colloid and Interface Sci., 42, 270 (1973).

44. Langbein,D., J. Adhesion, 1, 237 (1969).

45. Parsegian,V.A. and Weiss,G.H., J. Colloid and Interface Sci., 40, 35 (1972).

46. Weiss,G.H., Kiefer,J.E. and Parsegian,V.A., J. Colloid and Interface Sci., 45, 615 (1973).

47. Tabor,D. and Winterton,R.H.S., Proc. Roy. Soc., Series A, 312, 435 (1969).

UNIVERSITY OF SYDNEY LIBRARY
0000000601951014

Offprinted from the *Journal of The Chemical Society, Faraday Transactions I*, 1975, vol. 71.

Analytical Theories of the Steric Stabilization of Colloidal Dispersions

BY JAMES B. SMITHAM, ROBERT EVANS AND DONALD H. NAPPER*

Department of Physical Chemistry, University of Sydney, N.S.W. 2006, Australia

Received 21*st January*, 1974

Analytical theories are developed for the steric stabilization of colloidal spheres and flat plates by monodisperse tails. It is proposed that the reason for the failure of previous theories to predict the correct distance dependence of the repulsion resides in their neglect of lateral interactions between adjacent stabilizing chains. Theories are therefore formulated that implicitly allow for these lateral interactions. All that need be specified is the mathematical form of the relevant segment density distribution functions. Two models are examined in detail: a constant segment density model and a combined constant segment density and near symmetrical gaussian model. The latter gives the better agreement with experimental results. Both models, however, describe the distance dependence of the repulsion reasonably well over quite a wide range of separations.

There are currently two general methods for stabilizing colloidal dispersions.[1] For electrostatic stabilization, the most studied of these two methods, Deryagin, Landau, Verwey and Overbeek[2] (DLVO) have proposed a quantitative theory that is widely held to be definitive. No comparable definitive theory exists as yet for the alternative method of imparting colloid stability, so-called steric stabilization. Steric stabilization is the generic term that encompasses all mechanisms by which nonionic macromolecules can impart colloid stability.

To-date there have been several [3-5] attempts to develop a quantitative theory for steric stabilization. However, with the notable exception of Fischer's solvency theory [3] and its extension,[6] most of these theories can be criticized because they fail to describe properly even the qualitative features observed for the flocculation of sterically stabilized dispersions.[7] Moreover Doroszkowski and Lambourne [8] have shown that such theories are unable to predict with any accuracy the distance dependence of steric repulsion. We also note that these theories are somewhat inconvenient to use because they require considerable digital computation to generate numerical results.

In what follows we develop several possible theories to describe the steric stabilization of flat plates and spheres by monodisperse tails (i.e., polymer chains attached to an interface at only one end). These theories can be expressed analytically which circumvents the need for extensive digital computation. Comparison of the predictions of these theories with experiment suggests that they describe, both qualitatively and quantitatively, most of the features of steric stabilization by tails observed to-date.

SHORTCOMINGS OF PREVIOUS THEORIES

We have shown previously [6] that a simple extension of Fischer's solvency theory provides an excellent description of all of the observed, qualitative features of steric stabilization. This approach, which exploits the Flory–Huggins theory, predicts

that the repulsive potential energy (V_R) per unit area for two large flat parallel plates is given by [4-6]

$$V_R = 2(V_s^2/V_1)(\tfrac{1}{2} - \chi_1)v^2i^2RkT/\langle r^2\rangle^{\frac{1}{2}}, \quad (1)$$

where the meaning of the symbols is listed in the Glossary and

$$R = \langle r^2\rangle^{\frac{1}{2}}\left(\int_0^d \hat{\rho}_d^2 dx - \int_0^\infty \hat{\rho}_\infty^2\, dx + \int_0^d \hat{\rho}_d\hat{\rho}'_d\, dx\right). \quad (2)$$

Eqn (1) differs from those of previous theories [4, 5] in that the volume exclusion term is omitted. Using the Deryagin approximation [9] it is possible to utilize the theory for flat plates in calculating the repulsion between two identical spheres.[6] Provided that the thickness of the stabilizing layer is much less than the particle radius, the repulsive free energy becomes [5, 6]

$$V_R = \frac{(2\pi)^{\frac{1}{2}}}{27}\langle r^2\rangle_0^{\frac{3}{2}}v^2(\alpha^5 - \alpha^3)aSkT, \quad (3)$$

where $S = \int_{\delta_0}^\infty R\, d\delta$.

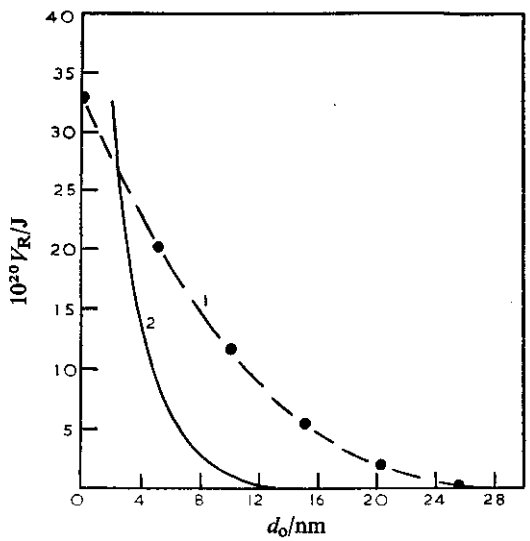

FIG. 1.—The distance dependence of the repulsive potential energy for two polyacrylonitrile sphere stabilized by polystyrene in toluene at 297 K. Curves: 1, experimental results; 2, theoretica prediction using isolated polymer chain distribution functions.

To evaluate the repulsion in any instance it is necessary to specify the respective segment density distribution functions. It has in the past proved convenient to use the segment density distribution derived by Hesselink [5, 10, 11] for isolated polymer chains at a planar interface. A comparison between theory and experiment for the repulsion between sterically stabilized particles is presented in fig. 1. The experimental data are those of Doroszkowski and Lambourne [8] for polyacrylonitrile particles stabilized by polystyrene ($\langle M_n\rangle$ = 6000) in toluene at 297 K (these appear to be the only distance dependent V_R data in the literature); the theoretical curve was calculated using the extended Fischer theory [6] and the Hesselink segment density functions.[5] The distance dependence of the repulsion calculated theoretically is clearly unsatisfactory: the theoretical repulsions are too small at large distances and too large at small distances.

In attempting to locate the source of the discrepancy between theory and experiment, we are drawn inevitably to the parameters R (for flat plates) and S (for spheres) which determine the distance dependence of V_R. The reason for this failure appears to reside in the use of segment density distribution functions relevant to isolated macromolecules. The particles used as model dispersions for steric stabilization are always fully coated so that each stabilizing chain is surrounded by, and interacts with, a number of contiguous chains. The segment density distribution functions for isolated polymer chains are thus unlikely to be applicable. This inference is borne out by the measured conformations of tails at interfaces. There is strong evidence to show that the extension of chains normal to the interface is greater than that predicted theoretically for an isolated chain; whereas theory predicts a value *ca.* 1.5 times [10-12] the free solution value for isolated tails, the experimental factor for close packed tails is usually closer to say, 2.[8, 13-16] This greater expansion is a consequence of the lateral repulsion that occurs between neighbouring chains. The theories developed below are formulated to allow for these lateral interactions.

DEVELOPMENT OF NEW THEORIES

The critical feature in the evaluation of V_R is the choice of the segment density distribution function. In fact all that need be specified is the general mathematical form of the distribution; normalization then ensures that the function is completely specified. It is also possible in the general specification of the form of the distribution to allow implicitly for lateral interactions by using the experimentally determined extension of the stabilizing chains. This avoids the difficult problem of actually calculating the magnitude of these lateral interactions and their effects on conformation. Several possible models of polymer chains at interfaces suggest themselves according to whether the tails are of low or high molecular weight. The tails are, however, assumed to be monodisperse.

MODEL I: INTERPENETRATION AND COMPRESSION AT CONSTANT SEGMENT DENSITY

The simplest model to adopt for the segment density distribution function of a tail is a constant segment density step function. At first sight this would appear to be an artificial simplification but Ottewill and Walker [17] have shown that poly(ethylene oxide) tails of low molecular weight are apparently fully extended when functioning as steric stabilizers in water. This conclusion has been fully confirmed by several later studies on other low molecular weight polymers in other dispersion media.[8, 13-16] We conclude that the constant segment density model is likely to be applicable to the stabilization by low molecular weight tails provided that they are not significantly compressed.

The evaluation of R and S for a constant segment density model must be performed in two stages because of the change in the form of $\hat{\rho}_d$ if $d < L$.

(*a*) If $L \leqslant d < 2L$, interpenetration alone can occur. Here $\hat{\rho}_d = \hat{\rho}_\infty = \hat{\rho}'_d = 1/L$ since $\int_0^L \hat{\rho}_d \, dx = 1$. Thus

$$R_i^{Ia} = \langle r^2 \rangle^{\frac{1}{2}} \int_{d-L}^{L} \hat{\rho}_d \hat{\rho}'_d \, dx = \frac{\langle r^2 \rangle^{\frac{1}{2}}}{L^2} \int_{d-L}^{L} dx$$

$$= \frac{2\langle r^2 \rangle^{\frac{1}{2}}}{L}(1 - d/2L), \qquad (4)$$

where the subscript i denotes interpenetration. Note that at $d = L$, $R_i^{Ia} = \langle r^2\rangle^{1/2}/L$. Hence for spheres

$$S_i^{Ia} = \int_{\delta_0}^{\delta_\infty} R_i^{Ia}\, d\delta,$$

where $\delta_\infty = 2L/\langle r^2\rangle^{1/2}$. Accordingly

$$S_i^{Ia} = \int_{\delta_0}^{\delta^\infty} (4/\delta_\infty)(1-\delta/\delta_\infty)\, d\delta$$
$$= 2(\delta_0/\delta_\infty - 1)^2 = 2(1-d_0/2L)^2. \quad (5)$$

This relationship holds provided $L \leqslant d_0 < 2L$. Note that when $d_0 = L$, $S_i^{Ia} = 0.5$.

(*b*) If $0 < d < L$, $\hat{\rho}_d = \hat{\rho}_d' = 1/d$ and $\hat{\rho}_\infty = 1/L$.

Now both interpenetration and compression can occur. For interpenetration

$$R_i^{Ib} = \langle r^2\rangle^{\frac{1}{2}} \int_0^d \hat{\rho}_d \hat{\rho}'_d\, dx = \frac{\langle r^2\rangle^{\frac{1}{2}}}{d^2} \int_0^d dx$$
$$= \langle r^2\rangle^{\frac{1}{2}}/d = 1/\delta. \quad (6)$$

For compression (denoted by the subscript c)

$$R_c^{Ib} = 2\langle r^2\rangle^{\frac{1}{2}} \left[\int_0^d \hat{\rho}_d^2\, dx - \int_0^L \hat{\rho}_\infty^2\, dx\right]$$
$$= 2\langle r^2\rangle^{1/2}(1/d - 1/L)$$
$$= 2/\delta - 2/\delta_\infty, \quad (7)$$

since $\delta_\infty = L/\langle r^2\rangle^{1/2}$ between these limits. Thus for both interpenetration and compression,

$$R_i^{Ib} + R_c^{Ib} = 3\langle r^2\rangle^{\frac{1}{2}}/d - 2\langle r^2\rangle^{\frac{1}{2}}/L. \quad (8)$$

Note that at $d = L$, $R_i^{Ib} + R_c^{Ib} = \langle r^2\rangle^{1/2}/L$. This is identical with the value of R_i^{Ia} at that point. Thus eqn (8) gives the total value of R in this domain and eqn (4) and (8) are properly continuous at $d = L$.

The value of S in this domain is obtained by integration of eqn (8):

$$S_i^{Ib} + S_c^{Ib} = \int_{\delta_0}^{\delta\infty} (3/\delta - 2/\delta_\infty)\, d\delta$$
$$= 3 \ln(\delta_\infty/\delta_0) + 2(\delta_0/\delta_\infty) - 2 \quad (9)$$
$$= 3 \ln(L/d_0) + 2(d_0/L) - 2. \quad (10)$$

Note that if $d_0 = L$, $S_i^{Ib} + S_c^{Ib} = 0$ and the steric repulsion would be zero. This is obviously incorrect; it arises because the upper limit of the Deryagin integration prevents any allowance being made for the interpenetration that occurs when $d_0 > L$. We must therefore add in the value of S_i^{Ia} at $d_0 = L$. Thus the total value of $S(S_{i+c}^{Ib})$ becomes

$$S_{i+c}^{Ib} = 3 \ln(\delta_\infty/\delta_0) + 2(\delta_0/\delta_\infty) - 1.5$$
$$= 3 \ln(L/d_0) + 2(d_0/L) - 1.5 \quad (11)$$

provided $0 < d_0 < L$. The coupling of eqn (5) and (11) means that S is continuous for all non-zero d_0 as is shown in fig. 2.

To calculate the repulsion between two flat plates or two spheres we merely substitute the relevant values of R or S into eqn (1) or eqn (3) for each of the domains

(*a*) and (*b*). We compare in fig. 2 the curve predicted by model I for the repulsive potential energy between pairs of spherical polyacrylonitrile particles stabilized by polystyrene tails in toluene at 297 K with the experimentally determined repulsions.[8] For convenience we have used the most basic form of eqn (3) for calculating the repulsion:

$$V_R = 2\pi a\omega^2 N_A(\bar{v}_2^2/\bar{V}_1)\psi_1(1 - \theta/T)SkT. \quad (12)$$

The values of the relevant parameters are $a = 100$ nm,[8] $\omega = 5.2 \times 10^{-8}$ g cm^{-2},[8] $\bar{v}_2 = 0.91$ cm^3 g^{-1},[18] $\bar{V}_1 = 107$ cm^3 mol^{-1},[19] and $\theta = 160$ K.[20] The value of ψ_1 for polystyrene of $\langle M_n \rangle = 6000$ was determined experimentally by preparing a sample of unfractionated polymer of comparable molecular weight and measuring α_η viscometrically [21] at 297 K. The experimental value of $\alpha_\eta = 1.057$ is somewhat less than that calculated ($\alpha = 1.08$) from data [22] relevant to high molecular weight polystyrene, as would be expected for such a low molecular weight sample. We have thus calculated $\psi_1 = 0.07$ using the Flory–Fox relationship.[22] These values give $V_R = 10.6 \times 10^{-20} S$ J per pair of interacting particles. Setting $L = 14.7$ nm, we can calculate S for any specific value of d_0.

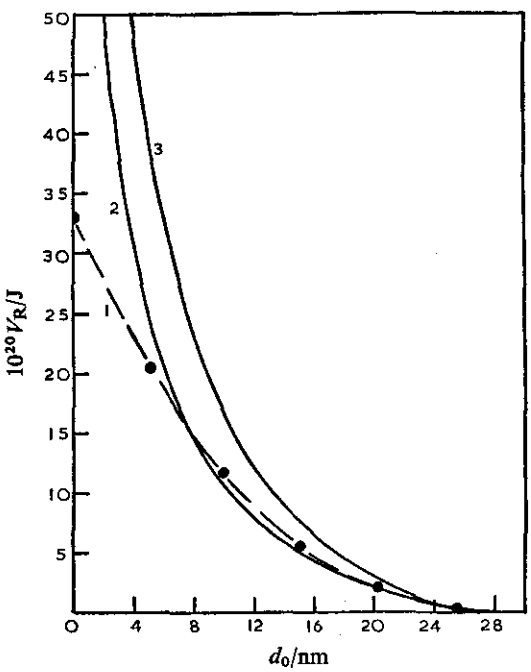

FIG. 2.—The distance dependence of the repulsive potential energy for two polyacrylonitrile spheres stabilized by polystyrene in toluene at 297 K. Curves: 1, experimental results; 2, theoretical curve assuming constant segment density with interpenetration and compression; 3, theoretical curve for constant segment density with denting.

It is obvious from fig. 2 that over quite a wide range of d_0 values (5-30 nm), the simple analytical theory developed above provides an accurate quantitative description of the repulsive potential energy. Steric repulsions of order 100 kT are predicted theoretically. Unfortunately for values of $d_0 < 5$ nm, the theoretical repulsions exceed the measured values significantly. However, it is scarcely surprising that the theory may give erroneous predictions under these conditions: first, perhaps the

tails adsorb onto the surfaces of the opposing particles; second, the constant segment density assumption may possibly break down when d_0 is significantly less than L as the chains are not fully extended; third, the tails are so compressed that the theoretical segment density on very close approach exceeds that in the solid polymer, which appears most unlikely in practice. We are unable to suggest at present how such highly compressed systems may be rendered more tractable to theory. Note that the good agreement between theory and experiment in fig. 2 may be somewhat misleading in that we have not so far been able to develop an analytical theory that properly allows for polydispersity. Accordingly we have been forced to use the theory for monodisperse tails coupled with the number average molecular weight of the sample. Nevertheless the agreement between theory and experiment is noticeably better than has been achieved before. Note that we have here ignored the van der Waals attraction between the core polyacrylonitrile particles as discussed previously [6]; inclusion of the attraction would alter the potential energy of interaction imperceptibly over the range depicted.

MODEL II: DENTING AT CONSTANT SEGMENT DENSITY.

Bagchi [23] has proposed that when sterically stabilized particles interact, the polymer chains crumple rather than undergo interpenetration and compression. This he has termed the denting mechanism. It corresponds to compression of the chains attached to one particle on contact with the chains attached to the other. We can calculate the repulsion for this denting model, given the assumption of a constant segment density. Under these conditions, $\hat{\rho}_d = (2/d)$ and $\hat{\rho}_\infty = (1/L)$. For the mutual denting of two surfaces there is no interpenetration term. Therefore,

$$\begin{aligned} R_c^{II} &= 2\langle r^2\rangle^{\frac{1}{2}}\left[\int_0^{d/2} \hat{\rho}_d^2 \, dx - \int_0^{L} \hat{\rho}_\infty^2 \, dx\right] \\ &= 2\langle r^2\rangle^{1/2}(2/d - 1/L) \\ &= 4(1/\delta - 1/\delta_\infty), \end{aligned} \tag{13}$$

since $\delta_\infty = 2L/\langle r^2\rangle^{1/2}$ for this model. Hence for spheres

$$\begin{aligned} S_c^{II} &= 4\int_{\delta_0}^{\delta_\infty} (1/\delta - 1/\delta_\infty)\, d\delta \\ &= 4\{\ln(2L/d_0) + (d_0/2L) - 1\}. \end{aligned} \tag{14}$$

The predicted repulsion for the denting model is compared as before with experiment in fig. 2 for polystyrene stabilized particles. The repulsive potential energy calculated for this model appears to be too large. The results suggest that interpenetration and compression are more likely to occur than denting.

MODEL III: INTERPENETRATION AND COMPRESSION FOR A GAUSSIAN SEGMENT DENSITY DISTRIBUTION

Whereas low molecular weight tails are likely to be fully extended normal to the surface if $d > L$, high molecular weight tails are unlikely to be fully extended. The reason for this is that $\langle r^2\rangle^{1/2}$ for low molecular weight chains is an appreciable fraction (e.g., 50%) of the contour length of the chains. Hence extension of the chain on attachment to a surface by a factor of say, 2 means that the contour length is approached (or even exceeded, which is physically impossible). But $\langle r^2\rangle^{1/2}$ for high molecular weight chains may only be say, 5% of the contour length; attachment to the interface does not produce an extension that approaches the contour length.

There is some experimental evidence to support this reasoning.[13] In addition, low molecular weight tails cannot be fully extended if $d < L$ and the assumption of constant segment density may well be invalid.

The distribution of end-to-end lengths of monodisperse polymer chains in free solution is given by the gaussian distribution [20]

$$W(r) = 4\pi(3/2\pi\langle r^2\rangle)^{\frac{3}{2}}r^2 \exp(-3r^2/2\langle r^2\rangle).$$

We will assume that the same form of the gaussian distribution function holds for tails constrained between two parallel flat plates. Only the appropriate value of $\langle r^2\rangle^{1/2}$ in terms of d need be specified. Thus we write in one-dimension for $0 < d < L$,

$$\hat{\rho}_d = 4\pi(3/2\pi F^2d^2)^{\frac{3}{2}}x^2 \exp(-3x^2/2F^2d^2) \tag{15}$$

where $\langle r^2\rangle^{1/2} = Fd$. It is readily shown that $\hat{\rho}_d$ is normalized. By varying F it is possible to explore several different assumptions: thus if $F = \frac{1}{2}$ we have $\langle r^2\rangle^{1/2} = d/2$ and this corresponds to assuming that the one-dimensional root mean square end-to-end length of the tails is the size parameter that determines the occupation of the available half-space; alternatively if $F = (3/2)^{1/2}/2$, the maximum in the gaussian distribution occurs at $d/2$ and the distribution of segments is essentially symmetrical between the plates. The latter assumption is reminiscent of the symmetrical distribution of ions that is assumed to occur between flat plates in the development of the DLVO theory.[2] The implication of this is that the segments attached to one flat plate freely interpenetrate right up to the approaching plate and are not preferentially associated with either plate apart from the point of attachment.

We point out that as $d \to L$, $\langle r^2\rangle^{1/2} \to FL$ where typically we set $F \approx 0.5$-0.6. This limiting value of $\langle r^2\rangle^{1/2}$ appears reasonable in light of the data of Doroszkowski and Lambourne [8] who found experimentally that the barrier layer thickness for polystyrene tails was $\sim 0.8L$. The direct proportionality between $\langle r^2\rangle^{1/2}$ and d may seem to be an oversimplification but the correct variation for close packed chains is unknown; the simplest, and to us the most physically reasonable, dependence was therefore adopted. Note that the gaussian function does not tend to zero at $d = L$ but it can be truncated at that point. However $\hat{\rho}_d$ is not then exactly normalized. In the theory developed below we have checked numerically that this does not produce serious errors. Note too that for $0 < d < L$

$$\hat{\rho}'_d = 4\pi(3/2\pi F^2d^2)^{\frac{3}{2}}(d - x)^2 \exp\{-3(d - x)^2/2F^2d^2\}. \tag{16}$$

The precise form chosen for $\hat{\rho}_\infty$ is not critical and we have examined two likely functions. First a gaussian distribution function corrected by an extension factor f to allow for the presence of the interface and the lateral interactions between contiguous chains:

$$\hat{\rho}_\infty = 4\pi(3/2\pi f^2\langle r^2\rangle)^{\frac{3}{2}}x^2 \exp\{-3x^2/2f^2\langle r^2\rangle\}. \tag{17}$$

The extension factor f, which is the ratio of the effective stabilizer thickness to the free solution value of $\langle r^2\rangle^{1/2}$, is best determined experimentally.

The second, and more likely, mathematical form for $\hat{\rho}_\infty$ is that derived by Hesselink [5, 10, 11] for isolated polymer chains at an interface but with f included to allow for lateral interactions:

$$\hat{\rho}_\infty = (6/f^2\langle r^2\rangle)\int_x^{2x} \exp\{-3t^2/2f^2\langle r^2\rangle\}\,dt$$
$$= (3\pi^{1/2}/f^2\langle r^2\rangle A)[\mathrm{erf}(2Ax) - \mathrm{erf}(Ax)] \tag{18}$$

where $\mathrm{erf}(x)$ is the error function of x and $A = (3/2f^2\langle r^2\rangle)^{1/2}$. Again it is readily

shown that $\hat{\rho}_\infty$ is normalized (i.e., $\int_0^\infty \hat{\rho}_\infty \, dx = 1$). Note that because we have explored several possibilities for $\hat{\rho}_\infty$, $\hat{\rho}_d$ does not in general approach $\hat{\rho}_\infty$ as $d \to \infty$. We point out, however, that $\hat{\rho}_d$ is not used in that limit but only for $d < L$; moreover, the magnitude and the distance dependence of the steric repulsion is insensitive to the precise form chosen for $\hat{\rho}_\infty$.

The integrals constituting R can all be evaluated analytically for $0 < d < L$, given the foregoing specification of $\hat{\rho}_d$ and $\hat{\rho}_\infty$. This requires a considerable number of tedious integrations by parts, the complete details of which are omitted here.* However, a typical example is set out in Appendix 1.

We find the following results for $0 < d < L$:

$$\int_0^d \hat{\rho}_d^2 \, dx = (9/\pi F^4 d)\{-(1+F^2/2)\exp(-3/F^2)+(F^3/4)(\pi/3)^{\frac{1}{2}}\operatorname{erf}(3^{\frac{1}{2}}/F)\}, \tag{19}$$

$$\int_0^d \hat{\rho}_d \hat{\rho}_d' \, dx = (54/\pi F^6 d)\exp(-3/2F^2)\{F^2/24 - F^4/12 + (1/16 - F^2/12 + F^4/12)(\pi/3)^{\frac{1}{2}}F\exp(3/4F^2)\operatorname{erf}(3^{\frac{1}{2}}/2F)\}, \tag{20}$$

$$\int_0^\infty \hat{\rho}_\infty^2 \, dx = B/f\langle r^2\rangle^{\frac{1}{2}}, \tag{21}$$

where $B = 0.9964$ for the Hesselink function and $B = 0.7329$ for the gaussian form. Physically the last integral must be independent of d. The first two integrals show that the steric repulsion for flat plates varies simply as $(1/d)$. We may therefore write for $0 < d < L$

$$R^{\mathrm{III}}_{\mathrm{i+c}} = (9\langle r^2\rangle^{1/2}/\pi F^4 d)\{-(1 + F^2/2)\exp(-3/F^2) + (F^3/4)(\pi/3)^{1/2}\operatorname{erf}(3^{1/2}/F) + (6/F^2)\operatorname{erf}(-3/2F^2)[F^2/24 - F^4/12 + (1/16 - F^2/12 + F^4/12)(\pi/3)^{1/2}F \times \exp(3/4F^2)\operatorname{erf}(3^{1/2}/2F)]\} - B/f. \tag{22}$$

For the particular values of $F = (3/2)^{1/2}/2$ and $F = 1/2$, R assumes the very simple forms:

$$R^{\mathrm{III}} = 2.3484/d - B/f; \quad F = (3/2)^{1/2}/2, \tag{23}$$

and

$$R^{\mathrm{III}} = 2.7759/d - B/f; \quad F = (1/2). \tag{24}$$

For spheres the factor S thus becomes on integration

$$S^{\mathrm{III}}_{\mathrm{i+c}} = (9/\pi F^4)\ln(L/d_0)\{-(1 + F^2/2)\exp(-3/F^2) + (F^3/4)(\pi/3)^{1/2}\operatorname{erf}(3^{1/2}/F) + (6/F^2)\exp(-3/2F^2)[F^2/24 - F^4/12 + (1/16 - F^2/12 + F^4/12)(\pi/3)^{1/2}F \times \exp(3/4F^2)\operatorname{erf}(3^{1/2}/2F)]\} - B(L - d_0)/f\langle r^2\rangle^{1/2}. \tag{25}$$

The special cases mentioned previously yield simple forms for S:

$$S^{\mathrm{III}} = 2.3484\ln(L/d_0) - B(L - d_0)/f\langle r^2\rangle^{1/2}; \quad F = (3/2)^{1/2}/2, \tag{26}$$

and

$$S^{\mathrm{III}} = 2.7759\ln(L/d_0) - B(L - d_0)/f\langle r^2\rangle^{1/2}; \quad F = 1/2. \tag{27}$$

The accuracy of eqn (26) and (27) is easily checked by performing a Deryagin integration on eqn (23) and (24). Note that for both cases $S^{\mathrm{III}} = 0$ if $d_0 = L$ because

* The authors will supply details of these integrations on request.

the upper limit of the Deryagin integration prevents any allowance being made for the interpenetration that occurs if $d_0 > L$. Therefore the value of S^{III} at $d_0 = L$ must be added into eqn (25), (26) and (27) if S^{III} is to be properly continuous.

The foregoing theory does not apply when $L \leqslant d$ (or d_0) $< 2L$. Unfortunately the interpenetration terms that result when the foregoing functions for $\hat{\rho}_\infty$ are employed in this domain are so complex that simple analytical functions for S in this domain have not yet been obtained, although formulae for R have been derived. We will therefore content outselves for low molecular weight polymers with using the constant segment density function for $d \geqslant L$ because this is probably the correct function to employ anyway. Thus for $L \leqslant d_0 < 2L$, V_R may be calculated from eqn (5) whereas for $0 < d_0 < L$ the repulsion is obtained by using eqn (25) to which must be added the value of S_1^{Ia} at $d_0 = L$ to allow for the interpenetration up to that point. So, for example, we use eqn (5) to calculate S for $L \leqslant d_0 < 2L$; for $0 < d_0 < L$ we employ

$$S = 0.5 + 2.3484 \ln (L/d_0) - 0.9964(L - d_0)/f\langle r^2\rangle^{1/2} \qquad (28)$$

if we assume a Hesselink distribution function for $\hat{\rho}_\infty$ and a near symmetrical gaussian function for $\hat{\rho}_d$.

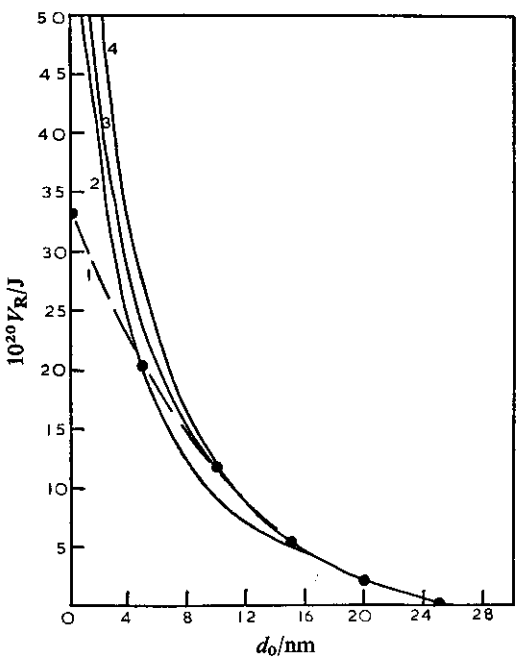

FIG. 3.—The distance dependence of the repulsion between two polyacrylonitrile spheres stabilized by polystyrene in toluene at 297 K. Curves: 1, experimental results; 2, 3, 4, theoretical curves using a gaussian function for $\hat{\rho}_d$ and a Hesselink function for $\hat{\rho}_\infty$. 2, $F = (3/2)^{1/2}/2, f = 2^{1/2}$; 3, $F = (3/2)^{1/2}/2, f = 2$; 4, $F = 1/2, f = 2$.

We compare in fig. 3 the predictions of this model with the experimental results of Doroszkowski and Lambourne.[8] For $d_0 < L$ the gaussian model gives closer agreement with experiment than does the constant segment density model. Apparently even low molecular weight tails may deviate from a constant segment density if significantly compressed. In these calculations we prefer to set $F = (3/2)^{1/2}/2$

because it gives closer agreement with experiment than $F = 1/2$, and we have used the experimental value for α in eqn (3). The extension factor f is best set equal to 2 because not only does this give good agreement with the experimental extension of the tails but it also ensures that only a small fraction of the segments in the Hesselink distribution exceeds the contour length (Appendix II). The latter distribution function for $\hat{\rho}_\infty$ is used exclusively in fig. 3 because it yields better agreement with experiment than does the gaussian function for $\hat{\rho}_\infty$. However, again it must be admitted that on very close approach the theoretical repulsions are greater than the measured values.

One interesting point that arises from this new theory is the possibility of the total potential energy curves exhibiting a maximum when due allowance is made for the van der Waals attraction. This is illustrated in fig. 4 (curve 1) for polyacrylonitrile particles assumed to have an effective Hamaker constant equal to 3×10^{-21} J. Note, however, that the maximum will only occur when T is close to θ and at very close distances of approach. The other curves in fig. 4 show that even if the van der Waals attraction is neglected, flocculation will occur close to $T = \theta$, as observed experimentally.

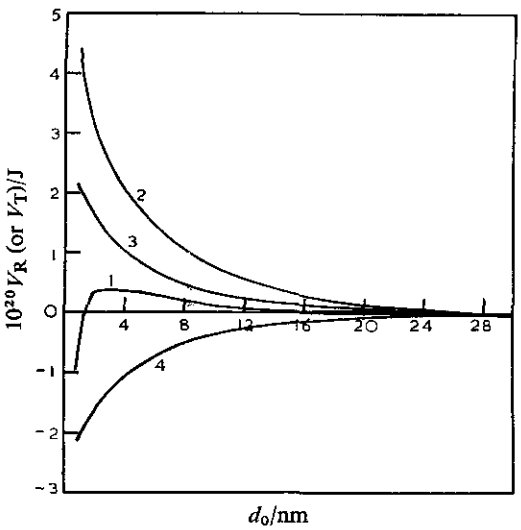

FIG. 4.—The distance dependence of the repulsive potential energy for two polyacrylonitrile spheres, stabilized by polystyrene in toluene, at different temperatures near $\theta = 160$ K. Curve 1, V_T for $T = 165$ K; curves, 2, 3 and 4 V_R for 170, 165 and 155 K respectively. For all curves $F = (3/2)^{1/2}/2$, and $f = 2$.

Finally we note that the foregoing theories fail to predict the small repulsions (comparable to thermal energies) that were measured by Doroszkowski and Lambourne [8] for $T < \theta$. All the above theories predict a nett attraction that should give rise to flocculation. Flocculation was in fact observed by Doroszkowski and Lambourne as the theories predict.[1, 7] We suggest that the small repulsions observed in flocculated systems were an experimental artifact: if successive compressions of the particles took place in a period of time less than that required for equilibrium interpenetration and compression of the tails, an apparent repulsion would be observed even in flocculated systems. The converse of this relaxational effect, an apparent attraction of the order of kT between stable sterically stabilized particles near to the θ-temperature, has been observed rheologically.[24]

CONCLUSIONS

We have shown previously [7] that eqn (1) and (3) on which the foregoing theories are based describe qualitatively all the observed features of steric stabilization. This study has illustrated how it is possible to develop analytical theories that describe many of the quantitative features of steric stabilization reported thus far for low molecular weight tails. The theory presented herein is therefore able to account for many of the qualitative and quantitative features of steric stabilization observed to-date. The comparisons presented above suggest that interpenetration and compression occur rather than denting in the types of experiments described by Doroszkowski and Lambourne.[8] The best model for low molecular weight tails appears to be near symmetrical gaussian distributions of segment densities when the distance of separation between the plates is less than the contour length of the tails. For larger distances of separation the constant segment density model appears to be applicable. The latter model, however, seems unlikely to hold for higher molecular weight polymers. The major weakness of the theory at present is its failure to allow for polydispersity. Very close approach of the particles also presents major difficulties. A further weakness of the theory is that it requires experimental knowledge of the barrier layer thickness before the distance dependence of the repulsion can be specified.

We thank the Australian Research Grants Committee for support of this work. Two of us (J. B. S. and R. E.) gratefully acknowledge the award of Commonwealth Post-graduate Scholarships.

GLOSSARY

a	= particle radius	$\bar{v}_2$	= partial specific volume of polymer
d	= plate separation	V_1	= volume of solvent molecule
d_0	= minimum distance of surface separation to two spheres	V_s	= volume of segment
		V_R	= steric repulsive free energy
f	= extension factor	α	= intramolecular expansion factor
F	$= \langle r^2\rangle^{1/2}/d$	δ	$= d/\langle r^2\rangle^{1/2}$
i	= number of segments per chain	δ_0	$= d_0/\langle r^2\rangle^{1/2}$
k	= Boltzmann's constant	θ	= theta-temperature
L	= contour length of the tail	ν	= number of chains per unit area
M	= molecular weight	$\hat{\rho}_d$	= normalized segment density distribution function at separation d
N_A	= Avogadro's constant		
$\langle r^2\rangle^{1/2}$	= r.m.s. end-to-end chain length in free solution	$\hat{\rho}'_d$	= mirror image of $\hat{\rho}_d$
		ψ_1	= entropy of dilution parameter
$\langle r^2\rangle_0^{1/2}$	= unperturbed r.m.s. end-to-end chain length	ω	= weight of polymer per unit area ($= \nu M/N_A$)

APPENDIX I

We show here a sample integration by parts that permits the development of analytical formulae for the assumed gaussian distributions. Given that

$$\hat{\rho}_d = 4\pi(3/2\pi F^2 d^2)^{\frac{3}{2}} x^2 \exp(-3x^2/2F^2d^2)$$

we have that

$$\int_0^d \hat{\rho}_d^2 \, dx = K \int_0^d x^4 \exp(-ax^2)\, dx,$$

where $K = (2/\pi)(3/F^2d^2)^3$ and $a = 3/F^2d^2$. Integration by parts yields:

$$\int_0^d x^4 \exp(-ax^2)\,dx = [-x^3 \exp(-ax^2)/2a]_0^d + \int_0^d (3x^2/2a)\exp(-ax^2)\,dx$$
$$= [-x^3 \exp(-ax^2)/2a]_0^d - [3x/(2a)^2\exp(-ax^2)]_0^d + (3/2a)^2 \int_0^d \exp(-ax^2)\,dx.$$

The correctness of this integration can easily be checked by differentiation. The last integral is a standard error function integral:[25]

$$(3/2a)^2 \int_0^d \exp(-ax^2)\,dx = (1/2)(\pi/a)^{\frac{1}{2}}[\mathrm{erf}(a^{\frac{1}{2}}x)]_0^d$$
$$= (1/2)(\pi/a)^{\frac{1}{2}}\,\mathrm{erf}(a^{\frac{1}{2}}d).$$

Evaluating the limits and substituting for K and a gives

$$\int_0^d \hat{\rho}_d^2\,dx = (9/\pi F^4 d)[-\exp(-3/F^2)(1+F^2/2)+(F^3/4)(\pi/3)^{\frac{1}{2}}\,\mathrm{erf}(3^{\frac{1}{2}}/F)].$$

APPENDIX II

Our theories use the segment density distribution functions, normalized by setting $\int_0^\infty \hat{\rho}\,dx = 1$, over the contour length of the chain. To calculate what fraction of chains exceeds the contour length we need to find $\int_0^L \hat{\rho}\,dx$. For example, for the Hesselink $\hat{\rho}_\infty$ we have from eqn (18):

$$\int_0^L \hat{\rho}_\infty\,dx = (3\pi^{\frac{1}{2}}/f^2\langle r^2\rangle A)\int_0^L [\mathrm{erf}(2Ax)-\mathrm{erf}(Ax)]\,dx$$
$$= (3\pi^{\frac{1}{2}}/f^2\langle r^2\rangle A)\{[x\,\mathrm{erf}(2Ax)]_0^L - [x\,\mathrm{erf}(Ax)]_0^L + (1/a\pi^{\frac{1}{2}})[\exp(-4A^2x^2)/2-\exp(-a^2x^2)]_0^L\}$$
$$= L\{\mathrm{erf}(2AL)-\mathrm{erf}(AL)\}+(1/a\pi^{\frac{1}{2}})\{1/2+\exp(-4A^2L^2)/2-\exp(-a^2L^2)\}.$$

Substituting in this relationship $L = 14.7$ nm, $\langle r^2\rangle^{1/2} = 6.2$ nm and $f = 2$ gives

$$\int_0^L \hat{\rho}_\infty\,dx \approx 0.958.$$

Hence less than 5% of the segments of the model chain lie beyond the contour length of the real chain.

For a gaussian chain we find

$$\int_0^L \hat{\rho}_\infty\,dx = K\{(\pi^{\frac{1}{2}}/a)\,\mathrm{erf}(a^{\frac{1}{2}}L)/4a-(L/2a)\exp(-3L^2/2f^2\langle r^2\rangle^{\frac{1}{2}})\}$$

where $K = 4\pi(3/2f^2\langle r^2\rangle^{1/2})^{3/2}$. We find that $f = 2^{1/2}$ gives 4% of chains greater than the contour length. Clearly, significantly greater values of f for the Hesselink function are permissible than for the gaussian function before the normalization procedure introduces serious errors.

[1] D. H. Napper and R. J. Hunter, *M.T.P. Int. Rev. Sci. Series* 1, 1972, **7**, 241.
[2] E. J. Verwey and J. Th. G. Overbeek, *Theory of the Stability of Lyophobic Colloids* (Elsevier, Amsterdam, 1948).
[3] E. W. Fischer, *Kolloid-Z.*, 1958, **160**, 120.
[4] D. J. Meier, *J. Phys. Chem.*, 1967, **71**, 1861.
[5] F. Th. Hesselink, A. Vrij and J. Th. G. Overbeek, *J. Phys. Chem.*, 1971, **75**, 2094.
[6] R. Evans and D. H. Napper, *Kolloid-Z. Z. Polymere*, 1973, **251**, 329.
[7] R. Evans and D. H. Napper, *Kolloid-Z. Z. Polymere*, 1973, **251**, 409.
[8] A. Doroszkowski and R. Lambourne, *J. Colloid Interface Sci.*, 1973, **43**, 97.
[9] B. V. Deryagin, *Kolloid-Z.*, 1934, **69**, 155.
[10] F. Th. Hesselink, *J. Phys. Chem.*, 1969, **73**, 3488.
[11] F. Th. Hesselink, *J. Phys. Chem.*, 1971, **75**, 65.
[12] E. A. Di Marzio and F. L. McCrackin, *J. Chem. Phys.*, 1965, **43**, 539.
[13] D. W. J. Osmond and D. J. Walbridge, *J. Polymer Sci. C*, 1970, **30**, 381.
[14] A. Doroszkowski and R. Lambourne, *J. Polymer Sci. C*, 1971, **34**, 253.
[15] A. Doroszkowski and R. Lambourne, *J. Colloid Interface Sci.*, 1968, **26**, 214.
[16] S. J. Barsted, L. J. Nowakowska, I. Wagstaff and D. J. Walbridge, *Trans. Faraday Soc.*, 1971, **67**, 3598.
[17] R. H. Ottewill and T. W. Walker, *Kolloid-Z. Z. Polymere*, 1968, **227**, 108.
[18] *Polymer Handbook* (Interscience, New York, 1966), p. IV-90.
[19] G. H. Aylward and T. J. V. Findlay, *SI Chemical Data* Wiley (Sydney, 1973), p. 42.
[20] P. J. Flory, *Principles of Polymer Chemistry* (Cornell, Ithaca, 1953).
[21] D. H. Napper, *J. Chem. Educ.*, 1969, **46**, 305.
[22] T. G. Fox and P. J. Flory, *J. Amer. Chem. Soc.*, 1951, **73**, 1909.
[23] P. Bagchi, personal communication.
[24] B. A. Firth, P. C. Neville and R. J. Hunter, *J. Colloid Interface Sci.*, in press.
[25] M. Abramowitz and I. A. Stegun, *Handbook of Mathematical Functions* (Nat. Bur. Stand., Washington, 1970), p. 303.

PRINTED IN GREAT BRITAIN AT
THE UNIVERSITY PRESS
ABERDEEN

Enthalpic Stabilization in Nonaqueous Media

ROBERT EVANS AND DONALD H. NAPPER

Department of Physical Chemistry, University of Sydney, N.S.W. 2006, Australia

Received September 30, 1974; accepted April 14, 1975

It is shown that polyacrylonitrile latexes stabilized by polyisobutylene in 2-methylbutane (isopentane) flocculate on heating to the θ-point for the stabilizing chains in free solution. This demonstrates unequivocally that the latexes are enthalpically stabilized, at least just below the critical flocculation temperature; the latexes represent the first quantitative documentation of enthalpic stabilization in nonaqueous media. The occurrence of enthalpic stabilization in nonaqueous media is attributed to the difference in free volume between the polymeric stabilizing chains and the dispersion medium.

INTRODUCTION

One of the characteristic features of sterically stabilized dispersions is their response to temperature changes (1). Some sterically stabilized latexes flocculate on heating to a critical temperature (2–5); others flocculate on cooling to below a critical temperature (6, 7). Still others cannot, at least in principle, be flocculated at any accessible temperature (1, 4). These different types of temperature responses contrast with the much less dramatic effect of temperature on the stability of electrostatically stabilized dispersion (8).

It is possible to show (5) by rigorous thermodynamic arguments that those dispersions that flocculate on heating are enthalpically stabilized, at least just below the critical flocculation temperature (cft). In contrast, those dispersions that flocculate on cooling are entropically stabilized, at least just above the cft. By enthalic stabilization we simply mean that the total enthalpy change that accompanies close approach of the particles is positive and opposes flocculation, whereas the corresponding positive entropy change favors flocculation (1). In entropic stabilization both the signs and the roles of the enthalpy and entropy changes are reversed.

Ottewill (9) was the first to point out that while entropic stabilization is most commonly encountered in nonaqueous media, enthalpic stabilization is most frequently exhibited in aqueous media. Nevertheless, modern theories of the thermodynamics of polymer solutions imply that by a judicious selection of the polymeric stabilizers, both types of steric stabilization should be observable in either type of dispersion medium. We have previously shown (7) how it is possible to prepare both entropically and enthalpically stabilized dispersion in aqueous media. However, all sterically stabilized dispersions prepared to-date in nonaqueous media have been found to be entropically stabilized. We now report the preparation of the first enthalpically stabilized dispersions in nonaqueous media. Their incipient flocculation behavior is also presented.

EXPERIMENTAL

Two samples of polyisobutylene (PIB) were kindly supplied by Essochem Australia Ltd. One sample was Esso Butyl Rubber grade 035 containing about 0.8 mole% unsaturation (isoprene). The second sample was Vistanex grade LM MH polyisobutylene containing

Copyright © 1975 by Academic Press, Inc.
All rights of reproduction in any form reserved.

negligible unsaturation. The viscosity average molecular weights M_v were measured as $(1.5 \pm 0.1) \times 10^5$ and $(2.3 \pm 0.2) \times 10^4$, respectively. These measurements were made in benzene at 24°C (a θ-solvent) so that the following Mark–Houwink equation was applicable (10):

$$[\eta]/dl\ g^{-1} = 1.07 \times 10^{-3} M_v^{\frac{1}{2}}.$$

Acrylonitrile and benzoyl peroxide were Fluka purum grade. The 2-methylbutane was BDH laboratory reagent and its vapor pressure was calculated (11) from: $\log_{10}(P/\text{mm Hg}) = -(1.4139 \times 10^3)/(T/K) + 7.54468$.

The amphipathic stabilizers, poly(isobutylene-*g*-acrylonitrile) were prepared, e.g., by heating the grade 035 PIB (2 g), dissolved in *n*-heptane (38 g), with acrylonitrile (0.2 g) at 60°C for 20 hr. Benzoyl peroxide (0.1 g) was added as initiator. The resultant copolymeric stabilizer was precipitated by the addition of ether and, on separation, dried *in vacuo*.

The corresponding polyacrylonitrile (PAN) latex was prepared by dissolving the stabilizer (2 g) in *n*-heptane (100 cm^3) and heating it with acrylonitrile (2 g) at 70°C, using benzoyl peroxide as initiator. The latex was produced after several hours. It was centrifuged several times to remove excess stabilizer; each time the particles were redispersed in 2-methylbutane. The weight average particle radius, as measured turbidimetrically, was 53 nm. (The particle radius for the PAN latex stabilized by the lower molecular weight PIB was 47 nm).

The θ-temperature of the PIB in free solution was determined in both sealed glass tubes and in a pressure bomb using the phase separation method of Cornet and van Ballegooijen (12). The cft of each latex was similarly determined (2–6). In all cases, the pressure in the system was closely approximated by the vapor pressure of 2-methylbutane.

RESULTS AND DISCUSSION

One difficulty encountered in these studies was the small but nonetheless significant variation (e.g., several atmospheres) of the temperature was varied. To render the results of our experiments at different temperatures internally consistent, we adopted the procedure common in polymer solution thermodynamics of correcting all measurements to the hypothetical state of $P = 0$ atm (13–15). Both Allen and Barker (12) and Gaeckle and Patterson (13) have shown that the lower critical solution temperature (LCST) of PIB in 2-methylbutane increases by approx. 0.5 K atm^{-1} and our experiments confirmed this small pressure dependence. Accordingly, this numerical factor was applied proportionately to correct the results to zero pressure.

Figure 1(a) displays the phase diagram determined in the pressure bomb for the phase separation of the higher molecular weight PIB in 2-methylbutane. The existence of an LCST is obvious. The shape of the phase diagram is quite characteristic for the liquid phase separation of macromolecules from a solvent for which the enthalpy and entropy of dilution parameters are both negative (16). These negative signs presage the manifestation of enthalpic stabilization by dispersions sterically stabilized by PIB in 2-methybutane. The phase separation data may be used to determine the θ-temperature of PIB in 2-methylbutane if plotted as described by Cornet and van Ballegooijen (12) [Fig. 1(b)]. The values

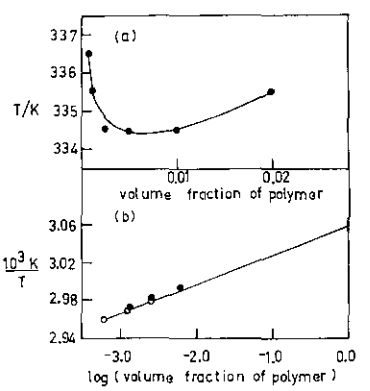

FIG. 1. (a) Phase diagram for PIB ($M_v = 1.5 \times 10^5$) in 2-methylbutane. (b) Cornet and van Ballegooijen plot to determine the θ-temperature: ● sealed tubes; ○ pressure bomb.

of θ so obtained were 325 ± 2 K (sealed tubes) and 326 ± 2 K (pressure bomb). These values are slightly higher than the θ-temperature reported (14) by Gaeckle and Patterson (316 K) for a fully saturated sample of PIB. Unfortunately, we were unable to measure θ for our fully saturated PIB sample because of the elevated temperatures needed to induce phase separation. Therefore, we are inclined to attribute the above small difference in θ-temperatures to either different degrees of unsaturation and/or different degrees of branching in the two PIB samples. Perhaps the different methods of measuring θ also contributed to the discrepancy. Certainly the discrepancy is unlikely to have originated in the purity of the 2-methylbutane; addition of 5% v/v *n*-pentane only increased θ by approx. 0.5 K and this is the most probable impurity in the dispersion medium.

The PAN latex stabilized by PIB of $M_v = 1.5 \times 10^5$ was found to flocculate on heating at 325 ± 1 K in both sealed tube and bomb experiments. [The cft is above the normal boiling point of 2-methylbutane, 301 K (17)]. This cft is in almost exact agreement with the measured θ-temperature for PIB in free solution. The cft for the latex stabilized by the lower molecular weight PIB was also found to be 325 ± 1 K. Hence, although the molecular weight of the stabilizing chains was reduced by a factor of 10, no significant change in cft was observed. This would be expected if the cft correlated with the θ-temperature, which is independent of molecular weight (18). However, these experimental results are in sharp conflict with the theoretical conclusions of Hesselink, Vrij, and Overbeek (19), who predict a very strong molecular weight dependence for the cft and the absence of a correlation between the cft and the θ-temperature. The errors in their theory have been pointed out elsewhere (20, 21). These new experimental results are in excellent agreement with our previous experimental studies (2–7) of incipient instability of sterically stabilized dispersions. They are also in accord with the quantitative theory of steric stabilization developed by us recently (21, 22).

Note that the origins of enthalpic stabilization in aqueous media are likely to be quite different from, and/or supplementary to, those generating enthalpic stabilization in nonaqueous media. The former may possibly arise from the strong interactions (e.g., H-bonding) between the stabilizing polymer chains and the water (23, 24); such enthalpic stabilization is likely to exist quite far removed from the critical point of water ($T_c = 374$°C, $P_c = 218$ atm). The origin of enthalpic stabilization in nonaqueous media probably resides in the difference in free volume between the polymeric stabilizing chains and the dispersion medium; such enthalpic stabilization is likely to be observed in dispersion media much closer to their critical point [for 2-methylbutane $T_c = 188$°C, $P_c = 33$ atm (25)]. The classical theories of polymer solution thermodynamics, such as those due to Flory and Huggins (26, 27), which only calculate the combinatorial entropy of mixing of polymer and solvent, are quite unable to predict (16) the existence of an LCST and the related flocculation on heating. They predict solely flocculation on cooling. Nevertheless, it is possible to modify empirically the Flory–Huggins theory to include noncombinatorical terms (18) and this modified theory predicts implicitly flocculation on both heating and cooling (16). The more sophisticated free volume theories (28, 29) provide a semiquantitative understanding of the physical bases underlying the empirical modifications of the classical Flory–Huggins theory.

With the preparation of these latexes we have completed the demonstration that both entropic and enthalpic stabilization should be evident in both aqueous and nonaqueous dispersion media. Therefore, we have assembled in Table I a summary of all the well-characterized sterically stabilized dispersions that have been prepared to-date. The nature of the disperse phase is usually unimportant (2–7). Note that both poly(ethylene

TABLE I

CLASSIFICATION OF STERICALLY STABILIZED DISPERSIONS

Stabilizer	Dispersion medium		Type	References
	Type	Example		
Poly(lauryl methacrylate)	Nonaqueous	*n*-heptane	Entropic	(6)
Poly(12-hydroxystearic acid)	Nonaqueous	*n*-heptane	Entropic	(6)
Polystyrene	Nonaqueous	Toluene	Entropic	(30)
Polyisobutylene	Nonaqueous	*n*-heptane	Entropic	(31)
Poly(ethylene oxide)	Nonaqueous	Methanol	Entropic	(5)
Polyisobutylene	Nonaqueous	2-methylbutane	Enthalpic	
Poly(ethylene oxide)	Aqueous	0.48 *M* $MgSO_4$	Enthalpic	(2,3)
Poly(vinyl alcohol)	Aqueous	2 *M* NaCL	Enthalpic	(4)
Poly(methacrylic acid)	Aqueous	0.02 *M* HCl	Enthalpic	(7)
Poly(acrylic acid)	Aqueous	0.2 *M* HCL	Entropic	(7)
Polyacrylamide	Aqueous	2.1 *M* $(NH_4)_2SO_4$	Entropic	(7)
Poly(vinly alcohol)	Mixed	Dioxan/water	Combined[a]	(4)
Poly(ethylene oxide)	Mixed	Methanol/water	Combined[a]	(5)

[a] Combined is combined enthalpic–entropic stabilization.

oxide) and PIB apparently function as both entropic and enthalpic stabilizers in different dispersion media. Of course modern theories of polymer solutions (28, 29) imply that each stabilizer should display both entropic and enthalpic stabilization in any given dispersion medium if only a wide enough temperature–pressure domain can be scanned. Unfortunately, this has not proven possible thus far.

ACKNOWLEDGMENT

We thank the Australian Research Grants Committee for support of these studies. The first author gratefully acknowledges the award of a Commonwealth Post-Graduate Scholarship. We thank Dr. A. Ewald for advice on the construction of the high pressure bomb.

REFERENCES

1. NAPPER, D. H., AND HUNTER, R. J., *MTP Int. Rev. Sci., Series 1.* **7**, 280 (1972).
2. NAPPER, D. H., *J. Colloid Interface Sci.* **29**, 168 (1969).
3. NAPPER, D. H., *J. Colloid Interface Sci.* **32**, 102 (1970).
4. NAPPER, D. H., *Kolloid Z. Z. Polymere* **234**, 1149 (1969).
5. NAPPER, D. H., AND NETSCHEY, A., *J. Colloid Interface Sci.* **37**, 528 (1971).
6. NAPPER, D. H., *Trans. Faraday Soc.* **64**, 1701 (1968).
7. EVANS, R., DAVISON, J. B., AND NAPPER, D. H., *J. Polymer Sci.* **B10**, 449 (1972).
8. VERWEY, E. J. W., AND OVERBEEK, J. T. G., "Theory of the Stability of Hydrophobic Colloids." Elsevier, Amsterdam, 1948.
9. OTTEWILL, R. H., *Ann. Rep. Progr. Chem.* (*Chem. Soc. London*) **A66**, 212 (1969).
10. BRANDRUP, J., AND IMMERGUT, E. H. (Eds.), "Polymer Handbook," p. I V-8. Wiley-Interscience, New York, 1966.
11. "Handbook of Chemistry and Physics," 54th ed., p. D-162. CRC Press, Cleveland, 1973.
12. CORNET, C. F., AND VAN BALLEGOOIJEN, H., *Polymer* **7**, 293 (1966).
13. ALLEN, G., AND BAKER, C. H., *Polymer* **6**, 181 (1965).
14. GAECKLE, D., AND PATTERSON, D., *Macromolecules* **5**, 136 (1972).
15. ZEMAN, L., BIROS, J., DELMAS, G., AND PATTERSON, D., *J. Phys. Chem.* **76**, 1206 (1972).
16. FLORY, P. J., ELLENSON, J. L., AND EICHINGER, B. E., *Macromolecules* **1**, 279 (1968).
17. AYLWARD, G. H., AND FINDLAY, T. J. V., "Chemical Data Book," p. 27. Wiley, Sydney, 1968.
18. FLORY, P. J., "The Principles of Polymer Chemis-

try," Chapt. 12. Cornell University Press, Ithaca, New York, 1953.
19. HESSELINK, F. T., VRIJ, A., AND OVERBEEK, J. T. G., *J. Phys. Chem.* **75**, 2094 (1971).
20. EVANS, R., AND NAPPER, D. H., *Kolloid Z.Z. Polymere* **251**, 409 (1973).
21. EVANS, R., AND NAPPER, D. H., *Kolloid Z.Z. Polymere* **251**, 329 (1973).
22. SMITHAM, J. B., EVANS, R., AND NAPPER, D. H., *J. Chem. Soc. Faraday I*, **71**, 285 (1975).
23. NAPPER, D. H., *J. Colloid Interface Sci.* **33**, 384 (1970).
24. NAPPER, D. H., *Ind. Eng. Chem. Prod. R. D.* **9**, 467 (1970).
25. "Handbook of Chemistry and Physics," 54th ed. p. F-75. CRC Press, Cleveland, 1973.
26. HUGGINS, M. L., *J. Chem. Phys.* **9**, 440 (1941).
27. FLORY, P. J., *J. Chem. Phys.* **9**, 660 (1941).
28. FLORY, P. J., *Discuss. Faraday. Soc.* **49**, 7 (1970).
29. PATTERSON, D., *Macromolecules* **2**, 672 (1969).
30. DOROSZKOWSKI, A., AND LAMBOURNE, R., *J. Colloid Interface Sci.* **43**, 97 (1973).
31. BUECHE, F., *J. Colloid Interface Sci.* **41**, 374 (1972)

J. POLYMER SCI.: Symposium No. 49, 159-167 (1975)

THE CHEMICAL REACTIVITIES OF MACROMOLECULES ATTACHED TO AN INTERFACE

PETER M. WENT, ROBERT EVANS, and DONALD H. NAPPER

Department of Physical Chemistry, University of Sydney, N.S.W. 2006, Australia

SYNOPSIS

The rates of alkaline hydrolysis of polyacrylamide chains attached to polystyrene latex particles have been measured and compared with the corresponding values in free solution. The attached chains exhibited a significant reduction in rate. The magnitude of this reduction increased with decreasing molecular weight. Consequently, the rates of hydrolysis of attached chains were a function of their molecular weight; this contrasted with the apparent second-order rate constants for the chains in free solution, which were insensitive to the molecular weight. The reduction in rate was attributed to the decreased accessibility of the amide groups to the hydroxyl anions when the polymer chains were attached to an impenetrable interface.

INTRODUCTION

The chemical reactivities of synthetic macromolecules when attached, either chemically or physically, to an impenetrable interface have apparently not been studied in any detail. Yet such studies may well cast light upon the biological activity of natural macromolecules at interfaces, both in vivo and in vitro (e.g., the catalytic activity of enzymes attached to a solid), and on the behavior of polymers in situations of technological importance (e.g., macromolecules acting as bridging flocculants).

The preparation [1] of latex particles sterically stabilized by polyacrylamide (PAM) provides a model system for studying the chemical reactivity of attached macromolecules. On alkaline hydrolysis, PAM yields poly(acrylic acid), which is itself an effective steric stabilizer [1]. Hence, the kinetics of the alkaline hydrolysis of attached PAM can be studies in the absence of complications arising from flocculation of the latex particles. Moreover, studies of the rates of alkaline hydrolysis of PAM in free solution have provided a reasonably detailed picture of the factors that control the kinetics [2-5].

EXPERIMENTAL

Polyacrylamide

Three samples of PAM with different viscosity average molecular weights ($\bar{M}_v$) were studied. The lowest molecular weight sample ($\bar{M}_v$ = 18,000) was

prepared by polymerization of acrylamide (50 g) in ethanol (500 cm^3) at 323°K using benzoyl peroxide (0.7 g) as initiator. The other two samples were prepared in a similar fashion, except that acetone was used as the monomer solvent. In the presence of *n*-butyl mercaptan (0.1 cm^3) as a chain transfer agent, the product had $\bar{M}_v = 60{,}000$, but in its absence $\bar{M}_v = 180{,}000$.

The values of $\bar{M}_v$ were measured in 1.0 M NaNO3 at 303°K and calculated by application of the Mark-Houwink equation [6]

$$[\eta]\ (\text{dl g}^{-1}) = 3.73 \times 10^{-4}\ M_v^{0.66}$$

Poly(acrylamide-g-acrylonitrile)

Poly(acrylamide-g-acrylonitrile) was prepared by refluxing PAM (10 g) in water (400 cm^3) in the presence of potassium persulfate (0.35 g), followed by the addition of a saturated aqueous solution of acrylonitrile (5 g) with further reflux for 30 min. A clear solution of the graft copolymer resulted when PAM was present, whereas a precipitate of polyacrylonitrile was formed in its absence.

Polystyrene Latex Particles

Polystyrene latex particles, sterically stabilized by PAM, were prepared by dispersing styrene (5 g) in an aqueous solution (400 cm^3) containing a known weight of poly(acrylamide-g-acrylonitrile). Potassium persulfate (0.5 g) was then added and the reaction mixture stirred magnetically at room temperature for 3 days. Excess stabilizer was removed, after dialysis of the resultant latex, by centrifugation and redispersion of the particles. The amount of unused graft copolymer present in the supernatant liquid was determined gravimetrically so that the concentration of adsorbed PAM could be calculated by difference. To check that the particles were fully coated by the steric stabilizer, measurements were made of their critical flocculation temperatures in 2.1 M $(NH_4)_2SO_4$ [1]. Only those latices that exhibited reversible (or almost reversible) flocculation in the range 285 ± 20°K were studied kinetically.

The mean particle size of each latex was determined by electron microscopy, some 300-600 particles being measured.

Kinetic Studies

The alkaline hydrolysis of polyacrylamide was studied for equimolar (0.05 M) concentrations of amide group and sodium hydroxide. The degree of hydrolysis was always less than 20%. The kinetics were followed by potentiometric titrations as described by Nagase and Sakaguchi [4]. Apparent second-order rate constants were calculated from [3, 4]

$$k_2 = \frac{[1/(a - x_2)] - [1/(a - x_1)]}{t_2 - t_1}$$

where a is the initial amide concentration and x is the amide concentration at time t. Note that this gives a mean rate constant for the average time $(t_2 - t_1)/2$.

RESULTS AND DISCUSSION

Polyacrylamide in Free Solution

As a basis for comparison of the rates of hydrolysis of adsorbed PAM, the corresponding rates were measured for PAM in free solution. Three different molecular weight polymers were studied at three different temperatures (338, 348, and 358°K). Typical plots of the apparent second-order rate constants as a function of the reaction time are shown in Figure 1 for the three different molecular weights at 358°K. The characteristic reduction [2-5] in k_2 as hydrolysis proceeds is obvious, as is the virtual independence of the rate on molecular weight.

The "initial" value of k_2 at 358°K (52×10^{-4} dm^3 mol^{-1} s^{-1}) was somewhat larger than the value (39×10^{-4} dm^3 mol^{-1} s^{-1}) reported by Moens and Smets [3]. However, as noted above, these rates do not refer to the rate at t = 0 but to the mean rate from t =0 to the time of the first measurement. This mean rate will be approximately equal to the rate at a time equal to half the time of the initial readings in these studies; this corresponded to ca 2-5% hydrolysis. Because of the greater sensitivity of our analytical methods, we were able to take our first reading at a shorter time than Moens and Smets [3]. The "initial" k_2 is therefore correspondingly larger. This explanation is reinforced by the smaller activation energy (40 kJ mol^{-1}) that was calculated from our "initial" k_2 as compared with Moens and Smets activation energy (57 kJ mol^{-1}) [3]. The data presented in Table I show that the activation energy increases rapidly as hydrolysis proceeds. This increase would be expected if the electrostatic repulsion forces between the negatively charged carboxylic acid groups, formed by hydrolysis, and the hydroxyl anions are important.

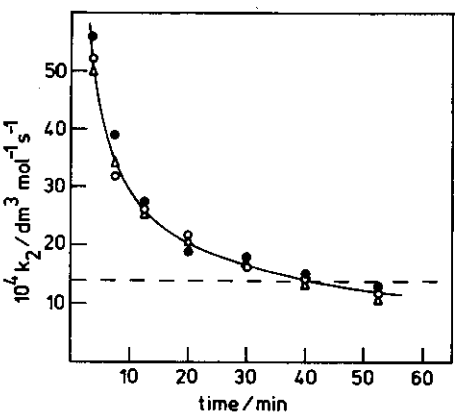

FIG. 1. The time dependence of the apparent second-order rate constants for the hydrolysis of PAM; (○) $\bar{M}_v = 18{,}000$; (●) $\bar{M}_v = 60{,}000$; (△) $\bar{M}_v = 180{,}000$; (- - -) acrylamide.

TABLE I

The Apparent Activation Energy at Different Degrees of Hydrolysis for PAM in Free Solution

% Hydrolysis	Activation Energy, kJ mol^{-1}	Correlation Coefficient of Arrhenius Plot
3	40	0.997
9	51	0.990
13	54	0.999
17	68	0.996

Further evidence that electrostatic repulsions play a significant role is given in Figure 2, where the rates of hydrolysis of PAM ($\bar{M}_v$ = 18,000) at 338°K in the presence and absence of 0.10 M NaCl are compared. At low degrees of hydrolysis, the k_2 values are almost identical for the two ionic strengths. However, as hydrolysis proceeds, differences in k_2 of a factor of two appear. The higher rates are observed at the higher ionic strength, as would be expected if electrostatic repulsions between the ionized carboxylic acid and the hydroxyl groups are significant. Changing the ionic strength from 0.05 M to 0.15 M decreases the Debye ionic atmosphere parameter, $1/\kappa$, from 1.4 nm to 0.8 nm, so that a primary salt effect is observed.

We note, in passing, that the observation that the rate of hydrolysis was virtually independent of molecular weight is in accord with the orthodox view that the reactivity of a functional group attached to a polymer is essentially independent of the polymer molecular weight [7]. Moreover, as the intrinsic viscosity of the polymer solution increased by a factor of about four in going from the lowest to the higher molecular weight sample, the results agree with Flory's classical finding that the viscosity does not influence the rate of reaction of a polymer and a small molecule, except in extreme cases [7].

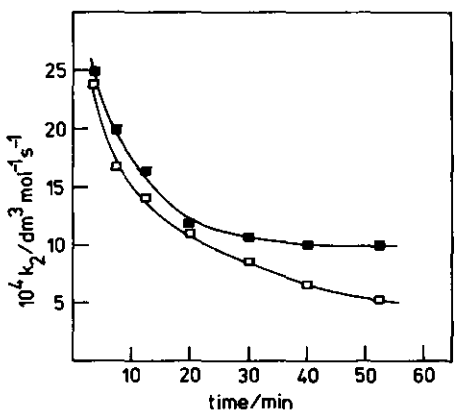

FIG. 2. The time dependence of the apparent second-order rate constants at two different ionic strengths: (□) no NaCl added; (■) 0.10 NaCl added.

Poly(acrylamide-g-acrylonitrile)

The reason for using this graft copolymer as a stabilizer, rather than PAM, was to ensure that the nominally insoluble polyacrylonitrile anchored the PAM to the surfaces of the latex particles, thus achieving both attachment and maximum colloid stability [8]. However, since the nitrile groups may also be hydrolyzed to carboxylic acid groups [9], it was necessary to check that this reaction did not contribute significantly to the measured rates. The rates of hydrolysis of the graft copolymers were therefore measured in free solution and were found to be identical, within the limits of experimental error, with those for PAM in free solution. This strongly suggests that the hydrolysis of polyacrylonitrile was not appreciable.

Attached Polyacrylamide

The time dependence of the apparent second-order rate constant for the hydrolysis of attached PAM ($\bar{M}_v$ = 18,000) at 358°K is shown in Figure 3. It is apparent that the value of k_2 decreases as hydrolysis proceeds in a manner qualitatively similar to that for PAM in free solution. However, the absolute values of k_2 for the attached polymer are only about half the free solution values.

Table II summarizes the "initial" rate data obtained at the three different temperatures for the three different molecular weight polymers when attached to polystyrene latex particles. All the "initial" k_2 values for the attached chains are smaller than those for the corresponding chains in free solution. Moreover, the values of k_2 clearly exhibit a molecular weight dependence; the smaller the molecular weight of the attached chain the larger is the reduction in rate. Indeed, for the highest molecular weight polymer studied ($\bar{M}_v$ = 180,000), the rate reduction scarcely exceeds the limits of experimental error.

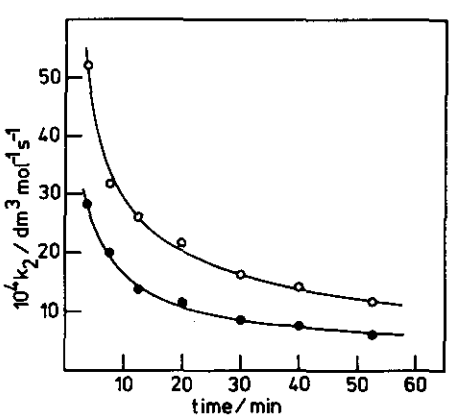

FIG. 3. The time dependence of the apparent second-order rate constants for the hydrolysis of PAM ($\bar{M}_v$ = 18,000): (•) attached; (○) free solution.

TABLE II

Initial Hydrolysis Rate Data for Adsorbed Polyacrylamide

Latex Code	Particle Radius, nm	$\bar{M}_v$	$10^4 k_2/dm^3\ mol^{-1}\ s^{-1}$		
			338°K	348°K	358°K
R10-190	51	18,000	11	–	–
R10-286	50	18,000	16	–	29 ± 2
R10-367	–	18,000	13	–	–
			Mean = 13 ± 3		
R10-213	30	60,000	13	–	–
R10-265	30	60,000	17	27 ± 2	41 ± 2
R10-316	29	60,000	16	–	–
			Mean = 15 ± 2		
R10-287	40	180,000	22	34 ± 2	48 ± 2
R10-317	36	180,000	26	–	–
R10-368	37	180,000	26	–	–
			Mean = 25 ± 3		
Free Solution Rate			26 ± 2	39 ± 3	52 ± 4

Table III displays the activation energies observed for the attached PAM of $\bar{M}_v = 60{,}000$. The values increase with the degree of hydrolysis, as they did for the chains in free solution. Although these activation energies are marginally greater than those for the free solution, the differences are probably not experimentally significant, except perhaps at the highest degree of hydrolysis. This lack of significance is borne out by the observed activation energies for the initial hydrolysis rates of attached chains of $\bar{M}_v = 18{,}000$ and $\bar{M}_v = 180{,}000$; both of these activation energies were ca. 40 kJ mol^{-1}, in good agreement with the free solution value. We conclude that there is probably no change in the basic chemical mechanism of hydrolysis on attachment; however, this conclusion is necessarily tentative because an increase in activation energy of only 2 kJ mol^{-1} would cause a reduction in rate by a factor of 2. This is comparable to the precision of our determination of activation energies.

Attachment of a coiled macromolecule to an impenetrable interface alters the conformation. An isolated chain would be expected to be extended by ca. 40% in the direction normal to the interface over its free solution r.m.s.

TABLE III

The Apparent Activation Energy at Different Degrees of Hydrolysis for Attached PAM

% Hydrolysis	Activation Energy, kJ mol^{-1}	Correlation Coefficient of Arrhenius Plot
3	46	0.999
8	54	0.994
12	64	0.999
17	80	0.999

end-to-end length [10]. For close-packed low molecular weight chains whose second virial coefficients are suitably positive, as required for good steric stabilization, the extension normal to the surface is found experimentally to be ca. 100% greater than the free-solution value [11-15]. This apparently results from the strong lateral repulsive interactions between contiguous molecules. However, in view of the absence of any effect of molecular weight on the rate of hydrolysis, it seems unlikely that these changes in conformation are sufficient to alter the neighboring group effects [5] that result in the higher rates of hydrolysis of the polymer (or polyfunctional compounds) compared with the monomer [4]. The activation energies measured for the attached polymers support this conclusion.

It should be pointed out, however, that for the attached polymers, replenishment of the hydrolyzing hydroxyl anions is not possible from the impenetrable-barrier side of the chains. Accordingly, we would expect that entry of the hydroxyl anions would proceed via the relatively fixed peripheral regions of the polymer chains, which would therefore become the predominant loci of hydrolysis. Thus the polymer chains would not likely be hydrolyzed uniformly along the chain length. If we ignore neighboring group effects, relatively uniform hydrolysis might be expected for a coil undergoing rapid conformational changes in free solution such that all amide groups are exposed at one time or another on the "surface" of the coil [7]. The conformational changes of an attached polymer are obviously restricted so that hydrolysis in the regions furthest removed from the surface are most likely. For a given degree of hydrolysis, this would be expected to concentrate the charged carboxylic acid groups in the peripheral zones. Repulsion of the incoming hydroxyl groups would be enhanced, leading to a reduced rate of hydrolysis.

The foregoing explanation would predict that the rate of hydrolysis should depend upon the relative sizes of the chains and the particles. For low molecular weight chains and large latex particles, the situation approximates attachment to a flat surface where we might expect maximum rate reduction. For high molecular weight chains and small particles, however, the situation more closely approximates the case of hydrolysis of the graft copolymer poly(acrylamide-g-acrylonitrile), which might be presumed to undergo almost normal conformational changes and was shown to give no reduction in rate. The ratio of the particle radius to the chain extension normal to the interface varied in these experiments from roughly 2.5/1 for the lowest molecular weight, through 1/1 for $\bar{M}_v$ = 60,000, to 1/2 for the highest molecular weight polymer. This variation could thus explain the observed molecular weight dependence.

A further factor that could reduce the rate of hydrolysis of adsorbed chains is the charge associated with the surface of the polystyrene latex particles. This can arise both from the incorporation of initiator fragments (sulfate anion free radicals) into the particles and from the formation of carboxylic acid groups [16, 17]. The charge on the particle surface is negative, so that repulsion of the hydroxyl anions could occur, leading to a lower rate. However, the double-layer thickness for the 0.05 M NaOH solutions is only ca. 1.4 nm, which is probably less than one-tenth of the attached polymer thickness of even the lowest molecular weight polymer studied. Accordingly, it seems unlikely that the

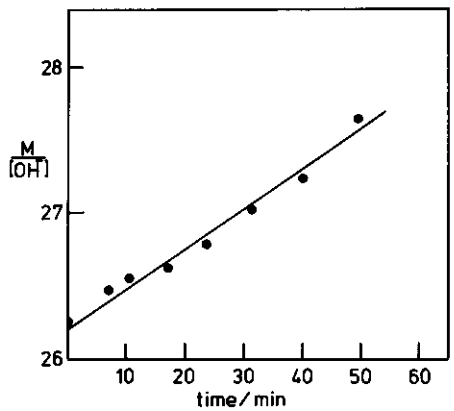

FIG. 4. A second-order rate plot of the reciprocal of the molar concentration of hydroxyl ions as a function of time for the hydrolysis of PAM attached to flocculated latex particles.

surface charge is responsible for the reduction in rate. This inference is supported by the measured "initial" activation energies of the attached chains.

Finally, we show in Figure 4 the second-order rate curve for the hydrolysis of polyacrylamide ($\bar{M}_v$ = 18,000) attached to flocculated latex particles at 338°K. The surfaces of the particles were incompletely covered, so that flocculation was induced by addition of hydroxyl ions. Hydrolysis proceeded at a rate that was only one-third of the initial rate for chains attached to stable latex particles or one-sixth the value for chains in free solution. Second-order kinetics were also obeyed approximately, presumably because the extent of hydrolysis studied was so small. Flocculation would be expected to render many of the amide groups relatively inaccessible to hydroxyl anions and so diminish the rate of hydrolysis.

The authors thank the Australian Research Grants Committee for their support of these studies. R. E. gratefully acknowledges the award of a Commonwealth Postgraduate Scholarship.

REFERNCES

[1] R. Evans, J. B. Davison, and D. H. Napper, *J. Polym. Sci. B, 10*, 449 (1972).
[2] G. Smets, *Makromol. Chem., 34*, 190 (1959).
[3] J. Moens and G. Smets, *J. Polym. Sci., 23*, 931 (1957).
[4] K. Nagase and K. Sakaguchi, *J. Polym. Sci. A, 3*, 2475 (1965).
[5] H. Morawetz, *Macromolecules in Solution*, Interscience, New York, 1965, Chap. IX.
[6] American Cyanamid Co. Bulletin MDD-9236, June 1959.
[7] P. J. Flory, *Principles of Polymer Chemistry*, Cornell Univ. Press, Ithaca, N. Y., 1953, pp. 75-78.
[8] D. H. Napper and R. J. Hunter, *MTP Int. Rev. Sci., Phys. Chem. Series 1, 7*, 241 (1972).
[9] L. F. Fieser and M. Fieser, *Organic Chemistry*, Harrap, London, 1953, p. 167.
[10] E. A. Di Marzio and F. L. McCrackin, *J. Chem. Phys., 43*, 539 (1965).
[11] R. H. Ottewill and T. W. Walker, *Kolloid-Z. Z. Polym., 227*, 108 (1968).

[12] D. W. J. Osmond and D. J. Walbridge, *J. Polym. Sci. C, 30*, 381 (1970).
[13] A. Doroszkowski and R. Lambourne, *J. Polym. Sci. C, 34*, 253 (1971).
[14] A. Doroszkowski and R. Lambourne, *J. Colloid Interface Sci., 26*, 214 (1968).
[15] S. J. Barsted, L. J. Nowakowska, I. Wagstaff, and D. J. Walbridge, *Trans. Faraday Soc., 67*, 3598 (1971).
[16] R. H. Ottewill and J. N. Shaw, *Kolloid-Z. Z. Polym., 215*, 161 (1967).
[17] R. H. Ottewill and J. N. Shaw, *Kolloid-Z. Z. Polym., 218*, 34 (1967).

ERRATA

The compressional terms included in both models I and II(but not model III) are too large by a factor of 2. On correction we have:

Model I

$$R_c^{Ib} = 1/\delta - 1/\delta_\infty \tag{7}$$

$$R_i^{Ib} + R_c^{Ib} = 2\langle r^2\rangle^{\frac{1}{2}}/d - \langle r^2\rangle^{\frac{1}{2}}/L \tag{8}$$

$$S_i^{Ib} + S_c^{Ib} = 2\ \ln(L/d_o) + (d_o/L) - 1 \tag{10}$$

$$S_{i+c}^{Ib} = 2\ln(L/d_o) + (d_o/L) - 0.5 \tag{11}$$

Model II

$$R_c^{II} = 2(1/\delta - 1/\delta_\infty) \tag{13}$$

$$S_c^{II} = 2\left\{ \ln(2L/d_o) + (d_o/2L) - 1\right\} \tag{14}$$

A revised Fig. 2 is shown overleaf where it is seen that the predictions of both models I and II are very similar indeed. Clearly it is difficult to discriminate experimentally between the predictions of models I and II (or III for that matter), although model I still appears to be the better. (The situation is somewhat reminiscent of the similar predictions of the constant charge vs. constant potential assumptions in DLVO theory).

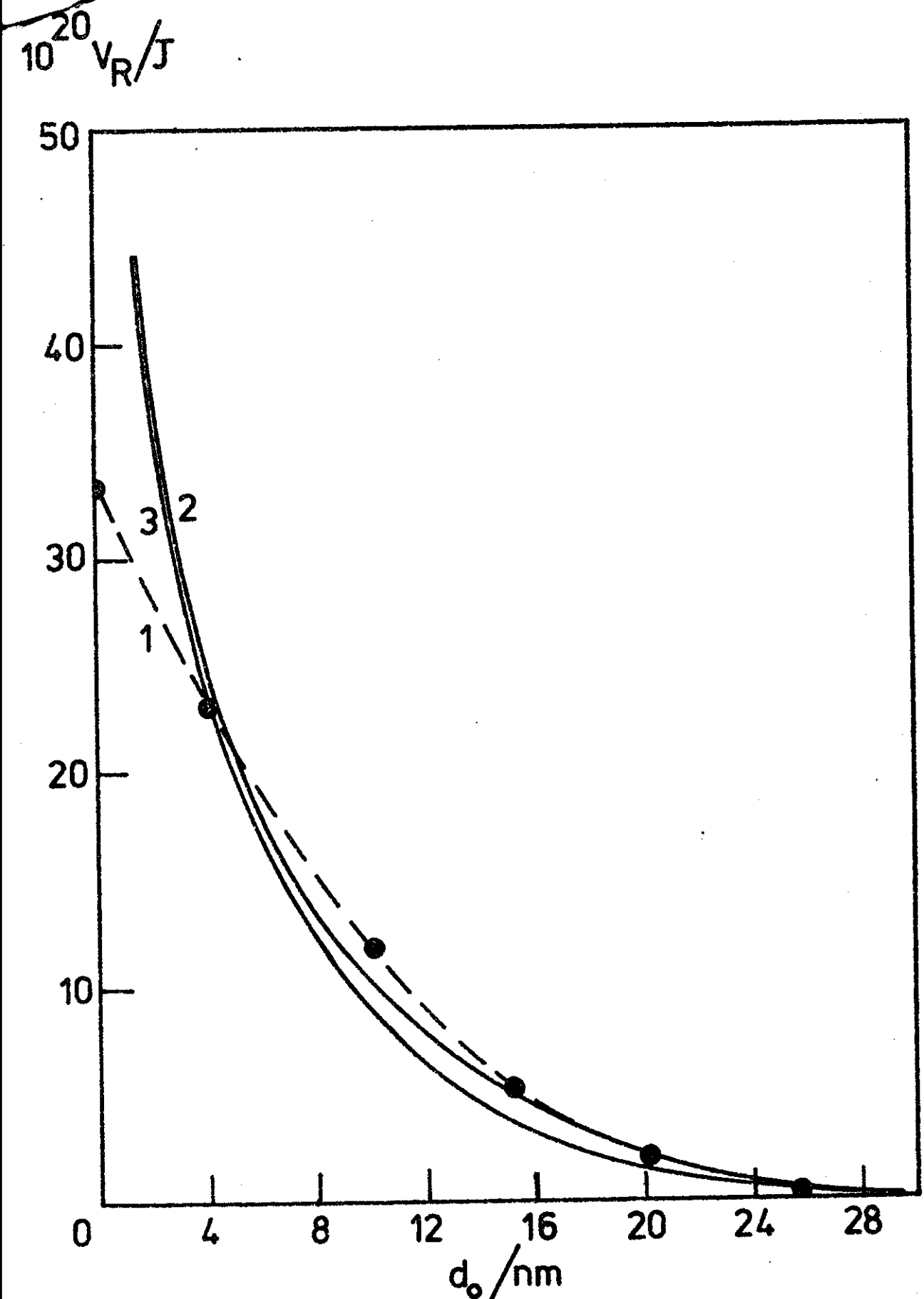
$10^{20} V_R/J$
50
40
30
20
10
0
4
8
12
16
20
24
28
d_o /nm
1
2
3

A Correlation Between Critical Flocculation Pressures and Theta-Pressures

One characteristic feature of sterically stabilized dispersions is the strong correlation that is usually observed between the attainment of theta (θ)-conditions and the onset of instability of the particles (1). The θ-point represents the limit of incipient phase separation for a hypothetical polymer of infinite molecular weight (2). It follows from this limit, by a simple application of the phase rule, that a binary solvent-polymer system has two degrees of freedom at the θ-point, one of which is lost on specification of the limiting concentrations. Hence if one intensive variable such as the pressure is specified (commonly a pressure of 1 atm is of interest), the θ-temperature is automatically fixed. Alternatively, however, θ-conditions can in principle be attained by fixing the temperature and varying the pressure. By analogy with θ-temperatures, we shall refer to such pressures as θ-pressures; θ-pressures are, however, likely to prove much less useful in general than θ-temperatures because of the incompressibility of liquids.

The concept of θ-pressures raises the possibility of inducing flocculation in sterically stabilized latexes, held at constant temperature, by the application of pressure alone. This note reports the observation of the new phenomenon of pressure-induced flocculation of sterically stabilized latexes. A correlation is established between the limiting pressures required to induce flocculation and the θ-pressures.

EXPERIMENTAL

The preparation of poly(ethylene oxide) stabilized latexes has been described previously (3). Poly(vinyl acetate) was the disperse phase; water was the dispersion medium. Viscosity average molecular weights ($\langle M_v \rangle$) were determined as before (3). The poly(ethylene oxide) used for the determination of θ-conditions had $\langle M_v \rangle = 2.08 \times 10^5$; that used to stabilize the latexes had $\langle M_v \rangle = 1.0 \times 10^4$, except for those latexes subjected to pressures in excess of 800 atm when $\langle M_v \rangle$ was increased to 2.08×10^5.

The pressure cell was a glass syringe that had been modified by removal of the flange and subsequent sealing; the plunger, also suitably modified, was used

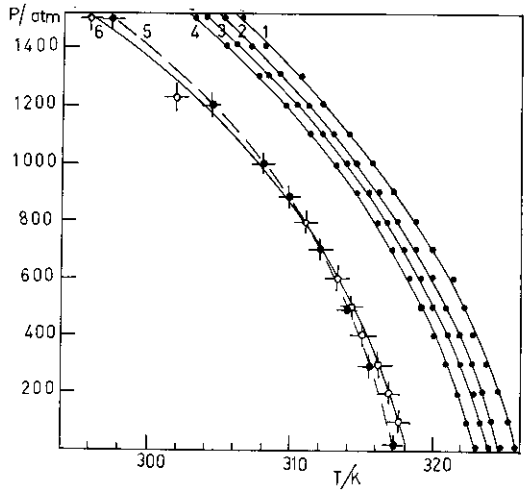

FIG. 1. Plots of phase separation pressure, θ-pressure and critical flocculation pressure as a function of temperature. Curves 1–4 show phase separation pressures for polymer volume fractions: (1) 2.5×10^{-3}; (2) 5×10^{-3}; (3) 1×10^{-2}; (4) 2×10^{-2}. Curves 5 and 6 show the θ-pressure and cfp, respectively.

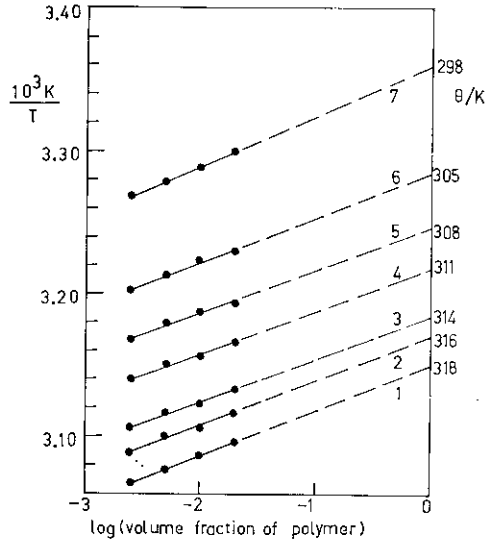

FIG. 2. Cornet and van Ballegooijen plots for poly(ethylene oxide) in 0.43m $MgSO_4$ at different pressures: (1) 1; (2) 300; (3) 500; (4) 800; (5) 1000; (6) 1200; (7) 1500 atm.

Copyright © 1975 by Academic Press, Inc.
All rights of reproduction in any form reserved.

as a piston. This cell, containing the latex or the polymer solution, was placed in a stainless steel bomb and pressure applied via a clear paraffin oil. Glass windows allowed the cell to be monitored visually. The temperature of the pressure bomb could be varied by a heating mantle. Small differences in the visually determined onset of flocculation and phase separation were detected at 1 atm pressure for samples inside and outside the bomb. This apparently arose from the decreased sensitivity of observations inside the bomb; all measurements taken inside the bomb were therefore corrected for these differences.

RESULTS AND DISCUSSION

The θ-temperatures for different specified pressures in the range 1–1600 atm were first determined for poly(ethylene oxide) in 0.43*m* $MgSO_4$ solution by the extrapolation method of Cornet and van Ballegooijen (4). (The electrolyte concentration is expressed on a molal basis because this scale is pressure independent.) The requisite phase separation curves as a function of pressure are shown in Fig. 1. The linear extrapolation plots for finding θ are presented in Fig. 2. It is clear from the variation of θ-temperature with pressure in Fig. 2 that θ decreases as pressure increases; hence aqueous latexes stabilized by poly(ethylene oxide) should become less stable on the application of pressure.

To measure the critical flocculation pressure (cfp) of a latex, the temperature of the cell was fixed and the pressure increased until incipient flocculation was observed. The flocculation thus induced was reversible at pressures below 800 atm: lowering the pressure below the cfp resulted in spontaneous redispersion. However, above 800 atm some irreversibility of flocculation was evident, despite a significant increase in the molecular weight of the stabilizing moieties used for these latexes. The temperature dependence of the cfp is compared in Fig. 1 with the temperature dependence of the θ-pressure. It is obvious that a strong correlation exists between the cfps and the θ-pressures over a wide range of pressure. This is in excellent agreement with previous observations (1) that θ-temperatures or θ-volumes form a practical limit to the stability of sterically stabilized latexes. Attainment of θ-conditions is also the theoretically predicted limit of stability in most systems (5, 6).

ACKNOWLEDGMENTS

We thank the Australian Research Grants Committee for support of these studies. R. E. gratefully acknowledges the award of a Commonwealth Post-Graduate Scholarship.

REFERENCES

1. NAPPER, D. H., AND HUNTER, R. J., *MTP Int. Rev. Sci. Ser. 1* **7**, 280 (1972).
2. FLORY, P. J., "The Principles of Polymer Chemistry," Chap. 13, Cornell University Press, Ithaca, New York, 1953.
3. NAPPER, D. H., *J. Colloid Interface Sci.* **32**, 102 (1970).
4. CORNET, C. F., AND VAN BALLEGOOIJEN, H., *Polymer* **7**, 293 (1966).
5. DOBBIE, J. W., EVANS, R., GIBSON, D. V., SMITHAM, J. B., AND NAPPER, D. H., *J. Colloid Interface Sci.* **45**, 557 (1973).
6. EVANS, R., AND NAPPER, D. H., Kolloid-Z.Z.Polymere **251**, 329 (1973).

ROBERT EVANS
DONALD H. NAPPER

Department of Physical Chemistry,
University of Sydney,
N.S.W. 2006,
Australia

ARNOLD H. EWALD

Mineral Research Laboratories,
C.S.I.R.O. Division of Mineralogy,
P.O. Box 136,
North Ryde, N.S.W. 2113,
Australia

Received February 3, 1975

Reprinted from JOURNAL OF COLLOID AND INTERFACE SCIENCE, Volume 45, No. 3, December 1973
Copyright © 1973 by Academic Press, Inc. *Printed in U.S.A.*

Enhanced Steric Stabilization

J. W. DOBBIE, ROBERT EVANS, D. V. GIBSON,
J. B. SMITHAM, AND D. H. NAPPER

Department of Physical Chemistry, University of Sydney, N.S.W. 2006, Australia

Received January 25, 1973; accepted June 8, 1973

An extensive series of experiments has previously demonstrated that for model sterically stabilized dispersions, θ-solvents for the stabilizing chains in free solution represent the limit of colloid stability. It has now been shown that by anchoring the stabilizing chains to the particle surfaces at many points along the chains, the pattern of flocculation behavior may be profoundly altered. Polystyrene latices stabilized by poly(ethylene oxide) have been prepared that are stable in dispersion media with solvency for the stabilizing moieties markedly worse than θ-solvents for the chains in free solution. Multipoint anchoring in these systems results from the hydrogen bonding between the ether oxygens of the stabilizer and surface carboxylic acid groups. The enhancement of steric stabilization is a function of the pH and the molecular weight of the stabilizing chains. It originates in the perturbation of the conformation of the stabilizing macromolecules that renders the free solution properties of the chains no longer relevant.

INTRODUCTION

An extensive series of experiments (1–5) has shown that for model sterically stabilized dispersions, a strong correlation exists between the point of incipient instability and the corresponding theta (θ)-point for the stabilizing moieties in free solution. This correlation has been demonstrated for both aqueous and nonaqueous dispersion media, irrespective of whether flocculation is induced by heating or cooling, or by the addition of nonsolvent. At least sixty critical flocculation points (cfp's) have now been correlated with their corresponding θ-points. A quantitative theoretical description of steric stabilization has also been developed recently (6, 7).

Whether or not stable sterically stabilized dispersions can be prepared in θ-solvents themselves remains a moot point. Certainly by definition the second, and therefore the third (8), virial coefficients of the stabilizing moieties in free solution must vanish in θ-solvents. As the major component of the repulsion in steric stabilization originates in these two nonideal components, any repulsion in θ-solvents must necessarily be relatively small. The fourth and higher virial coefficients are, however, nonzero in θ-solvents; presumably these nonideal components may be sufficiently large at high segment densities to impart stability in θ-solvents. In addition Born repulsion between polymer segments, which is disregarded in all theories advanced to date, may also contribute to stabilization. Unfortunately the experimental results to date lack sufficient precision to establish whether or not stable dispersions may be prepared in θ-solvents.

Nonetheless it can be stated quite categorically that there are no previously reported examples of sterically stabilized dispersions that exhibit stability in dispersion media which are markedly worse solvents than θ-solvents for the chains in free solution. By markedly worse solvency we mean that

Copyright © 1973 by Academic Press, Inc.
All rights of reproduction in any form reserved.

incipient flocculation would only be evident in excess of 10 K beyond the free solution θ-temperature. Flory (9) and others (7, 10) have stated clearly the reason for this: in solvents worse than θ-solvents the stabilizing sheaths are self-attracting, i.e., collisions are "sticky," and so the particles flocculate. Recent calculations have verified the essential correctness of this view (7).

We have now found that by using the phenomenon of multipoint anchoring of the stabilizing moieties to the particle surface, it is possible to prepare latices that display stability in dispersion media of considerably worse solvency than θ-solvents for the chains in free solution. This is possible because the anchoring of the macromolecules at many points along the chains so changes their conformation that the free solution properties of the chains are no longer relevant. An experimental investigation of this phenomenon, which we have termed "enhanced steric stabilization" (6), is now presented.

THEORY

We begin by establishing via a new theoretical route that, to a first approximation, θ-solvents for the stabilizing chains in free solution are the limit of colloid stability for dispersions sterically stabilized by tails or loops. By tails and loops we imply linear high polymers that are attached to the particle surface at one and both ends, respectively. We will assume that the configurational entropy of the core particles in the dispersion medium may be neglected; this is, of course, a standard assumption in colloid stability theory (e.g., in DLVO theory) but it could perhaps introduce some inaccuracy in certain circumstances. We shall, of course, take into account the configurational entropy of the stabilizing chains.

We want now the free energy of mixing ($\Delta\tilde{G}_M$) of randomly oriented tails or loops, whose centers of gravity are fixed in space, with solvent molecules. This is readily obtained from the theory developed by Flory and Krigbaum (11):

$$\Delta G_M{}^{FK} = \Delta G^{ATT} + \Delta\tilde{G}_M. \qquad [1]$$

Here $\Delta G_M{}^{FK}$ is the free energy of mixing of pure randomly oriented polymer chains, whose centers of gravity are fixed in space, with pure solvent, and ΔG^{ATT} is the free energy of attachment of randomly oriented chains to form tails or loops in the absence of solvent molecules. Thus

$$\Delta\tilde{G}_M = -\Delta G^{ATT} + kT[\tilde{n}_1 \ln (1 - \tilde{v}_2) + \tilde{n}_1\chi_1\tilde{v}_2^2]. \qquad [2]$$

where n_1 is the number of solvent molecules, v_2 is the volume fraction of the polymer segments, and χ_1 the polymer–solvent interaction parameter for chains in free solution. Note that the tilde is used to denote that the quantity refers not to the total system but only to that part of the system which is accessible to the stabilizing chains if the particles were all fixed in space. This differentiation is necessary because the Flory–Krigbaum theory (11) cannot be applied to the system as a whole: those regions of the dispersion medium between the coated particles contain a negligibly small polymer concentration which violates one of the basic requirements for the application of the Flory–Krigbaum theory. Only in the spatial regions occupied by the stabilizing chains is the segment density function sufficiently large and continuous to justify the Flory–Krigbaum approach.

To calculate the excess chemical potential of the solvent in the volume accessible to the polymer we need $[\partial(\Delta\tilde{G}_M)/\partial\tilde{n}_1]_{T,P}$. This differential is easily evaluated if we recall that $\tilde{v}_2 = (\tilde{n}_2 x)/(\tilde{n}_1 + \tilde{n}_2 x)$, where $\tilde{n}_2$ is the number of tails or loops and x is the number of lattice sites occupied by each chain, assumed to be monodisperse. Consequently, on differentiation we have

$$\tilde{\mu}_1 - \mu_1{}^0 = RT[\ln (1 - \tilde{v}_2) + \tilde{v}_2 + \chi_1\tilde{v}_2^2], \qquad [3]$$

where $\mu_1{}^0$ is the standard chemical potential of the solvent (i.e., the chemical potential of

pure solvent). Note that we have here ignored the configurational entropy of the core particles and so for equilibrium we may set $\tilde{\mu}_1 = \mu_1$, where the absence of the tilde denotes the system as a whole.

Flory (12) has shown that the requirements for incipient noncrystalline phase separation of the polymer solutions are

$$[\partial\mu_1/\partial v_2]_{T,P} = 0, \quad [4]$$

$$[\partial^2\mu_1/\partial v_2^2]_{T,P} = 0. \quad [5]$$

Phenomenologically we may relate incipient phase separation to incipient flocculation of sterically stabilized particles. Equations [4] and [5] can then be used to identify the critical flocculation point. The equivalent relationships in this case are

$$[V_T/\tilde{V}_T][\partial\tilde{\mu}_1/\partial\tilde{v}_2] = 0, \quad [6]$$

$$[V_T/\tilde{V}_T][\partial^2\tilde{\mu}_1/\partial\tilde{v}_2^2] = 0, \quad [7]$$

where V_T is the total available volume and $\tilde{V}_T$ is the volume accessible to the chains.

Combining Eqs. [3] and [6] yields

$$1/(1 - \tilde{v}_2) - 1 = 2\chi_1\tilde{v}_2, \quad [8]$$

whereas Eqs. [3] and [7] yield

$$1/(1 - \tilde{v}_2)^2 = 2\chi_1. \quad [9]$$

The solution of Eqs. [8] and [9] that is relevant is $\chi_1 = \frac{1}{2}$. This shows that to a first approximation θ-solvents, which are characterized by $\chi_1 = \frac{1}{2}$, are the limit of stability of particles stabilized by loops and tails (8). A very considerable body of experimental evidence (1–5) supports this theoretical conclusion. The conclusion is, however, at odds with that of Hesselink, Vrij, and Overbeek (13) who predict stability in dispersion media considerably worse than θ-solvents for dispersions stabilized by either tails or loops. The reason for their erroneous prediction has been pointed out elsewhere (6) but briefly it resides in assuming in the calculation of polymer compression that all θ-solvents are athermal. Flory (14) has asserted that θ-solvents are only athermal at the experimentally inaccessible temperature of absolute zero.

The foregoing discussion implies that if stability is observed in solvents markedly worse than θ-solvents, specific interactions may be operative between the stabilizing chains and the particles so that the chains are no longer tails or loops.

EXPERIMENTAL

Two types of polystyrene latices were prepared by emulsion polymerization. The first, termed "high carboxyl" latices, were prepared according to the method of Ottewill and Shaw (15) at elevated temperatures ($\gtrsim 50°C$), using potassium persulphate or hydrogen peroxide as the initiator and sodium dodecyl sulphate as the surfactant. Potentiometric titrations and electron microscopy established that the latex particles so prepared contained surface carboxylic acids (ca. one carboxyl group per 150–500 Å^2). The "low carboxyl" latices were prepared in a similar fashion but initiation by potassium persulphate was effected at 20–30°C and oxygen was rigorously excluded from the system. The complete absence of surface carboxyl groups could not be established unequivocally for these latices but the surface concentration of carboxyl groups was sufficiently small for them not to be detectable by potentiometric titration. Poly(vinyl acetate) latices were prepared by the solution polymerization of vinyl acetate in the absence of surfactant (16); no surface carboxyl groups could be detected with these latices.

The preparation of the amphipathic block copolymers of poly(ethylene oxide) with polystyrene and poly(vinyl acetate) has been described previously (2), as have the measurements of the critical flocculation temperatures and the poly(ethylene oxide) viscosity average molecular weights.

RESULTS

The critical flocculation temperature (cft) of various aqueous latices coated with well-anchored poly(ethylene oxide) (PEO) chains was determined in 0.39 M $MgSO_4$. All latices

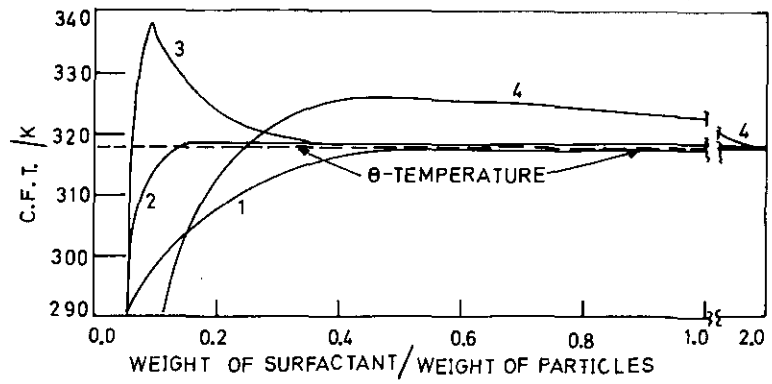

FIG. 1. Plots of the cft versus the ratio of the nominal weight of stabilizer in the bulk phase to the weight of latex particles. PEO molecular weight is 10,000 and pH = 4.65. Curve 1—poly(vinyl acetate) latices; curve 2—"low carboxyl" polystyrene latices; curve 3—"high carboxyl" polystyrene latices; curve 4—poly(styrene-*co*-acrylic acid) latex particles.

flocculated on heating, demonstrating that the latices were enthalpically stabilized (4). The cft of these latices is defined as the minimum temperature at which flocculation was evident (2, 3).

Shown in Fig. 1 are plots of the cft versus the nominal concentration of the amphipathic PEO stabilizer, the PEO chains having a viscosity average molecular weight ($\langle M_V \rangle$) of 10,000. Although these plots are not strictly adsorption isotherms, the adsorption of the stabilizer presumably increases monotonically to a constant value as the abscissa increases. Smooth curves have been drawn through the large number of points that were determined for each curve.

For poly(vinyl acetate) latices, the cft increased monotonically with increasing concentration of stabilizer (curve 1) to the limiting value corresponding to the θ-temperature (318 K) for free PEO chains in 0.39 M $MgSO_4$ (2, 17). Similar results were obtained for "low carboxyl" polystyrene latices (curve 2). The "high carboxyl" latices, however, exhibited a definite maximum (curve 3) in their cft. The maximum (in this case 338 K) was significantly higher than the θ-temperature, showing that in the vicinity of the cft it is possible to prepare latices that are stable in dispersion media considerably worse than θ-solvents. This is the phenomenon of enhanced steric stabilization. Note that the position of the maximum along the abscissa axis depends upon the efficiency of the anchor group in attaching the PEO to the particle surface. Beyond the maximum the cft decreased to the θ-temperature. Clearly it was only at the lower concentrations of stabilizer that enhanced steric stabilization was observed and then only with the "high carboxyl" latices.

Dispersions that exhibited enhanced steric stabilization flocculated irreversibly. Only at higher stabilizer concentrations, when the cft was close to the θ-temperature, was reversible flocculation observed.

It was suspected that the existence of enhanced steric stabilization was associated with the hydrogen (H) bonding between the –OH groups in the surface carboxyl groups and the ether oxygen of the PEO chains. To test this hypothesis the cft's were determined for a PEO of $\langle M_V \rangle$ = 10,000 at three pH values (2.06, 4.65, and 10.6). Some results are shown in Fig. 2. At the lowest pH the cft maximum was significantly higher than that for pH =4.65. No curve is shown for the alkaline pH because at the concentrations of stabilizer corresponding to the maximum in the cft curves, the "high carboxyl" polystyrene latices flocculated at temperatures well below room temperature.

The influence of the molecular weight of the

stabilizing PEO on enhanced steric stabilization is displayed in Fig. 3. The same "high carboxyl" latex was used in all experiments. Very high molecular weight PEO ($\langle M_V \rangle$ = 800,000) did not seemingly exhibit a maximum in the cft and no enhanced steric stabilization was observed with this polymer at this pH. However, as the molecular weight was decreased the maximum in the cft plots appeared. The maximum was small for a PEO of $\langle M_V \rangle$ = 96,000 but it increased significantly as the molecular weight decreased. For a PEO of $\langle M_V \rangle$ = 1540 the enhancement of steric stabilization was so large that the cft in the range of the dotted line of Fig. 3 exceeded the boiling point of the aqueous dispersion medium and so could not be measured. The data are, however, strongly suggestive of a maximum in the curve. The cft in this case decreased only very slowly at higher stabilizer concentrations.

Particles of polystyrene into which 10% acrylic acid had been copolymerized were also used as the adsorbent for anchored PEO. These particles were prepared under conditions that normally gave "low carboxyl" latices. The latices, which also possessed surface carboxyl groups, exhibited enhanced steric stabilization (curve 4 in Fig. 1). The cft peak was, however, quite broad.

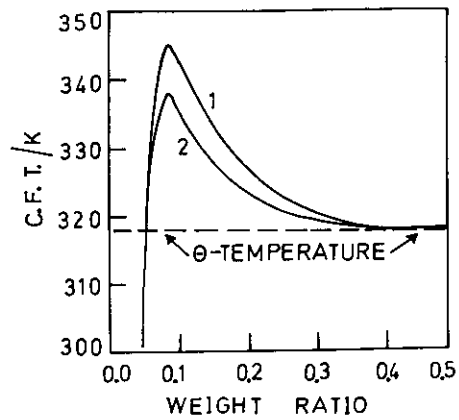

FIG. 2. Effect of pH on the plots of cft versus the ratio of the weight of stabilizer to the weight of latex particles. PEO molecular weight is 10,000. Curve 1—pH = 2.06; 2—pH = 4.65.

DISCUSSION

The foregoing results are consistent with the hypothesis that enhanced steric stabilization results from H bonding between the –OH group of the surface carboxyl species and the PEO ether oxygens (Fig. 4). In the absence of surface carboxyl groups, e.g., with poly(vinyl acetate) latices, no definite maximum was observed in the cft plots. As the bulk stabilizer concentration was increased more PEO chains were presumably adsorbed; in the plateau region the particles were fully coated. Reversible flocculation was then observed close

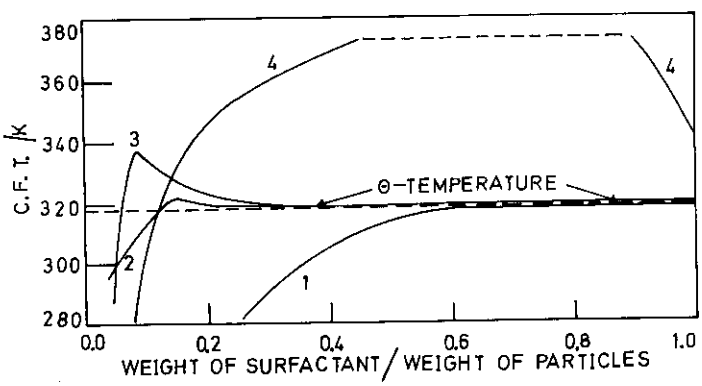

FIG. 3. Effect of PEO molecular weight on the plots of cft versus the ratio of the weight of stabilizer to the weight of latex particles at pH = 4.65. $\langle M_V \rangle$: curve 1—800,000; curve 2—96,000; curve 3—10,000; curve 4—1540.

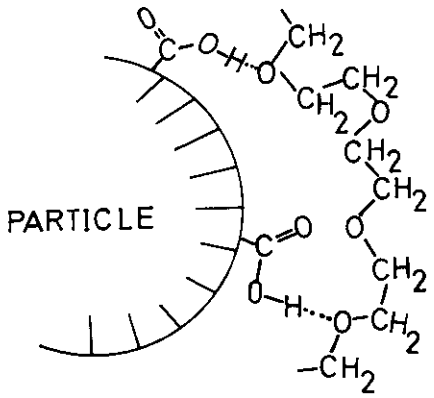

FIG. 4. Schematic representation of the hydrogen bonding interaction between the ether oxygens in PEO and the surface carboxylic acids.

to the θ-temperature for the stabilizing chains in free solution. This is the normal behavior of sterically stabilized latices (1–15), as predicted by the above theoretical discussion. Note that the electrostatic contribution to stability is negligible at the high ionic strengths studied, as was shown previously (4).

Enhanced steric stabilization was only observed when, in the absence of surface carboxyl groups, the surface would be incompletely covered. This suggests that under these conditions the conformation of the stabilizing moieties is changed because of the many H-bonding interactions between the PEO and the surface carboxyl groups. Presumably the chains interact with the surface so as to adopt a less extended conformation [the transformation (a) to (b) shown in Fig. 5]. As a result of this flat conformation, the thermodynamic parameters that govern segment-solvent and segment–segment interactions are no longer those relevant to the chains in free solutions or to chains attached to interfaces with which they do not interact strongly.

That the change in conformation due to multipoint anchoring can be significant is illustrated by the following approximate calculation. Potentiometric titration studies suggested that there was one carboxyl group per, say, 200 Å^2. For a PEO of molecular weight 10,000, the area occupied by the macromolecule on the surface is approximately 5000 Å^2. Hence, each chain could interact with 25 carboxyl groups. This would on the average lower the molecular weight of the PEO between anchor points to only 200, i.e., pentamer ($-CH_2CH_2O-$) groups. Clearly even interaction with only half of the surface carboxyl groups (as occurs at pH = 4.65) would significantly change the conformation of the PEO chains to one with only a small number of segments between anchor points.

The foregoing discussion suggests that if the surface carboxyl groups were deprotonated, the H bonding could not occur. Thus latices exhibiting enhanced steric stabilization would be converted into latices exhibiting incomplete surface coverage [transformation (b) to

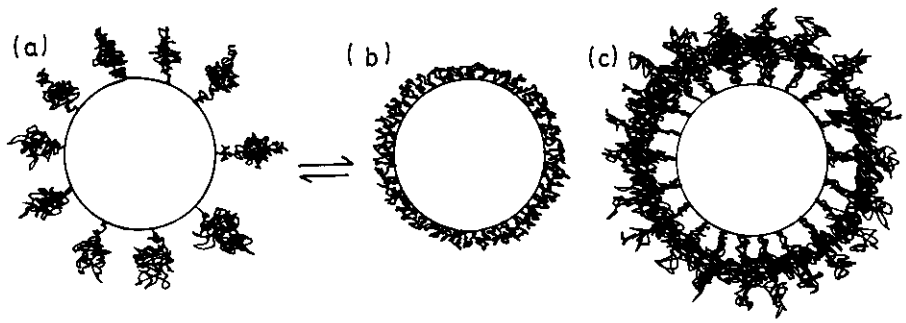

FIG. 5. Schematic representation of the effect of multipoint anchoring on the polymer conformation; (a) incomplete surface coverage and no interaction of PEO with the surface; (b) as in (a) but with a flat conformation due to surface interactions; (c) complete surface coverage with little surface interaction allowed.

(a) in Fig. 5]. Latices with incomplete PEO surface coverage were shown previously (2) to flocculate at lower temperatures. This explains why latices exhibiting enhanced steric stabilization flocculated when the pH of the dispersion medium was made alkaline. Moreover, it explains the increase in the cft maximum when the pH was lowered from 4.65 to 2.06. The surface carboxyl groups have a pK_a corresponding to a bulk pH of 4.6 (15, 18). Thus at pH = 4.65 only about half the surface groups would be protonated. Lowering the pH to 2.06 results in increased protonation of the surface carboxyl groups. The increased interaction of these groups with the PEO chains perturbs the conformation of the stabilizing chains even more than at pH = 4.65. An even greater cft maximum is thus observed.

The decrease in the cft values beyond the maximum is presumably associated with the increased adsorption of the anchored PEO chains on the particle surface. The upshot of this is that to accommodate further stabilizer adsorption, the adsorbed chains must adopt a more vertically oriented conformation [see (c) in Fig. 5] rather than a flat one. Moreover the anchor polymers may well cover many of the surface carboxyl groups. It is scarcely surprising that under these conditions high carboxyl latices flocculate reversibly near to the θ-point for chains in free solution.

The influence of the PEO molecular weight on the enhancement of steric stabilization was marked. Very high molecular weight chains were not significantly influenced by interactions with the surface, presumably because most of the segments are distant from the surface and are not affected by surface interactions. Conversely for very low molecular weight chains almost all the segments are perturbed as the calculation presented above shows. This accentuates the enhancement of steric stabilization.

The experiment on the poly(styrene-*co*-acrylic acid) particles confirms the importance of surface carboxyl groups. The very broad cft observed for this latex probably arises from the projection of the polyacid chains into solution.

The preceding discussion provides a qualitative picture of the likely origin of enhanced steric stabilization. It is necessary to consider more closely why the cft at the maximum is greater than the θ-temperature for the chains in free solution. It is not known as yet whether the cft's observed near the maximum correlate strongly with the θ-temperatures of the perturbed chains. However, in view of the strong correlations reported previously (1–5), this seems likely and we will adopt this assumption in the following discussion.

The critical flocculation temperature (T_C) is obtained by setting ΔG_R ($=\Delta H_R - T\Delta S_R$) $=0$, where ΔG_R is the free energy of close approach of two sterically stabilized particles. Thus for model sterically stabilized PEO lattices (2–5)

$$T_C = \theta = \Delta H_R/\Delta S_R.$$

Experimentally it was found that dispersions that exhibited enhanced steric stabilization flocculated irreversibly. This suggests that in order to induce flocculation it is necessary to break some H-bonding interactions. Bond breakage converts the particles into a system with incomplete surface coverage, which has been shown previously to result in irreversible flocculation (2). Therefore, we may write

$$T_C = \frac{\Delta H_R + (n/N_A)\Delta\bar{H}_{HYD}}{\Delta S_R + (n/N_A)\Delta\bar{S}_{HYD}}, \quad [10]$$

where N_A is Avogadro's constant, n the number of H bonds formed in the interaction zone, and $\Delta\bar{H}_{HYD}$ and $\Delta\bar{S}_{HYD}$ are the molar enthalpy and entropy changes associated with H-bonding. If we consider the H-bonding terms as perturbations of ΔH_R and ΔS_R, we can use the binomial theorem to transform Eq. [10] into

$$T_C = \theta + \theta\left(\frac{n}{N_A}\right)\left(\frac{\Delta\bar{H}_{HYD}}{\Delta H_R}\right) - \theta\left(\frac{n}{N_A}\right)\left(\frac{\Delta\bar{S}_{HYD}}{\Delta S_R}\right), \quad [11]$$

where terms higher than the first are neglected and θ refers to chains in free solution.

We have shown previously (4) that ΔH_R and ΔS_R are both positive. Intuitively both $\Delta \bar{H}_{HYD}$ and $\Delta \bar{S}_{HYD}$ should be negative. Provided that $|\Delta \bar{S}_{HYD}/\Delta S_R| > |\Delta \bar{H}_{HYD}/\Delta H_R|$, Eq. [11] predicts cft values larger than θ. In agreement with the preceding discussion enhanced steric stabilization should therefore result from the significant decrease in configurational entropy that H-bonding interactions impose on the stabilizing chains. Moreover, Eq. [11] predicts a maximum in the cft as n increases to a maximum and then decreases to near zero. It also suggests that as

$$\Delta S_R \gg (n/N_A)\Delta \bar{S}_{HYD}$$

for high molecular weight chains, surface interactions should not perturb the cft greatly in this case; conversely a large increase in cft should be evident for low-molecular-weight chains, as observed experimentally.

The foregoing discussion hinges on the assumption that surface carboxylic acids can H-bond with ether oxygens. Pimentel and McClellan (19) in their classic book on H-bonding list carboxylic acids and ethers as well recognized H-bonding acids and bases, respectively. They also assert that the properties of any combination of these compounds will be affected by H-bond formation. The occurrence of strong H-bonding between the ether oxygens of PEO and the carboxyl groups of poly(acrylic acid) is evident from the mutual precipitation of the two polymers from aqueous solutions at suitably acid pH (20–22). There seems little doubt that the H-bonding postulated to explain enhanced steric stabilization can occur.

CONCLUSIONS

These experiments show that by anchoring the stabilizing moieties at a large number of points along the chain, the pattern of flocculation behavior of sterically stabilized dispersions may be profoundly altered. No longer are θ-solvents for the chains in free solution the limit of colloid stability. Instead stability may be observed in solvents of considerably worse solvency for the stabilizing chains than θ-solvents. This is because the multipoint anchoring so perturbs the polymer conformation that the thermodynamic parameters that govern the chains in free solution are no longer relevant. For PEO chains multipoint anchoring may be achieved through H-bonding interactions between the ether oxygen of the stabilizing chains and surface carboxyl groups. However, it ought to prove possible to anchor polyfunctional macromolecules, e.g., poly(vinyl alcohol), at many points along their chains; thus they should also impart enhanced steric stabilization.

ACKNOWLEDGMENTS

It is a pleasure to thank the Australian Research Grants Committee for supporting this project. R. E. gratefully acknowledges receipt of a Commonwealth Postgraduate Scholarship.

REFERENCES

1. NAPPER, D. H., *Trans. Faraday Soc.* **64**, 1701 (1968).
2. NAPPER, D. H., *J. Colloid Interface Sci.* **32**, 106 (1970).
3. NAPPER, D. H., *J. Colloid Interface Sci.* **33**, 384 (1970).
4. NAPPER, D. H., AND NETSCHEY, A., *J. Colloid Interface Sci.* **37**, 528 (1971).
5. EVANS, R., DAVISON, J. B., AND NAPPER, D. H., *J. Polymer Sci.* **B10**, 449 (1972).
6. EVANS, R., AND NAPPER, D. H., *Kolloid Z. Z. Polymere* **251**, 409 (1973).
7. EVANS, R., AND NAPPER, D. H., *Kolloid Z. Z. Polymere* **251**, 329 (1973).
8. FLORY, P. J., "Principles of Polymer Chemistry," p. 533. Cornell University Press, Ithaca, New York, 1953.
9. FLORY, P. J., private communication (1971).
10. DOROSZKOWSKI, A., AND LAMBOURNE, R., *J. Polymer Sci.* **C34**, 253 (1971).
11. FLORY, P. J., AND KRIGBAUM, W. R., *J. Chem. Phys.* **18**, 1086 (1950).
12. FLORY, P. J., *in* "Principles of Polymer Chemistry," p. 543. Cornell University Press, Ithaca, New York, 1953.
13. HESSELINK, F. TH., VRIJ, A., AND OVERBEEK, J. Th. G., *J. Phys. Chem.* **75**, 2094 (1971).
14. FLORY, P. J., *in* "Principles of Polymer Chemistry,"

p. 525. Cornell University Press, Ithaca, New York, 1953.
15. OTTEWILL, R. H., AND SHAW, J. N., *Kolloid Z. Z. Polymere* **215**, 161 (1967).
16. NAPPER, D. H., AND PARTS, A. G., *J. Polymer Sci.* **61**, 113 (1962).
17. BAILEY, F. E., AND CALLARD, R. W., *J. Appl. Polymer Sci.* **1**, 56 (1959).
18. OTTEWILL, R. H., AND SHAW, J. N., *Kolloid Z. Z. Polymere* **218**, 34 (1967).
19. PIMENTEL, G. C., AND MCCLELLAN, A. L., *in* "The Hydrogen Bond," pp. 195–196. Freeman, San Francisco, 1960.
20. BAILEY, F. E., LUNDBERG, R. D., AND CALLARD, R. W., *J. Polymer Sci.* **A2**, 845 (1964).
21. BAILEY, F. E., AND KOLESKE, J. V., *in* "Nonionic Surfactants" (M. J. Schick, Ed.), Vol. 1, p. 819. Marcell Dekker, New York, 1967.
22. SMITH, K. L., WINSLOW, A. E., AND PETERSEN, D. E., *Ind. Eng. Chem.* **51**, 1361 (1959).

(*Reprinted from Nature, Vol. 246, No. 5427, pp. 34–35, November 2, 1973*)

Flocculation of Latices by Low Molecular Weight Polymers

POLYELECTROLYTES are increasingly being used as flocculants for electrostatically stabilised dispersions of colloidal particles in such diverse fields as water treatment and mineral processing[1]. Suitable polyelectrolytes, which are usually effective at low concentrations ($\leqslant$10 p.p.m.), invariably have a high molecular weight[2] (a viscosity average molecular weight $M_V > 10^5$). They seem to function by a bridging mechanism whereby the flocculant interferes with the free movement of the particles[1–6].

We now report that even low molecular weight non-ionic polymer molecules ($M_V \geqslant 10^3$ to 10^4) are able to flocculate some polymer latices. They also seem to function by a bridging mechanism but require the presence at the particle surfaces of suitable groups with which the flocculant can interact specifically.

The new phenomenon was first discovered with an apparently electrostatically stabilised aqueous polystyrene latex (mean radius 24 nm), prepared by the method of Ottewill and Shaw[7]. Figure 1*a* displays the course of flocculation, which was followed turbidimetrically, on addition of poly(ethylene oxide) (PEO) to the latex at 35° C. (The initial light scattering was compensated for.) Several samples of low molecular weight PEO (ex Union Carbide Australia Ltd) were examined using the latex at a particle concentration of $\sim 10^{12}$ cm^{-3}. In the absence of PEO the particles exhibited long term stability, whether or not 0.2 M HCl was present (line 1). When low molecular weight PEO was added in the absence of 0.2 M HCl no flocculation could be detected at any polymer concentration. But the addition of PEO, at 20 p.p.m., of either $M_V = 4{,}000$ or 23,000 in the presence of 0.2 M HCl resulted in rapid flocculation of the latex (curves 2 and 3). The higher molecular weight polymer was the more effective. Very high molecular weight polymer $M_V = 1 \times 10^6$ was also an effective flocculant at concentrations of only a few p.p.m.

Polystyrene latices prepared by the method of Ottewill and Shaw[7] possess surface carboxylic acid groups[8,9]. To investigate the role of these groups, polystyrene latices were prepared at low temperatures (<30° C); as we have shown elsewhere[10], such latices possess no detectable surface carboxylic acid groups. Interestingly these latices failed to flocculate on addition of PEO in the presence of 0.2 M HCl. On the other hand, polystyrene latices sterically stabilised[11] by poly(acrylic acid) (PAA) of $M_V = 19{,}300$ were also found to be flocculated by low (and high) molecular weight PEO (Fig. 1*b*). Again 0.2 M HCl was necessary for flocculation. We note that in the absence of PEO these latices exhibit long term entropic stabilisation[11] (line 4).

The foregoing experiments point to the central role played by the surface carboxylic acid group in promoting flocculation. They suggest the following mechanism for flocculation by low molecular weight polymers: At suitably low *p*H the surface carboxylic acid groups are predominantly unionised and so can H bond with the ether oxygens of the PEO chains. The occurrence of such H bonding is forcefully demonstrated by the phase separation of mixtures of PAA and PEO from aqueous solutions at low *p*H (refs 12 and 13). For the conditions relevant to curve 3 in Fig. 1*a*, the centres of the particles were separated, on average, by ~1,000 nm, if a cubic array is assumed. The r.m.s. end-to-end length of the PEO chains was calculated[14] to be only ~10 nm. Obviously on average the polymer chains could not possibly span the distance between the particle surfaces. Therefore the PEO chains may reasonably be inferred to have become attached to one particle by H bonding to the surface carboxylic acid groups and to have become attached to a second (or more) particle(s) in subsequent Brownian collisions. Free movement of the latex particles was thus prevented, corresponding to bridging flocculation. According to this postulated mechanism, no flocculation would be expected at higher *p*H values because the ionised carboxylic acid groups would be unable to H bond with the PEO. Also no flocculation would be expected in the absence of surface carboxylic acid groups. Both expectations were realised.

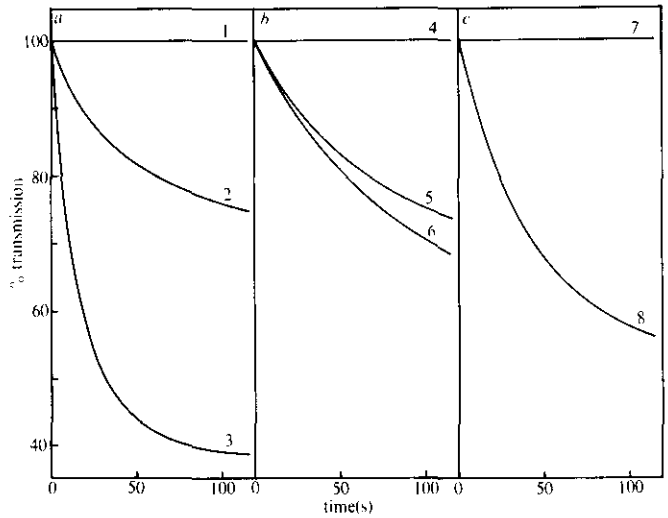

Fig. 1 The % transmission as a function of time for polystyrene latices. *a*, Curves for latices containing surface carboxylic acid groups: 1, no PEO added; 2, PEO of $M_V = 4{,}000$ added; 3, PEO of $M_V = 23{,}000$ added. *b*, Curves for latices stabilised by PAA: 4, no PEO added; 5, PEO of $M_V = 4{,}000$ added; 6, PEO of $M_V = 23{,}000$ added. *c*, Curves for latices stabilised by PEO: 7, no PAA added; 8, PAA of $M_V = 19{,}300$ added. Flocculant added at 20 p.p.m. in *a* and *c* and 50 p.p.m. in *b*.

If this explanation is correct then it is also predicted that low molecular weight PAA should be able to flocculate latices stabilised solely by PEO chains. Figure 1*c* shows the flocculation induced by the addition of PAA ($M_V = 19{,}300$) to a polystyrene latex sterically (in this case enthalpically) stabilised by PEO ($M_V = 23{,}000$). Again no flocculation was evident unless 0.1 M HCl was also present to convert most of the carboxylic acid groups into the unionised form.

The phenomenon seems to be closely analogous to the bridging flocculation observed with high molecular weight polyelectrolytes. Both are characterised by the intervention of the polymeric flocculant by promoting 'sticky' collisions between the particles, the flocculated particles often being separated by some distance[15]. There is thus no need to reduce to near zero the repulsive potential energy between the particles, whether electrostatically or sterically generated, to permit flocculation to occur.

We thank the Australian Research Grants Committee for financial support.

ROBERT EVANS
D. H. NAPPER

Department of Physical Chemistry,
University of Sydney,
NSW 2006

Received September 3, 1973.

1 Napper, D. H., and Hunter, R. J., *M.T.P. Int. Rev. Sci., phys. Chem. Ser.*, **1**, 7, 294 (1972).
2 La Mer, V. K., and Healy, T. W., *Rev. pure appl. Chem.*, **13**, 112 (1963).
3 Ries, jun., H. E., and Meyers, B. L., *Science, N.Y.*, **160**, 1449 (1968).
4 Gregory, J., *Trans. Faraday Soc.*, **65**, 2260 (1969).
5 Ries, jun., H. E., *Nature*, **226**, 72 (1970).
6 Williams, D. J. A., and Ottewill, R. H., *Kolloid-Z. Z. Polym.*, **243**, 141 (1971).
7 Ottewill, R. H., and Shaw, J. N., *Kolloid-Z. Z. Polym.*, **215**, 161 (1967).

[8] Ottewill, R. H., and Shaw, J. N., *Kolloid-Z. Z. Polym.*, **218**, 34 (1967).
[9] Shaw, J. N., and Marshall, M. C., *J. Polym. Sci. Pt A-1*, **6**, 449 (1968).
[10] Smitham, J. B., Gibson, D. V., and Napper, D. H., *J. Colloid Interface Sci.* (in the press).
[11] Evans, R., Davison, J. B., and Napper, D. H., *J. Polym. Sci., Pt. B*, **10**, 449 (1972).
[12] Bailey, F. E., Lundberg, R. D., and Callard, R. W., *J. Polym. Sci. Pt. A*, **2**, 845 (1964).
[13] Bailey, F. E., and Koleske, J. V., *Nonionic Surfactants* (edit. by Schick, M. J.), **1**, 819 (Dekker, New York, 1967).
[14] Kurata, M., Iwama, M., and Kamada, K., *Polymer Handbook* (edit. by Brandrup, J., and Immergut, E. H.), IV-58 (Interscience, New York, 1966).
[16] Walles, W. E., *J. Colloid Interface, Sci.*, **27**, 797 (1968).

Printed in Great Britain by Henry Ling Ltd., at the Dorset Press, Dorchester, Dorset

POLYMER LETTERS VOL. 10, PP. 449–453 (1972)

THE PREPARATION OF AQUEOUS ENTROPICALLY STABILIZED LATICES

Steric stabilization is the generic term used to describe the stability against flocculation that nonionic macromolecules impart to dispersions of colloidal particles (e.g., polymer latices) (1). The thermodynamic changes which generate the positive repulsive potential energy in steric stabilization may be classified as either entropic (2–4) or enthalpic (3,4), or a combination of both (4). For example, in entropic stabilization the net entropy change on close approach of two latex particles is negative and opposes flocculation whereas the overall enthalpy change is negative and promotes it.

To-date entropically stabilized latices have been prepared only in nonaqueous dispersion media (5). Conversely all aqueous sterically stabilized latices have hitherto exhibited enthalpic stabilization (4,6). Ottewill (1) has properly summarized the current position by tentatively concluding that "it would appear that enthalpic contributions are probably the most important in the stabilization of aqueous dispersions and entropic contributions in nonaqueous systems."

The type of steric stabilization imparted by a given macromolecule can be predicted from the signs, and relative magnitudes, of the enthalpy (κ_1) and entropy (ψ_1) of dilution parameters of the stabilizing moieties in free solution in the dispersion medium (4,7).

Negative values for κ_1 and ψ_1, when coupled with obedience to the inequality $|\kappa_1| > |\psi_1|$, presage enthalpic stabilization. Enthalpic stabilization may be shown theoretically (7) to be characterized at least in principle by flocculation of the dispersion on heating. Experimentally incipient flocculation has been found to occur on heating to the θ-temperature of the stabilizing moieties in free solution in the dispersion medium (4,8).

In contrast, positive values for κ_1 and ψ_1, such that $\psi_1 > \kappa_1$, result in entropic stabilization (4,5). Theory implies that entropically stabilized dispersions are characterized by flocculation on cooling to the θ-temperature (7).

Before these studies were undertaken, only enthalpically stabilized latices exhibiting flocculation on heating had been prepared in aqueous dispersion media. There appeared, however, to be no valid thermodynamic reason why entropically stabilized dispersions could not be prepared in water.

Silberberg et al. (9) found that for poly(acrylic acid)(PAA) in 0.2M HCl ψ_1 and κ_1 are both positive. Moreover, ψ_1 is greater than κ_1 if the temperature exceeds the θ-temperature (287°K). These data imply that aqueous latices stabilized by PAA should be entropically stabilized. This inference is strictly correct only in the presence of 0.2M HCl (to suppress any electrostatic effects) and at temperatures immediately above the point of incipient flocculation (7).

© 1972 by John Wiley & Sons, Inc.

We now report the preparation of aqueous latices stabilized by PAA and the verification that these latices are entropically stabilized.

Experimental

PAA was prepared by the heterogeneous polymerization of acrylic acid (B.D.H. laboratory grade purified by fractional crystallization at 0°C (10)) in butanone. The initiator was azobisisobutyronitrile. Samples differing in molecular weight were obtained by the addition before polymerization of various amounts of n-butyl mercaptan. However, the highest molecular weight PAA (89,700) was prepared by the solution polymerization of acrylic acid in water, using hydrogen peroxide as initiator (11).

To ensure that the PAA chains were strongly anchored onto the surfaces of the latex particles, nominally insoluble poly(vinyl acetate) chains were grafted onto the PAA. Poly(acrylic acid-g-vinyl acetate) was prepared by reacting PAA with glycidyl methacrylate (e.g., 5% by weight) in 1,4-dioxane at 50°C for, say, one week. Hydroquinone (0.1%) was added to inhibit polymerization of the resulting macromonomer adduct. Subsequent polymerization in dioxane of the macromonomer with vinyl acetate (30% w/w based on PAA) produced the desired graft copolymer. All copolymers were completely soluble in water.

Poly(vinyl acetate-g-acrylic acid) was also used as a stabilizer. It was prepared by copolymerizing vinyl acetate and glycidyl methacrylate (10% v/v) in dioxane. PAA was then dissolved in the resulting copolymer solution and grafting effected by refluxing for 16 hr.

Poly(methacrylic acid-g-vinyl acetate) was prepared in a fashion analogous to that for the acrylic acid copolymer.

All latices were generated by the heterogeneous polymerization of vinyl acetate (2.5% w/w) in water at 50°C in the presence of an excess of graft copolymer. Potassium persulfate was used as the initiator because it had been demonstrated that at relatively high ionic strengths, any electrostatic contribution to stability may be ignored (7).

Acrylamide (ex Fluka AG) was polymerized in refluxing butanone on addition of benzoyl peroxide. Vinyl acetate (40% w/w based on acrylamide) was grafted onto the resulting polyacrylamide in water, using potassium persulfate as initiator at 50°C. The resulting poly(acrylamide-g-vinyl acetate) was completely soluble in water. Subsequent polymerization at 50°C of an excess of vinyl acetate (2.5% w/w) in an aqueous solution of this graft copolymer generated the desired latex.

All number average molecular weights ($<M_n>$) were measured with a Hewlett Packard Series 500 rapid membrane osmometer. Particle diameters were determined by use of a Spinco Model E analytical ultracentrifuge (12). Relative diameters only are of significance because the particle densities were assumed to be unchanged by the adsorption of stabilizer.

Critical flocculation temperatures were measured visually by noting the temperature at which the turbidity increased rapidly (4).

TABLE I

Incipient Flocculation Results for Poly(vinyl Acetate) Latices Stabilized by Poly(acrylic acid) in 0.2M HCl

PAA $\langle M_n \rangle$	Particle Diam., Å	c.f.t., °K	θ,[a] °K	Reversibility
9800	390	287±2	287(±5)	irrev.
19300	120	289±2	287(±5)	rev.
19300	340	289±2	287(±5)	rev.
19300	470	293±3	287(±5)	some irrev.
51900	370[b]	283±2	287(±5)	rev.
51900	620	287±3	287(±5)	some irrev.
89700	110	281±1	287(±5)	rev.
89700	160	281±2	287(±5)	some irrev.
89700	500	280±3	287(±5)	rev.

[a] Literature θ-temperature (9). The probable error is a conservative estimate.

[b] Prepared using poly(vinyl acetate-*g*-acrylic acid) as stabilizer.

Results and Discussion

The results obtained for aqueous poly(vinyl acetate) latices stabilized by PAA in the presence of 0.2M HCl are shown in Table I. All dispersions flocculated on cooling. This demonstrates unequivocally that the latices are entropically stabilized at temperatures immediately above the critical flocculation temperature (c.f.t.) (7). The c.f.t. is in essence the point of incipient flocculation, being the maximum temperature at which flocculation was observed. The results show that the c.f.t. was relatively insensitive to the molecular weight of the stabilizing PAA over almost a decade range. A strong correlation of the c.f.t. with the θ-temperature reported by Silberberg et al. (9) is evident. No apparent dependence of the c.f.t. on the particle radius was observed. Whether the anchor polymer was grafted onto the stabilizing moieties or vice versa did not apparently influence the observed c.f.t. With the exception of the latex stabilized by the lowest molecular weight PAA, all dispersons exhibited flocculation that could in the main be reversed by warming to above the c.f.t.

The general pattern of results obtained with the aqueous entropically sta-

bilized latices is identical with that observed previously for aqueous latices enthalpically stabilized by poly(ethylene oxide) (4). Moreover both sets of data are in fair agreement with results obtained for entropically stabilized nonaqueous latices (5). Apparently the same general thermodynamic considerations govern steric stabilization whether it is operative in aqueous or nonaqueous dispersion media, whether enthalpic or entropic changes provide stability, or whether flocculation is induced by heating or cooling.

These experimental results, as well as those obtained previously (4,5), may be compared with the recent theoretical predictions of Hesselink et al. (13). Their theory of steric stabilization demands a strong dependence of the c.f.t. upon molecular weight; the absence of any correlation of the c.f.t. with the θ-temperature; the stability of latices in dispersion media of solvency worse than θ-solvents; and a strong dependence of the c.f.t. upon particle size. Unfortunately none of their theoretical predictions appears to be borne out by these experiments.

Silberberg et al. (9) found that for polyacrylamide (PAM) in water at room temperature, ψ_1 and κ_2 were both positive with $\psi_1 > \kappa_1$. It may therefore be inferred that aqueous latices stabilized by PAM are entropically stabilized. However, as the θ-temperature of PAM in pure water is 235°C, such latices cannot be flocculated simply by cooling because the water freezes before the θ-point is reached.

Aqueous latices stabilized by PAM have been found to be remarkably stable to the presence of normally effective flocculating reagents. Neither magnesium sulfate nor urea when present in the dispersion medium at saturation concentrations induced flocculation; both saturated potassium chloride and 10M sulfuric acid were also ineffectual. However, at pH = 3.0 the presence of 2.1M ammonium sulfate in the continuous phase permitted flocculation to be observed on cooling. Four different PAM stabilized latices exhibited c.f.t.'s in the range 294°-299°K on cooling. Aqueous latices stabilized by PAM are thus confirmed to be entropically stabilized, at least in the presence of 2.1M ammonium sulfate. Some uncertainty, however, attends these c.f.t. values because of the possible hydrolysis of PAM during latex preparation. The observation that the c.f.t.'s increased only slowly as the latices aged suggests, however, that hydrolysis was probably minimal.

Finally, preliminary experiments on aqueous latices stabilized by poly(methacrylic acid) (PMAA) indicated that flocculation was induced on heating. This implies that these dispersions are enthalpically stabilized as would be expected from the negative values for ψ_1 and κ_1 reported previously (9). Apparently the rather subtle differences in chemical constitution between PAA and PMAA are sufficient to reverse the roles of the net enthalpy and entropy changes controlling stabilization. Molecular model considerations suggest that PMAA should be a stiffer chain than PAA. This stiffness, coupled with the greater intramolecular hydrogen bonding in PMAA, provides a simple, if incomplete, rationalization of the reduced significance of entropy effects in steric stabilization by PMAA.

The authors are grateful to the Australian Research Grants Committee for financial support of these studies.

References

(1) R. H. Ottewill, Ann. Rep. Progr. Chem. (Chem. Soc. London), A66, 212 (1969).
(2) M. van der Waarden, J. Colloid Sci., 5, 317 (1950).
(3) R. H. Ottewill and T. Walker, Kolloid Z. Z. Polym., 227, 108 (1968).
(4) D. H. Napper, J. Colloid Interface Sci., 32, 106 (1970).
(5) D. H. Napper, Trans. Faraday Soc., 64, 1701 (1968).
(6) D. H. Napper, Kolloid Z. Z. Polym., 234, 1149 (1969).
(7) D. H. Napper and A. Netschey, J. Colloid Interface Sci., 37, 528 (1971).
(8) D. H. Napper, J. Colloid Interface Sci., 33, 384 (1970).
(9) A. Silberberg, J. Eliassaf, and A. Katchalsky, J. Polym. Sci., 23, 259 (1957).
(10) T. R. Paxton, J. Polym. Sci., B, 1, 73 (1963).
(11) A. Alexandrowics, J. Polym. Sci., 40, 91 (1959).
(12) T. Svedberg and J. B. Nichols, J. Amer. Chem. Soc., 45, 2910 (1923).
(13) F. Th. Hesselink, A. Vrij, and J. Th. G. Overbeek, J. Phys. Chem., 75, 2094 (1971).

Robert Evans
Jenny B. Davison
D. H. Napper

Dept. of Physical Chemistry
University of Sydney
Sydney, N.S.W., 2006, Australia

Received January 14, 1972

Kolloid-Z. u. Z. Polymere **251**, 409–414 (1973)

From the Department of Physical Chemistry, The University of Sydney (Australia)

Steric stabilization I

Comparison of theories with experiment

By R. Evans and D. H. Napper

With 2 figures and 1 table

(Received September 5, 1972)

Introduction

Steric stabilization refers to the stabilization of colloidal particles (e.g., polymer latex particles) against flocculation that is imparted by nonionic macromolecules (1, 2). Several statistical thermodynamic theories of steric stabilization have been proposed since the early experiments by *Zsigmondy* (3) on the "protective action" of natural macromolecules. More recent experimental studies (4–8) on model latices now permit the qualitative validity of the various theories to be assessed. These model latices, which are designed to ensure that the stabilizing macromolecules are attached irreversibly to the surfaces of the particles, appear to undergo reversible, thermodynamic flocculation (4–8).

In what follows we will show that with the notable exception of *Fischer*'s solvency theory (9), all of the theories of steric stabilization advanced heretofore are apparently in conflict with experiment. Possible reasons for these discrepancies are then explored.

Comparison of theories with experiment

We begin by comparing the predictions of the various theories of steric stabilization with the results of experiments.

(i) Entropy theories

Mackor (10, 11) was the first to attempt to calculate the repulsive potential energy in steric stabilization. He argued that the close approach of the two colloidal particles resulted in a decrease in the volume accessible to the stabilizing moieties and thus to a decrease in the configurational entropy of the stabilizing chains. The loss of configurational entropy was calculated for short rods, freely jointed at the particle surface, by using the *Planck-Boltzmann* relationship ($S_{\text{conf}} = k \ln W$) (10). The free energy of repulsion (ΔG_R) was then calculated from $\Delta G_R = -T\Delta S_{\text{conf}}$. Using essentially this approach *Clayfield* and *Lumb* (12–15) have performed elaborate *Monte Carlo* calculations for stabilizing polymer chains to find ΔS_{conf} and hence ΔG_R.

It is clear that calculations of this type seemingly ignore the presence of any molecules of the dispersion medium (hereafter also termed the solvent) that are associated with the chains. The macromolecules alone are assumed to contribute to ΔS_{conf}. This approach implies that a stable dispersion once formed, cannot be flocculated merely by changing the solvency of the dispersion medium. Yet there is compelling experimental evidence (4–8) to show that the solvency of the dispersion medium critically determines the stability of sterically stabilized dispersions. Moreover there exist thermodynamic arguments (7) which imply that those dispersions that flocculate on heating (e.g., many aqueous latices) are enthalpically stabilized, not entropically stabilized. *Mackor*'s approach ignores all enthalpy changes.

We infer that theories of steric stabilization that are couched solely in terms of the configurational entropy of the polymer and that ignore the presence of the solvent are, in general, incompletely formulated. Possibly they may be applicable to some dispersions

for which the dispersion medium is an athermal solvent for the stabilizing chains.

We also conclude that the synonymous use (16–18) of the terms "steric" and "entropic" stabilization is both incorrect and misleading. Sterically stabilized dispersions may be stabilized either entropically or enthalpically, or by a combination of enthalpic and entropic mechanisms (5, 7, 19).

(ii) Fischer's solvency theory

In an article published in this journal, *Fischer* (10) was the first to point out the critical importance in steric stabilization of the quality of the solvency that the dispersion medium displays towards the stabilizing chains. According to *Fischer*'s theory, if the dissolved polymer sheaths surrounding two sterically stabilized particles were to interpenetrate, the chemical potential of the solvent in the interaction zone would decrease. A gradient in chemical potential would thus be established between the solvent molecules in the interaction zone and those in the external dispersion medium. As a result, solvent external to the interaction zone would diffuse into the zone and so force the stabilizing moieties, and the particles, apart. This corresponds to the generation of an excess osmotic pressure. *Fischer* related the repulsive potential energy to the second virial coefficient (B) of the polymer in *free* solution using the *Flory-Huggins* theory:

$$\Delta G_R \sim 2BRT\langle c_g\rangle(\Delta V) \qquad [1]$$

where $\langle c_g\rangle$ is the mean segment concentration and (ΔV) is the overlap volume.

It must be admitted that several important criticisms of *Fischer*'s theory may be raised: first, the use of a mean segment concentration is obviously an approximation because the segment density is a function of the distance from the particle surface; second, *Fischer*'s theory by concentrating on interpenetration tends to ignore the compression of the polymer chains that must occur when the minimum distance between the particle surfaces is less than the contour length of the polymer chains. We note also that *Fischer*'s theory disregards all virial coefficients higher than the second.

Despite these obvious quantitative shortcomings, *Fischer*'s theory predicts all the qualitative features of incipient flocculation that have been observed thus far (4–8). These features are discussed in detail below but briefly *Fischer*'s theory predicts (i) that instability should be evident in solvents worse than θ-solvents, (ii) that the transition from stability to instability should occur near to the θ-point and (iii) that no marked dependence of the incipient instability point upon the molecular weight of the stabilizing moieties or the particle radius should be observed. Although all of these qualitative predictions have been verified experimentally (4–8), this does not imply that *Fischer*'s theory is necessarily correct quantitatively.

(iii) Entropy plus solvency theories

The assumption by *Fischer* that the mean segment concentration may be used to calculate the distance dependence of the repulsive potential energy is obviously an approximation. It corresponds to approximating the segment density by a step function. *Meier* (20) therefore evaluated the segment density distribution function at planar interfaces for linear chains terminally attached at one end ("tails"). His calculations are incorrect due to the inclusion of certain conformations that actually penetrate the impenetrable particle surfaces (21).

Hesselink (21, 22), has corrected this mistake and extended the theory to "loops" (i.e., linear chains which are attached at both ends). The distribution functions of both *Meier* and *Hesselink* fail to go to zero at distances greater than the contour lengths of the attached chains; however, this shortcoming may be neglected for many purposes.

Meier (20) also combined the entropy approach of *Mackor* (10) and *Clayfield* and *Lumb* (12–15) with *Fischer*'s solvency theory (9) to produce a generalized hybrid theory of steric stabilization. His quantitative predictions are in error because of the use of an incorrect segment density function as mentioned previously. Again, *Hesselink*, *Vrij* and *Overbeek* (23) (HVO) have corrected this error and extended the theory to stabilization by loops.

The major predictions of the HVO theory for dispersions of flat plates stabilized by tails are succinctly presented in fig. 1. This displays the predicted lines of demarcation between stable and unstable dispersions for varying molecular weight of the stabilizing polymer, different surface coverages and different edge lengths. The abscissa, the intramolecular expansion factor α, is a measure of the quality of the solvency of the dispersion medium for the stabilizing macro-

molecules. Although these results apply to tails, HVO theory for loops undoubtedly predicts qualitatively similar conclusions. Moreover, HVO admit that qualitatively similar findings will hold for spheres, although quantitative differences will be evident; this is substantiated in Part II by the use of the *Deryagin* (24) method for calculating the repulsion for spheres from the repulsion potential for flat plates.

The following comparisons of the predictions of the HVO theory (23) with experiment may be made:

(a) It is clear from fig. 1 that the points corresponding to $\alpha = 1.00$ (i.e., to θ-solvents) have no special significance *vis-à-vis* flocculation. Theta points are just like other

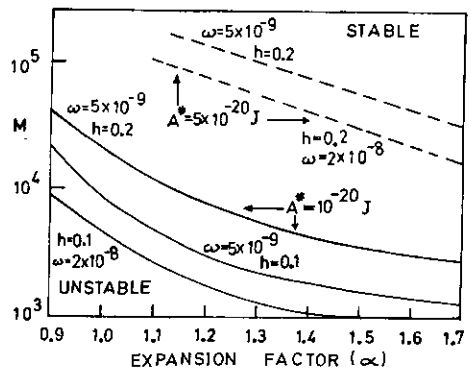

Fig. 1. The lines of demarcation between stable and unstable dispersions of flat plates according to HVO theory. The stabilizing moieties are tails: ω is the weight of stabilizer per unit surface area (g/cm²), h is the plate length (μm)

points on the curves. Yet there is abundant experimental evidence (4–8), which will not be fully retabulated here because it is too extensive, that the θ-point corresponds closely to the limit of stability of sterically stabilized dispersions. (Some typical results are, however, included below in table 1.) The θ-point and the critical flocculation point (c.f.p.) correlate strongly for both aqueous and non-aqueous latices whether flocculation is induced by addition of non-solvent, or by heating or cooling the latices. Over 40 different c.f.p.s. have been shown to correlate with their corresponding θ-points (4–8, 19).

Apparently HVO theory fails to predict this correlation between the c.f.p. and the θ-point.

(b) The HVO theory implies that the boundary between stability and instability is strongly dependent upon the molecular weight (M) of the stabilizing moieties (fig. 1). For a decade increase in M, α is predicted to decrease from e.g., 1.7 to 1.1. This is a large change in α. These two α values may be substituted into, e.g., the *Flory* relationship (25):

$$\alpha^5 - \alpha^3 = 2C_M\psi_1(1 - \theta/T)M^{1/2} \qquad [2]$$

where ψ_1 = entropy of dilution parameter and $\theta = (\varkappa_1/\psi_1)T$, where $\varkappa_1$ = enthalpy of dilution parameter. The parameter C_M in eqn. [2] is a constant for a given polymer in a given solvent such that

$$C_M = (27/2^{5/2}\pi^3)(\bar{v}_2^2/N_A\bar{V}_1)(M^{3/2}/\langle r^2\rangle_0^{3/2})$$

where $\bar{v}_2$ = partial specific volume of the polymer, $\bar{V}_1$ = molar volume of the solvent and $\langle r^2\rangle_0^{1/2}$ = unperturbed r.m.s. end-to-end length of the polymer chains in *free* solution. It is found from eq. [2] that the large change in α from 1.7 to 1.1 corresponds to a change in the c.f.p. of at least 100–200°K, for a θ-temperature within 50 °K of room temperature. The flocculation temperature of two latices stabilized by polymer chains which differ in molecular weight by a factor of ten should thus differ by 100–200 °K according to the HVO theory.

Table 1. Molecular weight dependence of the critical flocculation temperature (C.f.t.)

Stabilizing moieties	$\langle M\rangle$	C.f.t. (°K)	θ (°K)
PEO	1.0×10^6	317 ± 2	315 ± 3
PEO	8.0×10^5	316	316
PEO	3.2×10^5	315	314
PEO	9.6×10^4	316	315
PEO	4.9×10^4	316	314
PEO	2.3×10^4	314	315
PEO	1.0×10^4	318	319
PAA	9.8×10^3	287 ± 2	287 ± 5
PAA	1.9×10^4	289	287
PAA	5.2×10^4	283	287
PAA	9.0×10^4	281	287

Table 1 summarizes the incipient instability results obtained with latices stabilized by poly(ethylene oxide) (PEO) (5) and by poly(acrylic acid) (PAA) (8). The critical flocculation temperature (c.f.t.) is the temperature at which a sharp transition from stability to instability is observed. This was achieved by heating the latices stabilized by PEO but by cooling the latices stabilized by PAA. The former are enthalpically stabilized whereas the latter are entropically stabilized (4, 7, 8). The molecular weight of the PEO was varied over three decades

and that of PAA over one decade. Although small changes (< 10 °K) were evident, the c.f.t. was quite insensitive to M. Certainly any changes in c.f.t. are at least an order of magnitude less than those predicted by the HVO theory.

These experimental results, moreover, are consistent with those discussed in paragraph (a) above where it was mentioned that the c.f.p. correlates strongly with the θ-point. Because the θ-point is in principle independent of M, so must the c.f.p. (in this case the c.f.t.) be independent of M if the results are to be internally consistent.

Clearly the predictions of the HVO theory with respect to M are not substantiated by experiments with model dispersions.

HVO (23) cited the early data of *Heller* (2) as evidence for the validity of their theory. *Heller* did in fact observe a molecular weight dependence of the flocculation point (at least for lower values of M) of electrostatically stabilized latices that were additionally stabilized by *unanchored* PEO. These latices flocculated, e.g., in 0.5 M KCl at 20 °C. We have repeated *Heller*'s experiments and confirm the essential correctness of his observations. However latices stabilized by *anchored* PEO chains are quite stable in 0.5 M KCl. Indeed they are quite stable in 3 M KCl, which is a substantially worse solvent for PEO than is 0.5 M KCl. Apparently dispersions stabilized by unanchored PEO chains flocculate in 0.5 M KCl because the chains are not sufficiently well-anchored to the particle surface. This may be due to either lateral movement of the PEO away from the interaction zone or even desorption, both of which are expressly forbidden by the assumptions of the HVO theory. The molecular weight dependence observed with unanchored chains appears to be an artifact of displacement flocculation (7). *Molau*'s emulsion studies (25–28) suffer from the same artifact: our emulsion studies suggest that it is very difficult to eliminate displacement flocculation with emulsions (29).

Of course the values of M cited in table 1 refer to the overall molecular weight of the chains. The possibility must be considered that adsorption onto the surface at various points along the chains may drastically reduce these nominal values. There exists, however, convincing experimental evidence against this possibility: first, ultracentrifuge studies of the conformation of the chains attached to the particles (30) suggest that the stabilizing chains are quite extended normal to the surface, as indeed *Ottewill* (31) has also found in similar systems; second, for fully covered particles the surface area needed to convert extended polymers of nominal $M = 1 \times 10^6$ into polymers of actual $M = 1 \times 10^3$ by adsorption (either on close approach of the particles or on changing the solvency) is greater than the available area by a factor of ca. 10^3; third, when suitable surface groups are provided to generate additional adsorption of the stabilizing chains onto the surface in this way, experiments show that no longer is it possible to apply the thermodynamic parameters for the polymers in free solutions because the chains are too constrained (32). The θ-temperatures in table 1 all refer to the chains in free solution. We conclude that adsorption at points along the chains cannot explain the large discrepancy between HVO theory and experiment.

(c) HVO theory predicts that stability may be observed in solvents considerably worse than θ-solvents. It follows from what has been summarized in paragraphs (a) and (b) that such stability has not been observed for either tails or loops. We have in fact observed stability in solvents somewhat worse than θ-solvents but only when the polymer chains have been anchored at so many points (multipoint anchoring) that the free solution properties of the polymer are no longer relevant (32). This phenomenon may be termed "enhanced" steric stabilization.

(d) The HVO theory predicts that the stability of latices should be inversely dependent upon the particle radius in *Deryagin*'s approximation. We have shown that the c.f.p. of both aqueous and non-aqueous sterically stabilized latices are quite insensitive to the particle radius (4, 5, 7, 8). Again the HVO theory appears to lead to erroneous predictions.

We conclude that the major predictions of the HVO theory appear to be at odds with the results of experiments on model latices. The validity of the HVO theory must therefore be called into question. In particular, the experimental results suggest that the HVO theory appears to contain a significant term that improperly fails to become small near the θ-point

Formulation of entropy plus solvency theories

We now offer one possible origin for the disagreement between HVO theory and

experiment. It is proposed that the discrepancy arises from an insidious difficulty that intrudes when the entropy and solvency theories are combined. The HVO theory (23), following that of *Meier* (9), calculates the repulsive free energy by considering two processes:

(i) The loss of configurational free energy of the polymer molecules *alone* on the approach of the second particle. This is termed the volume restriction (VR) effect and is the effect postulated by *Mackor* (10).

(ii) An osmotic pressure (OP) effect that results from the interpenetration and compression of the polymer chains on close approach of the particles. This is, at least in part, the contribution first discussed by *Fischer*.

Contribution (i) was calculated from the loss of configurational entropy of random flight "lines-in-space" chains, composed of non-interacting segments. Contribution (ii) was calculated using the *Flory-Krigbaum* theory (33).

Fig. 2 provides a diagrammatic representation of what happens when two sterically stabilized flat plates are brought from infinite separation to a finite separation (d). The concomitant free energy change (ΔG_R) is the repulsive potential energy. When

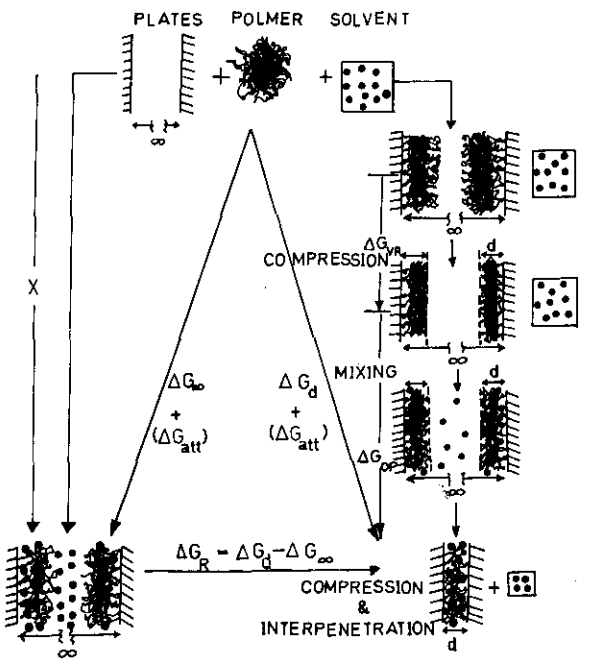

Fig. 2. Diagrammatic representation of the close approach of two flat plates and the calculation of the *Gibbs* free energy change using the *Flory-Krigbaum* theory

$L \leqslant d < 2L$, where L is the contour length of the polymer chains (assumed to be monodisperse), only interpenetration can be opertive. But when $d < L$, both interpenetration and compression may occur (4, 5).

To illustrate precisely what HVO have calculated, we have split up the process in fig. 2 into various steps. The standard state for the polymer in *Flory-Krigbaum* theory is pure, randomly oriented polymer chains whose centres of gravity are fixed in space. No problems arise in step X where the plates are coated with stabilizing chains at infinite separation. Note that we need not include the free energy of attachment (ΔG_{att}) of the chains to the plates in the following discussion; the centres of gravity are fixed in the standard state and ΔG_{att} may reasonably be assumed to be independent of the distance of separation. *Flory-Krigbaum* theory is directly applicable to find ΔG_∞, but step Y, which produces compressed polymer, is not straightforward in the HVO formulation. The prior calculation of the free energy of volume restriction (ΔG_{VR}) results in the solvent being mixed with *compressed* polymer chains in this step. Note, however, that compressed chains are not the standard state for the polymer in *Flory-Krigbaum* theory, yet the HVO theory is forced to treat them as such if the results of the *Flory-Krigbaum* theory are to be applicable to this step and the volume restriction term is calculated separately. It is this difficulty with the standard state that appears to render the predictions of the HVO theory inapplicable to real chains.

Assuming that the free energy of attachment of the polymer chains is independent of the distance of separation of the plates, thermodynamic considerations of fig. 2 yield

$$\Delta G_R = \Delta G_d - \Delta G_\infty. \qquad [3]$$

This shows that the volume restriction term is allowed for implicitly in this type of application of *Flory-Krigbaum* theory. (This is explicitly proven in the development of the basic dissolution equation in Part II). The origin of the improperly vanishing term in HVO theory thus becomes apparent. It is the volume restriction term, which clearly is non-zero in a θ-solvent or any solvent for that matter.

There is a sense in which this non-zero term is inevitable if a polymer chain in a θ-solvent is considered to be thermodynamically (as distinct from conformationally) equivalent to a random flight chain, com-

posed of non-interacting lines-in-space, as assumed by HVO. The latter model chain loses configurational entropy on compression and no enthalpy changes need be considered because the non-interacting system is essentially athermal. Real polymer chains in θ-solvents also lose configurational entropy on compression; however, because θ-solvents, are not athermal [except at the experimentally inaccessible absolute zero of temperature (34)] but rather slightly poor solvents there is an additional (usually counteracting) enthalpy change that is involved in compression. It is this enthalpy term associated with compression that is apparently unaccounted for in the HVO theory. In Part II we show that an extension of *Fischer*'s solvency theory permits this term to be included.

Finally we note in agreement with the foregoing discussion that *Doroszkowski* and *Lambourne* (35), as a result of their measurements on steric barriers, have concluded that models which ignore the volume restriction term best describe their experimental results.

Acknowledgements

We are grateful to the Australian Research Grants Committee for support of these studies. *R. E.* gratefully acknowledges the award of a Commonwealth Post-Graduate Scholarship.

Summary

A comparison is presented between the qualitative predictions of the various theories of steric stabilization with the results of experiments. It is shown that with the notable exception of *Fischer*'s solvency theory, all of the theories advanced to-date are at odds with results of experiments.

Possible reasons for these discrepancies are discussed.

References

1) *Heller, W.* and *T. L. Pugh*, J. Chem. Phys. **22**, 1778 (1954).
2) *Heller, W.*, Pure Appl. Chem. **12**, 249 (1966).
3) *Zsigmondy, R.*, Z. anal. Chem. **40**, 697 (1901).
4. *Napper, D. H.*, Trans. Faraday Soc. **64**, 1701 (1968).
5) *Napper, D. H.*, J. Colloid Interface Sci. **32**, 106 (1970).
6) *Napper, D. H.*, J. Colloid Interface Sci. **33**, 384 (1970).
7) *Napper, D. H.* and *A. Netschey*, J. Colloid Interface Sci. **37**, 528 (1971).
8. *Evans, R., J. B. Davison*, and *D. H. Napper*, J. Polymer Sci. **B10**, 449 (1972).
9) *Fischer, E. W.*, Kolloid-Z. **160**, 120 (1958).
10) *Mackor, E. L.*, J. Colloid Sci. **6**, 492 (1951).
11) *Mackor, E. L.* and *J. H. van der Waals*, J. Colloid Sci. **7**, 535 (1952).
12) *Clayfield, E. J.* and *E. C. Lumb*, Disc. Faraday Soc. **42**, 314 (1966).
13) *Clayfield, E. J.* and *E. C. Lumb*, J. Colloid Sci. **22**, 269 (1966).
14) *Clayfield, E. J.* and *E. C. Lumb*, J. Colloid Sci. **22**, 285 (1966).
15) *Clayfield, E. J.* and *E. C. Lumb*, Macromolecules **1**, **133** (1968).
16) *Elworthy, P. H., A. T. Florence*, and *J. A. Rogers*, J. Colloid Interface Sci. **35**, 23 (1971).
17) *Elworthy, P. H., A. T. Florence*, and *J. A. Rogers*, J. Colloid Interface Sci. **35**, 34 (1971).
18) *Shaw, D. J.*, Introduction to Colloid and Surface Chemistry, p. 185 (1970).
19) *Napper, D. H.*, Kolloid-Z. u. Z. Polymere **234**, 1149 (1969).
20) *Meier, D. J.*, J. Phys. Chem. **71**, 1861 (1967).
21) *Hesselink, F. Th.*, J. Phys. Chem. **73**, 3488 (1969).
22) *Hesselink, F. Th.*, J. Phys. Chem. **75**, 65 (1971).
23) *Hesselink, F. Th., A. Vrij*, and *J. Th. G. Overbeek*, J. Phys. Chem. **75**, 2094 (1971).
24) *Deryagin, B. V.*, Kolloid-Z. **69**, 155 (1934).
25) *Flory, P. J.*, Principles of Polymer Chemistry, Chap. **14** (New York 1953).
26) *Molau, G. E.*, Kolloid-Z. u. Z. Polymere **238**, 493 (1970).
27) *Molau, G. E.*, J. Polymer Sci. **A3**, 1267 (1965).
28) *Molau, G. E.*, J. Polymer Sci. **A3**, 4235 (1965).
29) *Dobbie, J. W.* and *D. H. Napper*, unpublished observations (1972).
30) *Smitham, J. B.*, B. Sc. Honours Thesis, University of Sydney (1972).
31) *Ottewill, R. H.* and *T. W. Walker*, Kolloid-Z. u. Z. Polymere **227**, 108 (1968).
32) *Gibson, D. V.*, B. Sc. Honours Thesis, University of Sydney (1971).
33) *Flory, P. J.* and *W. R. Krigbaum*, J. Chem. Phys. **18**, 1086 (1950).
34) *Flory, P. J.*, Principles of Polymer Chemistry, p. 525 (New York 1953).
35) *Doroszkowski, A.* and *R. Lambourne*, J. Polymer Sci. **C34**, 253 (1971).

Authors' address:
Mr. *R. Evans* and Dr. *D. H. Napper*
Department of Physical Chemistry
University of Sydney
N. S. W. 2006
(Australia)

Kolloid-Z. u. Z. Polymere **251**, 329–336 (1973)

From the Department of Physical Chemistry, The University of Sydney (Australia)

Steric stabilization II

A generalization of Fischer's solvency theory

By R. Evans and D. H. Napper

With 6 figures and 2 tables

(Received September 5, 1972)

Introduction

In the preceding paper (1) we showed that with the exception of *Fischer*'s germinal solvency theory (2), the qualitative predictions of the theories of steric stabilization advanced to-date (3–5) appear to be at odds with the results of experiments. It seems reasonable to infer that the quantitative predictions of such theories may also disagree with experiment.

We also noted that *Fischer*'s germinal solvency theory is not without its quantitative limitations; it calculates the repulsive potential energy primarily from the interpenetration process without much regard for compression; it uses a mean segment density step function rather than the more exact segment density distribution function; and it ignores all virial coefficients higher than the second. We now show, using a lattice approach, how *Fischer*'s theory may be extended to allow for both compression and a more exact segment density distribution function.

This approach differs from those proposed previously (4, 5) in that it does not consider the compression of the polymer chain in terms of a random flight chain, composed of non-interacting segments. The latter model regards θ-solvents as being equivalent to athermal solvents. However, θ-solvents are not athermal but somewhat poor solvents; only at the experimentally inaccessible temperature $\theta = 0$ °K may θ-solvents be taken as athermal (6).

The basic dissolution equation for attached polymer chains

We will develop a theory of steric stabilization through the basic dissolution equations for attached polymer chains. This is derived from the *Flory-Krigbaum* theory (7) for the mixing of randomly oriented polymer chains, whose centres of gravity are fixed in space, with pure solvent. This will show explicitly how conformational changes of the polymer are allowed for in this approach.

Consider a volume element δV located completely within a dissolved macromolecule. We will assume that this volume element resulted from the telescoping of two volume elements, each of size δV, that were separately situated in the pure solvent and in the pure, disoriented polymer respectively. The *Gibbs* free energy change for mixing in the volume element may be written:

$$\delta(\Delta G) = \delta(\Delta G_M^*) + \delta(\Delta G_{SP}) \qquad [1]$$

where ΔG_M^* = free energy of mixing calculated solely from external considerations of mixing segments and solvent and ΔG_{SP} = free energy changes due to all other interactions, including specific interactions between near neighbours. The *Flory-Krigbaum* theory yields, on the respective evaluation of each term, that

$$\delta(\Delta G) = kT\{\ln(1 - v_2) + \chi_1 v_2\}\delta n_1 \qquad [2]$$

where the subscripts 1 and 2 refer to the solvent and polymer respectively, v = volume fraction, χ_1 = interaction parameter (χ_1 =

$1/2 + \varkappa_1 - \psi_1$) and n_1 = the number of solvent molecules in δV. But

$$\delta n_1 = \frac{(1 - \varrho_2 V_s)}{V_1} \delta V \qquad [3]$$

where V_1 = volume of a solvent molecule, V_s = volume of a segment and ϱ_2 = number of polymer segments per unit volume. Substitution of relation [3] into eq. [2] yields on expansion of the logarithmic terms:

$$\delta(\Delta G) = kT \frac{V_s^2}{V_1} \left(\frac{1}{2} - \chi_1\right) \varrho_2^2 \delta V - kT \frac{V_s}{V_1} \left(\frac{1}{2} - \chi_1\right) \times \varrho_2 \delta V - \frac{1}{2} kT \frac{V_s}{V_1} \varrho_2 \delta V \qquad [4]$$

where powers higher than the second are neglected.

Eq. [4] is the basic dissolution equation for polymer chains attached to particles. We now formulate a term-by-term interpretation of this relation.

First consider the dissolution of randomly oriented polymer segments into a θ-solvent in a volume element δV. The *Flory-Krigbaum* relationship yields

$$\delta(\Delta G_\theta) = kT \{\ln(1 - v_2) + v_2 \chi_1^\theta\} \delta n_1.$$

Since $\chi_1^\theta = 1/2$, we have for small $v_2 (= \varrho_2 V_s)$

$$\delta(\Delta G_\theta) = -\frac{1}{2} kT \frac{V_s}{V_1} \varrho_2 \delta V. \qquad [5]$$

This is the third term in the basic dissolution equation. We note that it is negative so that attached polymer molecules dissolve spontaneously in a θ-solvent.

Next at constant T, we increase the quality of the solvent from a θ-solvent to some value of $\chi_1 < 1/2$, *whilst retaining the random coil θ-solvent conformation*. Clearly for this process $\delta(\Delta G_M^*) = 0$ and from the *Flory-Krigbaum* theory we have

$$\delta(\Delta\Delta G_{\chi_1}) = kT \left\{\chi_1 v_2 - \frac{1}{2} v_2\right\} \delta n_1$$

which for small v_2 gives

$$\delta(\Delta\Delta G_{\chi_1}) = -kT \frac{V_s}{V_1} \left(\frac{1}{2} - \chi_1\right) \varrho_2 \delta V. \qquad [6]$$

This is the second term in the basic dissolution equation. Note that it too is negative as would be expected.

The remaining term

$$+ kT \frac{V_s^2}{V_1} \left(\frac{1}{2} - \chi_1\right) \varrho_2^2 \delta V$$

is associated with the conformational change of the polymer that occurs in a solvent better than a θ-solvent. It includes both enthalpy and entropy changes associated with this conformational change and allows for the presence of the solvent. The positive sign denotes that the loss of configurational entropy due to the adoption of a less random conformation outweighs the favourable, but here truncated, enthalpy changes that usually accompany this process. This term would be expected intuitively to vary as the square of the segment density because it corresponds to intramolecular interpenetration (or the reverse) [8]. Note that the sum of the first two terms in eq. [4] is negative as must be the case in going from a θ-solvent to a good solvent.

It is this first term in the basic dissolution equation that formally allows for changes in the conformation of the attached polymer chains such as those caused by compression. In this case the conformational change is induced by a solvency change but suitable thermodynamic cycles may easily be devised so that this term properly allows for *all* conformational changes, wherever their origin (e.g., attachment to an interface, compression, etc.).

We can therefore write the basic dissolution equations

$$\delta(\Delta G) = \delta(\Delta G_\theta) + \delta(\Delta G_{\chi_1}) + \delta(\Delta G_{\text{conf}}) \qquad [7]$$

where $\delta(\Delta G_{\text{conf}})$ = free energy change due to conformational changes. It is this latter term that renders the volume restriction term used by *Meier* (4) superfluous.

Calculation of steric repulsion

Flat plates

The basic dissolution equation applies to polymer chains attached to colloidal particles because the centres of gravity of the macromolecules are incapable of independent motion. We will assume that there are ν monodisperse chains attached to unit area of the flat plates, each chain being composed of i segments. The chains are irreversibly attached to the plates; we need not include the free energy of attachment (ΔG_{att}) in the following discussion because the term cancels if it is assumed that ΔG_{att} is independent of the distance of separation of the plates. We assume a constant segment density parallel to the surface (i.e., high and complete surface coverages) and a continuous segment distribution normal to the interface.

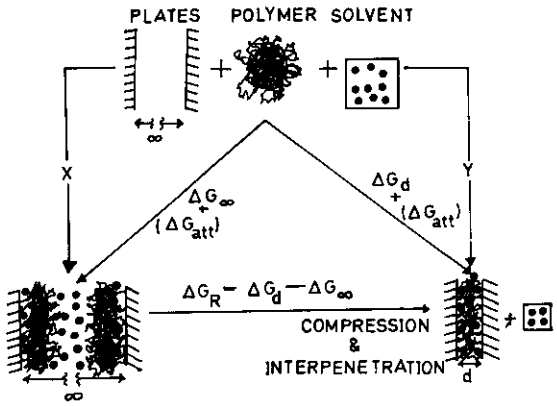

Fig. 1. Schematic representation of the close approach of two sterically stabilized plates

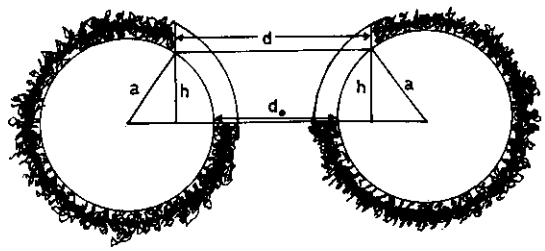

Fig. 2. The *Deryagin* method for calculating the repulsive potential for two equal spheres from that of flat plates (Not to scale)

For step X envisaged in fig. 1 we may write on integration of eq. [4] that for one plate

$$\Delta G_\infty = kT \frac{V_s^2}{V_1} (1/2 - \chi_1) \int_{x=0}^{\infty} \varrho^2{}_\infty dV - kT \times \frac{V_s}{V_1} (1/2 - \chi_1) \int_{x=0}^{\infty} \varrho_\infty dV - kT \frac{V_s}{2V_1} \int_{x=0}^{\infty} \varrho_\infty dV$$

where ϱ_∞ = segment density distribution function at infinite separation of the plates. Since ϱ_∞ is a function only of x,

$$dV = A\,dx = dx$$

if we consider unit surface area. Denoting the normalized distribution function by $\hat{\varrho}_\infty$ we have

$$\int_{x=0}^{\infty} \hat{\varrho}_\infty dV = \int_{x=0}^{\infty} \hat{\varrho}_\infty dx = vi$$

where vi = total number of segments in the volume normal to unit surface area. Accordingly.

$$\Delta G_\infty = kT \frac{V_s^2}{V_1} \left(\frac{1}{2} - \chi_1\right) v^2 i^2 \int_0^{\infty} \hat{\varrho}^2{}_\infty dx - kT \times \frac{V_s}{V_1} \left(\frac{1}{2} - \chi_1\right) vi - kT \frac{V_s}{2V_1} vi. \qquad [8]$$

We can perform an analogous dissolution to describe step Y in fig. 1 and so find ΔG_d for the dissolution of polymer when the separation is d:

$$\Delta G_d = kT \frac{V_s^2}{V_1} \left(\frac{1}{2} - \chi_1\right) v^2 i^2 \int_0^{d} \hat{\varrho}_d{}^2 dx - kT \times \frac{V_s}{V_1} \left(\frac{1}{2} - \chi_1\right) vi - \frac{kTV_s}{2V_1} vi \qquad [9]$$

where $\hat{\varrho}_d$ = normalized segment density distribution function when the separation is d such that $\int_0^d \hat{\varrho}_d\,dx = vi$.

The *Gibbs* free energy of compression per unit area (ΔG_C) for two plates is obtained by subtracting eq. [8] from eq. [9] and multiplying by two to allow for the interaction of two plates:

$$\Delta G_C = \Delta G_d - \Delta G_\infty = 2kT \frac{V_s^2}{V_1} \left(\frac{1}{2} - \chi_1\right) v^2 i^2 \times \left[\int_0^d \hat{\varrho}_d{}^2 dx - \int_0^{\infty} \hat{\varrho}^2{}_\infty dx\right] \qquad [10]$$

This is the free energy change resulting from the compression of the stabilizing moieties.

Eq. [10] makes no allowance for the interpenetration of the polymer chains attached to the two surfaces that occurs when $d < 2L$. The form of the free energy of interpenetration per unit area (ΔG_I) must be similar to that derived by *Flory* and *Krigbaum* (7) for the interpenetration of two chains in free solution:

$$\Delta G_I = 2kT \frac{V_s^2}{V_1} \left(\frac{1}{2} - \chi_1\right) v^2 i^2 \int_0^d \hat{\varrho}_d \hat{\varrho}_d{}' dx \qquad [11]$$

where $\hat{\varrho}'_d$ is the mirror image of $\hat{\varrho}_d$ obtained by reflection and translation of the coordinate axis. The total free energy change per unit surface area on close approach is thus given by

$$\Delta G_R = \Delta G_C + \Delta G_I = 2kT \frac{V_s^2}{V_1} \left(\frac{1}{2} - \chi_1\right) v^2 i^2 \times \left[\int_0^d \hat{\varrho}_d{}^2 dx + \int_0^d \hat{\varrho}_d \hat{\varrho}_d{}' dx - \int_0^{\infty} \hat{\varrho}^2{}_\infty dx\right] \qquad [12]$$

This relation has been given previously (9, 10) without proof. The right hand side of eq. [12] was in fact first calculated by *Meier* (4) but regarded by him as excluding conformational changes of the polymer. The foregoing discussion shows that conformational changes are included.

Hesselink, Vrij and *Overbeek* (5) have tabulated the sum of the integral terms in eq. [12] for loops and tails as a dimensionless function that we denote by R [their $M(\bar{i}, d)$]:

$$R = \langle r^2\rangle^{1/2}\left[\int_0^d \hat{\varrho}_d^2\,dx + \int_0^d \hat{\varrho}_d\,\hat{\varrho}_{d'}\,dx - \int_0^d \hat{\varrho}^2_\infty\,dx\right]$$

where $\langle r^2\rangle^{1/2}$ = r.m.s. end-to-end length of the chains in *free* solution. We may therefore write

$$\Delta G_R = \frac{2kTV_s^2}{\langle r^2\rangle^{1/2}V_1}\left(\frac{1}{2} - \chi_1\right)\nu^2 i^2 R. \qquad [13]$$

Eq. [13] is the fundamental relationship for evaluating the repulsive *Gibbs* free energy in the steric stabilization of flat plates. Because it contains the lattice parameters V_s and V_1, eq. [13] is not the most convenient form for calculating ΔG_R. We can, e.g., substitute into eq. [13] the approximate *Flory* relationship for the expansion factor α

$$\alpha^5 - \alpha^3 = 2C_M\psi_1(1 - \theta/T)M^{1/2}$$

where ψ_1 = entropy of dilution parameter and $\theta = (\varkappa_1/\psi_1)T$, where $\varkappa_1$ = enthalpy of dilution parameter. This yields the more tractable form:

$$\Delta G_R \sim \frac{2(2\pi)^{3/2}}{27}\langle r^2\rangle\nu^2(\alpha^2 - 1)RkT. \qquad [14]$$

The value of ν is best determined experimentally from adsorption studies. Alternatively a crude estimate of ν may be obtained in the following way. It has been shown theoretically (11) that the mean extension of tails or loops from an impenetrable interface is ca. double their extension in the absence of that interface. *Tanford* (12) has suggested that in a good solvent the thermodynamic volume of a hard-core sphere equivalent to a free polymer is $0.18\langle r^2\rangle^{3/2}$. If we assume that this equivalent volume remains unchanged on attachment to the interface, the effective area per molecule becomes $0.25\langle r^2\rangle$. Therefore $\nu \sim 4/\langle r^2\rangle$. Substitution of this value into eq. [14] leads on simplification to:

$$\Delta G_R \sim \frac{32(2\pi)^{3/2}}{27}\frac{(\alpha^2 - 1)}{\langle r^2\rangle}RkT. \qquad [15]$$

The total interaction free energy (V_T) for two flat plates is obtained by summing the steric repulsion and the *London-van der Waals* attraction (13).

$$V_T = \frac{2kTV_s^2}{\langle r^2\rangle^{1/2}V_1}(1/2 - \chi_1)\nu^2 i^2 R - \frac{A^*}{12\pi\langle r^2\rangle\delta^2} \qquad [16]$$

where A^* = net *Hamaker* constant and $\delta = d/\langle r^2\rangle^{1/2}$.

Spheres

Model dispersions of sterically stabilized colloidal particles are usually composed of monodisperse spheres. It has not yet proved possible in general to solve the case of two sterically stabilized spheres of equal radius, a. We can, however, exploit the *Deryagin* approximation (14) to calculate the repulsive potential for spheres from that developed for flat plates, provided only that the thickness of the stabilizing layer is considerably less than the radius of the particles. This situation is commonly encountered in practice. The *Deryagin* method calculates the repulsive potential for spheres by summing the contributions of infinitesimally thick planar rings parallel to each other at a distance d (fig. 2). The repulsive potential per pair of spheres (ΔG_R^S) is given by

$$\Delta G_R^S = \int_0^\infty 2\pi h(\Delta G_R^{FP})\,dh \qquad [17]$$

where ΔG_R^{FP} = *Gibbs* free energy of repulsion per unit area for flat plates and h = radius of the ring.

(i) Equal spheres

Simple geometric considerations of fig. 2 give that

$$(d - d_0)/2 = a - (a^2 - h^2)^{1/2}$$

where d_0 = minimum distance of surface separation for the two spheres of equal radii. Therefore

$$2h\,dh = a(1 - (h^2/a^2))^{1/2}dd \sim a\,dd$$

since $h \ll a$ in the *Deryagin* approximation. Accordingly

$$\Delta G^S_{R(a,a)} = \pi a\int_{d_0}^\infty (\Delta G_R^{FP})\,dd$$

$$= 2\pi a\frac{V_s^2}{V_1}(1/2 - \chi_1)\nu^2 i^2 SkT \qquad [18]$$

where $S = \int_{\delta_0}^\infty R\,d\delta$ and $\delta_0 = d_0/\langle r^2\rangle^{1/2}$. Alter-

natively using eq. [15] we may write

$$\Delta G_R^S(a,a) = \frac{(2\pi)^{5/2}}{27}\langle r^2\rangle^{3/2}\nu^2(\alpha^2-1)aSkT \quad [19]$$

and if, as discussed above, we set $\nu = 4/\langle r^2\rangle$ the repulsive free energy becomes

$$\Delta G_R^S(a,a) \sim \frac{16(2\pi)^{5/2}}{27}\frac{(\alpha^2-1)}{\langle r^2\rangle^{1/2}}aSkT \quad [20]$$

The total free energy of interaction per pair of particles (V_T) is obtained by summing the steric repulsion and the *London-van der Waals* attraction [previously calculated by *Hamaker* (13)]:

$$V_T = \frac{(2\pi)^{5/2}}{27}\langle r^2\rangle^{3/2}\nu^2(\alpha^2-1)aSkT - \frac{A^*a}{12\langle r^2\rangle^{1/2}\delta_0} \quad [21]$$

Table 1. Values of the parameter S for tails (T) and loops (L) at different separations (δ_0) of the spheres

δ_0	S_T	δ_0	S_L
0.4	2.666	0.6	0.720
0.6	1.680	0.7	0.500
0.8	1.070	0.8	0.338
1.0	0.678	0.9	0.219
1.2	0.416	1.0	0.135
1.4	0.249	1.1	0.080
1.6	0.141	1.2	0.044
1.8	0.075	1.3	0.022
2.0	0.038	1.4	0.011
2.2	0.018	1.5	0.005
2.4	0.007	1.6	0.002

Values of S estimated graphically for various values of the distance parameter δ_0 are shown in table 1 for tails (T) and loops (L). The prerequisite functions for flat plates were taken from *Hesselink, Vrij* and *Overbeek* (5) and were interpolated before integration.

(ii) Unequal spheres

Consider two spheres of unequal radii a and b (fig. 3). The repulsion potential is again given by eq. [20]. We have from fig. 3

$$d - d_0 = (a+b) - (b^2-h^2)^{1/2} - (a^2-h^2)^{1/2}$$

so that

$$hdh = \frac{ab\,dd}{a\left(1-\frac{h^2}{b^2}\right)^{-1/2} + b\left(1-\frac{h^2}{a^2}\right)^{-1/2}} \sim \frac{ab}{a+b}dd$$

since $h \ll a, b$. Therefore the repulsion potential per pair of particles is

$$\Delta G_R(a,b) = \frac{2\pi ab}{(a+b)}\int_{d_0}^{\infty}(\Delta G_R^{FP})\,dd = \frac{2b}{a+b}\Delta G_R^S(a,a)$$

where $\Delta G_R^S(a,a)$ = steric repulsion per pair of monodisperse spheres of radius a calculated using eq. [18] or [19].

The total potential energy is thus (13)

$$V_T = \frac{2b}{a+b}\Delta G_R^S(a,a) - \frac{A^*ab}{6(a+b)\langle r^2\rangle^{1/2}\delta_0} \quad [23]$$

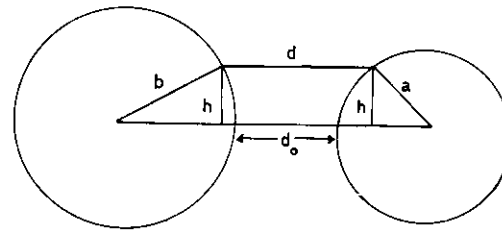

Fig. 3. The *Deryagin* method applied to unequal spheres

(iii) Flat plates and spheres

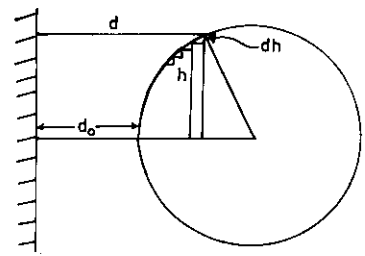

Fig. 4. The *Deryagin* method applied to sphere/plate interaction

For the case of a sphere interacting with a flat plate, which is another commonly encountered geometry in colloid studies, we have from fig. 4

$$d - d_0 = a - (a^2-h^2)^{1/2}.$$

Thus

$$hdh = (1-h^2/a^2)^{1/2}\,add \sim add.$$

Therefore the repulsive potential for a single sphere interacting with a flat plate is given by

$$\Delta G_R^{SP} = 2\pi a\int_{d_0}^{\infty}(\Delta G_R^{FP})dd = 2\Delta G_R^S(a,a). \quad [24]$$

Relation [24] can also be derived from eq. [22] by letting b tend to infinity:

$$\Delta G_R^{SP} = \Delta G_R^S(a,\infty) = \lim_{b\to\infty}(2/(1+a/b)[\Delta G_R^S(a,a)]) = 2\Delta G_R^S(a,a).$$

The total potential energy in this case is thus [13]

$$V_T = 2\Delta G_R^S(a,a) - \frac{A^* a}{6\pi\langle r^2\rangle^{1/2}\delta_0} \qquad [25]$$

Table 2 summarizes the results for the steric repulsive potential energy for the three geometrical situations frequently encountered in colloid studies.

Table 2. The relationship between the repulsive potentials for different geometries in the *Deryagin* approximation

System	*Repulsion energy*
Equal spheres (radii a)	$\Delta G_R^S(a,a)$
Unequal spheres (radii a, b)	$(2b/[a+b])\,\Delta G_R^S(a,a)$
Flat plate/sphere (radius a)	$2\Delta G_R^S(a,a)$

Comparison of the theory for spheres with experiment

Eq. [21] can be used to calculate the total potential energy curves for two sterically stabilized spherical particles. These are displayed in fig. 5 for two equal poly(vinyl acetate) particles in an aqueous latex sterically stabilized by PEO loops of $_M$ = 96,000 [corresponding (10) to Polyox WSRN80]. For convenience we have in fact used eq. [20] to calculate the repulsive potential. The effective *Hamaker* constant was taken as $A^* = 3\times10^{-21}\,J$ but as shown later, the exact value of A^* chosen has little influence in general on the curves if $\alpha > 1.000$. The radius of each particle was taken as 10^3 Å.

We will assume that flocculation is observed if the net attractive potential exceeds $2{,}5\,kT$. Precisely what value is chosen here for the potential energy of attraction will not influence the following discussion provided it is somewhat greater than thermal energy.

It becomes apparent from consideration of eq. [21] and fig. 5 that the steric repulsion usually increases faster than does the *van der Waals* attraction at all distances of separation. The upshot of this is that the potential energy curves for sterically stabilized particles do not usually exhibit the maximum that is so characteristic of electrostatically stabilized dispersions. We have carried out many different calculations apart from those presented and always found this to be true. The absence of this maximum explains why flocculated sterically stabilized dispersions, or stable latices that have been compacted by centrifugation, redisperse spontaneously

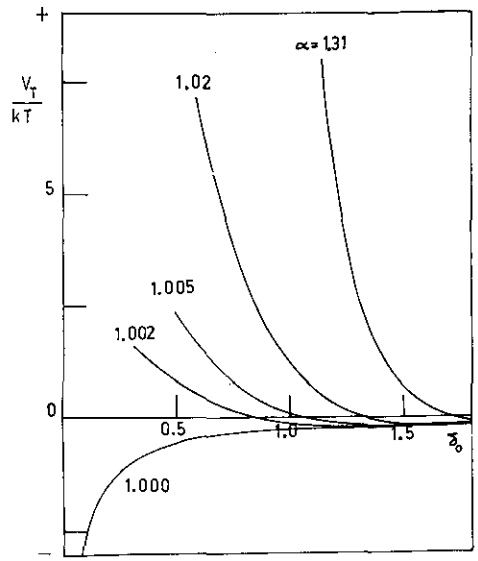

Fig. 5. The total potential energy curves for two spherical poly(vinyl acetate) particles stabilized by poly(ethylene oxide) loops of molecular weight 9.6×10^4. The radii of the particles is 10^3 Å, the effective *Hamaker* constant is 3×10^{-21} J and $T = 303$ °K

under suitable solvency conditions (9, 10). There is in all instances where $\alpha > 1.000$ a very shallow minimum at the larger distances of separation. This is analogous to the secondary minimum in electrostatic stabilization but it is too shallow for flocculation to be observed in it in the large number of different cases for which we have made calculations.

The curves also show that stable dispersions would be expected if $\alpha = 1.002$ but that instability would be evident if $\alpha = 1.000$. A sharp transition from stability to instability is thus predicted, as is observed experimentally (9, 10). These two values of α correspond, according to the *Flory* equation for α, to a temperature difference of less than 1 °K. Thus as $\alpha = 1.000$ corresponds to the θ-point, we see that the theory predicts the presence of a sharp transition from stability to instability very close to the θ-point. The strong correlation between the θ-point and the c.f.p. observed experimentally has already been described. Obviously the theory also predicts the observed insensitivity of the c.f.p. to the molecular weight of stabilizing moieties, since the θ-point is independent of molecular weight. Finally inspection of eq. [21] shows that as both the attraction and the repulsion increase linearly with a, the above conclusions will be almost independent of the particle radius a, since the

point at which $V_T \sim 0$ is independent of the radius; again experiments support this conclusion. All of the parameters for which we have chosen specific values in the above discussion can be varied over wide ranges without altering the general conclusions presented herein.

We conclude that the theory of steric stabilization outlined above is in agreement with all the qualitative features of steric stabilization that have been observed to-date. It is essentially an extension of *Fischer*'s solvency theory; it treats compression as an intramolecular interpenetration process characterized by the same enthalpy and entropy of dilution parameters as intermolecular interpenetration (8). This explains why the predictions of *Fischer*'s germinal theory are in qualitative accord with experiments.

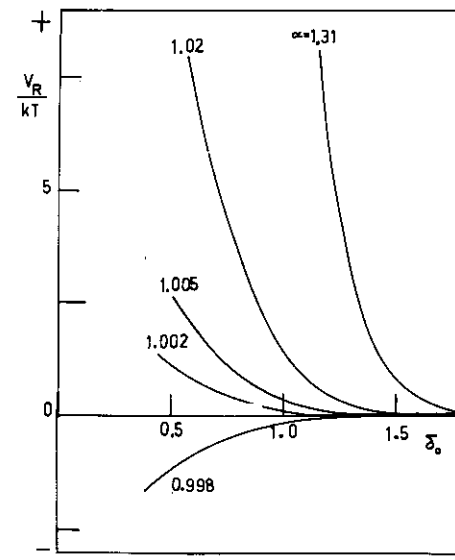

Fig. 6. The potential energy curves for two sterically stabilized particles if the *London-van der Waals* attraction is neglected. All parameters are as for fig. 6

An alternative explanation of flocculation

An alternative way of viewing sterically stabilized latex particles is to regard them as polymer molecules of (almost) infinite molecular weight. Attachment of the soluble stabilizing chains to the particles removes their ability to move separately in the solvent and hence removes their ideal contributions to the thermodynamic properties of the solution. Their non-ideal contributions, however, remain intact. The ideal contributions of the particles may be safely neglected. It is as if the sterically stabilized particles were graft homopolymers with a backbone polymer of almost infinite molecular weight but with soluble lower molecular weight side chains.

The θ-point has long been recognized as the critical miscibility limit of homopolymers of infinite molecular weight. Thus sterically stabilized particles would be expected to phase separate (i.e., flocculate) at the θ-point. This is, of course, what is observed experimentally (9, 10). It raises the question of the solubility of attached stabilizing moieties at or near the θ-point. We will explore this question elsewhere. However, we have shown above that attached polymer chains are soluble in θ-solvents.

Flory (15) has suggested that the experimental results obtained with sterically stabilized dispersions may well imply that the *London-van der Waals* attraction between the core particles is relatively unimportant in determining flocculation of latices. Fig. 6 presents some typical potential energy curves for sterically stabilized dispersions if the *London-van der Waals* attraction between the core particles is ignored completely. Other conditions are as shown for fig. 5 and a comparison of the curves in figs. 5 and 6 shows that if $\alpha > 1.000$, neglect of the attraction between the core particles scarcely changes the overall repulsive potential. Moreover if $\alpha < 1.000$, the attraction between the sheaths must become relatively large as δ_0 tends to zero. It is obvious that flocculation would be observed if, e.g., $\alpha = 0.998$, i.e., within 1 °K of the θ-point. Hence flocculation would still be observed near to the θ-point even if we ignore the *van der Waals* attraction between the core particles. Flocculation would also be independent of the particle radius since the θ-point is independent of the partial radius. Currently the accuracy of the experiments fails to distinguish between flocculation induced by *van der Waals* attraction between the core particles and that induced by attraction between the stabilizing sheaths. We would expect that sheaths of very high molecular weight polymer (e.g., $M \sim 1 \times 10^6$) would prevent the core particles from exhibiting significant attraction except at extremely high compressions. (This effect is apparent even in fig. 5.) Yet latices stabilized by PEO of $M = 1 \times 10^6$ flocculate very close to the θ-point (14). We therefore strongly favour *Flory*'s notion that flocculation of latices is induced as a result of the

attraction between the stabilizing sheaths, which in turn derives from the solvency of the dispersion medium being made marginally worse than a θ-solvent. Whether this conclusion will hold for metal sols, e.g., where the core attraction may be an order of magnitude larger, remains to be established experimentally.

We note also that *Doroszkowski* and *Lambourne* (16) have arrived at a similar conclusion from their studies of steric stabilization. There exists at least the theoretical possibility of preparing stable latices in θ-solvents because the fourth and higher virial coefficients fail to vanish in θ-solvents. Only the second and third coefficients are effectively zero. Interpenetration and compression of the polymer chains to high segment densities will permit these higher virial coefficient repulsions to become operative. This is not allowed for in the above theories or any theories developed to-date. All models probably break down under these conditions. In addition the *Born* repulsion between the segments is not included yet it too becomes operative at high segment densities. Note also that the traditional estimate of the *van der Waals* attraction may have to be adjusted in light of the more exact theories being developed by *Ninham* and *Parsegian* (17, 18). Finally the values for ψ_1 and $\varkappa_1$ to be used in the above theory are those derived from experiment.

Acknowledgements

We are grateful to the Australian Research Grants Committee for financial support. *R.E.* gratefully acknowledges the award of a Commonwealth Post-Graduate Scholarship.

Summary

A theory of steric stabilization is developed that is essentially an extension of *Fischer*'s solvency theory. It treats both interpenetration and compression using a latice approach. This permits the introduction of segment density distribution functions. One virtue of the new theory is that it is in good qualitative agreement with the results of experiment. Some limitations of the theory are also noted.

References

1) *Evans, R.* and *D. H. Napper*, Kolloid-Z. u. Z. Polymere preceding paper, (1973).
2) *Fischer, E. W.*, Kolloid-Z. **160**, 120 (1958).
3) *Clayfield, E. J.* and *E. C. Lumb*, Disc. Faraday Soc. **42**, 314 (1966).
4) *Meier, D. J.*, J. Phys. Chem. **71**, 1861 (1967).
5) *Hesselink, F. Th., A. Vrij*, and *J. Th. G. Overbeek*, J. Phys. Chem. **75**, 2094 (1971).
6) *Flory, P. J.*, Principles of Polymer Chemistry, p. 525 (New York 1953).
7) *Flory, P. J.* and *W. R. Krigbaum*, J. Chem. Phys. **18**, 1086 (1950).
8) *Flory, P. J.*, Principles of Polymer Chemistry, p. 529 (New York 1953).
9) *Napper, D. H.*, Trans. Faraday Soc. **64**, 1701 (1968).
10) *Napper, D. H.*, J. Colloid Interface Sci. **32**, 106. (1970).
11) *Di Marzio, E. A.* and *F. L. McCrackin*, J. Chem. Phys. **43**, 539 (1965).
12) *Tanford, C.*, Physical Chemistry of Macromolecules, p. 199 (New York 1961).
13) *Hamaker, H. C.*, Physica **4**, 1058 (1937).
14) *Deryagin, B. V.*, Kolloid-Z. **69**, 155 (1934).
15) *Flory, P. J.*, Comments on the substance of this paper at the Polymer Division Symposium of the Royal Australian Chemical Institute, Mildura, November 1971.
16) *Doroszkowski, A.* and *R. Lambourne*, J. Polymer Sci. C**34**, 253 (1971).
17) *Parsegian, V. A.* and *B. W. Ninham*, J. Colloid Interface Sci. **37**, 332 (1971).
18) *Mitchell, D. J.* and *B. W. Ninham*, J. Chem. Phys. **56**, 1117 (1972).

Authors' address:

Mr. *Robert Evans* and Dr. *D. H. Napper*
Department of Physical Chemistry
University of Sydney
N. S. W. 2006
(Australia)

Reprinted from JOURNAL OF COLLOID AND INTERFACE SCIENCE, Volume 45, No. 1, October 1973
Copyright © 1973 by Academic Press, Inc. *Printed in U.S.A.*

On the Calculation of the van der Waals Attraction Between Latex Particles

ROBERT EVANS AND D. H. NAPPER

Department of Physical Chemistry, University of Sydney, N.S.W., 2006, Australia
(Received November 27, 1972; accepted February 14, 1973

The van der Waals attraction between uncharged, spherical polymeric latex particles in both aqueous and non-aqueous dispersion media has been calculated using the quantum field theory approach due to Lifshitz and Ninham and Parsegian. It is shown that for close approach it is possible to define a Hamaker function, analogous to the classical Hamaker constant, that is a function of the ratio (δ) of the minimum distance of surface separation to the particle radius. Computations for polymer latex particles in water showed that the Hamaker function for close approach decreases linearly with δ. However for polymers in hydrocarbons, the Hamaker functions are in fact constant. Both results are also derived analytically. A major obstacle to accurate calculations using this approach is the difficulty of converting the readily available gaseous ionization potentials into values for solids and liquids by providing due allowance for the polarization energy of the dielectric medium.

INTRODUCTION

There have been several theoretical estimates (1–3) of the van der Waals attraction between polymer latex particles in both aqueous and nonaqueous media. These estimates have all assumed, following London (4) and Hamaker (5), that the interatomic interactions exhibit pairwise additivity. Moreover it has become customary to assume in these calculations that electronic correlations with frequencies in the ultraviolet region are primarily responsible for the attraction.

In a pioneering series of papers (6–10), Ninham and Parsegian have shown conclusively that for colloidal systems in general, this traditional approach is not without its deficiencies: pairwise additivity may well be appropriate for dilute gases but is scarcely reasonable in condensed systems where many-body effects become significant and correlations involve more than just a pair of molecules; additionally, correlations other than those propagated at ultraviolet frequencies can contribute significantly to the overall van der Waals attraction, especially if water is the dispersion medium.

The basis of the new approach devised by Ninham and Parsegian is the macroscopic continuum theory of Lifshitz (11, 12). This applies the methods of quantum field theory to the fluctuating electromagnetic fields that are always present inside material media and which extend beyond their physical boundaries. These electromagnetic spectra contain the characteristic absorption frequencies corresponding to resonant electronic and molecular frequencies. For condensed bodies the properties of the electronic envelopes of the atoms or molecules are different from those in the gas phase because of the close proximity of contiguous atoms or molecules. Hence the failure of the pairwise additivity approach. Moreover the presence of a medium between the interacting species alters the electromagnetic disturbance by which the attraction is propagated. Properly the fluctuating electromagnetic fields must include all

Copyright © 1973 by Academic Press, Inc.
All rights of reproduction in any form reserved.

long-wavelength spectral components (i.e., all correlations propagated at wavelengths large compared with atomic dimensions).

The power of the Lifshitz formalism lies in its ability to account for all many-body interactions, to deal properly with the effects of intermediate substances, and to include contributions from all spectral components. The interaction is expressed solely in terms of measurable dielectric properties of the materials considered. It further eventuates that for materials of similar density the whole dielectric spectrum need not be known accurately because the energy transfer occurs mainly at the principal absorption frequencies of the bodies, which are usually known or are measurable (6).

Mitchell and Ninham (13), using the Lifshitz theory, have derived the relevant formulae for the energy of interaction of spherical particles imbedded in a dispersion medium. These can be used to calculate the van der Waals attraction between latex particles in both aqueous and nonaqueous media. In what follows we discuss some algebraic and numerical implications of the theory developed by Mitchell and Ninham, pointing out certain difficulties that still reside in this approach.

THEORY AND COMPUTATIONS

The following symbols are used:

T = temperature
a = particle radius
d = minimum distance of particle separation
$\delta = d/a$
$s = \delta + 2$
n = refractive index
n_W = refractive index of water
n_{PHC} = refractive indes of polymer or hydrocarbon
ω = absorption frequency
ϵ = permittivity
I = ionization potential
ξ = eigenfrequency.

The problem to be discussed is that of calculating the free energy of attraction between two uncharged, spherical polymer latex particles, each of radius a, immersed in a uniform dispersion medium. We will assume that the minimum distance of separation between the surfaces of the spheres, d, is large compared with interatomic dimensions, although it may still be quite small. This allows each medium to be treated as a continuum.

An upper bound is also placed on d: d must be much less than the wavelengths of transitions between the ground states and the excited states of the constituent species so that retardation effects can be ignored.

The free energy of attraction (G) can be calculated for small separations from (13)

$$G = (kT/8\eta^2) \sum_{j=0}{}' \left[\int_0^\infty x \ln (1 - \Delta^2 e^{-x}) dx + 4\eta^2 (1 - \Delta) \ln \eta \ln (1 - \Delta^2) \right], \quad [1]$$

where

$$\eta = \ln \{ [(\delta^2/4) + \delta]^{\frac{1}{2}} + [(\delta^2/4) + \delta + 1]^{\frac{1}{2}} \},$$

$$\Delta = (\epsilon_1 - \epsilon_2)/(\epsilon_1 + \epsilon_2).$$

Here the subscripts 1 and 2 refer to the particles and the medium respectively and the prime on the summation symbol implies that the term for the eigenvalue $j = 0$ must be divided by 2 because it is a zero-point term.

Note that the positive sign of the second term in Eq. [1] is the same as that given by Mitchell and Ninham (13) in their Eq. 81 but is opposite in sign to that given in their Eqs. 85 and 86, said to be derived from Eq. 81. Ninham (14) has confirmed the correctness of the positive sign in Eq. [1] and suggested that this small separation approximation is valid only if the second term is, say, one-third of the numerical value of the leading term for each frequency. Larger values of the second term could, of course, reverse the sign of G, which does not seem physically permissible for two like spheres and implies that higher-order terms must be included.

Our calculations show that the useful approximation $\eta^2 = \delta$ is valid in the interval $0 < \delta \leqslant 0.2$ with an accuracy of better than 2%.

To calculate Δ we need the values of the dielectric permittivity of both the particles and the medium. By assuming that the dielectric susceptibility may be expressed as the sum of the average contributions from the eigenfrequencies in the microwave (mw), infrared (ir), and the ultraviolet (uv) regions, we may write (6)

$$\epsilon(i\xi) = \frac{\epsilon_0 - \epsilon_D}{1 + \xi/\omega_{mw}} + \frac{\epsilon_D - n^2}{1 + (\xi/\omega_{ir})^2} + \frac{n^2 - 1}{1 + (\xi/\omega_{uv})^2} + 1, \quad [2]$$

where $i = \sqrt{-1}$ and $\xi = (2\pi kT/\hbar)j$ where $\hbar = (h/2\pi)$ and $j = 0, 1, 2, \cdots$. This relation assumes that relaxation occurs first as a drop in permittivity from the static value for the substance ϵ_0 to a smaller value ϵ_D during the Debye relaxation. Then follows a decrease from ϵ_D to a smaller value relevant to the visible range, which because of its electronic character, obeys the Maxwell relationship $\epsilon = n^2$. Finally, during the ultra-violet relaxation, the permittivity drops from n^2 to the value for free space, 1. The infrared and ultraviolet relaxations are represented by the classical Lorentz electron dispersion equations.

The computations were performed with the aid of an IBM 7040 computer. All integrations were evaluated using Simpson's rule.

The Ionization Potential Problem

Examination of dielectric dispersion data for polystyrene and poly(vinyl acetate) at room temperature (15) shows that very little relaxation occurs from the static dielectric permittivity until the ultraviolet region is reached. We have chosen, therefore, to neglect the small infrared relaxations. The dispersion spectrum for poly(methyl methacrylate) does, however, exhibit a significant, if broad, relaxation near 100 Hz and this relaxation was included in the calculations. The most convenient frequency to use for ultraviolet relaxation is the value corresponding to the ionization potential. No suitable ionization potential data seem to be available for these three polymers. It was, therefore, necessary to adopt an approximate procedure.

We first assumed that the ionization potential of the polymers can be equated to the ionization potentials of molecules whose chemical structures closely resemble those of the repeating mer units. Thus ethyl benzene, isopropyl benzene or toluene would be cognate molecules for polystyrene repeating units and all have similar ionization potentials. Values of the ionization potentials of these molecules as isolated species in the gas phase are readily available (16). However, these values as such cannot be used for the polymers, as has previously been assumed (6–10, 17, 18). This is because there is a well-documented and significant change (usually a reduction) in ionization potentials of molecules in passing from the vapour phase to the solid or liquid phase (19, 20). The reason for this is precisely the same reason why pairwise additivity of interactions is inappropriate in condensed media; the attraction between an electron that is to be removed from a compound and the contiguous atoms in a condensed medium so weakens its interactions with the nuclei that hold it in its orbital that it is easier to remove that electron. Consequently the ionization potential of a solid or liquid is less than that of the same substance in the dilute gas phase.

The correction to be applied to the gaseous ionization potential (I_G) to yield the value for a condensed phase (I_C) is difficult to estimate theoretically. We may write (16)

$$I_C = I_G + P, \quad [3]$$

where P = polarization energy for a single charge in the dielectric medium. For many crystals, and even some liquids, Lyons and Mackie (20) have shown that P is approximately -1.5 ± 0.5 eV. The value of P for liquids, however, may be greater than this

because the liquid molecules can point their directions of maximum polarizability at the charge; thermal motions will, of course, tend to reduce by disorientation the value of P below that for maximum orientation. However, the value of P for liquid water may be as large as 5–7 eV (16). We have assumed that for polymers, the value of P is similar to that for crystals, as indeed some calculations by Wintle (21) for polyethylene suggest.

We note that Ninham and Parsegian (6–10) in their calculations on liquid films used gaseous values for the ionization potentials of liquids. Their numerical calculations must be viewed with caution until it is established that such an approximation does not introduce significant errors.

The final equations for the permittivity of water (ϵ_W) and of all polymers and hydrocarbons (ϵ_{PHC}) were (6):

$$\epsilon_W = \frac{\epsilon_{0W} - 5.2}{1 + 7.761 jT} + \frac{5.2 - n_W^2}{1 + 2.112 \times 10^{-6} j^2 T^2} + \frac{n_W^2 - 1}{1 + 2.931 \times 10^{-7} j^2 T^2 / I_W^2} + 1 \quad [4]$$

$$\epsilon_{PHC} = (\epsilon_{0PHC} - n^2_{PHC}) + \frac{n^2_{PHC} - 1}{1 + 2.931 \times 10^{-7} j^2 T^2 / I^2_{PHC}} + 1, \quad [5]$$

where the subscript o refers to zero frequency terms. Table I summarizes the values for the ionization potentials, refractive indices and the static dielectric constants (15, 16) of the polymers and hydrocarbons used in these computations. The temperature dependence of the zero frequency permittivity of water was approximated by the function (22)

$$\epsilon_0 = 182.5 - 0.348T.$$

RESULTS AND DISCUSSION

We begin by examining Eq. [1] in more detail because it facilitates the presentation of the computed results. First we define a Hamaker function H, exactly analogous to the classical Hamaker constant for spheres (5), by the relationship

$$H = -6G \Big/ \left[\frac{2}{s^2 - 4} + \frac{2}{s^2} + \ln\left(\frac{s^2 - 4}{s^2}\right)\right] = -6G \Big/ \left[\frac{2}{\delta^2 + 4\delta} + \frac{2}{\delta^2 + 4\delta + 4} + \ln\left(\frac{\delta^2 + 4\delta}{\delta^2 + 4\delta + 4}\right)\right] \quad [6]$$

since $\delta = s - 2$. Accordingly we also define a function F by

$$F = -G/H = \left[\left(\frac{2}{\delta^2 + 4\delta} + \frac{2}{\delta^2 + 4\delta + 4}\right) + \ln\left(\frac{\delta^2 + 4\delta}{\delta^2 + 4\delta + 4}\right)\right] \Big/ 6.$$

If we make the substitution $\eta^2 = \delta$, Eq. [1]

TABLE I

NUMERICAL VALUES FOR THE PARAMETERS USED IN THE COMPUTATIONS

Cognate compound	I_G/eV	Polymer	I_C/eV	n_P	ϵ_0
Ethylbenzene	8.8	polystyrene	7.0	1.587	2.52
Isopropylbenzene	8.4				
Toluene	8.8				
Isopropyl acetate	10.0	poly(vinyl acetate)	8.5	1.467	2.15
Ethylacetate	10.1				
Methyl isobutanoate	10.0	poly(methyl methacrylate)	8.5	1.500	3.35
n-Heptane	10.0		8.5	1.388	1.93

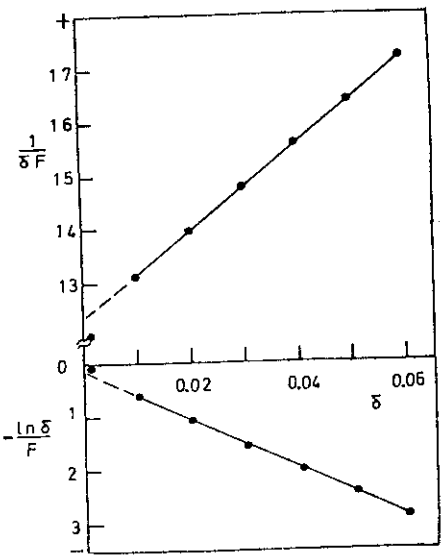

FIG. 1. Plots of $(1/\delta F)$ and $(\ln \delta)/F$ versus the distance parameter δ.

can be rewritten as

$$G = \alpha[(1/\delta) + \beta \ln (1/\delta)],$$

where α and β are independent of δ. Since $G = -HF$, we can write

$$-(H/\alpha) = [(1/\delta F) + \beta \ln (1/\delta)/F] \quad [7]$$

The virtue of Eq. [7] is that in the interval, say $0.005 \leqslant \delta \leqslant 0.1$ both $(1/\delta F)$ and $[\ln (1/\delta)]/F$ are linear functions of δ to a good approximation, as is shown in Fig. 1. Linear combinations of these two functions which yield H must also be linear. Actually the apparent linearity of these combinations is merely a good approximation for sigmoidal shaped curves with very shallow oscillations about the straight line. It must be admitted that significant deviations from linearity do occur for $\delta \leqslant 0.001$; however, for typical latex particles this corresponds to particle separations of less than, say, 1–2 Å where the validity of the continuum approach is suspect. We conclude that for close approach of latex spheres, H should be a linear function of δ.

Plots of some computed Hamaker functions as a function of δ are presented in Fig. 2 for polystyrene in water at room temperature (293 K). The expected linearity of these plots is confirmed. It was not possible to carry the calculations beyond $\delta = 0.03$ because the contribution of the zero frequency component of the second term of Eq. [1] became so large that Eq. [1] was no longer a valid approximation. Nevertheless $\delta = 0.03$ corresponds to a separational distance of, say 50 Å for a typical latex system so that Fig. 2 covers most of the interactional distance of interest. It must be admitted, however, that the verification of the quantitative correctness of these calculations, at least for the larger values of δ, must await a complete theoretical treatment of the attraction between two spheres.

The different lines in Fig. 2 display the predicted values for H using both gaseous and condensed values for the ionization potentials of both polystyrene and water. The reduction in the ionization potential of polystyrene from 8.5 eV (line 1) to 7.0 eV (line 4) significantly reduced the Hamaker function because the contributions of correlations at ultraviolet frequencies decreased. Clearly uncertainty in

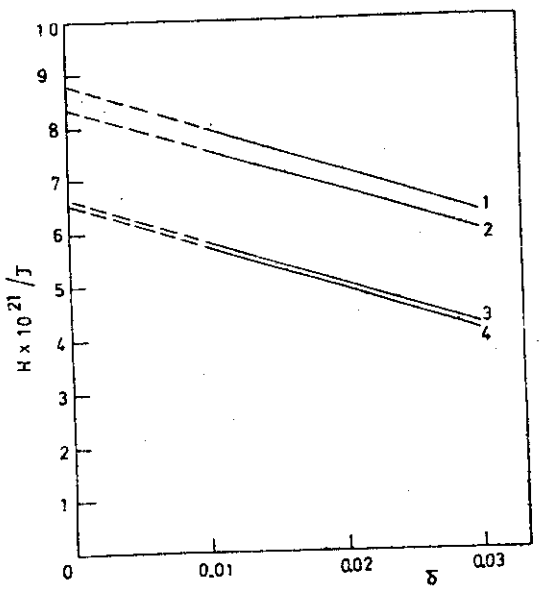

FIG. 2. Plots of the Hamaker function H versus the distance parameter δ for polystyrene in water at 293 K. Lines: (1) $I_P = 8.5$ eV, $I_W = 11.0$ eV; (2) $I_P = 8.5$ eV, $I_W = 12.62$ eV; (3) $I_P = 7.0$ eV, $I_W = 12.62$ eV; (4) $I_P = 7.0$ eV, $I_W = 11.0$ eV.

the ionization potentials of solids can introduce considerable uncertainty (ca. 40%) into values of the Hamaker function. However, a comparable reduction in the ionization potential of water (e.g., lines 3 and 4) altered the Hamaker function much less. Nonetheless because the polarization energy of liquid water may be as large as 7.0 eV (16), the uncertainty in H is probably larger than is indicated in Fig. 2. The contribution to the attraction by the ultraviolet correlations of water may be inferred from these results to be relatively small or, at least, not dominant.

Note that as $\delta = d/a$, the Hamaker function is determined both by the distance of separation and the particle radius. Of course pairwise additivity predicts that the Hamaker function is a constant, independent of either d or a. The negative slopes of the lines show that the fall-off in attraction between the latex particles is considerably faster than that predicted by pairwise additivity for a given value of a. However, preliminary calculations at large δ suggest that H increases with δ in that domain, implying that the Hamaker function for spheres may possess a minimum at intermediate distances.

The reason for the dependence of H upon δ presumably originates in the nonadditivity of the free energy of the bodies resulting from the long-range nature of the van der Waals forces. Any change in the electrical properties of the medium in a certain region will, by Maxwell's equations, lead to a change in the fluctuation fields which extend beyond that region. Therefore, the free energy is not determined solely by the properties of the substance at the point considered, i.e., it is nonadditive.

The straight lines in Fig. 2 have been extrapolated to $\delta = 0$ to give what we shall term "contact Hamaker constants." This extrapolation is a somewhat artificial device but it may perhaps be relevant to problems in adhesion. Of course, the continuum theory does not hold at very close distances. The values of the contact Hamaker constant obtained for polystyrene in water span the range (6.5–8.8) $\times 10^{-21} J$, with perhaps the best estimate being $6.5 \times 10^{-21} J$ (line 4). Napper and Hunter (23) have recently reviewed the experimental and theoretical values for the classical Hamaker constant, which is our Hamaker function, for polystyrene in water. The theoretical estimates span the interval 1×10^{-19}–$5 \times 10^{-21} J$ whereas the experimental values derived from colloid stability studies of the free energies of interaction cover the range 1×10^{-20}–$1 \times 10^{-21} J$. Perhaps the best experimental value to date is $3 \times 10^{-21} J$, which is smaller than the contact Hamaker function but is in rough agreement with values of H for $0 < \delta \leqslant 0.03$. Unfortunately the values of δ for the experiments reported in the literature must vary widely, but for most the measurements probably refer to $\delta < 0.05$. Perhaps some of the disagreement between the experimental values for latex particles resides in the nonconstancy of the Hamaker function.

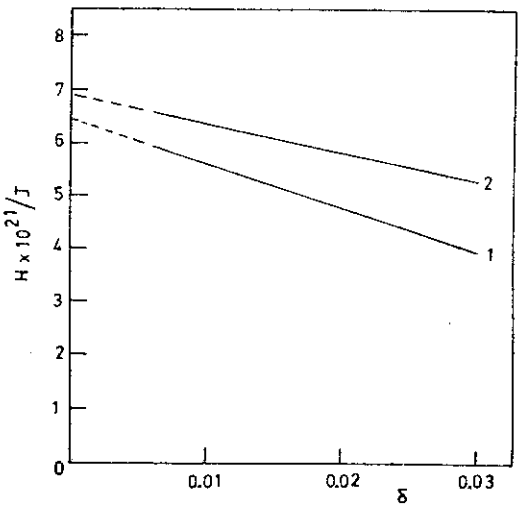

FIG. 3. Plots of the Hamaker function H versus the distance parameter δ for polystyrene in water, assuming $I_P = 7.0$ eV and $I_W = 11.0$ eV. Lines: (1) $T = 285$ K; (2) $T = 355$ K.

The temperature dependence of the Hamaker function for polystyrene in water is illustrated in Fig. 3. Only two temperatures, 285 and 355 K, are shown but several intermediate temperatures were also calculated and

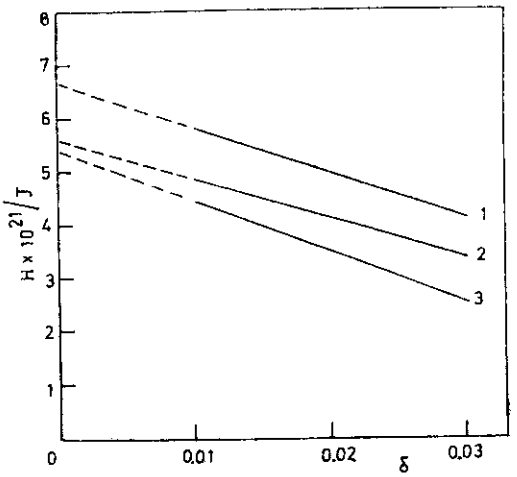

FIG. 4. Plots of the Hamaker function versus the distance parameter δ at 293 K. Lines: (1) polystyrene in water; (2) poly(methyl methacrylate) in water; (3) poly(vinyl acetate) in water. I_W = 12.62 eV.

fell monotonically within the lines shown. The temperature dependence is apparently quite small (<0.5%/K), H showing a monotonic increase with temperature in this range.

Shown in Fig. 4 are the Hamaker functions for polystyrene, poly(methyl methacrylate) and poly(vinyl acetate) in water. The Hamaker functions for a given value of δ decrease in that order. Polystyrene, with its conjugated delocalized π-electrons in the pendant benzene rings, exhibits an especially large Hamaker function. The slope of line 2 for poly(methyl methacrylate) is less than that for polystyrene because of its significant relaxation at near to zero frequencies. Perhaps the best values for the contact Hamaker constants for poly(vinyl acetate) and poly(methyl methacrylate) in water are ca. $5.5 \times 10^{-21} J$.

The Hamaker functions for polystyrene and poly(methyl methacrylate) in hydrocarbons (e.g., n-heptane) at 293 K are displayed in Fig. 5. Note that the values of H are less than the values for the same polymers in water for $\delta \leqslant 0.03$ because the zero frequency contributions are less in hydrocarbons. Moreover, the Hamaker function is a constant for these systems. It was possible in these nonpolar systems to extend the calculations to $\delta = 0.06$ before the contributions of the second terms in Eq. [1] became too large.

The value of the Hamaker function for poly(methyl methacrylate) in n-heptane is apparently $2.5 \times 10^{-21} J$ whereas that for polystyrene in a hydrocarbon is $3.5 \times 10^{-21} J$. However, uncertainty in the ionization potentials of the polymers leaves some residual uncertainty in H.

The reasons for the constancy of the Hamaker functions for polymers in hydrocarbons, and their linearity with δ in water, can be derived analytically from Eq. [1]. First we note that for small Δ

$$\sum_{j=1}^{\infty} \int_0^{\infty} x \ln (1 - \Delta^2 e^{-x}) dx \sim -\sum_{j=1}^{\infty} \Delta^2 \int_0^{\infty} x e^{-x} dx \sim -\sum_{j=1}^{\infty} \Delta^2$$

after integration by parts. In addition, for small Δ

$$\sum_{j=1}^{\infty} (1 - \Delta) \ln (1 - \Delta^2) \sim -\sum_{j=1}^{\infty} \Delta^2.$$

Therefore, Eq. [1] becomes

$$G \sim -(kT/8\delta) \sum_{j=1}^{\infty} \Delta^2 - (kT/2) \ln (\delta^{\frac{1}{2}}) \sum_{j=1}^{\infty} \Delta^2 + (kT/16\delta) \int_0^{\infty} x \ln (1 - \Delta_0^2 e^{-x}) dx + (kT/4)(1 - \Delta_0) \ln (\delta^{\frac{1}{2}}) \ln (1 - \Delta_0^2),$$

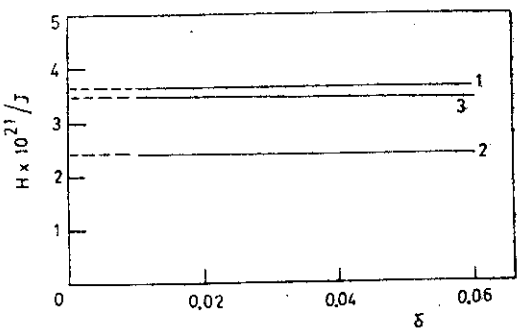

FIG. 5. Plots of the Hamaker function versus the distance parameter δ at 293 K. Lines: (1) polystyrene in n-heptane; (2) poly(methyl methacrylate) in n-heptane; (3) nonzero frequency component for polystyrene in water.

where the subscript o refers to zero frequency values. The terms in Δ_0 are important in aqueous systems where $\Delta_0 \sim -0.95$ but in nonpolar dispersion media the zero frequency terms can be neglected in the first order approximations. Separating the zero frequency ($j = 0$) from the nonzero frequency ($j \neq 0$) terms we may write

$$G_{j\neq 0} \sim -(kT/8)\left(\sum_{j=1}^{\infty} \Delta^2\right)(1/\delta + 2\ln\delta) \qquad [8]$$

$$G_{j=0} = (kT/16)\left\{[1/\delta]\int_0^{\infty} x\ln(1-\Delta_0^2 e^{-x})dx + 2(1-\Delta_0)\ln\delta\ln(1-\Delta_0^2)\right\}. \qquad [9]$$

Now for $\delta \leqslant 0.05$

$$H = -6G\Big/\left(\frac{2}{\delta^2+4\delta} + \frac{2}{\delta^2+4\delta+4} + \ln\frac{\delta^2+4\delta}{\delta^2+4\delta+4}\right)$$

$$\sim -6G\Big/\left[\frac{1}{2\delta}+\frac{1}{2}+\ln\left(\frac{\delta}{1+\delta}\right)\right]$$

$$\sim -12G\Big/\left(\frac{1}{\delta}+2\ln\delta\right).$$

Therefore, from Eq. [8]

$$H_{j\neq 0} \sim (3/2)kT\sum_{j=1}^{\infty}\Delta^2 \sim H. \qquad [10]$$

This shows analytically that for polymers in hydrocarbons, the total Hamaker function H, which approximates closely to $H_{j\neq 0}$, is independent of δ, i.e., it is a constant. This, of course, will also be true for the nonzero frequency contributions for polymers in water. Some actual numerical values computed for polystyrene in water are shown in Fig. 5 (line 3). Since $\sum_{j=1}^{\infty}\Delta^2$ is of the order of unity, the Hamaker function for polymers in hydrocarbons is of the order kT, i.e., of the order of thermal energy.

TABLE II

VALUES OF F ($=-G/H$) AS A FUNCTION OF δ

δ	F
0.005	15.85
0.010	7.63
0.015	4.92
0.020	3.57
0.025	2.78
0.030	2.25
0.035	1.88
0.040	1.60
0.045	1.39
0.050	1.22
0.055	1.08
0.060	0.97

The form of Eq. [9] may be simplified by introducing the approximations

$$\int_0^{\infty} x\ln(1-\Delta_0^2 e^{-x})dx \sim -1$$

and $(1/4)(1-\Delta_0)\ln(1-\Delta_0^2) \sim -1$ which hold, e.g., for $\Delta_0 \sim -0.95$, as can be verified by substitution. Thus from Eq. [9]

$$G_{j=0} \sim -(kT/16)(1/\delta + 8\ln\delta)$$

so

$$H_{j=0} \sim (3/4)kT\left\{\frac{1+8\delta\ln\delta}{1+2\delta\ln\delta}\right\}.$$

All the dependence of H upon δ for polystyrene in water is incorporated in $H_{j=0}$. We, therefore, have to a good approximation on differentiation

$$\frac{dH}{d\delta} = \frac{dH_{j=0}}{d\delta} \sim (9/2)kT\left\{\frac{1+\ln\delta}{1+4\delta\ln\delta}\right\}$$

$$\sim -19.5kT$$

since $(1+\ln\delta)/(1+4\delta\ln\delta) \sim -4.3$ for $0.005 \leqslant \delta \leqslant 0.03$. This demonstrates analytically that the plots of H versus δ should be linear with a negative slope of 19.5 kT. The slopes of the computed lines in Fig. 2 are in fact close to $-19.5\,kT$, confirming the correctness of the numerical computations. It is clear from the above discussion that the Hamaker function will be constant if Δ_0 is small (e.g., polymer

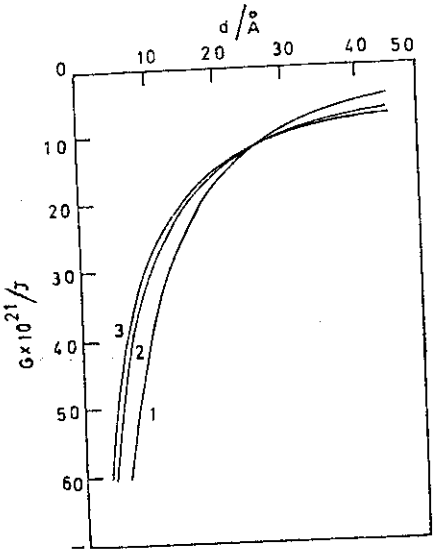

FIG. 6. Plots of the attractive potential energy versus the distance of separation for two polystyrene particles, each of radius 1000 Å, immersed in water. Lines: (1) Lifshitz formalism; (2) Assuming $G = -(A/12\delta)$, where $A = 3.6 \times 10^{-21}$ J; (3) Assuming $G = -AF$, where $A = 4.4 \times 10^{-21}$ J.

latex particles in media of weak or zero polarity).

Values of the function F for different values of δ are tabulated in Table II. These permit the free energy of attraction for a given value of δ to be calculated rapidly from our computed values of H using $G = -HF$. An example of this is given in Fig. 6. Curve 1 shows the calculated values of G as function of the separational distance for polystyrene particles, of radius 1000 Å, in water. Also included in the diagram are values for the free energy of attraction using the classical Hamaker constant procedure: curve 2 employs the crude approximation $G = -(A/12\delta)$ and curve 3 the more exact relationship $G = -AF$, where A = Hamaker constant. The values chosen for A were $3.6 \times 10^{-21}J$ and $4.4 \times 10^{-21}J$ to give concurrence of all curves at $d = 25$ Å but these values are close to the best experimental values to date. Clearly quite accurate experimental results would be needed to differentiate between the exact and the approximate theoretical results. Nevertheless the fact that H depends upon δ may well explain some of the discrepancies observed by Ottewill and Shaw (24) between their experimental results for polystyrene latices in water and the predictions of the well-known DLVO theory

Finally, we note that the uncertainty in the calculations using the Ninham and Parsegian approach would be minimized by direct measurements of the ionization potentials of solids and liquids. The most promising method devised to-date to provide this information is low-energy electron-reflection spectroscopy (25).

CONCLUSIONS

The foregoing discussion shows that it is possible to define a Hamaker function, analogous to the classical Hamaker constant, for spherical latex particles. It is proven that the Hamaker function for close approach of the particles is linearly dependent on the ratio of the minimum distance of separation of the surfaces to the radius of the particles (δ). For polymers in aqueous media, the Hamaker function decreases with δ; only in nonpolar media is the Hamaker function a constant, as is commonly assumed for all dispersion media.

The major difficulty encountered in calculating accurate values for the Hamaker function is the paucity of ionization potential data for condensed media. Nevertheless an approximate procedure can be devised to yield reasonable precise results.

Note added in proof: Fujihara and Inokuchi [*Chem. Phys. Letters*, 17, 554 (1972)] have now measured the I.P. of polyethylene as 8.5 eV. Our procedure predicts this value exactly because the I.P.'s of *n*-alkanes are known to approach asymptotically 10.0 eV as the number of carbon atoms increases.

ACKNOWLEDGMENTS

R. E. gratefully acknowledges the award of a Commonwealth Post-Graduate Scholarship. We are grateful to the Australian Research Grants Committee for support of these studies. Professor B. W. Ninham is thanked for his comments on the basic equation, as is Dr. J. C. Mackie for his advice on the ionization potential problem.

REFERENCES

1. FORCE, C. G., AND MATIJEVIC, E., *Kolloid-Z. Z. Polymere* **224**, 51 (1968).
2. LYKLEMA, J., *Pontif. Acad. Scient. Scripta Varia* **31**, Contribution 7 (1967).
3. WALBRIDGE, D. J., AND WATERS, J. A., *Discuss. Faraday Soc.* **42**, 294 (1966).
4. LONDON, F., *Z. Phys.* **63**, 245 (1930).
5. HAMAKER, H. C., *Physica* **4**, 1058 (1937).
6. PARSEGIAN, V. A., AND NINHAM, B. W., *Nature (London)* **224**, 1197 (1969).
7. NINHAM, B. W., AND PARSEGIAN, V. A., *Biophys. J.* **10**, 646 (1970).
8. PARSEGIAN, V. A., AND NINHAM, B. W., *Biophys. J.*, **10**, 664 (1970).
9. NINHAM, B. W., AND PARSEGIAN, V. A., *J. Chem. Phys.* **52**, 4578 (1970).
10. NINHAM, B. W., AND PARSEGIAN, V. A., *J. Chem. Phys.* **53**, 3398 (1970).
11. LIFSHITZ, E. M., *Soc. Phys. JETP* **2**, 73 (1956).
12. DZYALOSHINSKII, I. E., LIFSHITZ, E. M., AND PITAEVSKII, L. P., *Advan. Phys.* **10**, 165 (1961).
13. MITCHELL, D. J., AND NINHAM, B. W., *J. Chem. Phys.* **56**, 1117 (1972).
14. NINHAM, B. W., private communication (1972).
15. "Tables of Dielectric Materials," Vols. I and II. Massachusetts Institute of Technology, 1944.
16. GUTMANN, F., AND LYONS, L. E., *In* "Organic Semiconductors," Chap. 6. John Wiley, New York, 1967.
17. WATILLON, A., AND JOSEPH-PETIT, A.-M., *Discuss. Faraday Soc.* **43**, 143 (1966).
18. WALBRIDGE, D. J., AND WATERS, J. A., *Discuss. Faraday Soc.* **42**, 294 (1966).
19. LYONS, L. E., AND MACKIE, J. C., *Proc. Chem. Soc.* **71** (1962).
20. LYONS, L. E., AND MACKIE, J. C., *Nature (London)* **197**, 589 (1963).
21. WINTLE, H. J., *Photochem. Photobiol.* **3**, 249 (1964).
22. EISENBERG, D., AND KAUZMANN, W., *In* "The Structure and Properties of Water," Chap. 4. Oxford University Press, New York, 1969.
23. NAPPER, D. H., AND HUNTER, R. J., *M.T.P., Int. Rev. Sci., Phys. Chem. Series* 1, Vol. 7, Chap. 8 (1972).
24. OTTEWILL, R. H., AND SHAW, J. N., *Discuss. Faraday Soc.* **42**, 154 (1966).
25. HUNTER, L. M., LEWIS, D., AND HAMILL, W. H., *J. Chem. Phys.* **52**, 1733 (1970).